

**MICROPHYTOBENTHOS (MPB) BIOMASS VARIABILITY AND SEDIMENT- WATER
COLUMN EXCHANGES ON AN INTERTIDAL FLAT: INFLUENCE OF WEATHER-
RELATED ABIOTIC FACTORS ACROSS NEAP-SPRING-NEAP TIDAL CYCLES**

NURUL SHAHIDA REDZUAN

**Supervised by
PROF. GRAHAM J. C. UNDERWOOD**

**A thesis submitted for the degree of
DOCTOR OF PHILOSOPHY IN BIOLOGICAL SCIENCES**

**School of Biological Sciences
University of Essex
United Kingdom**

2017

***To my daughter, Aisha Nur Nasuha,
Sorry for the motherless toddler years***

SUMMARY

The spatio-temporal distribution of microphytobenthos (MPB) on the sediment surfaces during emersions and suspended in water column during immersions was investigated on transects across Fingringhoe Tidal Flat in Colne estuary, on three zones: the mud flat, the transition zone and the salt marsh. The results of this thesis suggest that MPB distribution on intertidal flat was controlled by a set of complex interaction between the MPB with both biotic and abiotic factors. How much MPB are there on the sediment surfaces determines the availability of MPB biomass after immersion period and in the water column during immersion. 'Sum of sun hours' and 'sum of rainfall' directly affected the MPB biomass on sediment surfaces, and consequently, indirectly affected the MPB that associated with suspended sediment in the water column during immersions. Tidal range did not have significant effect on MPB biomass on sediment surfaces, however was significantly negatively effected the suspended MPB on the mud flat and the transition zone. The Chl *a* on the salt marsh however was significantly positively correlated with the tidal range. Data of net settlement rate of suspended sediment per hour during immersions displayed positive relationship with MPB biomass availability after immersion. The sediment settlement on the intertidal flat was negatively correlated with mean wind speed and tidal range. Neap-spring-neap tidal cycles were found to nfluence MPB species composition across the tidal flat. Spring tide that was characterized by high water current and high tidal range (4.3 – 5.6 m) showed to increase the occurrence of centric diatom such as species from genus *Coscinodiscus*, genus *Actinoptychus* and *Odontella* on both mud flat and transition zone. Also, the spring tide was responsible to source the salt marsh with species that commonly recorded on the mud flat and transition zone such as *Pleurosigma angulatum* and species from genus *Gyrosigma*.

ACKNOWLEDGEMENTS

In the name of God the most merciful and honorable.

First and foremost I would like to express my special thanks and gratitude to my only supervisor, Professor Graham J. C. Underwood for his guidance, patience and supportive critics throughout my research and writing periods.

My sincere gratitude and appreciation go to University Malaysia Terengganu for approving my study leave, and also to the Ministry of Higher Education of Malaysia for funding my study here at University of Essex, UK.

My cordial appreciation to School of Biological Sciences members for all your help, especially to John Green, Russell Smart, Scott Warren, thanks for not making me went sampling alone. Not forgotten, thanks to Maddy Giles, you helped me a lot with the statistic and to Tania, for helping me with the labworks. I will always remember all of you and all the memories will remain intact in my mind. Also, thanks to Syila and Lana for your support and help, especially during the final stage of my PhD.

Finally, I would like to express my heartfelt regards to my dearest husband (Azrul Shah) and my daughter, Aisha Nur Nasuha, whom without, this thesis would not be possible. Thanks for always standing beside me through thick and thin. Finally, thanks to my parents Hj. Redzuan Othman and Hih. Rapih Amir, and my siblings for all your supports; physically, mentally and financially.

TABLE OF CONTENTS

Summary		i
Acknowledgements		ii
List of Tables		xi
List of Figures		xiv
List of Plates		xxiv
Abbreviations		xxv
Chapter 1	Introduction to microphytobenthos (MPB) and their importance on tidal flats ecosystem	
1.1	Microphytobenthos	1
1.2	General characteristics of mud flats and salt marshes	3
1.3	Distribution of microphytobenthos on tidal flats	5
1.4	Benthic pelagic coupling of microphytobenthos	11
1.5	Resuspension of microphytobenthos	12
1.6	Aims, objectives and hypotheses	15
1.7	Thesis outline	19
Chapter 2	General materials and methods	
2.1	Study site	21
2.2	Sampling strategy	25

2.3	Top 2 mm sediment Chl <i>a</i> analyses	27
2.4	Top 2 mm colloidal carbohydrate and EPS analyses	27
2.5	Diatom cells count and identification	28
2.6	Environmental and meteorological factors	29
Chapter 3	Microphytobenthos variability at multi spatio-temporal scales across an intertidal flat	
3.1	Introduction	30
3.2	Methodology	33
3.2.1	Sampling strategy	33
3.2.2	Statistical analyses	34
3.3	Results	35
3.3.1	Microphytobenthos biomass general spatial variability between the mud flat, transition zone and salt marsh	35
3.3.2	Microphytobenthos biomass general temporal variability across intertidal flat	39
3.3.3	Temporal variability of weather-related abiotic factors	43
3.3.4	Contribution of spatio-temporal scales to total variation of biomass proxies	47
3.3.5	Influence of weather-related abiotic factors on the variability of the biomass proxies	60
3.3.6	Characterization of the physical state of microphytobenthos patches at spatio-temporal scales	63

3.3.6.1	microphytobenthos biomass variability at temporal monthly scale across tidal flat	63
3.3.6.2	Daily variability of microphytobenthos biomass proxies across spatial scales	68
3.4	Discussion	79
3.4.1	Variability of microphytobenthos biomass proxies across the intertidal flat	79
3.4.2	Effect of weather-related abiotic factors on biomass proxies variability at multi scales	81
3.4.2.1	Biomass proxies variability at monthly or seasonal temporal scales	81
3.4.2.2	Daily variability of microphytobenthos biomass proxies across the tidal flat	83
3.4.2.3	Microphytobenthos biomass proxies variability at spatial scale < 5 m and < 0.5 m across tidal flat	86
3.5	Conclusions	87
Chapter 4	Variability in the Chl a concentration of the microphytobenthos biofilm patches on an intertidal flat: influence of species composition across neap-spring-neap tidal cycles	
4.1	Introduction	89
4.2	Methods	91
4.2.1	Sampling strategy	91

4.2.2	Samples preparation for analyses	92
4.2.3	Cells count	92
4.2.4	Statistical analyses	93
4.3	Results	94
4.3.1	General characteristic of microphytobenthos assemblage species composition	94
4.3.2	Variability of Chl <i>a</i> concentration and microphytobenthos assemblages diversity	99
4.3.3	Relationship between Chl <i>a</i> and microphytobenthos assemblages diversity	101
4.3.4	Relationship between Chl <i>a</i> concentration, species richness and species equitability (<i>E</i>)	108
4.4	Discussion	120
4.4.1	Community ecology theory and the relationship between Chl <i>a</i> and microphytobenthos assemblages diversity on an intertidal flat	120
4.4.2	Shifts in microphytobenthos assemblages species composition across neap-spring tidal cycle and possible resuspension event	122
4.5	Conclusions	124

Chapter 5

Sediment-water column exchanges of microphytobenthos on an intertidal flat

5.1	Introduction	127
-----	--------------	-----

5.2	Materials and methods	131
5.2.1	Sampling strategy	131
5.2.2	Sediment trap approach (sample collection and processing)	131
5.2.3	Microphytobenthic cells count for species composition	132
5.2.4	Sediment surface and suspended properties data	134
5.2.5	Statistical analyses	134
5.3	Results	136
5.3.1	Spatial variability in microphytobenthos biomass proxies on sediment surfaces and in suspended sediment across intertidal flat	136
5.3.2	Characterization in the relationship between suspended sediment and suspended Chl <i>a</i>	138
5.3.3	Characterization in the relationship between benthic biomass and suspended biomass	142
5.3.4	Exchanges of microphytobenthos species composition on the sediment surface and in the water column	148
5.3.5	Sediment settlement and microphytobenthos biomass on sediment surface	153
5.4	Discussion	157
5.4.1	Spatial variability in microphytobenthos biomass on sediment surface and in the water column	157
5.4.2	Does suspended sediment carry along microphytobenthos?	158

5.4.3	Evidence of microphytobenthos sediment-water column exchanges	159
5.4.4	Do weather-related abiotic factors drive the sediment-water column exchanges of microphytobenthos?	161
Chapter 6	Coupling of microphytobenthos biomass between the transition zone and the vegetated salt marsh during spring tides	
6.1	Introduction	165
6.2	Materials and methods	168
6.2.1	Sampling strategy and samples processing	168
6.2.2	Samples processing	169
6.2.2.1	Sediment surface samples	169
6.2.2.2	Sediment traps and tidal levels (flood and ebb tides) water samples	169
6.2.3	Microphytobenthic cells count	170
6.2.4	Weather-related abiotic factors	170
6.2.5	Statistical analyses	171
6.3	Results	173
6.3.1	Temporal variability in microphytobenthic and suspended biomass across weather-related abiotic factors gradient	173
6.3.2	Microphytobenthos coupling between the transition	180

	zone (mud flat) and the salt marsh	
6.3.2.1	Characterization of microphytobenthos across tidal levels, the flood tide and ebb tides in spring tidal immersion	180
6.4	Discussion	189
6.4.1	Temporal microphytobenthos biomass variability	189
6.4.2	Relationship between Chl a on sediment surface with suspended Chl a on the salt marsh	189
6.4.3	Contribution of tidal levels (flood and ebb tides) in spring tide to microphytobenthos variability on the salt marsh	191
Chapter 7	General discussion	193
7.1	Link between MPB biomass with weather-related abiotic factors, MPB assemblages diversity and sediment resuspension on mud flat and transition zone	193
7.2	Role of flood and ebb tides in MPB variability on salt marsh	195
7.3	Recommendations for further work	197
7.4	Concluding remarks	196
References		200
Appendices		218
Appendix 1	Daily ratio of colloidal carbohydrate (CC) and	218

extracellular polymeric substance (EPS) across July
2013 on mud flat and transition zone

Appendix 2

Plate of some recorded microphytobenthos diatom
species in Fingringhoe tidal flat, Colne estuary

219

LIST OF TABLES

Table 1.1	- Hypotheses and the chapters in which they were addressed	16
Table 3.1	- Pearson correlation coefficients between biomass proxies data across tidal flat with weather-related abiotic factors	67
Table 3.2	- Daily differences in the PC1 and PC2 scores in the three sampling months	72
Table 3.3	- Pearson correlation coefficients between Chl <i>a</i> , CC and EPS concentrations with weather-related abiotic factors in the April, July and Oct 2013.	76
Table 3.4	- Correlation coefficients between PC1 and PC2 scores with Chl <i>a</i> , CC and EPS concentrations variability (SE) at spatial scale < 5 m.	77
Table 3.5	- Hypotheses that were addressed in Chapter 3	88
Table 4.1	- Counted cells for sediment samples	93
Table 4.2	- Relative abundance of the top ten most common species on the mud flat	96
Table 4.3	- Relative abundance of the top ten most common species on the transition zone	97
Table 4.4	- Relative abundance of the top ten most common species on the salt marsh	98
Table 4.5	- Correlation coefficients between Chl <i>a</i> concentrations (daily) and MPB assemblages diversity index (H')	103

Table 4.6	- Hypotheses that were addressed in Chapter 4	126
Table 5.1	- Details of the sampling strategies for data set 1, set 2 and set 3	135
Table 5.2	- Slope of the regression line ($\mu\text{g Chl } a \text{ mg suspended sediment}^{-1}$) of the relationship between the suspended sediment and the suspended Chl <i>a</i>	141
Table 5.3	- Correlation coefficients between the slope of regression line and the weather-related abiotic factors	141
Table 5.4	- Pearson correlation coefficients between PC1 and PC2 with biological and weather-related abiotic factors	146
Table 5.5	- Temporal variability of the measured weather-related abiotic factors	146
Table 5.6	- Relative abundance of the diatom taxa on the sediment surfaces and in the trap on both mud flat and transition zone	150
Table 5.7	- Hypotheses that were addressed in Chapter 5	164
Table 6.1	- Similarity index of MPB species composition between mud flat, transition zone and salt marsh	167
Table 6.2	- Details of the sampling strategies for samples for data set 1, data set 2, data set 3 and data set 4.	172
Table 6.3	- Variability in the Chl <i>a</i> and CC concentrations in LT1 and LT2 across sampling survey 1 and 2 on transition zone and salt marsh	176
Table 6.4	- Daily changes in the chosen weather-related abiotic factors	177
Table 6.5	- Correlations between Chl <i>a</i> concentration on transition zone	178

and salt marsh with weather-related abiotic factors

Table 6.6	- Relative abundance of MPB species that potentially involved in movement between transition zone and salt marsh	187
Table 6.7	- Relative abundance of MPB species that potentially involved on the resuspension on the salt marsh during ebb tides.	188
Table 6.8	- Hypotheses that were addressed in Chapter 6	192

LIST OF FIGURES

Figure 2.1	-	Satellite view of study site at Fingringhoe tidal flat	22
Figure 2.2	-	Illustration of the quadrat (0.5 X 0.5 m) in which triplicate samples were obtained from fixed area using minicores	26
Figure 2.3	-	Temporal sampling in neap-spring-neap tidal cycle	26
Figure 2.4	-	Two carbohydrate calibrations that were used for colloidal carbohydrate and EPS analyses	28
Figure 3.1	-	Variability in Chl <i>a</i> , colloidal carbohydrate and EPS in top 2 mm sediment surface on the mud flat, the transition zone and the salt marsh	37
Figure 3.2	-	Spatial differences in the ratio of colloidal carbohydrate and EPS to Chl <i>a</i> across the intertidal flat	37
Figure 3.3	-	Relationship between Chl <i>a</i> and colloidal carbohydrate concentrations on the mud flat, the transition zone and the salt marsh	38
Figure 3.4	-	Temporal variability of Chl <i>a</i> and colloidal carbohydrate and EPS concentrations in the top 2 mm per cm ² sediment on the mud flat and on the transition zone in April, July and October 2013 across the neap-spring-neap tidal cycle.	41
Figure 3.5	-	Temporal variability in four weather-related abiotic factors across seven sampling days in April 2013, July 2013 and October 2013 over neap-spring-neap tidal cycle. The factors	45

are mean wind speed, sum of rainfall, sun of sun hours and tidal range

- Figure 3.6 - Significant positive relationship between the wind speed and the wave height 46
- Figure 3.7 - Contribution of spatio-temporal scale; temporal month scale, temporal day scale, spatial scale < 0.5 m within day and spatial scale < 0.5 m within quadrat to Chl a, CC and EPS variability in top 2 mm per cm² sediment on mud flat, transition zone and salt marsh. 50
- Figure 3.8 - Multi-scales variability of Chl a concentration in the top 2 mm per cm² sediment on mud flats at Fingringhoe, Essex at the smallest spatial scale < 0.5 m, spatial scale < 5 m at daily temporal scale over seven sampling days across neap-spring-neap tide tidal cycle and at the largest monthly and seasonal temporal scales in April 2013, July 2013 and October 2013. 51
- Figure 3.9 - Multi-scales variability of colloidal carbohydrate concentration in the top 2 mm per cm² sediment on mud flats at Fingringhoe, Essex at the smallest spatial scale < 0.5 m, spatial scale < 5 m at daily temporal scale over seven sampling days across neap-spring-neap tide tidal cycle and at the largest monthly and seasonal temporal scales in April 2013, July 2013 and October 2013. 52
- Figure 3.10 - Multi-scales variability of EPS concentration in the top 2 mm per cm² sediment on mud flats at Fingringhoe, Essex at the smallest spatial scale < 0.5 m, spatial scale < 5 m at daily

temporal scale over seven sampling days across neap-spring-neap tide tidal cycle and at the largest monthly and seasonal temporal scales in April 2013, July 2013 and October 2013.

- Figure 3.11 - Multi-scales variability of Chl a concentration in the top 2 mm per cm² sediment on transition zone at Fingringhoe, Essex at the smallest spatial scale < 0.5 m, spatial scale < 5 m at daily temporal scale over seven sampling days across neap-spring-neap tide tidal cycle and at the largest monthly and seasonal temporal scales in April 2013, July 2013 and October 2013. 54
- Figure 3.12 - Multi-scales variability of colloidal carbohydrate concentration in the top 2 mm per cm² sediment on transition zone at Fingringhoe, Essex at the smallest spatial scale < 0.5 m, spatial scale < 5 m at daily temporal scale over seven sampling days across neap-spring-neap tide tidal cycle and at the largest monthly and seasonal temporal scales in April 2013, July 2013 and October 2013. 55
- Figure 3.13 - Multi-scales variability of EPS concentration in the top 2 mm per cm² sediment on transition zone at Fingringhoe, Essex at the smallest spatial scale < 0.5 m, spatial scale < 5 m at daily temporal scale over seven sampling days across neap-spring-neap tide tidal cycle and at the largest monthly and seasonal temporal scales in April 2013, July 2013 and October 2013. 56
- Figure 3.14 - Multi-scales variability of Chl a concentration in the top 2 mm 57

per cm² sediment on salt marsh at Fingringhoe, Essex at the smallest spatial scale < 0.5 m, spatial scale < 5 m at daily temporal scale over seven sampling days across neap-spring-neap tide tidal cycle and at the largest monthly and seasonal temporal scales in April 2013, July 2013 and October 2013.

- Figure 3.15 - Multi-scales variability of colloidal carbohydrate concentration in the top 2 mm per cm² sediment on salt marsh at Fingringhoe, Essex at the smallest spatial scale < 0.5 m, spatial scale < 5 m at daily temporal scale over seven sampling days across neap-spring-neap tide tidal cycle and at the largest monthly and seasonal temporal scales in April 2013, July 2013 and October 2013. 58
- Figure 3.16 - Multi-scales variability of EPS concentration in the top 2 mm per cm² sediment on salt marsh at Fingringhoe, Essex at the smallest spatial scale < 0.5 m, spatial scale < 5 m at daily temporal scale over seven sampling days across neap-spring-neap tide tidal cycle and at the largest monthly and seasonal temporal scales in April 2013, July 2013 and October 2013. 59
- Figure 3.17 - Principal components 1 and 2 from PCA of log-transformed(n+1) variables: abiotic factors and biomass proxies (Chl *a*, colloidal carbohydrate and EPS) of MPB microspatial patches on sediment biofilm of the mud flat, transition zone and salt marsh 62
- Figure 3.18 - Variable factor map and the individual factor plots (at monthly 66

temporal scale) of the PCA on the mud flat, the transition zone and the salt marsh

Figure 3.19	- Individual plots of PCA of the mud flat at daily temporal scale, showing the samples scores for the physical state of biofilm patches at temporal daily scale in April 2013, July 2013 and October 2013	73
Figure 3.20	- Individual plots of PCA of the transition zone at daily temporal scale, showing the samples scores for the physical state of biofilm patches at temporal daily scale in April 2013, July 2013 and October 2013	74
Figure 3.21	- Individual plots of PCA of the salt marsh at daily temporal scale, showing the samples scores for the physical state of biofilm patches at temporal daily scale in April 2013, July 2013 and October 2013	75
Figure 3.22	- Percentage change of CC and EPS concentrations on 11 th April on the mud flat and the transition zone.	78
Figure 4.1	- Daily variability in three different sampling months (April 2013, July 2013 and October 2013) on the mud flat, the transition zone and the salt marsh in Fingringhoe tidal flat, Colne	100
Figure 4.2	- Daily Shannon-Wiener diversity index value of MPB assemblages on the mud flat, the transition zone and the salt marsh across the neap and spring tidal cycle in Colne estuary in three April 2013, July 2013 and October 2013	100
Figure 4.3	- Scatterplots showing the relationship between Chl a concentration and the MPB assemblage diversity on the mud	104

	flat in April 2013, July 2013 and October 2013	
Figure 4.4	- Scatterplots showing the relationship between Chl <i>a</i> concentration and the MPB assemblage diversity on the transition zone in April 2013, July 2013 and October 2013	105
Figure 4.5	- Scatterplots showing the relationship between Chl <i>a</i> concentration and the MPB assemblage diversity on the salt marsh in April 2013, July 2013 and October 2013	106
Figure 4.6	- Scatterplots showing positive correlations between Pearson correlation coefficients between Chl <i>a</i> and diversity index (H') and tidal range on the mud flat and the transition zone in spring tide	107
Figure 4.7	- Scatterplots showing positive correlations between Pearson correlation coefficients between Chl <i>a</i> and diversity index (H') and sum of sun below 24 hours on the salt marsh	107
Figure 4.8	- Relationship between Chl <i>a</i> concentration and MPB assemblages diversity (H') can be used to predict whether the Chl <i>a</i> variability in the samples was attributed to the evenness (E) or the species richness of the assemblage	108
Figure 4.9	- Scatterplot showing the relationship between Chl <i>a</i> concentration with the Evenness and the species richness of the samples which MPB assemblages were significantly positively, linearly and positively and curvilinear correlated with the Chl <i>a</i> concentration	113
Figure 4.10	- Scatterplot showing the relationship between Chl <i>a</i> concentration with the Evenness and the species richness of the samples which MPB assemblages were significantly	114

negatively and unimodal correlated with the Chl a concentration

- Figure 4.11 - Variable factor map and the individual factor map of the samples which Correlation A were $r > 0.90$ 115
- Figure 4.12 - Variable factor map and the individual factor map of the PCA that was performed on the samples which Correlation A showed significant positive curvilinear relationship on the salt marsh 116
- Figure 4.13 - Variable factor map and the; B) individual factor map of the PCA that was performed on the samples which Correlation A showed significant positive curvilinear relationship on the mud flat during spring (9th Apr and 9th Oct 2013) and neap (17th Apr 2013) tides 117
- Figure 4.14 - Variable factor map and the individual factor map of the PCA that was performed on the samples on the mud flat which Correlation A showed significant negative relationship and was only recorded during neap tide on the 4th April, 3rd and 17th July 2013 and on the 2nd Oct 2013 118
- Figure 4.15 - Variable factor map and the individual factor map of the PCA that was performed on the samples on the transition zone which Correlation A showed significant negative relationship and was only recorded during neap tide on the 2nd, 3rd, 16th and the 17th July 2013 119
- Figure 4.16 - Diagram on the possible cycle in the relationship between the Chl a concentration and the MPB assemblage diversity 126
- Figure 5.1 - Conceptual diagram on sediment-water column exchanges of 130

MPB that allows MPB resuspension to happen on an
intertidal flat

- Figure 5.2 - Spatial variability of Chl *a* and EPS on the sediment surface and, suspended sediment and suspended Chl *a* in the water column on two different zones across Fingringhoe tidal flat in Colne estuary 137
- Figure 5.3 - Relationship between suspended sediment and suspended Chl *a* on the mud flat and the transition zone in April 2013, July 2013 and October 2013 across the neap-spring tidal cycle 140
- Figure 5.4 - Individual variable map of principle component analyses (PCA) done on log-transformed of the pooled data (mud flat and transition zone data) of the biomass on the sediment surface and suspended properties across three sampling months April 2013, July 2013 and October 2013 and in neap-spring tidal cycle 145
- Figure 5.5 - Temporal variability of Chl *a* concentration on the sediment surface and extracellular polymeric substance (EPS) concentration on sediment surface with suspended sediment and suspended Chl *a* in the water column during immersion across the neap-spring-neap tidal cycle 147
- Figure 5.6 - Relationship between the suspended sediment load and the percentage similarity between the species composition of diatom on the sediment surface and in the sediment traps (suspended) of the mud flat and the transition zone in April, July and October 2013 152

Figure 5.7	- Relationship between Chl <i>a</i> on sediment surface daily changes in Chl <i>a</i> on sediment surface with the net settlement rate of sediment across three different sampling months.	155
Figure 5.8	- Relationship between the net settlement of sediment and mean wind speed for three days across the neap-spring-neap tidal cycle	156
Figure 5.9	- Relationship between the net settlement of sediment and tidal range across the neap-spring-neap tidal cycle	156
Figure 6.1	- Similarity (%) in MPB species composition between the transition zone and the salt marsh during spring and neap tides during the months of April, July and October 2013	167
Figure 6.2	- Sampling strategy in August and September 2015 that was carried out on the transition zone of the mud flat and salt marsh	172
Figure 6.3	- Daily changes in Chl <i>a</i> concentration in the top 2 mm per cm ² sediment surface on the transition zone and salt marsh and the colloidal carbohydrate on only the transition zone during low tide 1 and low tide 2 on the transition zone in sampling survey 1 and survey 2	175
Figure 6.4	- Daily changes in suspended sediment per L of water over the transition zone and the salt marsh and also the daily changes of the suspended Chl <i>a</i> per L of water over the transition zone and the salt marsh during two periods of sampling in August and September 2015	177
Figure 6.5	- Significant positive relationship between the Chl <i>a</i> and	178

colloidal carbohydrate concentration in the top 2 mm sediment surface of the transition zone during August and September 2015

- Figure 6.6 - Positive relationships between the suspended Chl *a* concentration over the salt marsh during slack high tide of the spring tide with the mean wind speed and the tidal range 179
- Figure 6.7 - Daily variability in Chl *a* in flood and ebb tidal water and also the concurrent Chl *a* concentration in the top 2 mm sediment surface on the transition zone and on the salt marsh in both survey 1 and 2 183
- Figure 6.8 - Relationship between Chl *a* concentration per L flood and ebb tidal water with the Chl *a* concentration in the top 2 mm per cm² sediment surface of the transition zone and the salt marsh 184
- Figure 6.9 - Relationship between the Chl *a* concentration in flood and ebb tides with the sum of rainfall for three days averaged wind speed for three days percentage of cloud cover and the tidal range across spring tide occasion on the salt marsh 185
- Figure 6.10 - Dendrogram on the similarity in the MPB species composition of ebb tide, salt marsh (on sediment surfaces), flood tide, sediment traps (deployed on transition zone) and transition zone (on the sediment surfaces) samples. 186

LIST OF PLATES

Plate 2.1	- The tidal flat of Fingringhoe Wick Reserve during flooding tide	23
Plate 2.2	- Salt marsh, the vegetated area of Fingringhoe Wick Reserve tidal flat	23
Plate 2.3	- Differences in sampling zones' sediment particle sizes	24
Plate 2.4	- <i>Hydrobia</i> sp.	24
Plate 5.1	- Sediment trap that was deployed on the sediment surface	133
Plate 5.2	- Illustration of the sediment traps on the sediment surface of mud flat and transition zone	133

ABBREVIATIONS

CBESS	Coastal biodiversity and ecosystem service sustainability
CC	colloidal carbohydrate
Chl <i>a</i>	chlorophyll <i>a</i>
EPS	extracellular polymeric substance
MPB	microphytobenthos
NERC	Natural Environment Research Council
NaCl	Sodium chloride
T	Transition zone
SM	salt marsh
PCA	Principal component analyses
MF	mud flat
SE	standard error
HCl	Hydrochloric acid
MVSP	Multi variate statistical package
PC1	Principal component 1
PC2	Principal component 2
<i>E</i>	evenness
H'	Shannon Weiner diversity index
+ve	positive

-ve	negative
NP	no pattern
UM	unimodal
+ve curv.	positive curvilinear

Word count of the thesis: 51 468 words

CHAPTER 1

INTRODUCTION TO MICROPHYTOBENTHOS (MPB) AND THEIR IMPORTANCE ON TIDAL FLATS ECOSYSTEM

1.1 Microphytobenthos

Microalgae found living amongst any inert material such as rock, coral, sand particle and those attached to detritus or living organism are known as microphytobenthos (MPB). The term micro suggested that they are very small with range of length from about 2 μm to 2 mm (Miklasz, 2012). MPB are associated with substrata in different coastal habitats within the sediment of intertidal areas. The habitats include estuaries, sand flats, mud flats and salt marsh.

Microphytobenthos have been long known as the base of food chain on sub-tidal and intertidal ecosystems. The MPB community consists of the diatoms, cyanobacteria, chlorophytes and some other divisions of microscopic algae that normally inhabit the sediment. Diatoms however, are often the most common (Mann, 1999). Though viable MPB are found to inhabit the top 10 cm within the sediment (Brito et al., 2012), they are normally located in muddy sediment, in the top 2 mm surficial sediment deeper in sand that are mobile (Blanchard & Forster, 2006). The distribution of MPB in the sediments is typically temporally varied; either at high temporal scale such as inter-annual (Benyoucef et al., 2013) to daily (Herlory et al., 2004) and to hourly (Du et al., 2010) scales; and spatially; at the smallest micro-scale between patches (Weerman et al., 2012), at centimetre to metre scales (Weerman et al., 2012) and between zones across the tidal flat (Brito et al., 2012).

Although only located and restricted in the uppermost part of sediment, MPB can have significantly high impact on the whole intertidal flats ecosystem functioning (Colijn et al., 1984; Aberle-Malzahn, 2004; Blanchard & Forster, 2006). Diatoms, which are also the major contributor to population in MPB communities, are vital as sediment stabilizers. They produce

extracellular polymeric substances (EPS) that are able to stabilize sediments (Underwood et al., 1995), and inhibit the resuspension or wash away of sediment by tidal currents and waves (Ubertini et al., 2015). MPB biofilms have been proven to effectively retain deposited sediment during tidal activity by preventing the sediment from being resuspended and carried away (Underwood & Paterson, 1993). This was further supported by de Brouwer et al. (2003), who suggested removal of biofilm from intertidal area shows to increase sediment erosion.

In order to understand the functions of EPS to the intertidal flat ecosystem, it is crucial to gain more information on its relationship to the physiology and biological processes of MPB community, other microorganisms and also in maintaining the ecological stability of the intertidal flat. De Brouwer et al. (2003) mentioned that the complex interaction between diatoms and the biological and physical environment they live in make the study on EPS difficult. Additionally, diatoms also secrete different types of EPS and the properties of this species-specific EPS also may vary between different species of diatoms (de Brouwer et al., 2006).

As the main primary producers on intertidal flat, MPB can contribute up to 50% of total primary production of the ecosystem (Cahoon, 1999). Lake & Brush (2011) suggested that on an annual basis, MPB production can be as high as or higher than phytoplankton production. To further supported this, Brito et al. (2012) reported that MPB may contribute almost 99 % of the total chlorophyll concentration when compared to phytoplankton in shallow and turbid coastal lagoon ecosystem. Thus, it is not a surprise as Underwood & Krompkamp (1999) stated that MPB are the most essential food source not only for benthic, but also the adjacent water channel ecosystem.

MPB are autotrophic microorganisms and therefore play a vital role as a processor for atmospheric carbon dioxide by utilizing this greenhouse gas during photosynthesis. Webster et al. (2002) suggested that the photosynthetic activity of MPB also aids in the production of oxygen and the return of nutrients to the sediment. Both oxygen and nutrients are crucial to allow the survival of organisms of both intertidal and aquatic ecosystems. Other ecological functions of MPB include their ability to retain the nutrients in sediment by preventing the

nutrient from escaping to the water column (Underwood & Kromkamp, 1999; Tyler et al., 2003). In addition, photosynthesizing MPB influence nitrogen turnover processes and help in exchanging process of phosphate between water and sediment (Risgaard-Peterson, 2003).

1.2 General characteristics of mud flats and salt marshes

Tidal flats are important coastal and estuarine habitats (Peterson & Peterson, 1979) that play a vital role in ecosystem services. Tidal flats occur along coastlines and are barriers to wave and wind energy (Leonardi et al., 2015; Scholz & Liebezeit, 2012). Coastal sediments are comprised of clay and sand that is carried by the riverine inputs and shoreline runoff that enter and settle on the sediment surfaces of the tidal flats (Arfi et al., 1994). Tidal flats are categorized by tidal level into supratidal, intertidal and subtidal flats (Fan et al., 2012). Of these, the intertidal flats (mud flats) and the supratidal flats (for instance the salt marshes) are the most well known zones to be researched.

Mud flats are the lowest area of the tidal flats. Therefore, the sediment surfaces are exposed to diurnal or semidiurnal cycles of tides. These tidal cycles cause high heterogeneity in the mud flats nutrients (Chesman et al., 2006) particularly nitrate, ammonium and phosphate (Peterson & Peterson, 1979). The concentrations of the mentioned nutrients were reported in higher concentration at mud flat than at upper marsh (Kocum et al., 2002). The high nutrients of the mud flats always correlate with high MPB biomass and high MPB diversity (Kocum et al., 2002; Thornton et al., 2002).

Salt marshes are located in the supratidal area and are often vegetated with herbs, grasses and low shrubs (Xin et al., 2013). This area is only subjected to tidal immersion during the highest spring tides. Therefore nutrients' concentrations in the salt marshes are lower than the lower tidal flats, such as the mud flat (Kocum et al., 2002). The salinity of salt marshes are

often far greater than in the mud flat (McKew et al., 2011). Underwood (1997) reported the high salinity ranged between 16 – 210 in the salt marsh of the Colne estuary, Essex, while in the mud flat, the salinity only ranged between 22 – 39. This high salinity of the salt marshes creates an extreme condition that only certain organisms can tolerate.

Both mud flats and salt marshes' sediments have been reported as important sites where denitrification takes place (Ogilvie et al., 1997; Underwood, 1997; Kocum et al., 2002; Sundbäck & Miles, 2002; Cibic et al., 2007). The denitrification in the tidal flats able to decrease the amount of continentally-derived nitrogen transported into the ocean (Seitzinger, 1988). The denitrification in tidal flats is greater than the denitrification that takes place in lakes and rivers (Seitzinger, 1973). Seitzinger (1973) documented that the amount of nitrogen removed by denitrification in six tidal flats, two rivers and six lakes was equivalent to between 20 and 50 %, 7 and 35 % and 1 and 36 % of the input of the nitrogen loading into the ecosystems, respectively.

Wave energy, tidal range and flood-ebb tides and spring-neap tidal cycles are the potential factors that affect the resuspension and deposition of sediment in the tidal flats. The resuspension and the deposition of sediment in this ecosystem ensures the sediment-water column exchanges of vital oxygen gas and nutrients flux that are important for the ecosystem's production (McIntyre et al., 1996; Piccard et al., 2010). Therefore, studies have been carried out to obtain more knowledge on the relationship between both sediment resuspension and deposition on tidal flats with wave (Arfi et al., 1994; Booth et al., 2000; Green, 2011) and tidal (Arfi et al., 1994; French et al., 2009) activities.

1.3 Distribution of MPB on tidal flats

Studies on the distribution of MPB normally discuss their variability at both spatial and temporal scales. Both distributions are crucial to provide information on MPB dynamics in the ecosystems they live in, for instance the shallow coastal lagoons, mud flats and finally the vegetated salt marshes. Numerous studies have been done to investigate their distribution in respect to their functions in the ecosystem.

Facca et al. (2002) suggested that the distribution of MPB in the sediment is mainly dependent on sampling site features, in particular on physical and chemical properties of sediment, specifically phosphate and nitrate concentrations (Thornton et al. 2002 & Yamaguchi et al., 2007) as well as light availability (Cibic et al., 2007). However, contrarily, some researchers suggested that MPB distribution and occurrence was statistically proven not to be significantly related to both nutrients and light availability. For instance, Du et al. (2009) found the distribution in MPB biomass was not significantly related to nutrients and light intensity in the Nakdong estuary, Thailand. Such contradictory findings must be due to the fact that MPB distribution is obviously controlled by the type and property of the sediment, thus different results were found at different places. A previous study done by Delgado (1987) found the effect of grain size on the occurrence and distribution of MPB. The study discussed that MPB are abundant in clay soils or silt. A more recent work by Du et al. (2009) revealed that MPB biomass was positively related to mud and very fine sand and negatively related to fine and medium grained sediment. High nutrient concentration and less physical disturbance must be responsible to cause the finding of Du et al. (2009).

When Cartaxana et al. (2006) did a comparative study on MPB distribution in muddy and sandy intertidal sediment, they found more Chl *a* was recorded in muddy sediment with the concentration of 77 $\mu\text{g g}^{-1}$ compared to only 21 $\mu\text{g g}^{-1}$ in sandy sediment. Higher water content in muddy sediment makes it more conducive to be inhabited by MPB. This is due to the fact that the mud must have higher water content (70 % water component) compared to sandy

sediment (28 % water component) (Perkins et al., 2003). Perkins et al. (2003) suggested that wetter sediment is more favourable for cell nutrient supply and gas exchange. An earlier study by Barranguet et al. (1997) found that motile diatoms vertically migrate downwards the sediments towards shaded area, as response to ensure protection from desiccation. Nevertheless, the study also suggested that the movement of diatoms towards deeper and wetter area facilitates access to nutrients and organic and inorganic carbon in the sediment. McKew et al. (2011) found further evidence for the downwards movement of diatom cells towards the wetter sediment below. Under stimulated desiccation, they found that the movement towards wetter sediment was exhibited by the cells even at the earlier stages of desiccation.

Spatially, MPB or benthic microalgae micro-vertically migrate upward to the sediment surface during low tide in daylight, then move downward as the immersing high tide returns (McIntyre et al., 1996 & Smith & Underwood, 1998). Blanchard et al., (2001) suggested MPB normally migrate in the uppermost mm of sediment during tidal exposure. MPB biomass is found in high concentrations in the top 1 mm of sediment and can be sampled within the top 0.2 mm during daytime (de Brouwer & Stal, 2001). Most researches mentioned the movement of MPB in mud sediment in distance of mm. However, Cartaxana et al. (2006) suggested that the vertical distribution study in muddy sediment is better to be expressed in μm instead of in mm. Since the MPB can migrate to as little as 5 μm within the sediment. Consalvey et al. (2004), in their investigation to study upward movement of benthic diatom further supported this by mentioning that MPB also do vertical movement within the biofilm.

Vertical distribution of MPB within sediment is strongly correlated with light intensity. Though light intensity sometimes shows a non-significant relation, it is frequently a positive relationship except during high light intensity when MPB can show a photophobic response. Serôdio et al. (2006) determined the photo-response by MPB surface biomass on light intensity and found MPB showed positive photo-response to light intensity below $100 \mu\text{mol m}^{-2} \text{s}^{-1}$ and showed photo-protection or photophobic response at light intensity over $250 \mu\text{mol m}^{-2} \text{s}^{-1}$. A

more detailed investigation on diatom response towards light intensity (in terms of photon flux) was carried out by McLachlan et al. (2009) on two diatom species, *Navicula permunita* and *Cylindrotheca closterium*. They found that motile diatoms demonstrated a complex response to not only the intensity or quantity of the light but also the quality of the light. This potentially further supported the MPB variability and dynamic on an intertidal flat across temporal, such as seasonal (Montani et al., 2003; Scholz & Liebezeit, 2012), monthly (Pan et al., 2013; Woelfel et al., 2007), daily (G. Du et al., 2009; Kwon et al., 2012) and hourly scales (Smith & Underwood 1998; Du et al. 2010). However, as mentioned, the type and grain size of the sediment is actually the main factor to control the distribution as well controlling the light penetration into the sediment, hence, affecting the MPB distribution.

Most studies on MPB spatial distribution often focus on vertical distribution within the sediment with less information on their horizontal distribution. As important as vertical distribution, the horizontal distribution is also essential to provide information not only on biomass, composition and diversity of MPB but also the relationships between MPB with nutrients and physical parameters. Vertical distribution of MPB strongly relates with the property of the sediment. Whereas, the study on MPB horizontal distribution is more relevant for detail on how MPB relates with both physical and chemical parameters. For instance, Ribeiro et al. (2013) did a horizontal study in the Tagus estuary, Portugal, to determine the MPB species variation along built transects that run perpendicular to the shore which covered a different types of sediment. And they successfully obtained knowledge on how MPB distribution varies in different sediment profile in each of the stations. They found that the species community in sandy were more diverse compared to muddy area with diversity indices (H') of 3.2 and 1.9 respectively. More attention has been given to the large spatial scale studies that normally cover up to kilometres horizontal in distance (Guarini et al., 1998; van der Wal et al. 2010). However, high levels of spatial patchiness and temporal variability is a typical feature of MPB (Spilmont et al. 2011; Weerman et al. 2012), and therefore, an understanding of the relative

contribution of either micro or macro spatial variability in MPB biomass are important in understanding the ecology of MPB within intertidal flats.

As important as spatial, the temporal distribution is also essential in contributing knowledge on the relationship of MPB biomass and species composition with their environmental as well biological factors. The temporal studies potentially have close relation to the weather condition of the study sites. Lots of information on how climate change could alter the composition and distribution of MPB (van der Wal et al., 2010; Nedwell et al., 2016) at study sites can be obtained.

In investigating the MPB temporal distribution, the main topics that are normally discussed are on the MPB occurrence and distribution between months (Easley et al., 2005), seasons (Cibic et al., 2007; Facca et al., 2002; Koh et al., 2007) on hourly basis (Kwon et al., 2012) and also between tidal variation (Cibic et al., 2007; Smith & Underwood, 1998). Most attention on MPB temporal distribution studies has been given to large temporal scale (Benyoucef et al., 2013; Montani et al., 2003), neglecting the fact that the distribution of MPB can easily change even at micro temporal scale period (Koh et al., 2007). There are physical parameters that can change in a short-term timescale (Koh et al., 2007). Therefore, high frequency short time scale sampling on MPB is also vital and must not be ignored in carrying out studies on the distribution (Kwon et al., 2012). Easley et al. (2005) however found that the high frequency short term variations in physical parameters (light and wind speed) that strongly affect the MPB, makes it hard to use the short term data to predict the seasonal pattern above such "background noise". Nevertheless, both short and long time scales are still vital and able to produce more significant and informative result on MPB occurrence and their relation with environmental changes.

An example of investigation was done by Koh et al. (2007) on MPB distribution in both short (less than an hour, 10-30 minutes) and long term time scale (seasonally). They found a significant net increase in within-day biomass pattern in winter but not in other seasons. In addition, they reported that physical parameters such as current and wind-induced waves had a

significant negative influenced on the short time dynamic of intertidal mud and also benthic diatom on the order of minutes to hours. This work attested that by incorporating the high frequency sampling and large temporal scales, more understanding on the ecology of MPB across the ecosystem can be unveiled. In addition, given the repeated and continuous sediment-water column exchanges of MPB that happens on an intertidal flat at daily basis, it would be necessary for investigations of MPB resuspension or benthic-pelagic coupling to be done over short temporal scale (Koh et al., 2006; Kwon et al., 2012).

Tidal range is an important factor that physically controls the occurrence and variability of microorganisms such as MPB on an intertidal flat. Tidal movement results in the exposure of intertidal system to the air at low tide and to the estuarine water during immersion (Fonseca et al., 2013). These changes may responsible to significantly control the MPB biomass on an intertidal flat. There are some studies reported on the negative effect of tidal range with the MPB variability on sediment surface across an intertidal flat (Koh et al. 2006; Koh et al. 2007; Kwon et al. 2012). Although these studies found the significant negative relationship between MPB biomass with the tidal range (in terms of neap-spring tidal cycle), their studies did not incorporate the information on the diversity of the MPB. As it significantly influences the MPB biomass, the tidal range must potentially influence the species composition and species richness of the MPB. However, there is no work published specifically discussing the relationship between MPB species diversity with the tidal range. Research by Underwood (1994) on changes in MPB diversity towards the low water mark stations in the Severn Estuary, UK, could be related to the effect of tidal range on the MPB species and diversity. Because the upper shore and the lower shore areas on the intertidal flat as stated in Underwood (1994) must have been affected at different strength by the tidal range (Le Hir et al., 2000).

The salt marshes in the North-west Europe that occur above the level of mean high water of neap tides only are covered with water during some spring tides (French and Stoddart, 1992). Tidal range, in terms of the high spring tides has a strong positive effect on the marsh soil condition (Xin et al., 2013), which is able to stimulate the MPB biomass on the area (Aspden

et al., 2004). Paterson (1986) found that water content of the sediment affects diatom locomotion. He suggested that the drying of sediment inhibits migratory behaviour possibly due to the drying of EPS layer. The increased sediment water content on salt marshes due to high tide cover might initiate the growth of MPB on this high area of salt marshes (McKew et al., 2011). However, contrarily to its contribution to MPB on the salt marsh, tidal ranges was reported to have negative relation in MPB wash away or resuspension phenomenon on the tidal flats (De Jonge & Van Beusekom, 1995; Hanlon et al., 2006; Kwon et al., 2012; Murphy et al., 2009). Hanlon et al. (2006) found tidal cover over 90 minutes on mud flats significantly decreased Chl *a* content from sediment. The percentage of the decrease was different according to sampling months, which mainly occurs within the top 2 mm depth sediment slice. Tidal range is undoubtedly an important factor controlling the MPB biomass variability and potentially the MPB diversity as well. Kwon et al. (2012) suggested that variations in tide-dependent production might contribute to the characteristics of MPB, and therefore should be considered when estimating long-term dynamic of MPB production on an intertidal flat. The different effect of tidal ranges on MPB at different area across tidal flats makes it interesting to be unveiled and discussed.

Climate change that may be resulting in hotter weather and more frequent storms (Jackson et al., 2010) showed to not only affect the intertidal flat ecosystem (Aspden et al., 2004) but also their associated microorganisms, such as MPB. Together with tidal range, storms can sometimes shows positive (Fonseca et al., 2013) and negative (Reiss et al., 2007) impacts on MPB biomass on tidal flats. Storms limit the deposition of sediment and organic matter by promoting resuspension of sediment and associated MPB (Underwood, 1994). This phenomenon benefits the water column food chain through the resuspension of the macrofauna and benthic bacterial of the flats (Facca et al., 2002; Reiss et al., 2006; Ubertini et al., 2012). Storm that are associated with high wind speeds and increased rainfall are believed to increase the resuspension or wash away effect on MPB (Garstecki et al., 2002; De Brouwer et al., 2003). However, there are also studies that showed positive correlation between the storm and MPB

biomass. For instance, Costa et al. (2002) concluded that sediment dynamics promoted by runoff due to heavy rain, seem to drive factors that positively influence the abiotic parameters and also the biological communities in estuarine and lagoon of Southwest Coast of Portugal. They also suggested that MPB biomass peaks were strongly dependent on the input of terrestrial nutrients from different origin, such as cattle-breeding or agriculture activities into intertidal flat.

1.4 Benthic-pelagic coupling of MPB

In studying MPB resuspension, knowledge on benthic-water column distribution of MPB is essential and has been ignored. For decades, research attention has only been given to the role of MPB on the sediment surface (Mitbavkar & Anil, 2006; Du et al. 2010) and MPB response to both physical and chemical factors (Blanchard et al.,1997; Perkins et al., 2001), neglecting their role in the water column when resuspended. Though they are known as microphytobenthos, and the term suggests that they are confined in sediment (De Jonge & Van Beusekom, 1995), MPB naturally play vital role in coastal phytoplankton dynamics. Their resuspension is also a natural part of this system (Facca et al., 2002). Therefore it is important to quantify and understand the whole picture of this phenomenon.

Brito et al. (2012) carried out a study to investigate on how resuspension of MPB influenced the dynamic of phytoplankton in respect of tidal variation and wind activities. It was suggested in the study that MPB resuspension from the sediment surface would have a significant positive impact on phytoplankton in water column especially in shallow water and also in the water channel (outside of the tidal flat). They also reported a non-significant correlation between phytoplankton biomass in the water column and the adjacent pelagic ecosystem. This finding further supported the idea of a significant contribution of MPB to

phytoplankton biomass in both the shallow water and in coastal ecosystems (Sahan et al., 2007).

Facca et al. (2002) studied the movement of MPB from sediment into water column due to increased sediment fluxes on Venice Lagoon, Italy. In the study, they mentioned that out of 166 identified diatoms species, 27 of them were recorded in both sediment (in tidal flat) and water column (outside the tidal flat). Species such as *Gyrosigma balticum*, *Pleurosigma distortum* and *Surirella ovata* were the most significant species inhabiting the water column and sediment. In addition, as much as planktonic diatoms, there were some MPB taxa for instance *Amphora*, *Cocconeis*, *Navicula*, *Nitzschia*, *Pleurosigma* and *Thalassiosira* that were recorded to be more abundant in the water column than the on the sediment surface. The finding mentioned in this study is very much similar to the study done by Brito et al. (2012), however with more details on the genus and the species of phytoplankton and MPB those recorded on the sediment surface, in the water column or both. Studies on the benthic-pelagic and benthic-water column have documented the connection between MPB on the tidal flats' sediment surfaces with the water column and pelagic ecosystems. However, the connection must firstly start with the sediment-water column exchanges or resuspension of MPB on the tidal flat.

1.5 Resuspension of MPB

Wash away activity that actively transports sediment between tidal flat and water column (also known as resuspension of the sediment) is an important phenomenon in sedimentology (Green, 2011). Sediment resuspension or sediment-water column exchange affects the MPB distribution patterns not only on tidal flats but also in the water column. Gabrielson & Lukatelich (1985) in their study on wind sediment resuspension in Peel Harvey estuary reported that an increased in Chl *a* concentration in water column is related to resuspension activity. They found that there was actively photosynthesizing microorganisms which were the MPB, transported

along with sediment during the resuspension event. Study on resuspension should incorporate investigation on sediment-water column exchanges (De Jonge & Van Beusekom 1995; Facca et al. 2002; Koh et al. 2006) and the benthic-pelagic coupling of MPB and also must include the information on the movement of MPB across the intertidal flat.

Movement of sediment and MPB between tidal flats and water column are controlled by a complex set of factors that interact direct or indirectly (Ubertini et al., 2012). De Jonge & Van Beusekom (1995) suggested that wind-induced waves are responsible in the movement of sediment between the water channel, water column and the mudflat. In addition, they also concluded that there is no fixed or actual threshold for optimum wind speeds to allow resuspension to happen. Instead, the saturation level for sediment resuspension at the study sites happened when all mobile sediment was suspended from the sediment surface. The study also reported that the effective wind threshold at the study site, the tidal flats of Ems estuary is always above 3 m s^{-1} and below 13 m s^{-1} .

Earlier investigations done by Ducker (1982) were also reported in De Jonge & Van Beusekom (1995). Ducker (1985) reported a sharp increase in suspended matter for a wind speed more than 13 m s^{-1} to 20 m s^{-1} , which is higher than their strongest recorded effective maximum wind speed of 13 m s^{-1} . Both findings showed that the effective wind speed potentially varies spatially at different areas (fetch) on an intertidal flat and also across temporal scales. Easley et al. (2005) also reported that it was the wind-induced wave dominated by fetch rather than the wind speed that was the major factor in controlling MPB resuspension in Breach Inlet, South Carolina, USA. In addition, the different findings between both works can also be attributed to the temporal variability of other meteorological and environmental factors.

More recently, Green (2011) investigated the effect of small waves on resuspension of sediment on Tamaki estuary and concluded that a very small (height < 10 cm), short period (1.0 – 1.8 second) waves associated with light winds are able to resuspend the sediment bed efficiently. The information in Green's study can be taken into account in studying the MPB resuspension by using the reported knowledge on the response of sediment towards the

conditions of the waves. Nevertheless, the study by Green (2011) also proved that the type of waves needed to trigger resuspension and rate of sediment resuspension on intertidal flats varied according to the location of sediment of the flats. For instance, at lower intertidal flat (site adjacent to water column), he found that waves associated with stronger, infrequent winds dominate the resuspension activity and were only able to resuspend 5 % of sediment during inundation. Contrarily on the top of intertidal flat (site adjacent to intertidal bank), waves were able to resuspend about 30 % sediment during inundation times that associated with waves associated with lighter and frequent winds.

Despite studies suggesting that both waves and wind velocity are the main factors to initiate resuspension of MPB and sediment, Ubertini et al. (2012) showed results which relates resuspension of MPB with grazing. MPB which comprised of diatoms secrete extracellular polymeric substance (EPS) to stabilize the sediment they live in (Underwood et al., 1995). The EPS are able to armour MPB cells and to minimize the effect of MPB resuspension. Ubertini et al. (2012) showed that active grazing activity by *Cerastoderma edule* (common cockle) did have negative effect on MPB occurrence by means of bioturbation. The low MPB occurrence decreases EPS secretion, therefore leads to biofilms instability which makes the sediment prone to erosion thus enhancing resuspension to happen. Nonetheless, the location of study sites in Bay des Veys that geographically protected from wind effect by the Cotentin Peninsular may responsible to minimise the effect of the wind speed on MPB and sediment resuspension at study sites (Ubertini et al., 2012).

Ubertini et al. (2012) reported that the factors that control the MPB and sediment resuspension vary according to annual season and weather changes (Koh et al., 2006; Ubertini et al., 2012; Orvain et al., 2014). Biologically, they found the increased in mollusc biomass activity in summer drastically doubled the increased in resuspension of MPB. Grazing by mollusc markedly increase the water turbidity due to sediment resuspension and enhances the disruption of benthic micro-layer due to low MPB on the sediment surfaces. The lower MPB on

the sediment surfaces promotes the resuspension or the sediment-water column exchanges of MPB.

1.6 Aims, objectives and hypotheses

Climate change such as global warming and the rise of the sea level that can disrupt the mud flat and salt marsh systems (Aspden et al., 2004) makes it more crucial to understand the way this systems form and work as the major 'ecosystem service'. As an associated part of the Coastal Biodiversity and Ecosystem Services Sustainability (CBESS) project, this study is important for better understanding on MPB in both mud flat and salt marsh zones, which is one of crucial elements to maintain the health of UK's coastline. The importance of MPB, for instance, as the main primary producer and their ability to retain the sediment to reduce the effect of erosion on the flats are the main reasons to increase understanding of their dynamics and occurrence in this ecosystem. Studies on the distribution and abundance of MPB have been conducted in micro and macro spatial scales all around the world across a variety of temporal scales. There are many conflicting studies that do not agree on the major findings, which possibly are attributed to the location of study sites, latitude and weather conditions.

This study specifically was done on a range of spatial scale over both large (month and seasonal) and small temporal (daily changes across tidal cycle) scales. With a dedicated focus on a small study area, the aim of this study was to investigate both spatial and temporal variability of MPB across different tidal cycles. The study also aimed to characterize the direct or indirect effect of weather-related abiotic factors on the MPB variability. Finally, this study set out to investigate the potential of sediment-water column exchanges (resuspension) of MPB in contributing to the spatial and temporal variability of MPB linked to the weather-related abiotic factors. The aims will be achieved by following sets of objective which are;

A. To characterise the distribution of MPB biomass across the tidal flat on three different chosen zones; mud flat, the transition zone and the salt marsh, across a transect from mean to low water to mean high water spring tide level.

Hypotheses (Table 1.1);

1. There is higher benthic Chl *a*, extracellular polymeric substance (EPS) and cells composition on the mud flat and the transition zone than on the salt marsh. The highest MPB biomass will be recorded on the transition zone.
2. There is higher MPB - diatom species richness and diversity on the mud flat and the transition zone than on the salt marsh.
3. There is high species similarity between mud flat and transition zone.
4. Species composition on the mud flat comprises of a more diverse community with higher occurrence of centric diatoms than on the transition zone.
5. Lower carbohydrate : Chl *a* ratios will be presented on both mud flat and transition zones than on salt marsh.

B. To characterise MPB distribution over temporal scales, the months, seasons and days across neap-spring-neap tidal cycle.

Hypotheses;

1. The highest benthic Chl *a* variability is between months or seasons followed by days and tidal types (spring and neap).
2. The highest benthic Chl *a* and species diversity are in summer month at all sites or zones.
3. The lowest benthic Chl *a* and species diversity are in colder (autumn and spring) months.
4. There is higher benthic Chl *a* in spring tide than in neap tide at all of the zones across the tidal flat.
5. Benthic Chl *a* and species richness on the salt marsh are higher during the spring tide than in the neap tide.

6. There is higher variability in species composition between months and seasons than at shorter temporal scales on all zones.

C. To determine the relationship between MPB biomass distribution with weather-related abiotic factors (mean wind speed, periods of sunshine, amount of rainfall and tidal range).

Hypotheses;

1. There will be different correlation strength and magnitude in the relationship between the dependent (biomass) variables and the abiotic factors in different temporal and spatial scales.
2. MPB biomass is positively correlated with longer periods of 'sun hours' on all the zones.
3. MPB biomass is negatively correlated with mean wind speed and amount of rainfall.

D. To investigate whether the horizontal movement of MPB between zones happens across the intertidal flat during immersion.

Hypotheses (Table 1.1);

1. There is higher movement of MPB from transition zone onto the salt marsh than from mud flat onto the salt marsh.
2. Mud flat and transition zone share high MPB species (overlapped species).

E. To determine the movement of sediment (suspended sediment) and its associated MPB (suspended Chl *a*, suspended species) from sediment surface into the water column.

Hypotheses (Table 1.1);

1. Sediment is being washed away from sediment surface during tidal immersion on all zones.
2. Spring tides have higher suspended sediment load with its associated MPB (wash away) than in neap tides.

F. To identify the significant abiotic factors those control the movement of sediment and its associated MPB.

Hypotheses (Table 1.1);

1. MPB in terms of benthic Chl *a*, colloidal carbohydrate (CC) and EPS on the sediment surface can lower the suspended sediment and suspended Chl *a* concentration as a result of biostabilisation.
2. Wind speed and tidal height are the important factors that positively control the suspended materials.

Table 1.1 : Hypotheses and the chapter in which they were adressed

Hypotheses (page 15-18)	Chapter
A1	3 and 4
A2	4 and 5
A3	4
A4	4
A5	3
B1	3
B2	3 and 4
B3	3 and 4
B4	3
B5	3 and 4
B6	4
C1	3
C2	3 and 5
C3	3 and 5
D1	5
D2	4 and 5
E1	5
E2	5
F1	5 and 6
F2	5 and 6

1.7 Thesis outline

Chapter 2 describes the study site, general sampling strategies and also general methodologies that were involved in this PhD study.

Chapter 3 presents and discusses the major data on MPB distribution including a) spatial distribution of MPB at the study site, b) temporal distribution of MPB at study site and c) correlations between MPB biomass proxies with the chosen weather-related abiotic factors. The findings that discussed in this chapter are important in formulating the hypothesis of more specific findings and discussions in the following chapters 4, 5 and 6.

Chapter 4 discusses the issue of high MPB biomass variability that was observed. Relationships between the Chl *a* concentration with MPB assemblage's diversity (the evenness and the species richness) are discussed in this chapter. The preliminary findings for this Chapter 4 have been presented in oral at the European Phycological Conference in August 2015 in London.

Chapter 5 discusses the sediment-water column exchanges of MPB (MPB resuspension) at the study site. This chapter presents the spatial dynamics of both suspended sediment and suspended biomass (suspended Chl *a* and suspended cells). Weather-related abiotic factors that control the MPB resuspension occasion are also described in this chapter. Specific attention is given to the relationship between MPB resuspension with MPB spatial and temporal variability. Finally, species composition data is used to verify the sediment-water column exchanges of MPB across the intertidal flat. The preliminary findings for this chapter have been orally presented at the Aquatic Sciences and Limnological (ASLO) Meeting in February 2015 in Granada, Spain.

Chapter 6 focuses on the details of the extended study that was done (in situ) on horizontal movement of MPB across the intertidal flat. In Chapter 6, the movement of MPB between the mud flat and the salt marsh zones and on MPB sediment-water column exchanges

of MPB on the salt marsh zone during a period of very high spring tides (super-moon spring tides) is discussed.

The final chapter is **Chapter 7** which includes the general discussion.

CHAPTER 2

GENERAL MATERIALS AND METHODS

2.1 Study site

This study was carried out on Fingringhoe tidal flat (51.8343°N, 1.0011°E) which is located in the vicinity of Fingringhoe Wick reserve in the Colne estuary that lies on the east coast of Essex, UK (Figure 2.1, Plate 2.1 & 2.2). The tidal flat is owned and managed by the Essex Wildlife Trust, and is listed as an important ecological site in the Nature Conservation Review (Chesman et al., 2006). The average tidal range is ~ 4.5 m; therefore it is classed as mesotidal.

During spring tide emersion, the mud flat (Plate 2.1) is the first zone to be covered by tidal water, followed by the transition zone and the salt marsh (Plate 2.2). Only the mud flat and the transition zone are covered with tidal emersion during neap tide. Visual assessment of the sediment particle size showed the fine sediment of both the mud flat (Plate 2.3A) and the transition zone (Plate 2.3B), whereas, the salt marsh (Plate 2.3C) has larger sediment particle size than the other zones. *Hydrobia* sp. (Plate 2.4) is the common grazer observed on the sediment surface of the mud flat and the transition zone, especially in summer.

The Colne estuary has been reported as hypernutrified (Kocum et al., 2002; Ogilvie et al., 1997) and exhibits a strong nutrient gradients (Ogilvie et al., 1997; Underwood et al., 1998; Thornton et al., 2002). This hypernutrified condition could potentially cause the nutrients to be the non-limiting factors for MPB growth in the estuary. Therefore, nutrients were not measured in this study. Underwood (1997) reported the high salinity ranged between 16 – 210 in the salt marsh of the Colne estuary, Essex, while in the mud flat, the salinity only ranged between 22 – 39.

Although the Colne estuary is sheltered from strong winds, it can be severely affected by the easterly storms that also influences the wave height and tidal currents (Midlen & Ferreira,

n.d.). According to data from the Coastal Geomorphology Partnership (2000), the proportions of the salt marshes lost from Colne estuary from 1988-1998 was about 7 %.

Fingringhoe tidal flat was chosen due to its location in the Fingringhoe Nature Reserve. Therefore, it is less likely to be impacted by people and other domestic disturbances. It was also one of the NERC CBESS study sites (<http://www.nerc-bess.net/index.php/bess-projects-list/research-projects/42-cbess>). Therefore it is the best site in Colne estuary to investigate the relationship between the MPB and the weather-related abiotic factors.

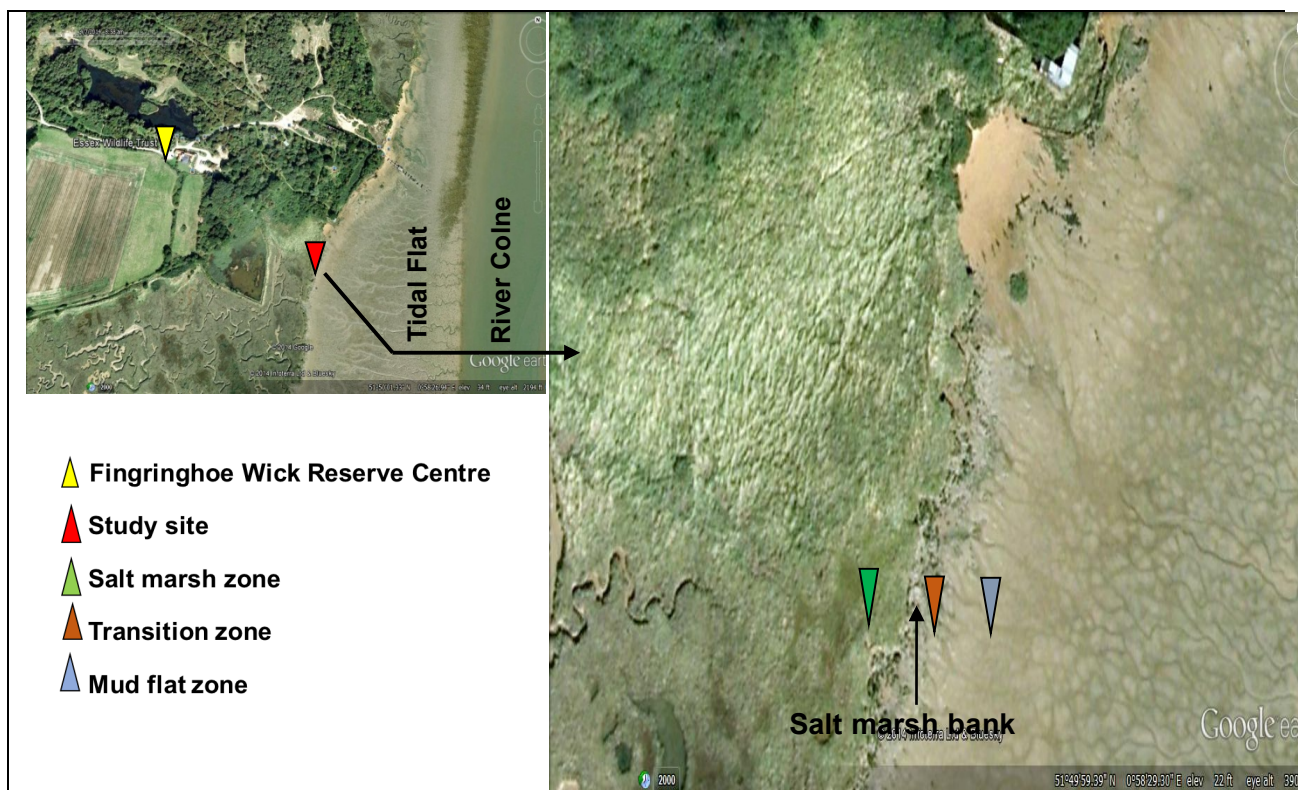


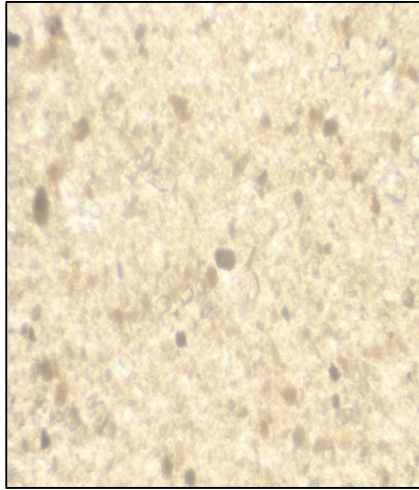
Figure 2.1: Satellite view of study site at Fingringhoe Intertidal Flat showing the three different zones, the mud flat, the transition zone and the salt marsh that > 5 m apart to each other.



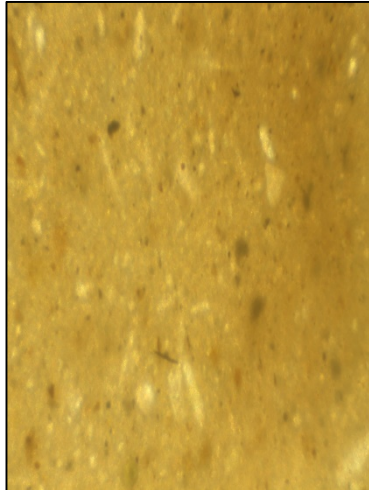
Plate 2.1: The tidal flat of Fingringhoe Wick Reserve during flooding tide.



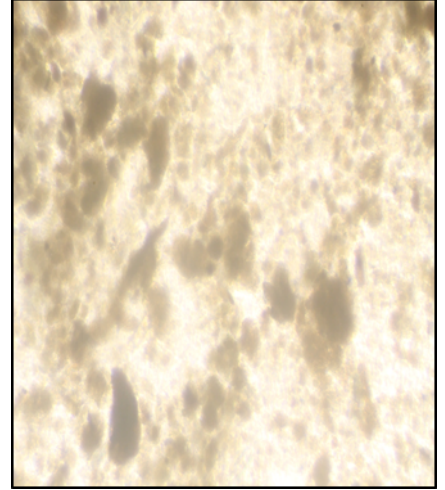
Plate 2.2: Salt marsh, the vegetated area Fingringhoe Wick Reserve tidal flat.



A. Mud flat



B. Transition zone



C. Salt marsh

Plate 2.3: Differences in the sediment particles size on the A. mud flat, the B. transition zone and the C. salt marsh.



Plate 2.4 : *Hydrobia* sp.

2.2 Sampling strategy

Benthic Chl *a*, CC, EPS and diatom cells number were determined at Fingringhoe intertidal flat in the Colne Estuary. The top 2 mm sediment surfaces were sampled from three different zones (the mud flat, the transition zone and the salt marsh) (Figure 2.2B). The zones were at > 5 m apart across the intertidal flat (Figure 2.2B). Triplicate ($n = 3$) minicores (area = 2.836 cm²) were used to obtain the sediment surface samples at fixed locations within 0.5 m X 0.5 m quadrats, at micro-scale < 0.5 m (Figure 2.2A). Eight quadrats were set up on each of the three zones at > 1 m apart (Figure 2.2B). The samplings were carried out at the largest temporal scale of the month ($n = 3$) in April 2013, July 2013 and October 2012. Within each month, sampling was done on seven days ($n = 7$) during neap (2 days in week 1), spring (3 days in week 2) and neap (2 days in week 3) tidal cycles (Figure 2.3). A total of (triplicate minicores (3) x scale > 1 m (8) x scale > 5 m (3) x days (7)) ($n = 504$) top 2 mm sediment samples were collected in each of the sampling month. Sediment samples on the salt marsh were obtained in between the vegetations.

In laboratory, each minicore was extruded so only the top 2 mm of the sample remained in the syringe. The lower portion of the sediment was discarded while the remaining sample was divided into two. Half of it was placed into 7 ml bijoux bottle for Chl *a*, extra polymeric substance (EPS) and CC analyses. Sediment samples for Chl *a*, CC and EPS analyses were freeze dried. The balance of the sediment was transferred into 15 ml falcon tube and was preserved using 0.5 % glutaraldehyde in 2.3 % NaCl for cells identification and cells count.

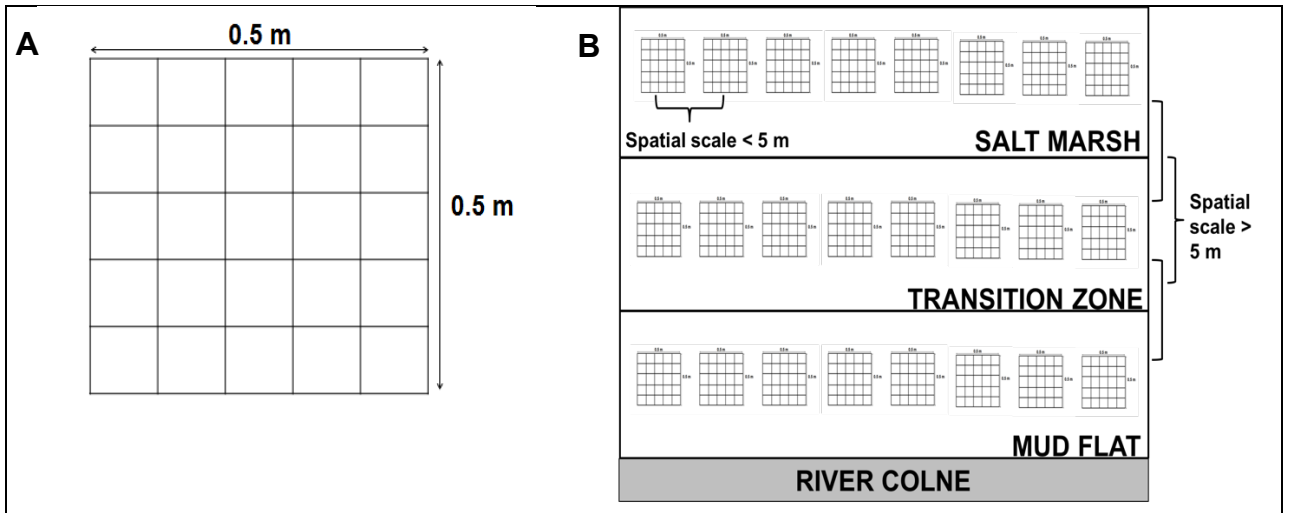


Figure 2.2: A) Illustration of the quadrat (0.5 x 0.5 m) in which triplicate top 2 mm sediment were obtained from fixed area using minicores. B) A total of eight quadrats were placed at scale < 5 m apart on each of the zones (spatial scale > 5 m) that located parallel to River Colne.

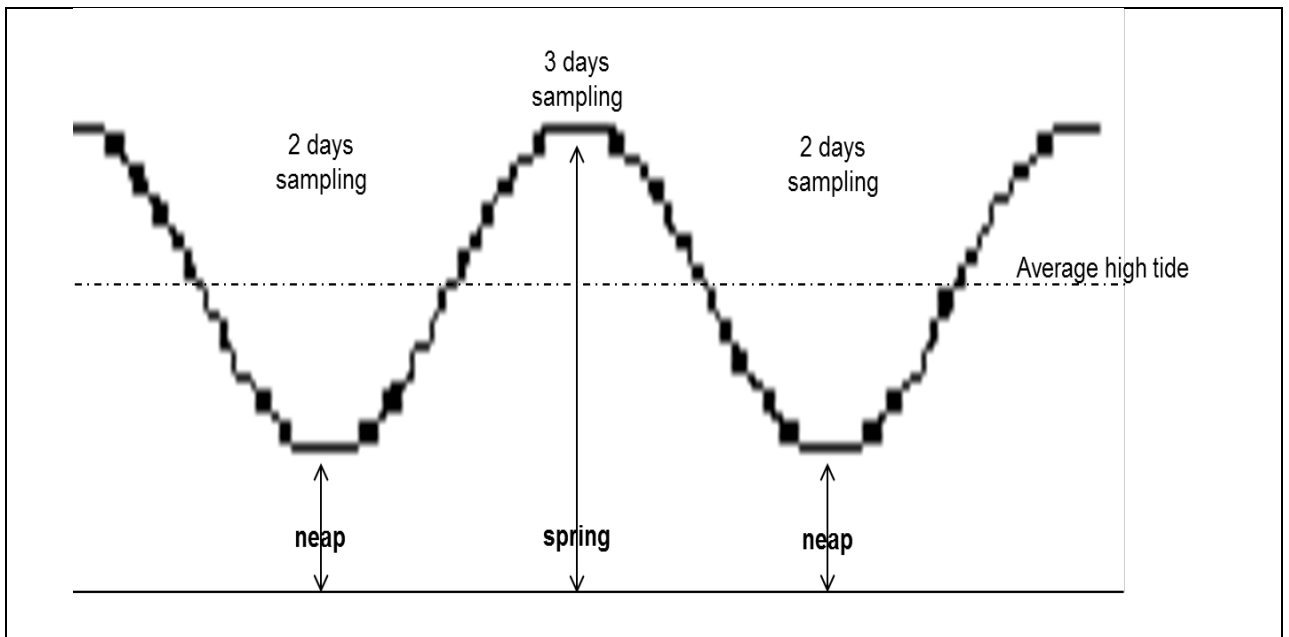


Figure 2.3: Temporal sampling in neap (two sampling days)-spring (three sampling days)-neap (two sampling days) tidal cycle, that were carried out in week 1, week 2 and week 3 of each sampling months, respectively.

2.3 Top 2 mm sediment Chl a analyses

Chl a was extracted from 100 mg lyophilised top 2 mm sediment in 4 ml 100 % buffered with MgCO₃-saturated methanol. After twenty four hours at 4°C in darkness, sediment sample and blank were centrifuged at 3650 g for fifteen minutes. Chl a content in supernatant was determined by spectrophotometry with absorbance reading at 665 nm and 750 nm (Lorenzen, 1967). Sediment sample was acidified using 10 % hydrochloric acid to correct for phaeopigment and the absorbance readings at both mentioned wavelengths were determined spectrophotometrically. Chl a content was expressed in µg Chl a per cm⁻² sediment (µg Chl a cm⁻²).

2.4 Top 2 mm CC and EPS analyses

CC and EPS concentrations were derived from the benthic dissolved organic material (DOM). Both the CC and EPS measured in this investigation were the water soluble (colloidal) fraction and no longer cell-associated carbohydrates.

A total weight of 200 mg lyophilised sediment was used to extract the water soluble carbohydrate or the CC from the sediment. Five ml of saline water (2.3 % NaCl) was added into the sediment before incubating it for thirty minutes at 20 °C. The incubated samples were centrifuged at 4760 g for fifteen minutes and 0.4 ml of the supernatant were collected and pipetted into boiling tube. Remaining supernatant from the incubated sediment was used for EPS analyses. Three ml of the supernatant was added into 7 ml ethanol (for 70 % v/v final concentration) to measure water soluble EPS fractionation. After twenty four hours incubation, the mixture was centrifuged at 4760 g for fifteen minutes. The supernatant that was contained with the ethanol was discarded as much as possible. While the precipitated EPS (pellet) was air dried and resuspended using 0.4 ml distilled water. Both the CC the EPS contents were measured spectrophotometrically using phenol-sulphuric assay (0.2 ml phenol and 1 ml

sulphuric acid were pipetted into boiling tube) at wavelength of 485 nm (Hanlon et al., 2006). Both contents in the top 2 mm sediment were expressed in μg glucose equivalents per cm^{-2} sediment (μg glucose equiv. cm^{-2}) using glucose (0 to $100 \mu\text{g ml}^{-1}$) as standard (Figure 2.4).

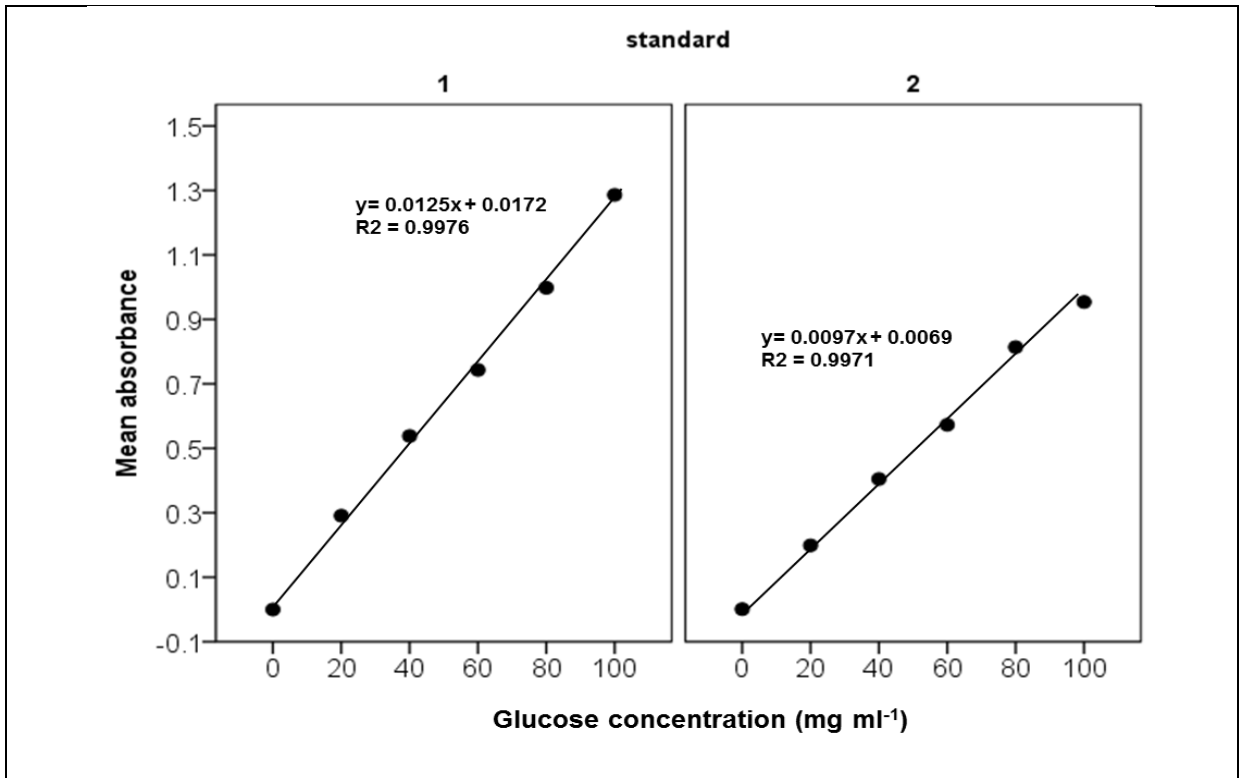


Figure 2.4: Two Carbohydrate calibrations that were used for CC and EPS analyses.

2.5 Diatom cells count and identification

Fresh materials were examined exactly after each sampling occasion showed that the samples mostly contained with diatom cells that were alive. The diatom taxa of the fresh materials were also proportional to the taxa in the fixed and oxidized materials.

Sample preserved in 0.5 % (v/v) glutaraldehyde in saline water (2.3 % NaCl) were centrifuged at 1570 g for fifteen minutes to separate the diatom cells from the glutaraldehyde. Excess glutaraldehyde (supernatant) was discarded using teat pipette. Five millilitres distilled water was added to the diatom cells and was agitated to mix. The sample was then cleaned

following an acid washing procedure for a permanent slide preparation mounted in naphrax solution (Underwood, 1994). Four hundred valves were identified and counted for each of the samples for mud flat and transition zones. Due to low numbers of valves observed in the permanent slides, only two hundred and fifty valves were counted on the salt marsh sample slides.

2.6 Environmental and meteorological factors

The daily data of weather-related abiotic factors; the rainfall and the periods of sun hours were obtained from Colchester Weather Site based in the Myland, Colchester, Essex, UK (<http://www.tijou.co.uk/weather/>). Both data for wind speed and wave height of Fingringhoe Tidal flat were courtesy of Dr. Tom Spencer and Ben Evans of University of Cambridge (CBESS consortium). Daily data of tidal variation were obtained from www.TideTimes.org.uk for Brightlingsea.

For the rainfall, the data that was used was the 'sum of rainfall' (mm), for three days, which includes the data of two days prior to sampling days plus on the sampling day. Period of sun hours of three days was used in the study and was expressed as 'sum of sun hours' (hour). The 'sum of sun hours' is the sum of period of sun hours data of; two days pre sampling day + on the sampling day. The average wind speed data for three days (two days before sampling day + on sampling day) was calculated and represents the 'mean wind speed' (m s^{-1}).

CHAPTER 3

MICROPHYTOBENTHOS (MPB) VARIABILITY AT MULTI SPATIO-TEMPORAL SCALES ACROSS AN INTERTIDAL FLAT

3.1 INTRODUCTION

Pronounced variability in MPB biomass has been reported at micro-spatial (Azovsky et al., 2004; Taylor et al., 2013), macro-spatial (Azovsky et al., 2004; Gottschalk et al., 2007), at short-term temporal (Koh et al., 2007; Orvain et al., 2014) and at long-term temporal (Wolfstein et al., 2000) scales. This high level of spatial patchiness and temporal variability is a typical feature of MPB (Spilmont et al., 2011; Weerman et al., 2012). Therefore, understanding the contribution of either micro or macro levels of spatial and temporal factors to variability in MPB biomass are important in investigating the ecology of MPB within intertidal flats.

Studies done on MPB ecology have often been focussed on single spatial and temporal scales, with the attention of most studies has been devoted to large spatio-temporal scales (Du et al., 2009; Murphy et al., 2009). A lack of multi-scale approaches in MPB spatio-temporal variability investigations may result a loss of key ecological information. MPB variability at micro-spatial scale ($< 1 \text{ m}^2$) is also as important as variability at larger scales. It is at this micro-scale ($< 1 \text{ m}^2$) where most of MPB ecologically relevant processes (Seuront & Leterme, 2006) take place. While at short term temporal scales, for instance at daily and hourly scales, the behaviour such as the micro-migration of MPB assemblages in response tidal variation (Koh et al., 2006) and also immersion and emersion periods (Herlory et al., 1998) can be observed more precisely than at broader temporal scale.

Work done by Azovsky et al. (2004) is one example of the studies done on MPB at multi spatial scale. Their study however was not solely done on MPB, but also on meiobenthos (harpacticoids) and microzoobenthos (ciliates). The work mostly investigated how the

organisms' body size affected their variability at the multi spatial scale (decimetres, meters and tens meters) and was carried out over daily temporal scale. Azovsky et al. (2004) reported that MPB species assemblages are distributed more varyly at spatial rather than at temporal scale and that MPB species community spatial variability increased sharply from decimetre to metre scale. They also found that microscopic organisms such as MPB, are distributed more heterogeneously at spatial scales than organisms with larger body size such as the meiobenthos. The study however did not take into account the abiotic factors that caused such heterogeneity at the spatial scale.

To date, there is still no published work exclusively investigating the MPB dynamics and ecology at simultaneous multiple-scales from the smallest micro-spatial patchiness to larger spatial scale and from short term to medium term temporal scales. Therefore, the main aim of this chapter was 1). to investigate multiple scales of spatial variability (at scale < 5 m and < 0.5 m) of not only chlorophyll *a* (Chl *a*) but also other biomass proxies which are colloidal carbohydrate (CC) and extracellular polymeric substance (EPS). The multi-spatial scales were observed across three different tidal zones (mud flat, transition zone and salt marsh) in the Colne estuary over daily, monthly and seasonal scales across the neap-spring-neap tidal cycle.

Tidal range during spring and neap tides has been reported to control the variability of the MPB on both the sediment surface and in the water column during immersion period (Koh et al., 2006). Brito et al., (2012) found that wind speed is the potential driver in the removal of MPB from the sediment surface and out of the intertidal flat into the lagoon during immersion. Effective wind speed that was associated with the wave activity was proven to significantly wash away the MPB from the MPB biofilm during immersion period (De Jonge & Van Beusekom, 1995). We hypothesized that MPB occurrence across the tidal range and wind induced wave variability is strongly related to the MPB biomass availability on the sediment surface before the immersion period. With respect to the rapid change of the world's climate that may increase the frequency of storms (Jackson et al., 2010), we also set out 2). to investigate the response of the MPB biomass proxies with the chosen weather-related abiotic factors; which were the 'period of

sun hours', and 'sum of rainfall' over preceding three days included the sampling day, and also the 'mean wind speed' across the neap-spring-neap tidal range.

Both weather-related abiotic factors the period of sun and sum of rainfall were hypothesized to control the MPB variability during emersion period. Longer periods of sun are expected to positively control the MPB biomass on sediment surface. Periods of illumination indirectly control the MPB biomass during immersion by enhancing more MPB production and stabilise the MPB biofilms during the preceding tidal emersion (Kwon et al., 2012). Frequent rainfall which causes higher sum of rainfall was hypothesized to wash away the MPB biomass on the sediment surface during emersion (Montani et al., 2003). Therefore, we hypothesized that increased rainfall and higher wind speed may result in less MPB biomass on the sediment surface during emersion period, which would have reduce the biostabilisation effect by MPB on the tidal flats.

I also hypothesized that the temporal variability in the measured weather-related abiotic factors will have different effect on the biofilm patches of different zones (the mud flat, the transition zone and the salt marsh). The Colne estuary that exhibits horizontal gradients of salinity and nutrients along the estuary (Ogilvie et al., 1997; Kocum et al., 2002), horizontally exposed to different tidal range level (Underwood, 1997) potentially comprises of different MPB community across the tidal flat. Therefore different effects of weather-related abiotic factors across different zones at the Colne estuary were expected. In addition, Taylor et al. (2013) reported that more than 30 % of the total variation in Chl a concentration in Colne estuary was attributed its variability at spatial scale within $< 1 \text{ m}^2$. Therefore it is hypothesized that the temporal variability in weather-related abiotic factors is also expected to have a different effect on each of the MPB biofilm patches of similar zones at both the $< 5 \text{ m}$ and 0.5 m spatial scales.

3.2 METHODOLOGY

3.2.1 SAMPLING STRATEGY

Benthic Chl *a*, CC, EPS and diatom cells were determined at Fingringhoe intertidal flat in the Colne Estuary. Top 2 mm sediment surface were sampled from three different zones (the mud flat, the transition zone and the salt marsh). The zones were at > 5 m apart across the tidal flat. On the salt marsh, the sediment cores were obtained from the sediment surfaces in between the salt marsh's vegetation. Triplicate ($n = 3$) minicores (area = 2.836 cm²) were used to obtain sediment surface samples at fixed location within 0.5 m X 0.5 m quadrats, at micro-scale < 0.5 m. Eight quadrats were set up on each of the three zones at > 1 m apart (The figures describing the quadrats and the zones are presented in chapter 2). The samplings were carried out over the highest temporal scale, the month ($n = 3$) in April 2013, July 2013 and October 2012. Each month, sampling was done on seven days ($n = 7$) during neap-spring-neap ($n = 2$) tidal cycle. The first two sampling days in neap tide was carried out in the first week of sampling followed by three days sampling in spring tide in week 2 and finally two more sampling days during neap tide in week 3.

A total of (triplicate minicores (3) x scale > 1 m (8) x scale > 5 m (3) x days (7)) $n = 504$ top 2 mm sediment samples were collected in each of sampling month. Sediment samples (top 2 mm) for Chl *a*, CC and EPS analyses were freeze dried and lyophilized. In laboratory, each minicore was extruded so only the top 2 mm of the sample remained in the syringe. Lower portion of the sediment was discarded while the remaining sample was divided into two. Half of it was placed into 7 ml bijoux bottle for Chl *a*, extracellular polymeric substance (EPS) and CC analyses. The other half was retained and preserved in 0.5 % (v/v) glutaraldehyde for cells count.

3.2.2 STATISTICAL ANALYSES

The basic units of replication were the triplicate minicores. One minicore sample was sampled from three 10 X 10 cm² regions within each of 0.5 x 0.5 m quadrat, here known as micro-spatial patchiness (spatial scale < 0.5 m). To estimate the contribution of each the temporal factors (day and month), the spatial scale < 5 m (quadrats) and the micro-spatial scale < 0.5 m (triplicate minicores), the Chl *a*, CC and EPS data were analysed separately using nested ANOVA in R package. Analysis of variance (ANOVA) with Tukey HSD test was performed on the overall data to investigate the spatial variability of the biomass proxies (the Chl *a*, CC and EPS) across the study site on the three different zones and across temporal daily and monthly scales on each of the zones using the R Package.

Principal component analyses (PCA) were performed log transformed data set ($\log_{10} n + 1$) of active variables (Chl *a*, CC and EPS concentrations and CC:Chl *a* and EPS:Chl *a* ratios) and the weather data as supplementary data (sum of rainfall (SOR), mean wind speed (MWS) and meteorological data (sum of sun and tidal range)) for all the three zones using the FactoMineR package in R. Individual scores of this PCA represents the physical state of the MPB biofilms. Analysis of variance (ANOVA) with Tukey HSD test was performed on the individual scores to investigate the daily and monthly pattern of the physical state of the biofilm across the study site on the three different zones. Function 'dimesc' in FactomineR was used to observe variables were significantly correlated to a certain principal component at $p < 0.05$.

Variability at spatial scale < 5 m were represented by calculating the value of standard error (SE) of the daily mean. The daily SE was used since the value was determined from the differences of data at the spatial scale < 5 m (between quadrats).

3.3 RESULTS

3.3.1 MPB biomass general spatial variability between the mud flat, transition zone and salt marsh

A combined data set from the three sampling months was used to investigate the spatial pattern of MPB biomass on the mud flat, the transition zone and the vegetated salt marsh at Fingringhoe tidal flat in the Colne estuary. There was a clear spatial variability in Chl *a* ($F_{5,1500} = 395.5$, $p < 0.001$) (Figure 3.1A) and carbohydrate concentrations (CC ($F_{5,1461} = 10.5$, $p < 0.001$) and EPS ($F_{5,1461} = 120.3$, $p < 0.001$)) (Figure 3.1B) in the top 2 mm microphytobenthic biofilm of the sediment. *Post hoc* analyses revealed no significant differences in Chl *a* and CC concentrations between the mud flat (Chl *a* = 8.8 ± 0.2 $\mu\text{g Chl } a \text{ cm}^{-2}$ and; CC = 350.8 ± 13.05 $\mu\text{g glucose equiv. cm}^{-2}$) and the transition zone (Chl *a* = 9.19 ± 0.25 $\mu\text{g Chl } a \text{ cm}^{-2}$ and; CC = 354.9 ± 13.6 $\mu\text{g glucose equiv. cm}^{-2}$) (Figure 3.1A (Chl *a*) & 3.1B (CC)). Both Chl *a* and CC contents on the mud flat and the transition zone however, were significantly higher than the concentration on the salt marsh (all at $p < 0.001$ except for CC on mud flat; at $p < 0.05$). EPS concentration on the salt marsh (211.7 ± 6.8 $\mu\text{g glucose equiv. cm}^{-2}$) was markedly greater than the transition zone ($p < 0.001$) and the mud flat ($p < 0.001$) (Figure 3.1B). The EPS concentration on the mud flat (119.8 ± 4.5 $\mu\text{g glucose equiv. cm}^{-2}$) and the transition zone (102.6 ± 4.2 $\mu\text{g glucose equiv. cm}^{-2}$) although displaying little variation was significantly different at $p < 0.05$ (Figure 3.1B).

The salt marsh was characterized by a low Chl *a* concentration (3.3 ± 0.1 $\mu\text{g Chl } a \text{ cm}^{-2}$) (Figure 3.1A), relatively high CC concentrations (319.1 ± 18.3 $\mu\text{g glucose equiv. cm}^{-2}$) (Figure 3.1B) and significantly high EPS concentrations (Figure 3.2B) than the other two zones. This was reflected by significantly high CC:Chl *a* and EPS:Chl *a* values of 276.1 ± 36.4 and 173.6 ± 29.1 , respectively (Figure 3.3). The ratios of CC:Chl *a* and EPS: Chl *a* were not significantly different between the mud flat and transition zone. Both average values were 39.4 ± 1.27 , 45.38 ± 4.24 and 13.97 ± 6.33 , 14.56 ± 1.46 $\mu\text{g glucose equiv. cm}^{-2}$, respectively (Figure 3.2).

The high Chl *a* concentration on both mud flat and transition zone was also reflected in their high CC concentrations (Spearman rank value of the correlation between Chl *a* and CC concentrations on the mud flat and the transition zone were $r = 0.714$ and $r = 0.667$ (both significant at $p < 0.001$)) in July 2013 (Figure 3.3). There was a reasonable mean percentage of EPS in colloidal extract of 34.1 % and 28.9 % on the mud flat and the transition zone, respectively (Figure 3.2). There was a relatively higher percentage of EPS in colloidal extract of 66.3 % (Figure 3.2) on the salt marsh, compared to the other two zones, and lack of any significant correlation of Chl *a* and CC on the salt marsh zone. The correlation between CC and Chl *a* on the mud flat and the transition zone although displayed significant strong correlation (Figure 3.3), showed to be non significant after certain Chl *a* threshold value (at about $10 \mu\text{g Chl } a \text{ cm}^{-2}$).

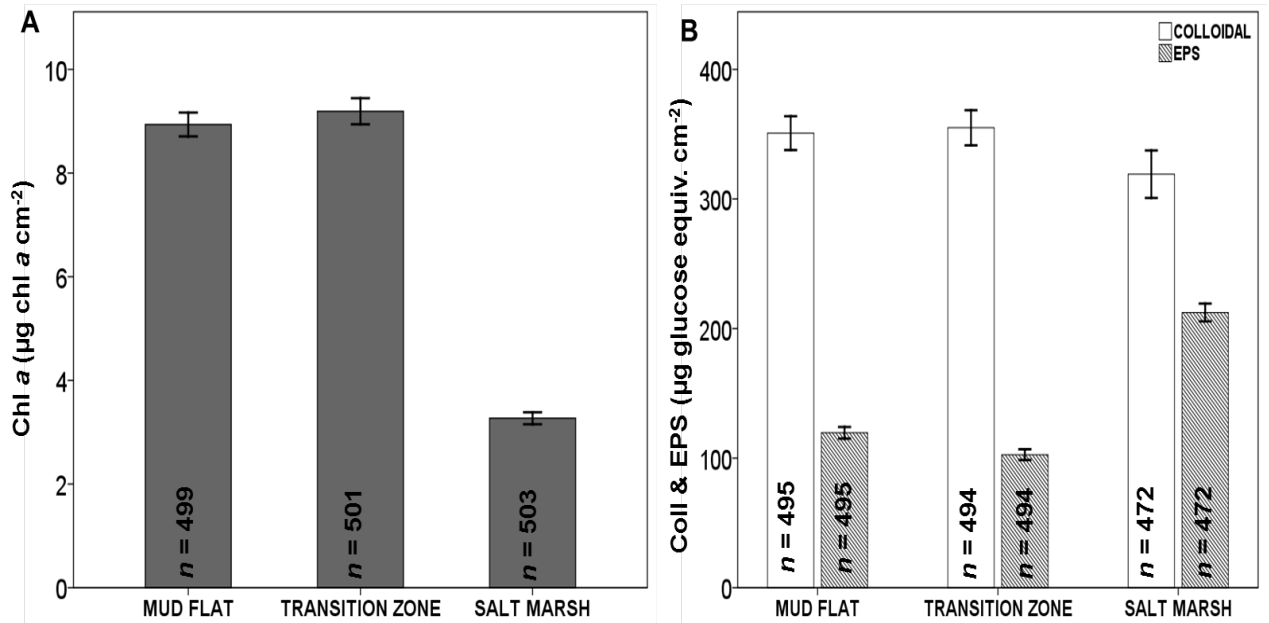


Figure 3.1: Variability in A) Chl a and B) colloidal carbohydrate (CC) and extracellular polymeric substance (EPS) in top 2 mm per cm^2 sediment surface in three zones across the intertidal flat, the mud flat, the transition zone and the salt marsh. The top 2 mm sediment surface was obtained using 2.836 cm^2 area minicore. Values are mean ± 1 SE. *n* value for each variable in the figure.

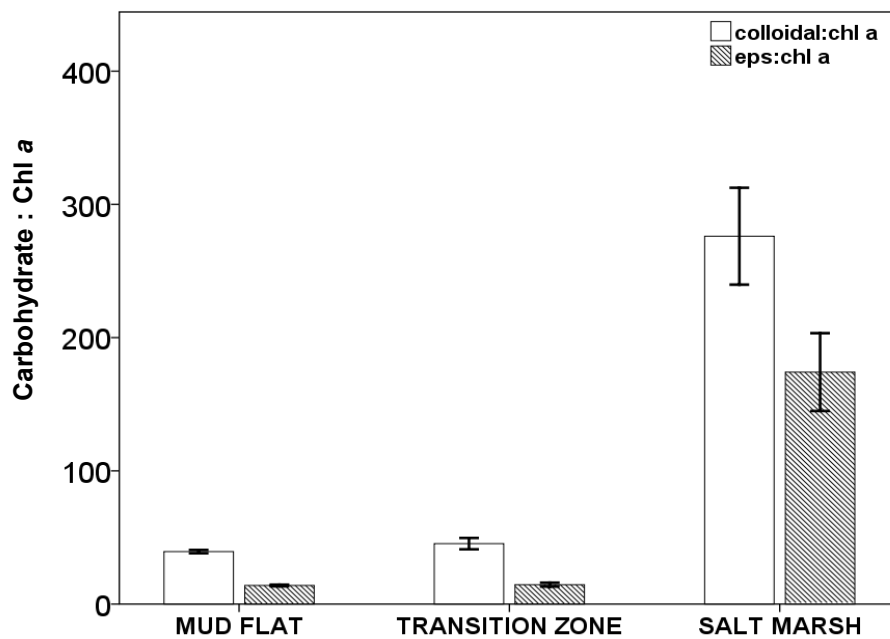


Figure 3.2: Spatial differences in the ratio of CC and EPS to Chl a across intertidal flat. Values are mean ± 1 SE, *n* = 504.

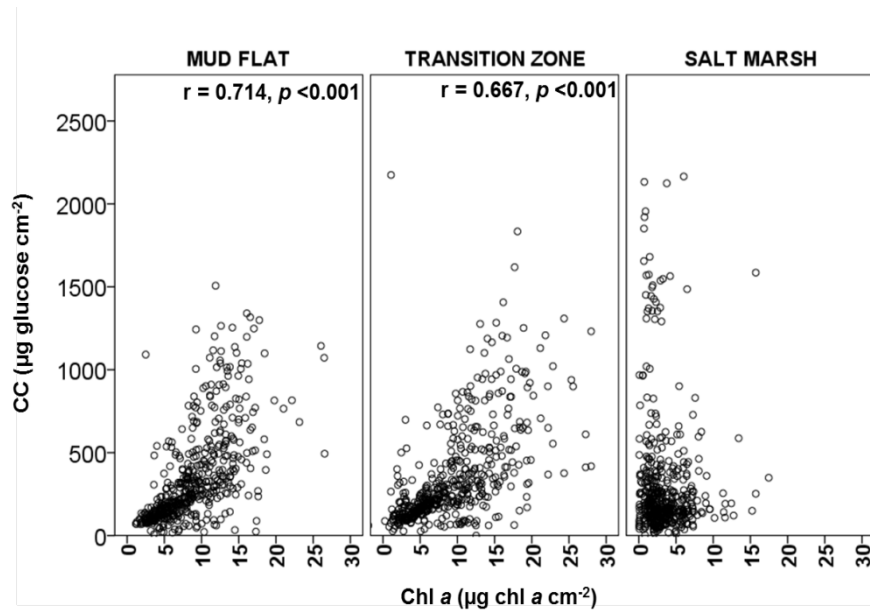


Figure 3.3: Relationship between Chl *a* and CC concentrations on the mud flat, the transition zone and the salt marsh. Note the significant correlation (Spearman correlation) on the mud flat and the transition zone. There was no significant correlation between both proxies on the salt marsh. Chl *a*, $n = 504$ (for all zones); CC, $n = 494$ (mud flat and transition) and $n = 472$ for the salt marsh. Overall Chl *a* and CC of July 2013 were used for this correlation analyses.

3.3.2 MPB biomass general temporal variability across intertidal flat

Monthly variability in the Chl *a*, CC and EPS concentrations in the top 2 mm sediment surface on the mud flat and the transition zone displayed similar pattern. All the biomass concentrations on both zones were the highest in July 2013 followed by the month of April and October 2013. In July, the mean Chl *a* concentration on the mud flat and the transition zone were 10.7 ± 0.3 and 11.9 ± 0.4 $\mu\text{g Chl } a \text{ cm}^{-2}$, respectively (Figure 3.4.1.A & 3.4.2.A, respectively). The highest Chl *a* value in July 2013 on both zones was concurrent with the zones' highest CC (mud flat; 538.7 ± 25.4 and transition; 535.2 ± 28.6 $\mu\text{g glucose equiv. cm}^{-2}$) and EPS (mud flat; 166.7 ± 7.5 and transition; 161.2 ± 7.8 $\mu\text{g glucose equiv. cm}^{-2}$) concentrations (Figure 3.4.1.B & 3.4.2.B). The lowest monthly mean of Chl *a* was in October 2013 with the recorded concentration below 6 $\mu\text{g Chl } a \text{ cm}^{-2}$ on both zones (Figure 3.4.1.A) and was concurrent with the lowest CC (mud flat; 166.7 ± 5.7 and transition; 183.6 ± 7.3 $\mu\text{g glucose equiv. cm}^{-2}$) and EPS (mud flat; 48.1 ± 1.6 and transition; 52.6 ± 2.1 $\mu\text{g glucose equiv. cm}^{-2}$) concentrations (Figure 3.4.1.B & 3.4.2.B).

In contrast to the other zones, the highest Chl *a* of 4.2 ± 0.2 $\mu\text{g Chl } a \text{ cm}^{-2}$ on the salt marsh was recorded in October 2013 (Figure 3.4.3.A). However, neither CC nor EPS were recorded as the highest in the month of October 2013. Both the highest CC and EPS concentrations on the salt marsh were in April 2013 (504.8 ± 42.3 $\mu\text{g glucose equiv. cm}^{-2}$) (Figure 3.4.3.B) and July 2013 (234 ± 13.4 $\mu\text{g glucose equiv. cm}^{-2}$) (Figure 3.4.3.B), respectively.

Chl *a* concentrations on the mud flat across seven days of sampling in April and July 2013 ranged between 8 to 12.5 $\mu\text{g Chl } a \text{ cm}^{-2}$ (Figure 3.4.1.A). The highest Chl *a* monthly mean was in July and were also reflected by the month's high CC and EPS concentration on three sampling days. With the CC concentration of 777.2 ± 80.0 , 741.6 ± 61.3 and 767.3 ± 72.6 $\mu\text{g glucose equiv. cm}^{-2}$ and EPS concentrations of 269.5 ± 23.8 , 227.7 ± 14.0 and 225.9 ± 20.1 μg

glucose equiv. cm^{-2} on the 3rd (neap), 10th (spring) and 11th (spring) July 2013, respectively (Figure 3.4.1.B).

Chl *a* concentration on the transition zone depicted a quite similar pattern with the mud flat. But the Chl *a* concentrations were higher on this zone compared to the mud flat, between 2 to 14.5 $\mu\text{g Chl a cm}^{-2}$, 10 to 13.5 $\mu\text{g Chl a cm}^{-2}$ and 4 to 6 $\mu\text{g Chl a cm}^{-2}$ in April, July and October 2013, respectively (Figure 3.4.2.B). The highest CC concentration was in July 2013 ($930.7 \pm 103.5 \mu\text{g glucose equiv. cm}^{-2}$) on the 3rd July 2013 (Figure 3.4.2.B). This was concurrent with Chl *a* concentration of $12.4 \pm 0.9 \mu\text{g Chl a cm}^{-2}$ (Figure 3.4.2.A), whereas, the lowest Chl *a* concentration was recorded on the 17th April with the value of $2.3 \pm 0.2 \mu\text{g Chl a cm}^{-2}$ (Figure 3.4.2.A) The lowest value coincided with relatively high CC of $277.7 \pm 31.2 \mu\text{g glucose cm}^{-2}$ and EPS of $110.7 \pm 19.6 \mu\text{g glucose equiv. cm}^{-2}$ (Figure 3.4.2.B).

Chl *a* across the seven days of sampling on the salt marsh in October 2013 were in a higher range than in the other two months which between 3.4 to 5.3 $\mu\text{g Chl a cm}^{-2}$ (Figure 3.4.3.A). The highest CC and EPS however were not recorded in October 2013, but on the 4th April for the CC ($940.6 \pm 125.9 \mu\text{g glucose equiv. cm}^{-2}$) and on the 5th April for the EPS ($369.9 \pm 27.1 \mu\text{g glucose equiv. cm}^{-2}$) (Figure 3.4.3.B).

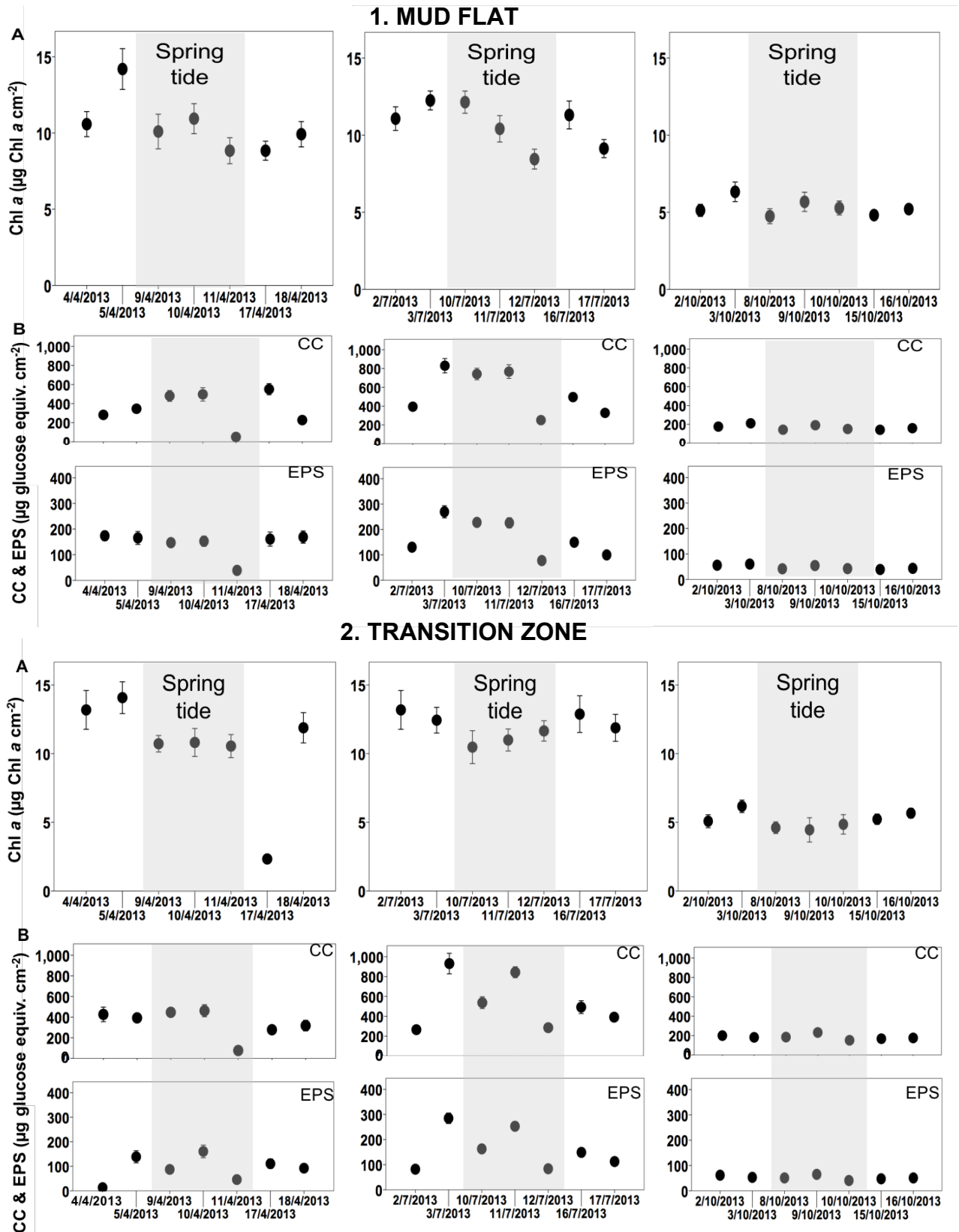


Figure 3.4: Temporal variability of A) Chl *a* and B) CC and EPS concentrations in the top 2 mm per cm² sediment on the; 1) mud flat and on the 2) transition zone in April, July and October 2013 across the neap-spring-neap tidal cycle. Values are mean \pm 1SE, $n = 24$. Shaded area represents spring tide while non shaded represents neap tide.

Continuation of figure

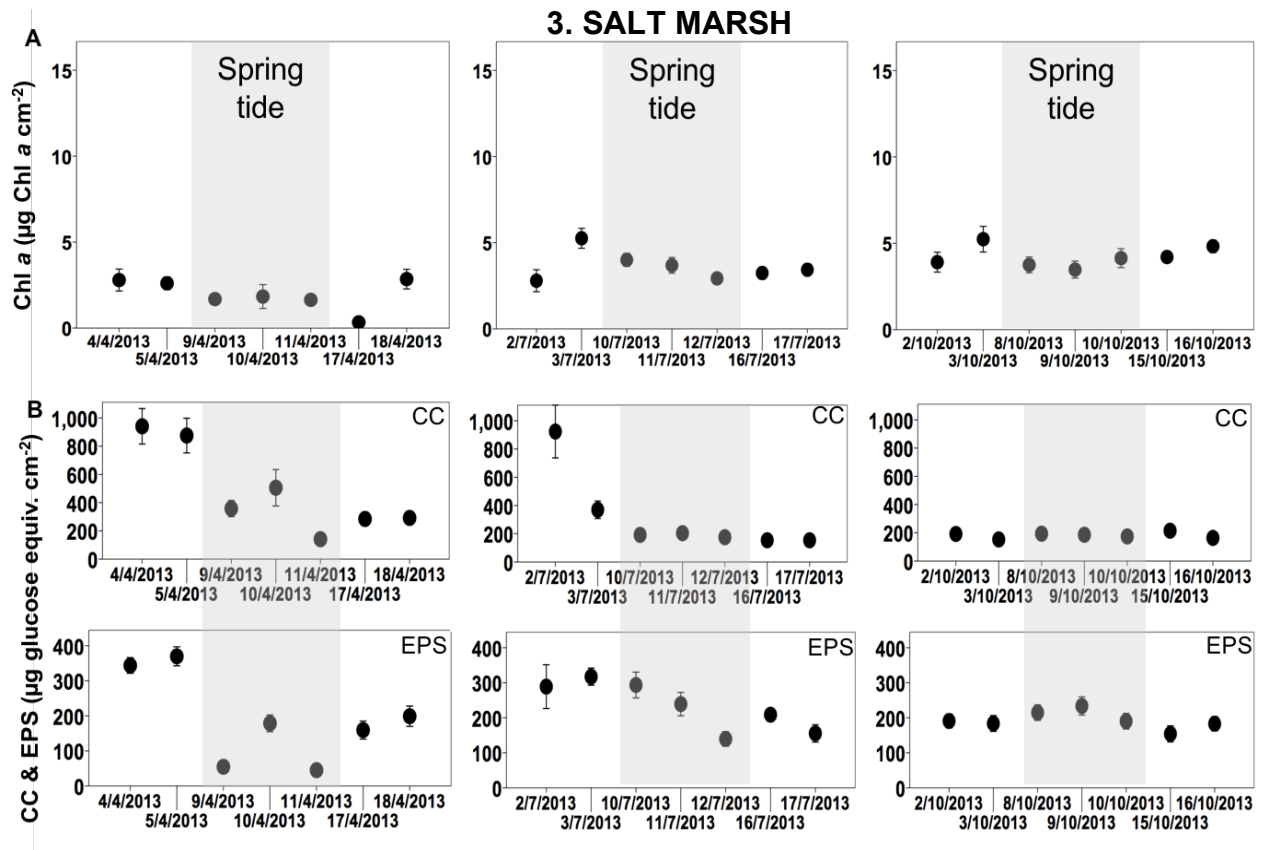


Figure 3.4: Temporal variability of A) Chl *a* and B) CC and EPS concentrations in the top 2 mm per cm² sediment on the; 3) salt marsh in April, July and October 2013 across the neap-spring-neap tidal cycle. Values are mean \pm 1SE, n= 24.

3.3.3 Temporal variability of weather-related abiotic factors

Mean wind speed (average value of wind speed on sampling day plus 2 days before sampling day) was significantly different between months ($p < 0.001$) (Figure 3.5A). The windiest month was April 2013 (spring) with a mean value of 9.4 m s^{-1} ; compared to July 2013 (4.0 m s^{-1} , $p < 0.001$) and October 2013 (4.8 m s^{-1} , $p < 0.001$) (Figure 3.5). Mean wind speed in July 2013 (summer) was significantly lower than in October 2013 (early autumn) ($p < 0.05$) (Figure 3.5A).

The wind speed data was closely linked to the wave height on the tidal flat. Both wind speed and the wave height in April 2013 sampling occasion showed significant positive correlation at $r = 0.648$, $p < 0.001$ (Figure 3.6). Therefore, the wind speed data was also used to depict the relationship between the MPB biomass distributions with the wave height at our study site.

Sum of rainfall was the sum of rain on and within 48 hours before the sampling day. This factor significantly varied between the sampling months ($p < 0.001$). October 2013 was the wettest sampling month with mean rainfall of 5.64 mm (Figure 3.5B). The highest sum of rain was on the 16th October 2013 with the record of 18.7 mm . The summer sampling occasion in July 2013 was the driest month. Only one day with 3.7 mm rainfall was recorded on the 3rd July 2013 (Figure 3.5B). Despite being the driest month, there was no significant difference between the sum of rain in July with April 2013. Both months however received significantly lower ($p < 0.001$) rain than October 2013.

Period of sun (sum of sun hours during sampling day plus 48 hours before the sampling day) showed significant variation between months ($p < 0.001$) (Figure 3.5C). Basically, period of sun represents the sun hours on the sampling days and 2 days prior to sampling day. Therefore, sampling during July 2013 had the longest period of sun and was significantly higher than April ($p < 0.001$) and October 2013 ($p < 0.001$) (Figure 3.2). Averaged daily period of sun in July 2013 was 23.1 hour . Maximum period of sun in July 2013's sampling occasion was 36.3

hours and the minimum was 8.3 hours on the 10th July 2013 and the 3rd July 2013, respectively (Figure 3.5C). The lowest period of sun on the 3rd July 2013 was coincided with the highest sum of rainfall in July 2013. The wettest October 2013 month had the lowest period of sun with the average of only 8.9 hours of sun in three days (Figure 3.5C). Minimum period of sun on the 15th (2.8 hours) and the 16th October 2013 (1.7 hours) were concurrent with both days' high sum of rainfall (Figure 3.5C).

Tidal range represents the vertical difference between high and low tides over the neap-spring-neap tidal cycle. Tidal range significantly varied between months ($p < 0.001$) and between tides ($p < 0.001$) (Figure 3.5D). The significantly highest mean tidal range was in July 2013 (4.6 m, $p < 0.001$) followed by October 2013 (4.3 m, $p < 0.001$) and finally April 2013 (4.1 m, $p < 0.001$) (Figure 3.5D). Seasonal or monthly variability of tidal range in all of the sampling months depicted a similar pattern. There was less difference between the tidal ranges in neap tide compared to the range in high energy spring tide occasions.

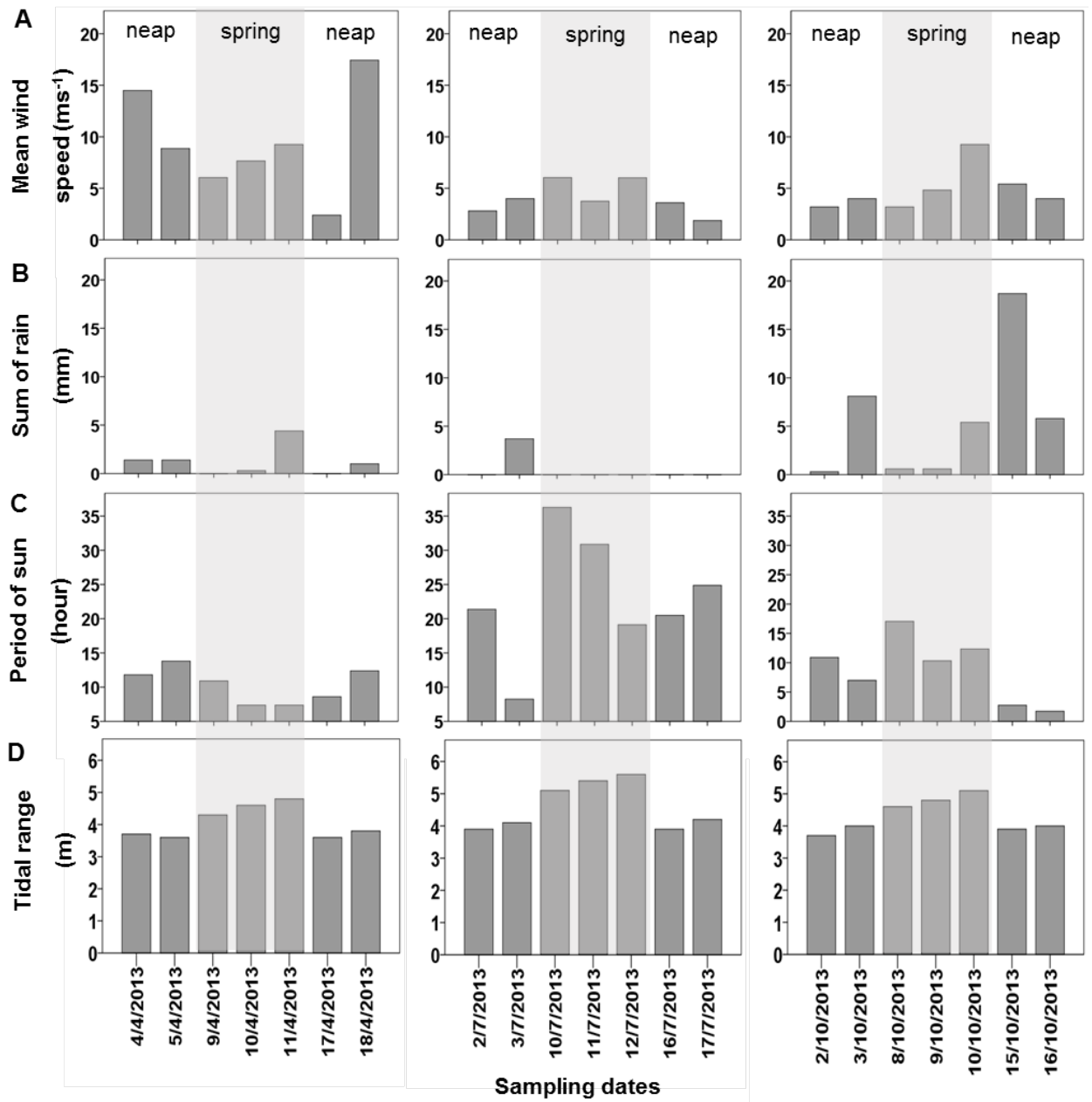


Figure 3.5: Temporal variability in four weather-related abiotic factors across seven sampling days in April 2013 (spring), July 2013 (summer) and October 2013 (early autumn / late summer) over neap-spring-neap tidal cycle (grey-shaded area)-neap tidal cycle. The factors are; A) mean wind speed (mean of wind speed for three days including the sampling days); B) sum of rainfall (accumulative rainfall on the sampling days + 48 hours before the sampling day); C) sun insolation (sum of sun hours during sampling days + 48 hours before the sampling days) and D) tidal range.

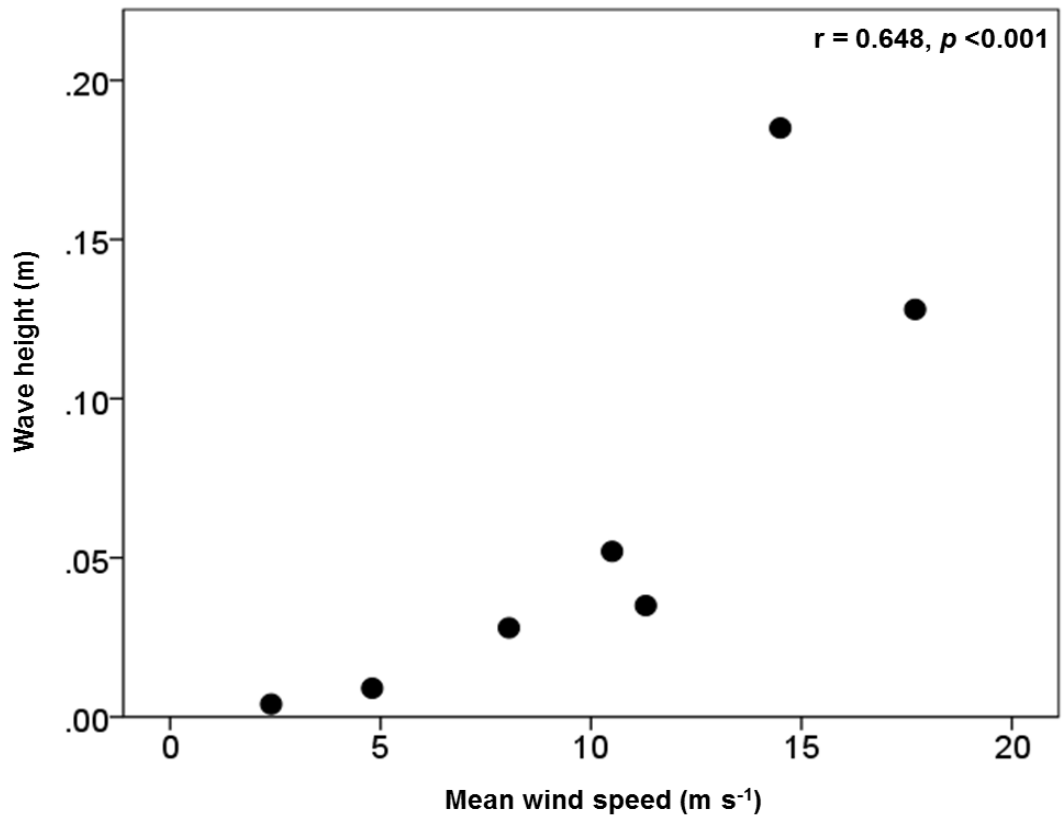


Figure 3.6: Significant positive relationship between the wind speed and the wave height. Calculated Pearson's correlation coefficients revealed $r = 0.648, p < 0.001$. $n = 1$.

3.3.4 Contribution of spatio-temporal scales to total variation of biomass proxies

Hierarchical nested ANOVA was used to investigate the variability of Chl *a*, CC and EPS concentrations at monthly temporal scale, daily temporal scale within month, spatial scale < 5 m (quadrat) within day and spatial scale < 0.5 m within quadrat on the mud flat, the transition zone and the salt marsh. The calculated percentage of total sum of square (SOS) revealed the contribution of each scale to the total variability of the measured biomass proxies on each zone. The percentage of SOS of the error or the differences between replicates (named as spatial scale < 0.5 m / micro-spatial patchiness) was also calculated to investigate the biomass variability at the smallest spatial scale in this study.

Figures 3.8, 3.9 and 3.10 depict the variability in Chl *a*, CC and EPS (respectively) at the spatial scale < 0.5 m (A), < 5 m (B) and temporal daily (C) and monthly (D) scales on the mud flat. However, only data from April 2013 was used to illustrate the variability of the biomass on the mud flat at both spatial < 0.5 m and < 5 m.

Chl *a* content within the mud flat had a strong spatial heterogeneity with 60.5 % of total variation (Figure 3.7A) explained by significant variability at spatial scale < 5 m ($F_{147,501}=1.653$, $p < 0.001$) (28.4 %) (Figure 3.5B) and spatial scale < 0.5 m (32.1 %) (Figure 3.7A). A total of 34 % of Chl *a* variability in this zone was attributed to significant differences at temporal monthly scales ($F_{2,501}=55.17$, $p < 0.001$) (Figure 3.7A). Daily temporal variability did not have a significant effect on Chl *a* total variation within the mud flat. In contrast to Chl *a*, both CC and EPS variability on the mud flat was greatly affected by temporal heterogeneity (Figure 3.7A). Both temporal scales, 'month' and 'day' significantly contributed to 25.9 % ($F_{2,493}=6.46$, $p < 0.01$) (Figure 3.7A and 3.9D) and 36.1 % ($F_{18,493}=1.653$, $p < 0.001$) (Figure 3.7A and 3.9C) of the CC total variation, respectively. EPS variability was mainly explained by the effect of monthly temporal scale, which significantly contributed to 34.3 % its total variation (Figure 3.7A). There was higher spatial heterogeneity in EPS than in CC content with respectively 27.5 % (Figure 3.7A and 3.10A) and 22.5 % (Figure 3.7A and 3.9A) of their total variation attributed to the effect of smallest spatial scale < 0.5 m. The larger spatial scale < 5 m significantly contributed 15.5 %

($F_{146,493}=1.54$, $p < 0.001$) and 17.2 % ($F_{149,493}=1.39$, $p < 0.001$), of CC (Figure 3.7A and 3.9C) and EPS (Figure 3.4A and 3.10C) total variation on the mud flat, respectively.

Both Chl *a* and CC concentrations on the transition zone displayed a high spatial heterogeneity (Figure 3.7B). By using only data of the 3rd, 11th and 17th July 2013, the variability of Chl *a*, CC and EPS on the transition zone at spatial scale < 0.5 m and < 5 m were depicted in figure 3.11 (A & B), 3.12 (A & B) and 3.13 (A & B), respectively. Figure 3.11 (C & D) to 3.13 (C & D) illustrates the biomass variability at temporal daily and monthly scales on the transition zone, respectively. The spatial heterogeneity was explained by 35.6 % and 28.2 % of total Chl *a* and CC variation at scales < 5 m (Chl *a*; $F_{147,497}=0.120$, $p < 0.001$ (Figure 3.7B and 3.11B) and CC; $F_{146,493}=0.135$, $p < 0.001$ (Figure 3.7B and 3.12B)), respectively. The spatial heterogeneity of CC however increased with decreasing spatial scale, with a higher percentage contribution at smaller spatial scale < 0.5 m, compared to spatial scale < 5 m with the value of 33.6 % (Figure 3.7B). As for EPS, the temporal daily scale significantly accounted for 30.1 % ($F_{18,494}=0.120$, $p < 0.001$) total variation on the transition zone (Figure 3.7B and 3.13C). Larger monthly temporal scales contributed significantly to ($F_{2,494}=7.287$, $p < 0.001$) lower percentage contribution (24.4 % EPS total variation) (Figure 3.7B and 3.13D). Spatial scale < 0.5 m was the second important factor (after the daily factor) affecting the EPS heterogeneity on the transition zone. The factor contributed to 28.3 % of total variation in EPS (Figure 3.7B and 3.13A).

The percentage of the contribution of Chl *a*'s total variability at spatial scale < 0.5 m, temporal daily and monthly scales on the salt marsh were depicted in Figure 3.14 A, C and D, respectively. Only data on the 3rd, 10th and 16th October 2013 were chosen in preparing the graphs for Chl *a* variability in at both spatial scales < 0.5 m (Figure 3.14A) and < 5 m (Figure 3.14B). While figure 3.15 and 3.16 shows the variability in CC and EPS on the salt marsh at the measured spatio-temporal scales, respectively.

Chl *a* concentration on the salt marsh displayed a stronger temporal heterogeneity than the mud flat and the transition zone. A total of 29.7 % and 26 % Chl *a* total variation was attributed to the contribution of temporal daily ($F_{18,502}=12.69$, $p < 0.001$) (Figure 3.7C and 3.14C) and monthly ($F_{2,502}=7.287$, $p < 0.001$) (Figure 3.7C and 3.14D) scales, respectively. Spatial

heterogeneity of Chl *a* on the salt marsh was best explained by variability at spatial scale < 0.5 m which accounted for 25.2 % total variation (Figure 3.7C and 3.14A). Larger spatial scale < 5 m ($F_{147,502}=1.728$, $p < 0.001$) contributed to relatively lower percentage of 19.1 % of the total variation (Figure 3.7C and 3.14B). Both CC and EPS concentrations on the salt marsh showed high spatial heterogeneity. The high spatial heterogeneity in CC on the salt marsh was significantly controlled by the spatial scale < 5 m ($F_{144,471}=2.56$, $p < 0.001$) which accounted for 33.6 % the total variation (Figure 3.7C and 3.15B). While 40.5 % of the EPS total variation was explained by spatial scale < 0.5 m factor (Figure 3.16A). Differences in temporal daily scale significantly contributed to both CC ($F_{18,471}=6.92$, $p < 0.001$) and EPS ($F_{18,471}=10.08$, $p < 0.001$) total variation. The temporal scale accounted for 29.1 % (Figure 3.7C and 3.15C) and 32.4 % (Figure 3.7C and 3.16C) of total variation of both biomass proxies within the salt marsh, respectively. Both CC and EPS total variation within the salt marsh was not significantly affected by the largest temporal scale, the month.

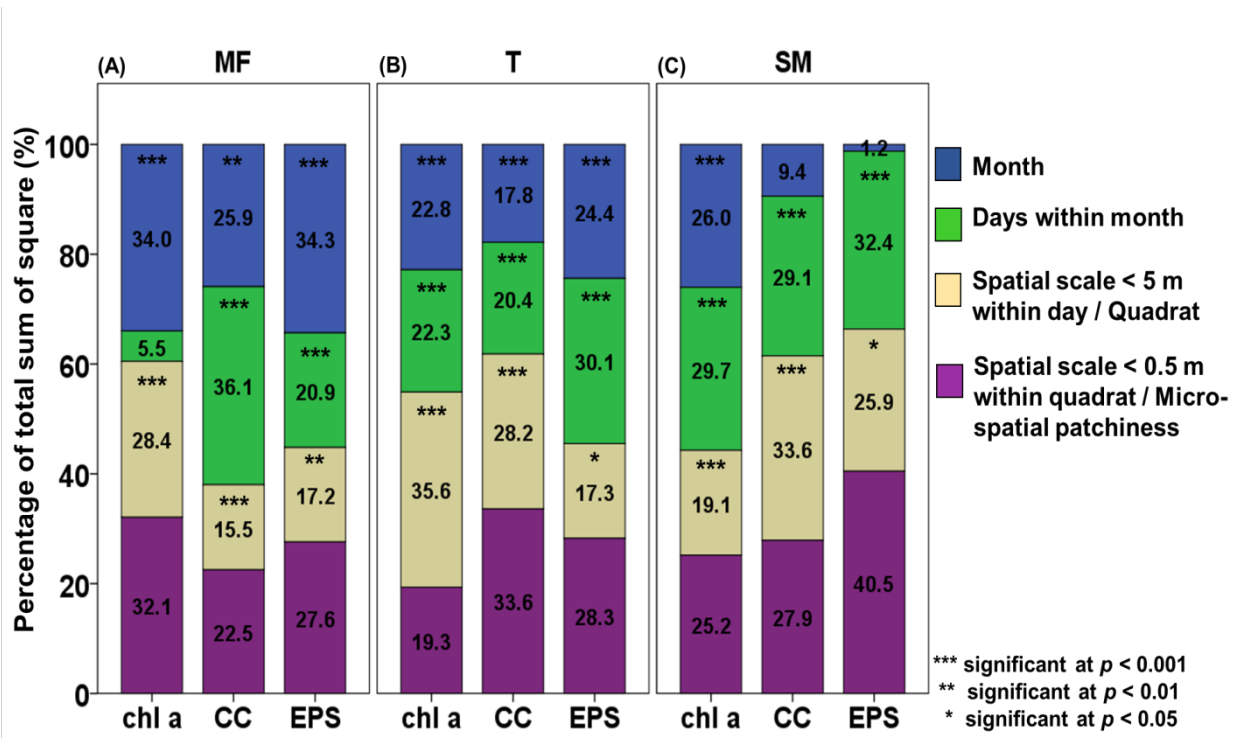


Figure 3.7: Contribution of spatio-temporal scale; temporal month scale, temporal day scale (days within month), spatial scale < 0.5 m (quadrat) within day and spatial scale < 0.5 m within quadrat (micro-spatial patchiness) to Chl a, CC and EPS variability in top 2 mm per cm² sediment on A) mud flat (MF), B) transition zone (T) and C) salt marsh (SM). Contributions are significant at: * $p < 0.05$, ** $p < 0.01$ and *** $p < 0.001$. Sum of square values were obtained from nested hierarchical ANOVA test done on the combined log-transformed biomass proxies data set for each zones (Chl a; mud flat, $n = 501$, transition zone, $n = 497$ and salt marsh, $n = 502$, CC and EPS; mud flat, $n = 493$, transition zone, $n = 493$, salt marsh, $n = 471$). Spatial scale < 0.5 m / micro-spatial patchiness is the lowest scale (between triplicate samples) which represents the variability between individual mini-core at spatial scale < 0.5 m within quadrats. There were no p value for microspatial patchiness since there are no replicates.

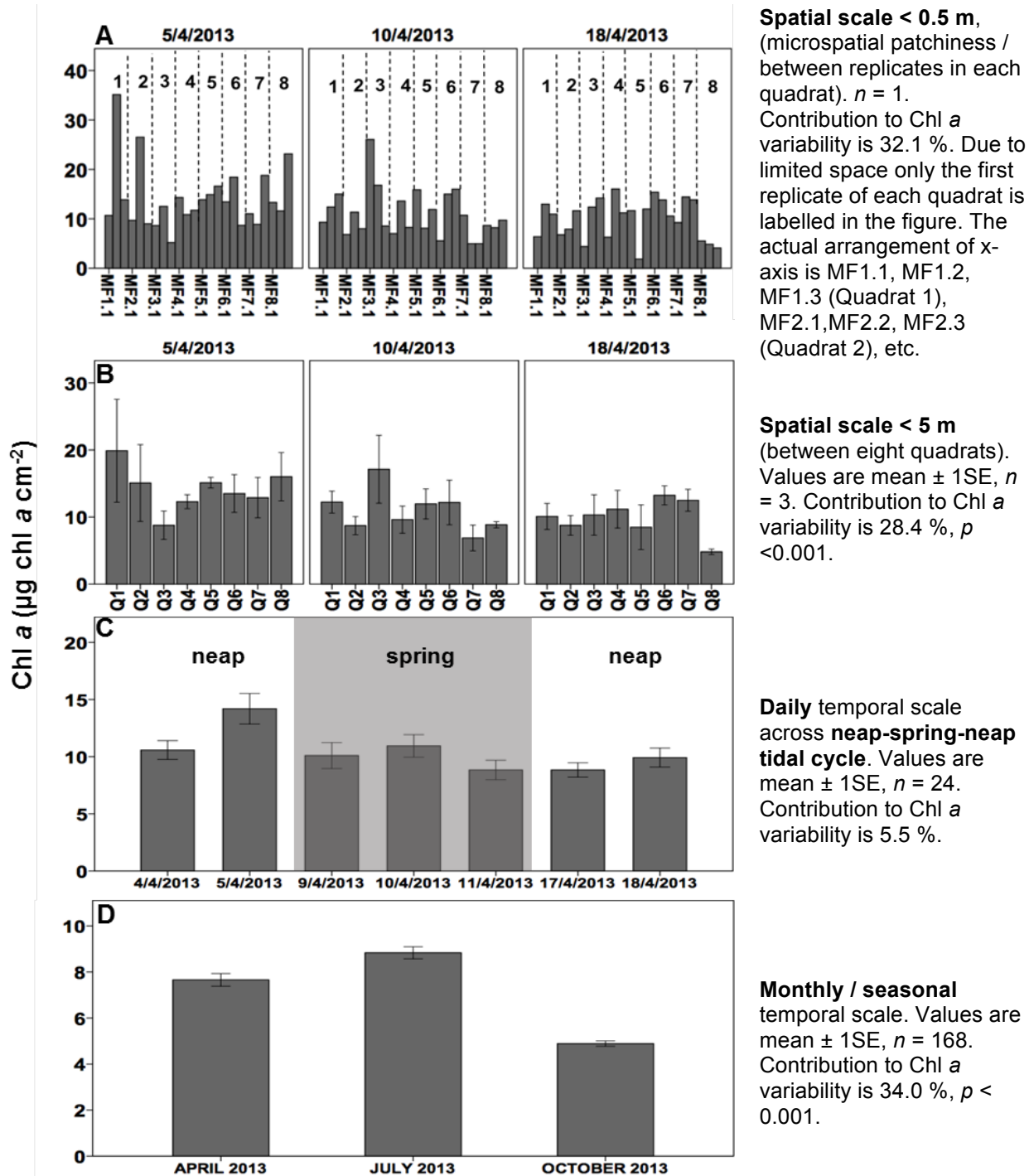


Figure 3.8: Multi-scales variability of Chl *a* concentration in the top 2 mm per cm² sediment on **mud flats** at Fingringhoe, Essex at; A) the smallest spatial scale < 0.5 m between three different biofilm patches in eight different quadrats (labelled by number in the figure); B) spatial scale < 5 m between quadrats (Q); C) at daily temporal scale over seven sampling days across neap-spring-neap tide tidal cycle and; D) at the largest monthly and seasonal temporal scale in the all three sampling months (April 2013, July 2013 and October 2013). Only representative data from three (5th April 2013, 10th April 2013 and 18th April 2013) of seven sampling days in April 2013 (out of three sampling months) are shown to display the Chl *a* variability at spatial scale < 0.5 m and spatial scale < 5 m.

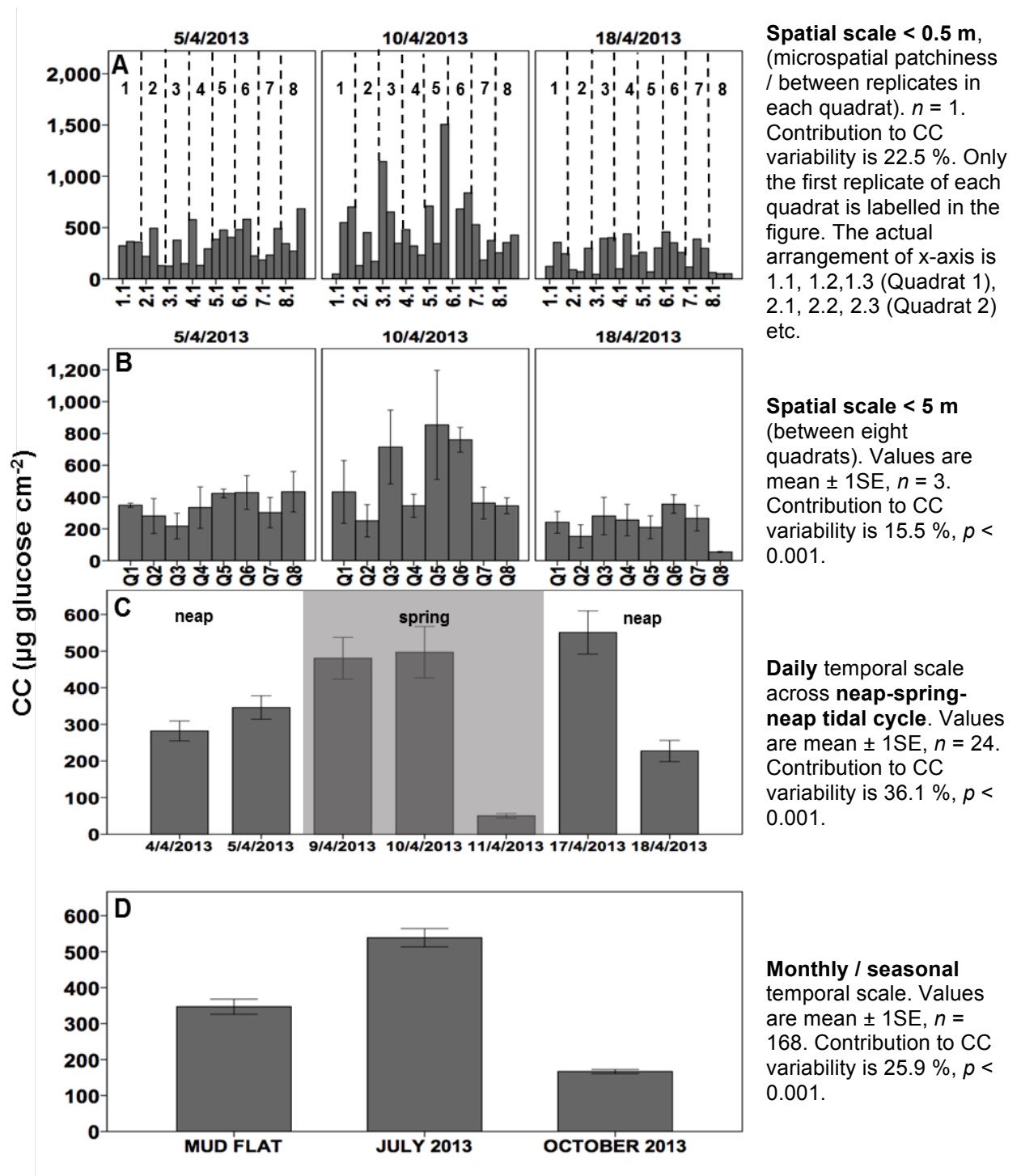


Figure 3.9: Multi-scales variability of CC (CC) concentration in the top 2 mm per cm^2 sediment on **mud flat** at Fingringhoe, Essex at; A) the smallest spatial scale $< 0.5\text{ m}$ between three different biofilm patches in eight different quadrats (labelled by number in the figure); B) spatial scale $< 5\text{ m}$ between quadrats (Q); C) at daily temporal scale over seven sampling days across neap-spring-neap tide tidal cycle and; D) at the largest monthly and seasonal temporal scale in the all three sampling months (April 2013, July 2013 and October 2013). Only representative data from three (5th April 2013, 10th April 2013 and 18th April 2013) of seven sampling days in April 2013 (out of three sampling months) are shown to display the Chl a variability at spatial scale $< 0.5\text{ m}$ and spatial scale $< 5\text{ m}$.

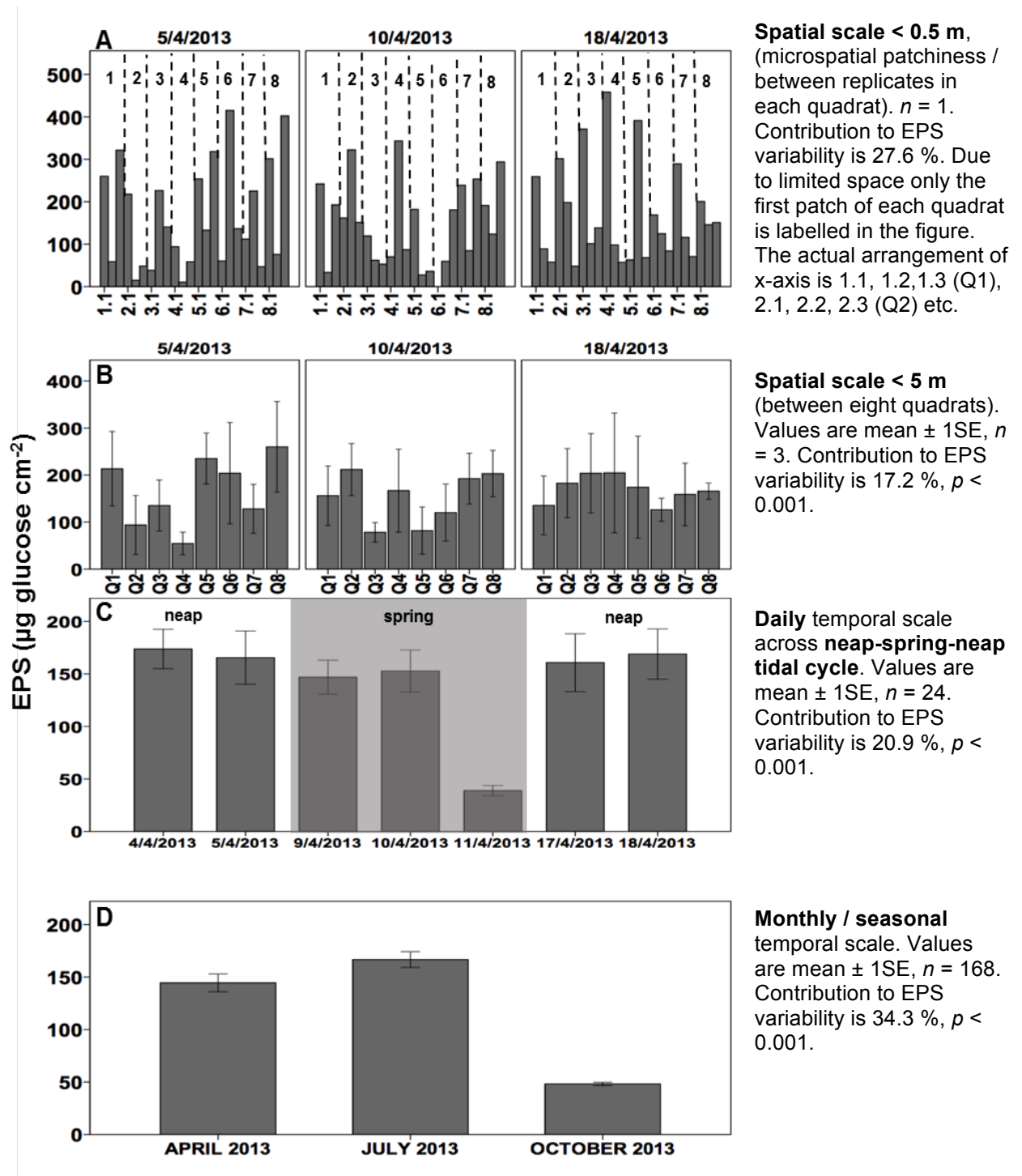
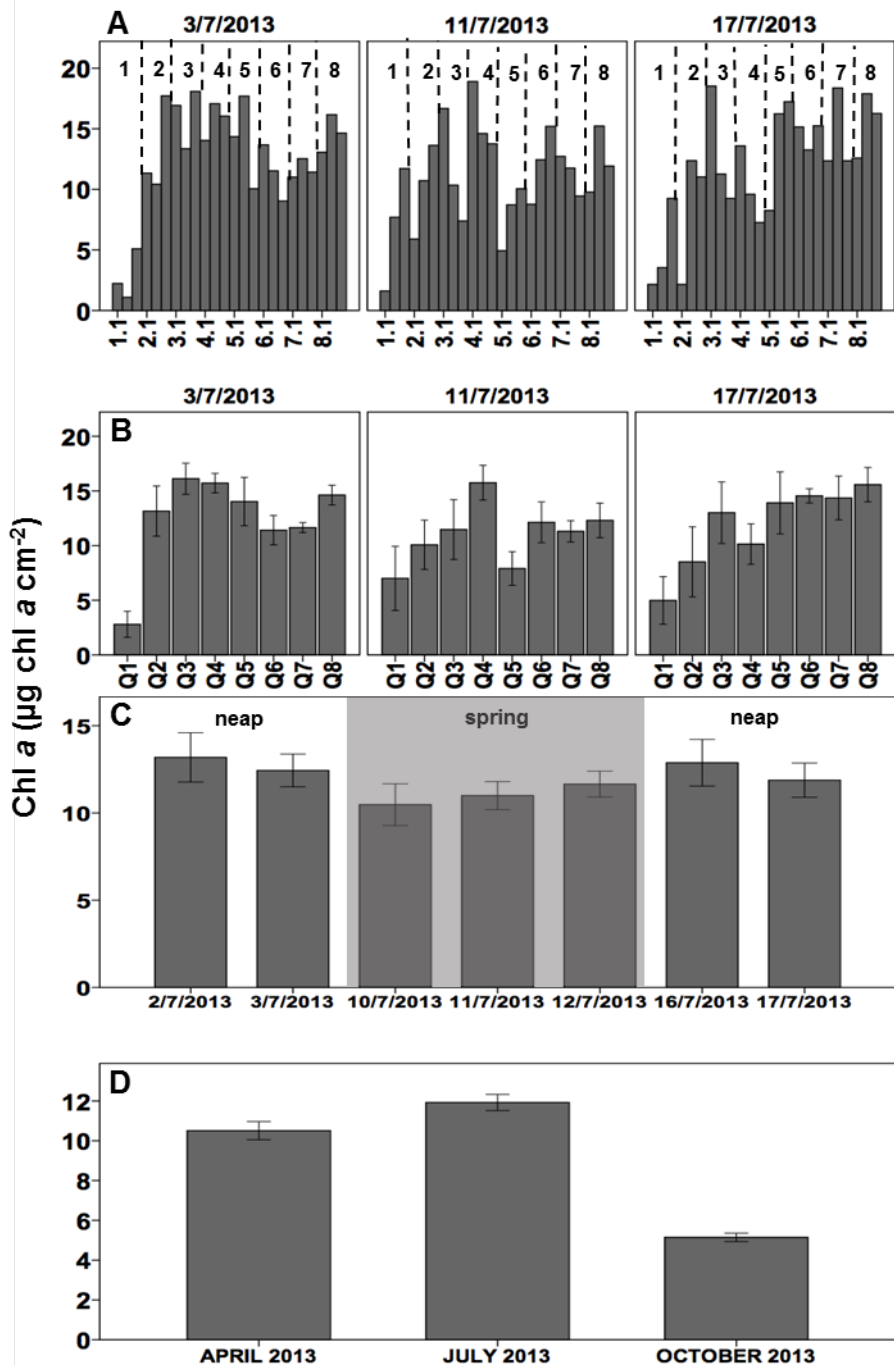


Figure 3.10: Multi-scales variability of EPS concentration in the top 2 mm per cm² sediment on **mud flat** at Fingringhoe, Essex at; A) the smallest spatial scale < 0.5 m between three different biofilm patches in eight different quadrats (labelled by number in the figure); B) spatial scale < 5 m between quadrats (Q); C) at daily temporal scale over seven sampling days across neap-spring-neap tide tidal cycle and; D) at the largest monthly and seasonal temporal scale in the all three sampling months (April 2013, July 2013 and October 2013). Only representative data from three (5th April 2013, 10th April 2013 and 18th April 2013) of seven sampling days in April 2013 (out of three sampling months) are shown to display the Chl a variability at spatial scale < 0.5 m and spatial scale < 5 m.



Spatial scale < 0.5 m, (microspatial patchiness / between replicates in each quadrat). $n = 1$. Contribution to Chl *a* variability is 19.3 %. Due to limited space only the first patch of each quadrat is labelled in the figure. The actual arrangement of x-axis is 1.1, 1.2, 1.3 (Q1), 2.1, 2.2, 2.3 (Q2), etc.

Spatial scale < 5 m (between eight quadrats). Values are mean \pm 1SE, $n = 3$. Contribution to Chl *a* variability is 35.6 %, $p < 0.001$.

Daily temporal scale across neap-spring-neap tidal cycle. Values are mean \pm 1SE, $n = 24$. Contribution to Chl *a* variability is 22.3 %, $p < 0.001$.

Monthly / seasonal temporal scale. Values are mean \pm 1SE, $n = 168$. Contribution to Chl *a* variability is 22.8 %, $p < 0.001$.

Figure 3.11: Multi-scales variability of Chl *a* concentration in the top 2 mm per cm² sediment on **transition zone** at Fingringhoe, Essex at; A) the smallest spatial scale < 0.5 m between three different biofilm patches in eight different quadrats (labelled by number in the figure); B) spatial scale < 5 m between quadrats (Q); C) at daily temporal scale over seven sampling days across neap-spring-neap tide tidal cycle and; D) at the largest monthly and seasonal temporal scale in the all three sampling months (April 2013, July 2013 and October 2013). Only representative data from three (3rd July 2013, 11th July 2013 and 17th July 2013) of seven sampling days in July 2013 (out of three sampling months) are shown to display the Chl *a* variability at spatial scale < 0.5 m and spatial scale < 5 m.

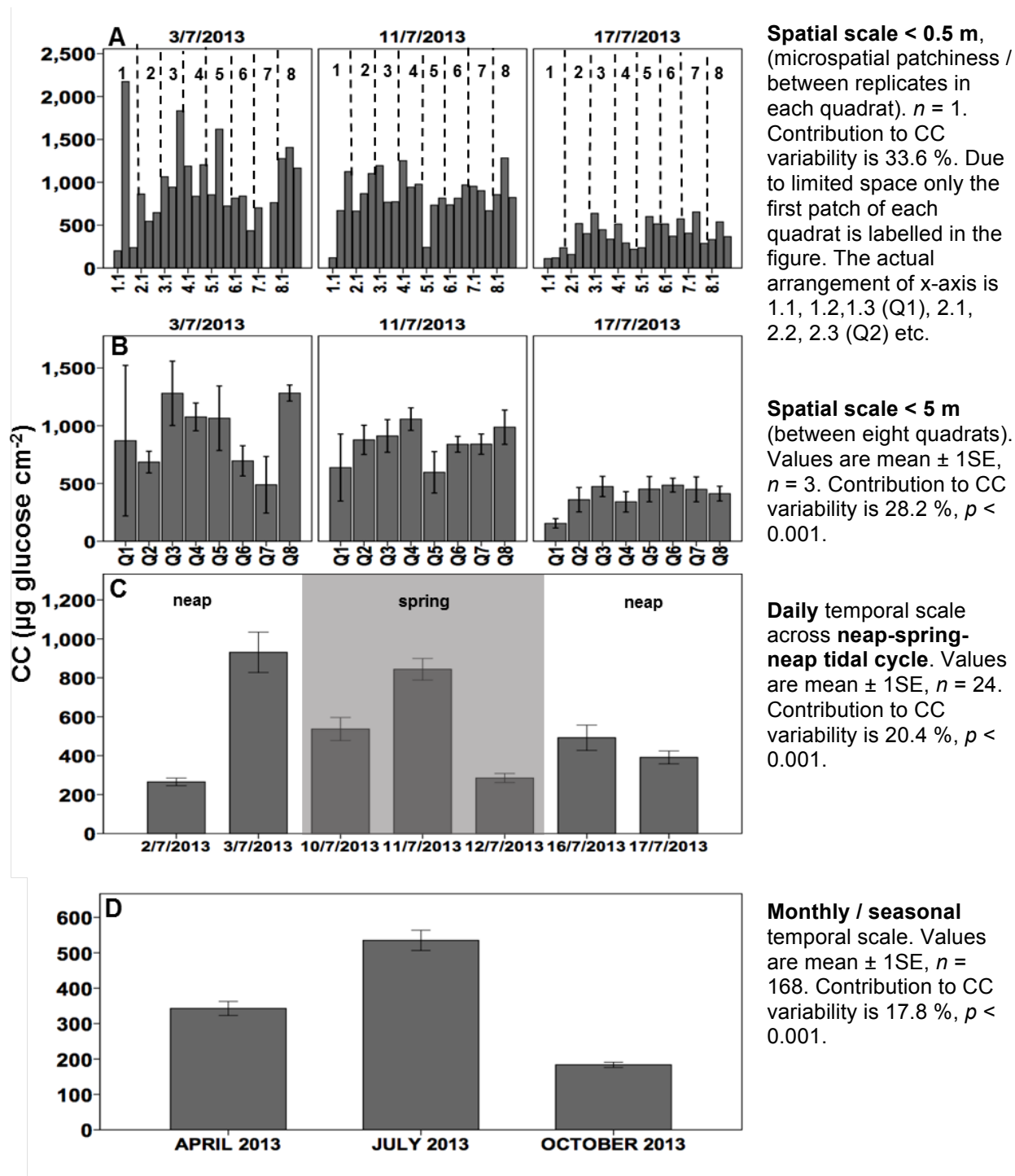


Figure 3.12: Multi-scales variability of CC concentration in the top 2 mm per cm² sediment on **transition zone** at Fingringhoe, Essex at; A) the smallest spatial scale < 0.5 m between three different biofilm patches in eight different quadrats (labelled by number in the figure); B) spatial scale < 5 m between quadrats (Q); C) at daily temporal scale over seven sampling days across neap-spring-neap tide tidal cycle and; D) at the largest monthly and seasonal temporal scale in the all three sampling months (April 2013, July 2013 and October 2013). Only representative data from three (3rd July 2013, 11th July 2013 and 17th July 2013) of seven sampling days in July 2013 (out of three sampling months) are shown to display the Chl a variability at spatial scale < 0.5 m and spatial scale < 5 m.

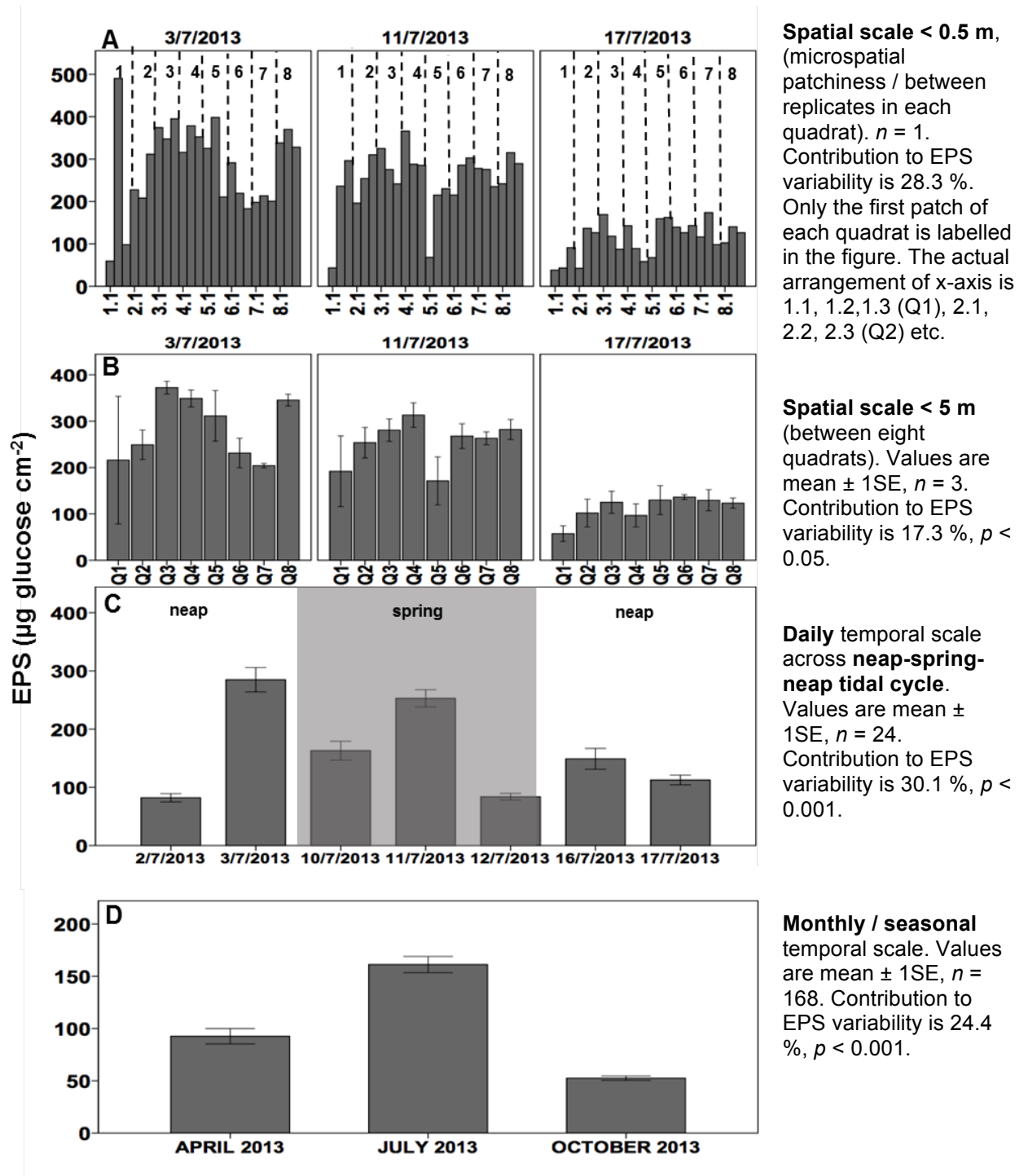


Figure 3.13: Multi-scales variability of EPS concentration in the top 2 mm per cm² sediment on **transition zone** at Fingringhoe, Essex at; A) the smallest spatial scale < 0.5 m between three different biofilm patches in eight different quadrats (labelled by number in the figure); B) spatial scale < 5 m between quadrats (Q); C) at daily temporal scale over seven sampling days across neap-spring-neap tide tidal cycle and; D) at the largest monthly and seasonal temporal scale in the all three sampling months (April 2013, July 2013 and October 2013). Only representative data from three (3rd July 2013, 11th July 2013 and 17th July 2013) of seven sampling days in July 2013 (out of three sampling months) are shown to display the Chl a variability at spatial scale < 0.5 m and spatial scale < 5 m.

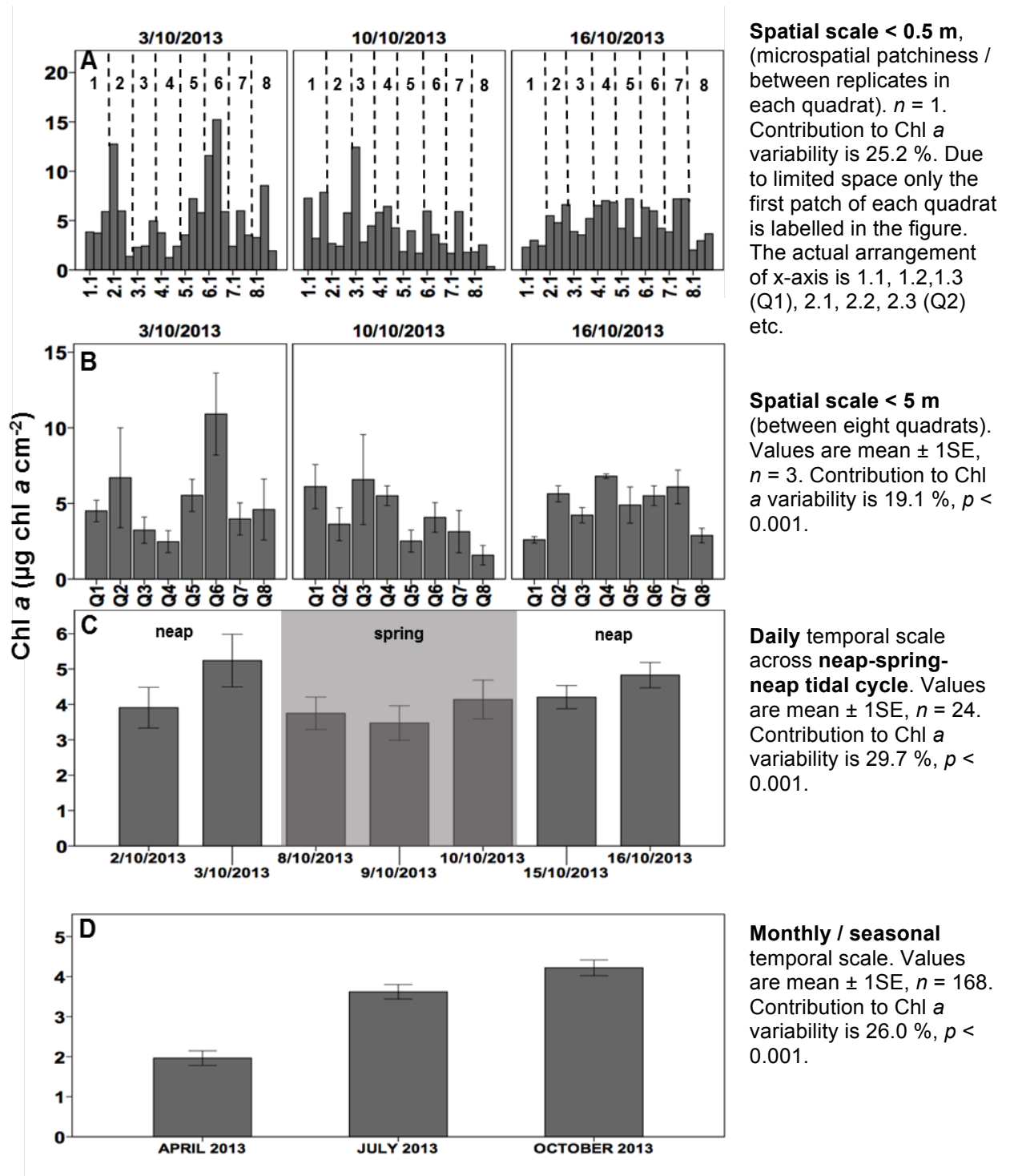


Figure 3.14: Multi-scales variability of Chl *a* concentration in the top 2 mm per cm² sediment on **salt marsh** at Fingringhoe, Essex at; A) the smallest spatial scale < 0.5 m between three different biofilm patches in eight different quadrats (labelled by number in the figure); B) spatial scale < 5 m between quadrats (Q); C) at daily temporal scale over seven sampling days across neap-spring-neap tide tidal cycle and; D) at the largest monthly and seasonal temporal scale in the all three sampling months (April 2013, July 2013 and October 2013). Only representative data from three (3rd Oct 2013, 10th Oct 2013 and 16th Oct 2013) of seven sampling days in July 2013 (out of three sampling months) are shown to display the Chl *a* variability at spatial scale < 0.5 m and spatial scale < 5 m.

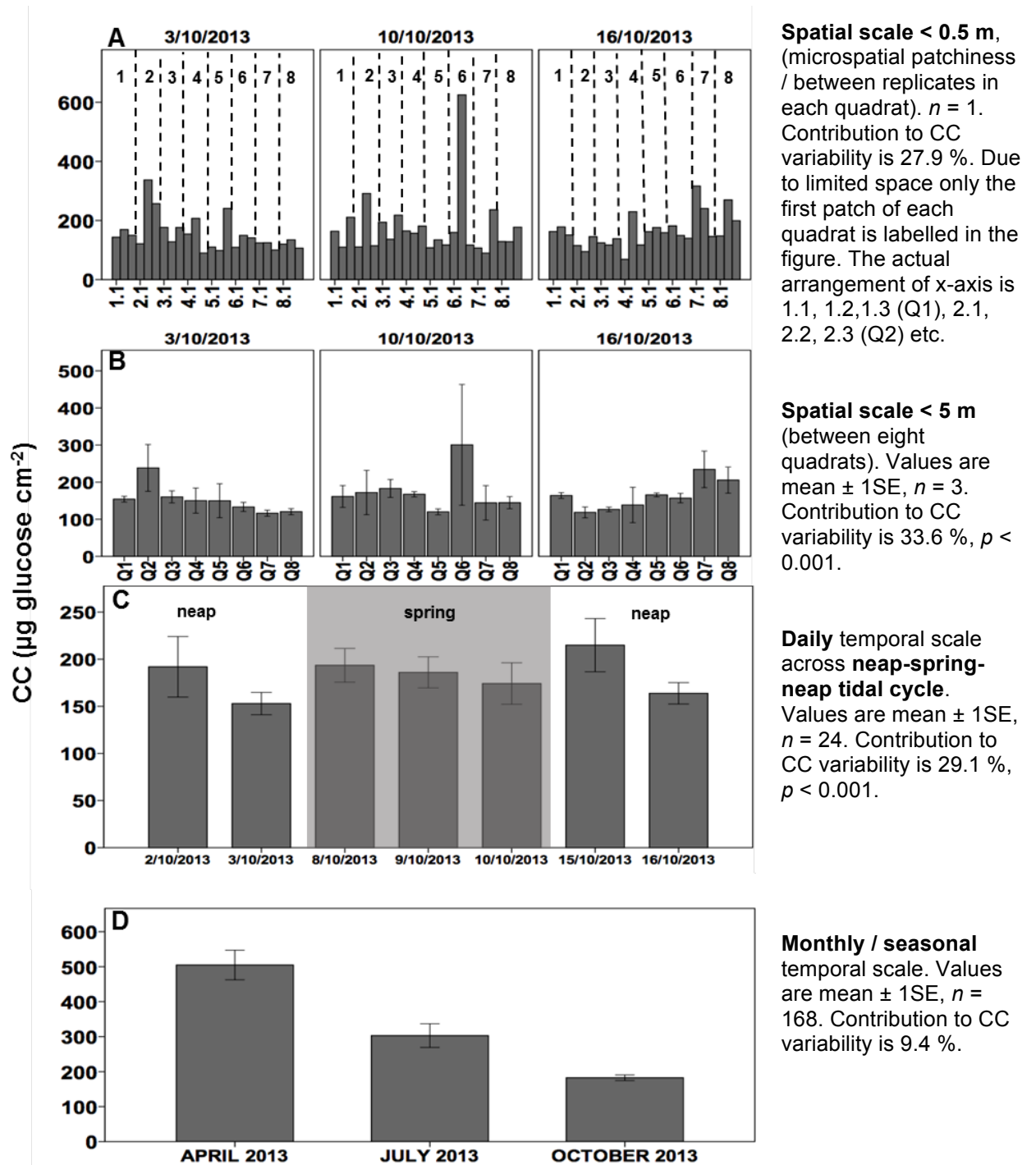


Figure 3.15: Multi-scales variability of CC (CC) concentration in the top 2 mm per cm² sediment on **salt marsh** at Fingringhoe, Essex at; A) the smallest spatial scale < 0.5 m between three different biofilm patches in eight different quadrats (labelled by number in the figure); B) spatial scale < 5 m between quadrats (Q); C) at daily temporal scale over seven sampling days across neap-spring-neap tide tidal cycle and; D) at the largest monthly and seasonal temporal scale in the all three sampling months (April 2013, July 2013 and October 2013). Only representative data from three (3rd Oct 2013, 10th Oct 2013 and 16th Oct 2013) of seven sampling days in July 2013 (out of three sampling months) are shown to display the Chl a variability at spatial scale < 0.5 m and spatial scale < 5 m.

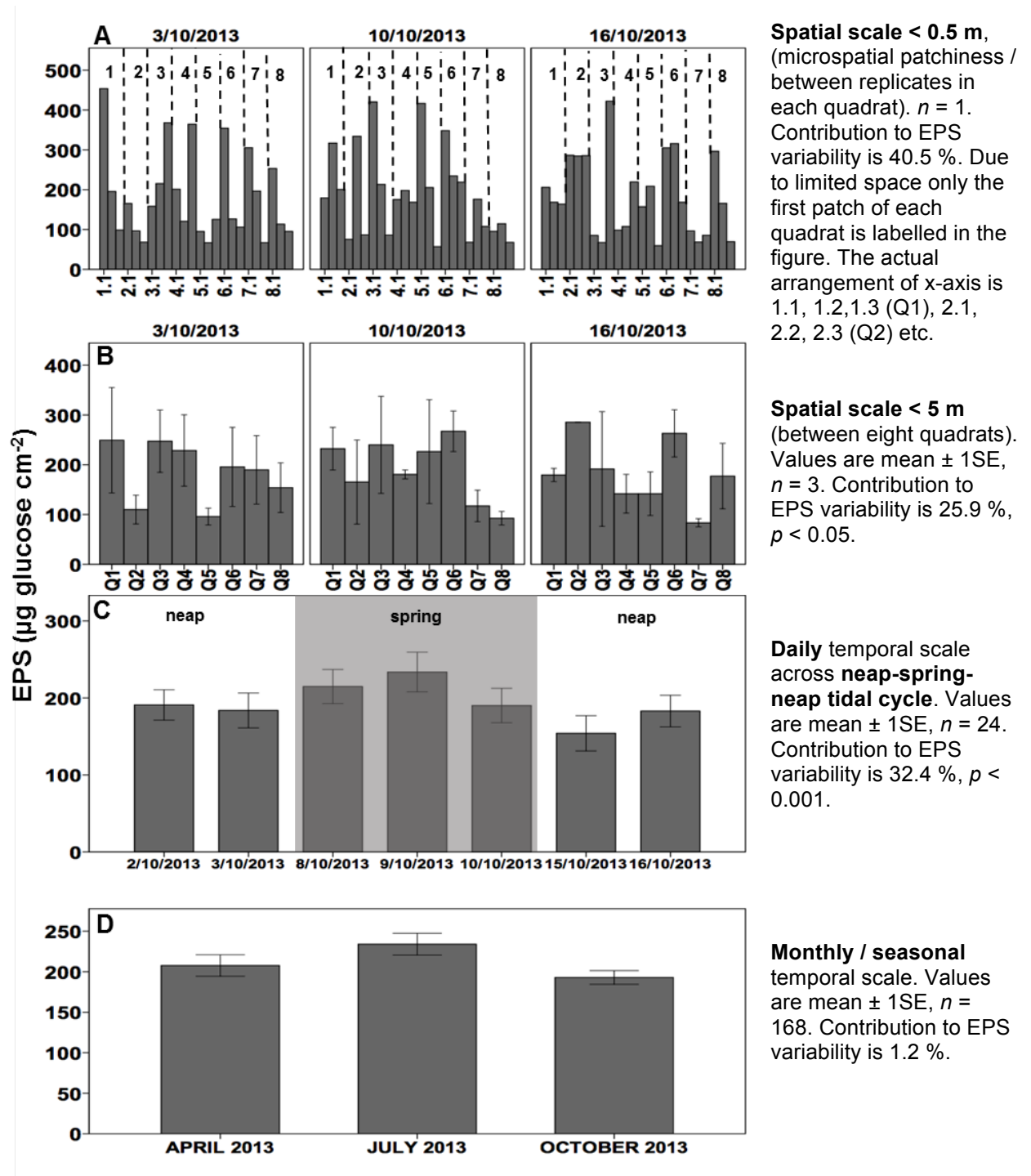


Figure 3.16: Multi-scales variability of EPS concentration in top 2 mm per cm² sediment on **salt marsh** at Fingringhoe, Essex at; A) the smallest spatial scale < 0.5 m between three different biofilm patches in eight different quadrats (labelled by number in the figure); B) spatial scale < 5 m between quadrats (Q); C) at daily temporal scale over seven sampling days across neap-spring-neap tide tidal cycle and; D) at the largest monthly and seasonal temporal scale in the all three sampling months (April 2013, July 2013 and October 2013). Only representative data from three (3rd Oct 2013, 10th Oct 2013 and 16th Oct 2013) of seven sampling days in July 2013 (out of three sampling months) are shown to display the Chl a variability at spatial scale < 0.5 m and spatial scale < 5 m.

3.3.5 Influence of weather-related abiotic factors on the variability of the biomass proxies

To investigate the relationship between the three biomass proxies (Chl *a*, CC and EPS) on the mud flat, the transition zone and the salt marsh with the chosen weather-related abiotic factors, a PCA was performed on log transformed ($n + 1$) data of Chl *a*, CC, EPS, CC: Chl *a*, EPS:Chl *a*, 'mean wind speed' (MWS), 'sum of rainfall' (SOR), 'sum of sun hours' (SOS) and tidal range. The PCA of each zone was done separately. The two principal components explained 56.4 % (Figure 3.17A), 57.7 % (Figure 3.17B) and 55.0 % (Figure 3.17C) of the variability in the data of the mud flat, transition zones and salt marsh, respectively.

Principal component 1 (PC1) and 2 (PC2) of the mud flat's data explained 39.8 % and 16.6 % total variability on the zone, respectively (Figure 3.17A). Biomass proxies together with 'sum of sun hours' were the significant positive contributors of the first principal component (PC1) gradient, whereas the 'sum of rainfall' was the negative (all significant at $p < 0.001$). Chl *a* together with mean wind speed and sum of rainfall were strongly and significantly positively ($p < 0.001$) represented the PC2. Tidal range and the 'period of sun hours' were the two factors that significantly negatively correlated with the PC2 at $p < 0.001$ (Figure 3.17A).

PC1 of the transition zone was significantly positively explained by the biomass proxies, the tidal range and the sum of sun (both significant at $p < 0.001$). The 'sum of rainfall' was negatively correlated with PC1 (Figure 3.17B). Notes that only the three biomass proxies, the Chl *a*, CC and EPS were significantly represented the PC1. Both CC: Chl *a* and EPS: Chl *a* ratios were significantly negatively correlated with the PC2 (both significant at $p < 0.001$). Whereas the mean wind speed and Chl *a* were significantly positively correlated with the PC2 (both significant at $p < 0.001$). Both PC1 and PC2 of the transition zone explained 34.6 % and 23.1 % variability on the transition zone, respectively.

Both mud flat and the transition zone's principal components depicted comparable patterns. The principal components however were possible to distinguish by the different

influence of tidal range in both zones' principal components. The different influence could possibly explain that tidal range was an important discriminator in controlling MPB biomass (especially the Chl *a*) on both zones.

Biomass proxies and two weather-related abiotic factors, the 'sum of rainfall' and the tidal range were the significant factors that correlated with the salt marsh PC1, which explained 32.5 % of the correlation data set (Figure 3.17C). Both CC and EPS concentrations and both CC:Chl *a* and EPS:Chl *a* ratios were the significant positive contributors of the PC1 (significant at $p < 0.001$), whereas the Chl *a* concentration, 'sum of rainfall' and tidal range were negative. PC 2 of the PCA (22.5 %) was significantly positively correlated with Chl *a* and CC concentrations (both proxies significant at $p < 0.05$), 'mean wind speed' ($p < 0.001$) and sum of rainfall ($p < 0.001$). The 'sum of sun hours' and tidal height significantly negatively correlated with the PC2 at $p < 0.001$ (Figure 3.17C).

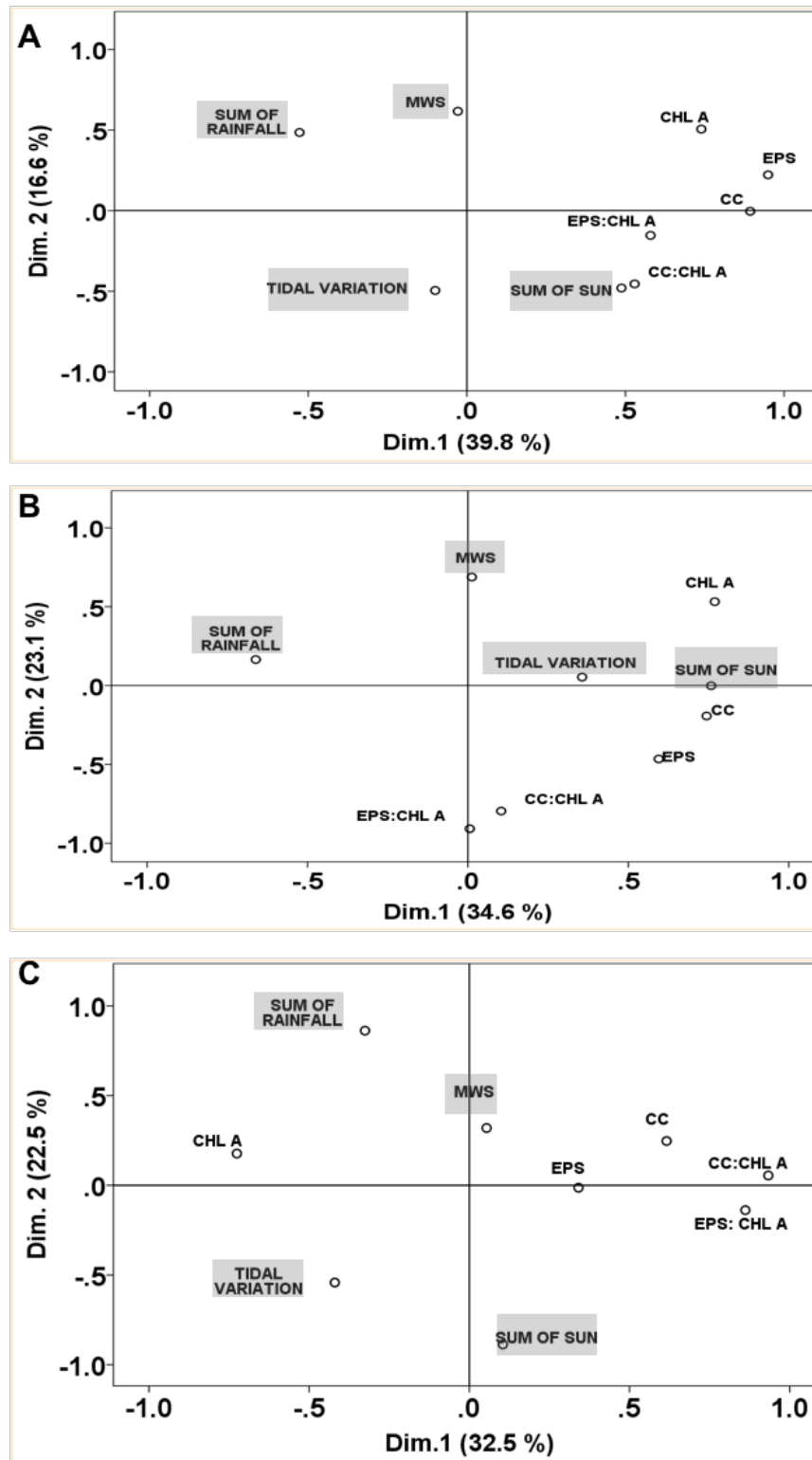


Figure 3.17: Principal components 1 and 2 from PCA of log-transformed(n+1) variables: abiotic factors (sum of rainfall (SOR) (mm), mean wind speed (MWS) (ms^{-1}), sum of sun (SOS) (hours) and tidal range (m)) and biomass proxies (Chl a ($\mu\text{g Chl a cm}^{-2}$), colloidal and EPS ($\mu\text{g glucose cm}^{-2}$)) of MPB microspatial patches (triplicates samples on each 8 quadrats) on sediment biofilm (top 2 mm) of the A) mud flat (n=495), B) transition zone (n=490) and C) salt marsh (n=471) based on data in April 2013, July 2013 and October 2013. Similar weather-related abiotic factors data were applied on all of the zones. Grey shaded variables are the supplementary variables.

3.3.6 Characterization of the physical state of MPB patches at spatio-temporal scales

Each point in the plots of individual scores of PCA represented the individual biofilm patch after taking into account the association between the biofilm patch biomass properties with weather-related abiotic factors. Hence in this study, the PC1 and PC2 coordinates were indicating measures of the physical state of the biofilm. Individual factor maps of the PCA were plotted to investigate any significant temporal, daily and spatial structures of the physical state of the biofilm patches.

3.3.6.1 MPB biomass variability at temporal monthly scale across tidal flat

Scores of both PC1 and PC2 of the mud flat (PC1; $F_{2,492}=105.3$, $p < 0.001$ and; PC2; $F_{2,492}=128.7$, $p < 0.001$), transition zone (PC1; $F_{2,487}=269.5$, $p < 0.001$ and PC2; $F_{2,487}=34.4$, $p < 0.001$) and the salt marsh (PC1; $F_{2,468}=87.9$, $p < 0.001$ and; PC2; $F_{2,468}=166.6$, $p < 0.001$) were significantly different between sampling months. There was potentially a close relationship between the monthly variability of the biomass proxies across the tidal flat with the chosen weather-related abiotic factors.

The mean PC1 score of mud flat in July 2013 was significantly more positive than the score in April 2013 ($p < 0.05$) and October 2013 ($p < 0.001$) (Figure 3.18B). Thus suggesting that the physical state of the biofilm patches in July 2013 were characterized by the factors that positively explained the PC1 gradient of the mud flat (Figure 3.18A). This observation was supported by a significantly higher Chl *a* ($10.41 \pm 0.81 \mu\text{g Chl } a \text{ cm}^{-2}$), CC ($536.38 \pm 48.83 \mu\text{g glucose equiv. cm}^{-2}$) and EPS ($168.55 \pm 13.85 \mu\text{g glucose equiv. cm}^{-2}$) in July 2013 (month that received the highest 'sum of sun' (Figure 3.5C)) than in October 2013. The CC and EPS concentrations in July was significantly higher ($p < 0.001$) than in April 2013 but not the Chl *a* concentration. The 'sum of sun for three days' was showed to be significantly positively correlated with all of the biomass proxies, Chl *a*, CC, EPS ($r=-0.384$, $p < 0.001$), and also the

CC:Chl *a* and EPS:Chl *a* ratios (Table 3.1). The significantly negative PC1 scores of October 2013 than the other two months (Figure 3.18B) corresponded with significantly lower biomass proxies (Chl *a* = $5.31 \pm 0.46 \mu\text{g Chl } a \text{ cm}^{-2}$, CC = $166.68 \pm 14.13 \mu\text{g glucose equiv. cm}^{-2}$, EPS = $48.10 \pm 3.82 \mu\text{g glucose cm}^{-2}$) concentration than July and April 2013 (both significant at $p < 0.001$). October's PC1 scores that plotting towards the left side of the PCA not only summarized the low biomass but also the high sum of rainfall (5.64 mm) (Figure 3.5B). There was significant negative correlation between the entire monthly mean of biomass proxies on the mud flat and the sum of rainfall for three days (Table 3.1).

There was higher monthly variability in PC1 score of the transition rather than in the PC2 scores (stated earlier). Comparable to the mud flat, July's biofilms' physical state (scores) on the transition zone also plotting towards the right side of the PC1 (Figure 3.18D). Therefore, indicated higher Chl *a* ($11.93 \pm 1.1 \mu\text{g Chl } a \text{ cm}^{-2}$), CC ($534.9 \pm 51.3 \mu\text{g glucose equiv. cm}^{-2}$) and EPS ($161.8 \pm 13.0 \mu\text{g glucose equiv. cm}^{-2}$) concentrations on the transition in July than in April 2013 (Chl *a*; $p < 0.01$, CC; $p < 0.001$, EPS; $p < 0.001$) and October 2013 (Chl *a*; $p < 0.001$, CC; $p < 0.001$ and EPS; $p < 0.001$). Similar to the mud flat, the high biomass proxies in July was potentially concurrent with this month high 'sum of sun for three days'. This coincided event was further supported by significantly positively correlation between the Chl *a*, CC and EPS concentrations on the transition zone with the 'sum of sun' (Table 3.1). Biofilms in October 2013 that plotted towards the left side of the PC1 was reflected by low biomass proxies' concentration and was also coincided with high sum of rainfall of the month. The negative relationship was supported by the significantly negative correlation between Chl *a*, CC, EPS, CC:Chl *a* and EPS:Chl *a* concentrations on the transition zone with the sum of rainfall (Table 3.1).

The average wind speed for three days showed to have significant positive relationship with the Chl *a* concentration on both the mud flat and the transition zone. With the Pearson correlation coefficients values of $r = 0.116$ and $r = 0.230$ (both significant at $p < 0.001$) (Table 3.1). The mean wind speed however was significantly negatively correlated with CC and CC:Chl *a* ratio of both zones and the EPS and the EPS:Chl *a* ratio of the transition zone (Table 3.1).

The tidal range did not have significant effect on the biomass proxies on both zones except on the EPS of the transition zone at (Table 3.1).

Post hoc output of the sample scores of July 2013 and October 2013 on the salt marsh were more significantly explained by the negative factors of PC1 gradient than April 2013 (both significant at $p < 0.001$) (Figure 3.18F), while the month of July was more significantly explained by the negative factor of PC1 than October 2013 (Figure 3.18F). The post hoc output reflected the significantly higher Chl *a* content in July 2013 ($3.6 \pm 0.4 \mu\text{g Chl } a \text{ cm}^{-2}$) and October 2013 ($4.2 \pm 0.5 \mu\text{g Chl } a \text{ cm}^{-2}$) than in April 2013 ($1.9 \pm 0.4 \mu\text{g Chl } a \text{ cm}^{-2}$) (both significant at $p < 0.001$). The high Chl *a* in July and October 2013 was also concurrent with the months' high tidal range (4.6 m) and high sum of rainfall (5.6 mm), respectively. The significantly positive correlation between Chl *a* with sum of rainfall and also the tidal range further supported the significant relationship between the Chl *a* and the abiotic factors (Table 3.1). In contrast, there was significantly higher CC in April 2013 ($485.3 \pm 78.8 \mu\text{g glucose equiv. cm}^{-2}$) rather than in July 2013 ($310.4 \pm 55.6 \mu\text{g glucose equiv. cm}^{-2}$) and October 2013 ($182.5 \pm 20.4 \mu\text{g glucose equiv. cm}^{-2}$) (both significant at $p < 0.001$).

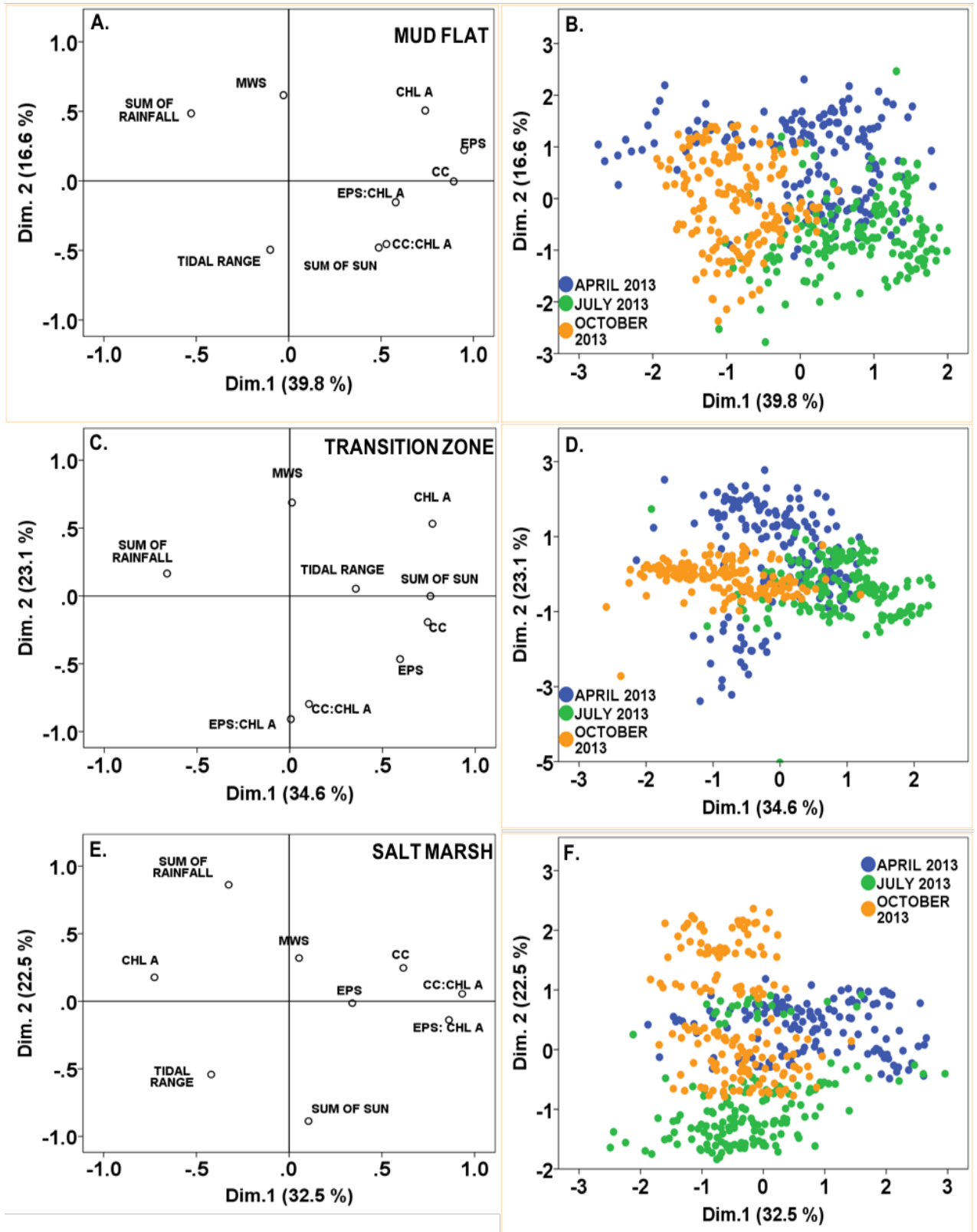


Figure 3.18: Variable factor map of the PCA on; A) the mud flat; C) the transition zone and; E) the salt marsh. Also, the individual factor plots at the temporal monthly scale of the; B) Mud flat; D) the transition zone and; F) the salt marsh.

Table 3.1: Pearson correlation output on the correlation between the overall data (n=504) of biomass proxies (Chl a, CC, EPS, CC:Chl a and EPS:Chl a) on the mud flat, the transition zone and the salt marsh with the weather-related abiotic factors, the mean wind speed, the sum of rainfall, the sum of sun and the tidal range across the three sampling months. *** indicates significant correlation at $p < 0.001$, ** significant at $p < 0.01$ and * significant at $p < 0.05$.

Biomass proxies	Mean wind speed	Sum of rainfall	Sum of sun	Tidal range
Mud flat				
Chl a	0.116***	-0.273***	0.288***	ns
CC	-0.224***	-0.419***	0.367***	ns
EPS	ns	-0.401***	0.384***	ns
CC:Chl a	-0.404***	-0.314***	0.238***	ns
EPS:Chl a	ns	-0.280***	0.251***	ns
Transition				
Chl a	0.230**	-0.174**	0.279**	ns
CC	-0.092*	-0.342***	0.326***	ns
EPS	-0.304***	-0.280***	0.284***	0.165***
CC:Chl a	-0.357***	-0.224***	0.107*	ns
EPS:Chl a	-0.473***	-0.155**	ns	ns
Salt marsh				
Chl a	ns	0.269***	ns	0.111*
CC	0.190***	ns	ns	-0.326***
EPS	ns	ns	0.125**	-0.119**
CC:Chl a	ns	-0.219***	ns	-0.357***
EPS:Chl a	ns	-0.258***	ns	-0.253***

3.3.6.2 Daily variability of MPB biomass proxies across spatial scales

The daily pattern of the scores for the physical state of the biofilm patches across the Fingringhoe tidal flat displayed different patterns according to the sampling months. The different pattern could be related to the daily variability of the weather-related abiotic factors. Clearer relationships between the biomass proxies and the weather-related abiotic factors were present at daily temporal scale compared to monthly temporal scale. The correlation coefficients were determined separately according to days within the three sampling months to investigate whether the biomass proxies responded differently to weather-related abiotic factors at daily temporal scale. Table 3.2 details the ANOVA output of the variability in the daily PC1 and PC2 scores of the biofilm patches on the mud flat, the transition zone and the salt marsh.

‘Sum of rainfall for three days’ could be a potential factor controlling daily variability in the biomass proxies across the tidal flat. The significantly lower CC and EPS contents on the mud flat and the transition zone on the 11th April 2013 than the other sampling days (all significant at $p < 0.001$) (Figure 3.19A & 3.20A) can be explained by the wet (4.4 mm) (the highest rainfall in April 2013) (Figure 3.5A) (Figure 3.6A) weather of the day. Both zones daily PC1 scores were also significantly lower than the other sampling days (all significant at $p < 0.001$). The red circle in Figure 3.5A and 3.6A show the biofilm patches on 11th April on both the mud flat and the transition zone respectively, that pointing toward the left part of PC1. Therefore, further supports that low daily biomass proxies were concurrent with the high ‘sum of rainfall’. There was significant negative correlation between both CC and EPS on both zones with the ‘sum of rainfall’ in April 2013 (Table 3.3). The Chl *a* concentrations on both zones in April 2013 were not significantly affected by the ‘sum of rainfall’. Daily CC and EPS data across the eight quadrats (spatial scale < 5 m) on both zones revealed that almost all of the biofilm patches on this day lost their carbohydrates content on the 11th April (Figure 3.22). There was no significant correlation between the CC and EPS concentrations in April 2013 on the salt marsh with the sum of rainfall. The ‘sum of rainfall’ in April 2013 was significantly positively correlated with the daily variability in Chl *a* concentration of the zone ($r = 0.295$, $p < 0.001$)

(Table 3.3). The 'sum of rainfall' in the wettest month (October 2013), only significantly negatively affected the variability in the EPS concentrations on the transition ($r = -0.187$, $p < 0.05$) and on the salt marsh ($r = -0.215$, $p < 0.01$), and was significantly positively correlated with the Chl *a* concentrations on the salt marsh ($r = 0.193$, $p < 0.05$) (Table 3.3).

The only rainfall in July occurred on the 3rd July 2013 coincided with the shortest sum of sun for three days (Figure 3.5C). The one day rainfall could possibly separate five biofilm patches on the mud flat (Figure 3.19B) and three biofilm patches on the transition zone away from the positive gradient of the PC1 (Figure 3.20B). There was a significantly positive correlation between the PC1 scores of samples of the mud flat in July 2013 with the standard error (SE) of daily mean of Chl *a* ($r=0.331$, $p < 0.001$), CC ($r=0.517$, $p < 0.001$) and EPS ($r=0.482$, $p < 0.001$) on the mud flat (Figure 3.19D) (Table 3.4). Therefore suggests that it was the 'sum of sun' that was responsible for high levels of heterogeneity at spatial scale < 5 m and < 0.5 m in the biofilm patches. Increasing 'sum of rainfall' caused homogeneity in the biofilm patches at the measured spatial scales (< 5 m and < 0.5 m) on the mud flat. In addition, increasing 'sum of rainfall' also enhanced the various biomass proxies on the mud flat in July 2013. The 'sum of rainfall' showed to significantly positively correlate with the Chl *a* (0.209 , $p < 0.01$), CC ($r=0.292$, $p < 0.001$) and EPS ($r=0.326$, $p < 0.001$) in July 2013 (Table 3.3).

Tidal range may also be an abiotic factor potentially controlling the biomass proxies across the tidal flat at temporal daily scale. The daily mean of carbohydrates concentrations of the biofilm patches in April 2013 was the most affected by the tidal range. There was significantly negatively correlation between the tidal range and the daily mean of CC and EPS concentrations on the mud flat and the salt marsh in April 2013 (Table 3.3). Whereas on the transition zone, the Chl *a* and the EPS were the biomass proxies that significantly positively ($r = 0.187$, $p < 0.05$) and negatively ($r = -0.278$, $p < 0.001$) correlated with the tidal range, respectively.

Mean wind speed was the positively correlated with the daily mean of biomass proxies in the biofilm patches of the salt marsh. High average wind speed for three days in April 2013 showed to significantly positively correlated with the Chl *a* ($r = 0.530$, $p < 0.001$), CC ($r = 0.178$,

$p < 0.05$) and EPS ($r = 0.250$, $p < 0.05$) of this zone (Table 3.3). The daily variability in 'mean wind speed' was showed to be an important factor in significantly positively controlling the daily mean of Chl *a* on the transition zone in April 2013 ($r = 0.611$, $p < 0.001$) (Table 3.3). However, the factor was significantly negatively correlated with both daily variability in EPS concentrations on the transition zone in April ($r = -0.285$, $p < 0.001$) and October 2013 ($r = -0.270$, $p < 0.001$) and also the CC in October 2013 ($r = -0.193$, $p < 0.05$) (Table 3.3).

Daily variability in the biomass proxies in the mud flat biofilm patches in October 2013 was not significantly affected by any of the weather-related abiotic factor (Table 3.3). The non-significant correlation was possibly obtained because the weather-related abiotic factor may have significantly affected the biomass proxies variability at the spatial scale < 5 m and < 0.5 m but not at the daily temporal scale. There were significant positive and negative relationships between the standard error (SE) of daily mean of Chl *a*, CC and EPS concentrations in October 2013 on the mud flat with PC1 and PC2 scores of samples on the PCA, respectively (Table 3.4). This suggests that the variability in biomass proxies' variability at spatial scale < 5 m were significantly affected by the abiotic factors that significantly explained both the PC1 and PC2 (Figure 3.19D). Based on the correlation output with the PC1, it can be stated that the variability in biomass proxies variability at spatial scale < 5 m was potentially increased in high 'sum of sun' and were decreased along the increasing 'sum of rainfall' (Figure 3.19D). The negative correlation with PC2 indicates that the increased in tidal variation that significantly correlated with the PC2 may cause higher heterogeneity in the biofilm patches on the mud flat in October 2013.

On the salt marsh, the high variability in the daily scores across the PC2 ($F_{6,159} = 600.7$, $p < 0.001$) of the salt marsh in July 2013, could possibly relate to the effect of the 'sum of rainfall' and the tidal range on the salt marsh biomass proxies (Figure 3.21B). The 'sum of rainfall' was significantly positively correlated with the Chl *a* ($r = 0.269$, $p < 0.001$), CC ($r = 0.174$, $p < 0.05$) and EPS ($r = -0.328$, $p < 0.001$) concentration in the biofilm patches (Table 3.3). Tidal range was significantly reduced the CC concentration of the salt marsh ($r = -0.328$, $p < 0.001$). The highest daily variability on the PC2 of the salt marsh was recorded in the month of October 2013, with

the value of $F_{6,160}=2347$, $p < 0.001$ (Table 3.2). The highest F-value was potentially related to the effect of 'sum of sun hours' and the 'sum of rainfall' on the Chl *a* concentration in the salt marsh's biofilm patches which significantly explained the PC2 of the salt marsh (Figure 3.21D). There was significantly positive and negative effect of the 'sum of rainfall' and the 'sum of sun hours' on the Chl *a* ($r = 0.193$, $p < 0.05$ and $r = -0.191$, $p < 0.05$) on the Chl *a* on the the salt marsh in October 2013, respectively (Table 3.3).

Overall, this study found that the biomass proxies in the biofilm patches of all the zones in April 2013 at both daily and at spatial scale < 5 m was the mostly affected by most of the weather-related abiotic factors. There was a significant correlation between at least one of the biomass proxies with the weather-related abiotic factors in April 2013 at daily temporal scales (Table 3.3). At least two of the SE of daily mean of the biomass proxies in the month of April 2013 was significantly correlated with the PC1 and the PC2 of the mud flat, the transition zone and the salt marsh PCA (Table 3.4). This suggests that the variability in biomass proxies at the spatial scale < 5 m in April 2013 were the mostly affected and significantly controlled by the weather-related abiotic factors.

Table 3.2: Daily differences in the PC1 and PC2 scores within the month of April, July and October 2013 of the biofilm patches of the mud flat, the transition zone and the salt marsh. n = 168.

	Mud flat		Transition		Salt marsh	
	PC1	PC2	PC1	PC2	PC1	PC2
Apr 2013	F6,159=50.3 ($p < 0.001$)	F6,158=86.3 ($p < 0.001$)	F6,157=23.4 ($p < 0.001$)	F6,157=110.9 ($p < 0.001$)	F6,131=39.7 ($p < 0.001$)	F6,131=99.5 ($p < 0.001$)
Jul 2013	F6,158=17.9 ($p < 0.001$)	F6,158=51.3 ($p < 0.001$)	F6,158=14.1 ($p < 0.001$)	F6,158=35.1 ($p < 0.001$)	F6,159=11.4 ($p < 0.001$)	F6,159=600.7 ($p < 0.001$)
Oct 2013	F6,157=16.6 ($p < 0.001$)	F6,157=95.8 ($p < 0.001$)	F6,154=46.4 ($p < 0.001$)	F6,154=39.2 ($p < 0.001$)	F6,160=4.7 ($p < 0.001$)	F6,160=2347 ($p < 0.001$)

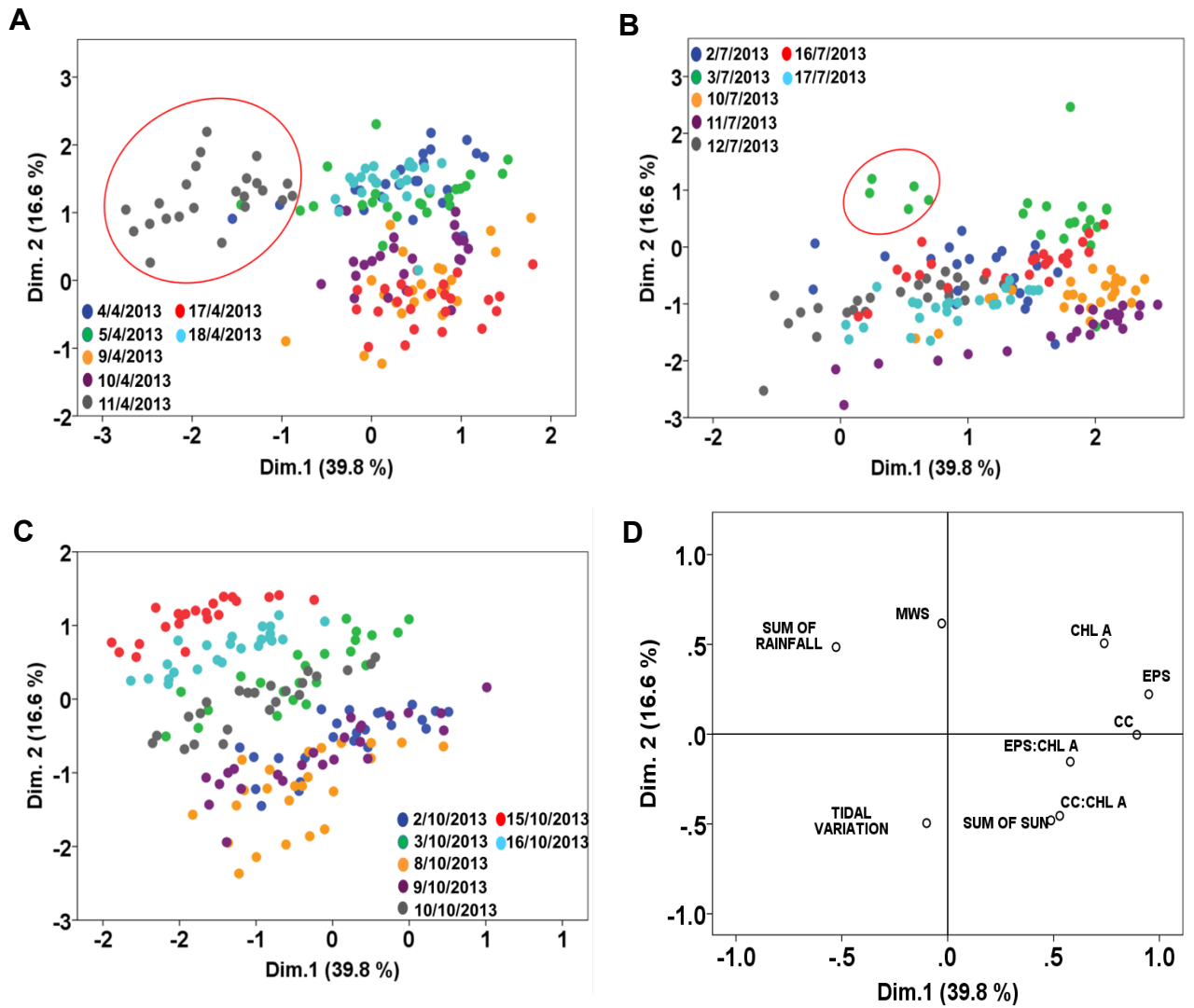


Figure 3.19: Individual plots of PCA of the mud flat at daily temporal scale, showing the samples scores for the physical state of biofilm patches at temporal daily scale in A) April 2013, B) July 2013 and C) October 2013. Also includes in the figure; D) the variables factor map of the mud flat. Circled in Figure 3.19A are the samples on the 11th Apr 2013 while in Figure 3.19B are the five biofilms on the 3rd July 2013 that pointing towards the negative gradient of PC 1.

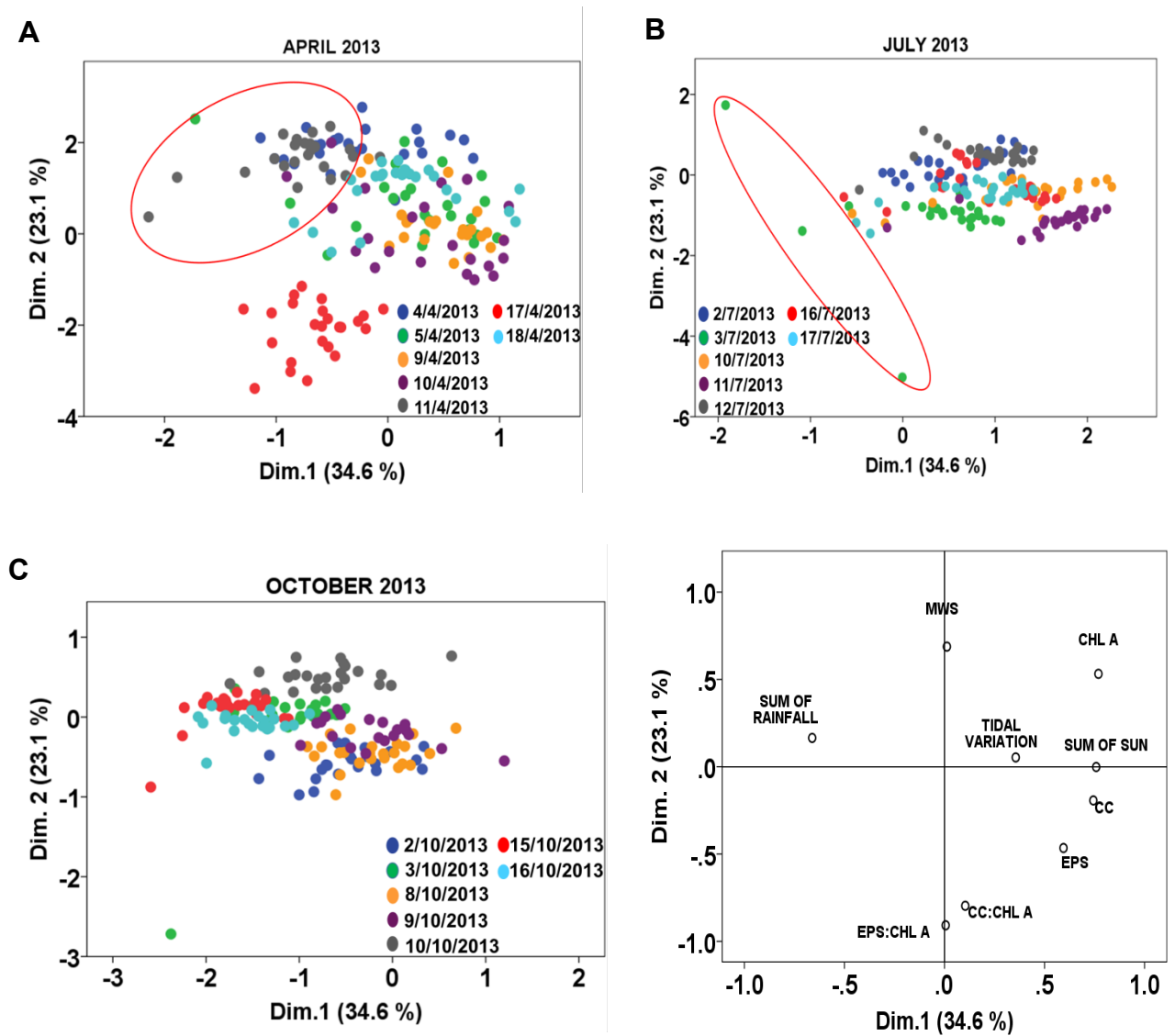


Figure 3.20: Individual plots of PCA of the transition zone showing the samples scores for the physical state of biofilm patches at temporal daily scale in A) April 2013, B) July 2013 and C) October 2013. Also includes in the figure; D) the variables factor map of the transition zone. Circled in Figure 3.20A are the samples on the 11th Apr 2013 while in Figure 3.20B are the three biofilms on the 3rd July 2013 that pointing towards the negative gradient of PC 1.

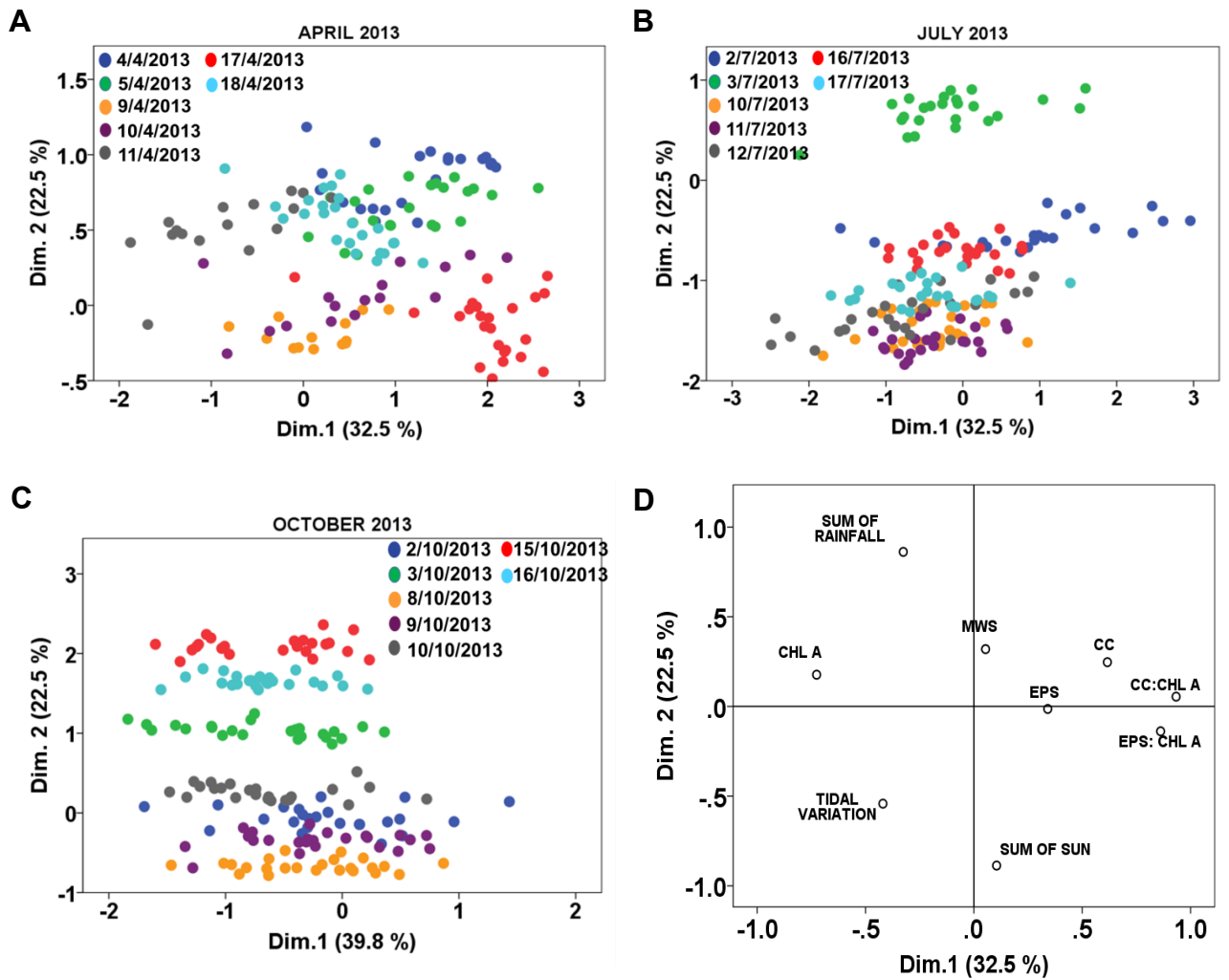


Figure 3.21: Individual plots of PCA of the salt marsh showing the samples scores for physical state of biofilm patches at temporal daily scale in A) April 2013, B) July 2013 and C) October 2013. Also includes in the figure; D) the variables factor map of the salt marsh.

Table 3.3: Pearson correlation coefficients (n= 168) between the Chl *a*, CC and EPS concentrations with the measured weather-related abiotic factors at daily temporal scale in April, July and October 2013. ***, ** and * indicates the correlation was significant at $p < 0.001$, $p < 0.01$ and $p < 0.05$, respectively.

	Tidal range	Mean wind speed	Sum of rainfall	Sum of sun
April 2013				
Mud flat				
Chl <i>a</i>	ns	ns	ns	0.195*
CC	-0.377***	-0.342***	-0.699***	0.198*
EPS	-0.355***	ns	-0.406***	0.302***
Transition				
Chl <i>a</i>	0.187*	0.611***	ns	0.315***
CC	-0.278***	ns	-0.495***	0.319***
EPS	ns	-0.285***	-0.280***	ns
Salt marsh				
Chl <i>a</i>	ns	0.530***	0.295***	0.359***
CC	-0.342***	0.178*	ns	0.434***
EPS	-0.546***	0.250*	ns	0.482***
July 2013				
Mud flat				
Chl <i>a</i>	-0.157*	ns	0.209**	ns
CC	ns	ns	0.292***	ns
EPS	ns	ns	0.326***	ns
Transition				
Chl <i>a</i>	ns	ns	ns	ns
CC	ns	ns	0.217**	ns
EPS	ns	ns	0.421***	-0.180*
Salt marsh				
Chl <i>a</i>	ns	ns	0.269***	ns
CC	-0.328***	-0.205**	0.174*	-0.167*
EPS	ns	ns	-0.328***	ns
October 2013				
Mud flat				
Chl <i>a</i>	ns	ns	ns	ns
CC	ns	ns	ns	ns
EPS	ns	ns	ns	ns
Transition				
Chl <i>a</i>	ns	ns	ns	ns
CC	ns	-0.193*	ns	ns
EPS	-0.187*	-0.270***	-0.187*	ns
Salt marsh				
Chl <i>a</i>	ns	ns	0.193*	-0.191*
CC	ns	ns	ns	ns
EPS	ns	ns	-0.215**	0.170*

Table 3.4: The PC1 and PC2 that significantly correlated with the Chl *a*, CC and EPS concentrations variability at spatial scale < 5 m. The variability at both spatial scales were represented by the calculated value of standard error (SE) of the daily mean. ***, ** and * indicates the correlation was significant at $p < 0.001$, $p < 0.01$ and $p < 0.05$, respectively.

	April		July		October	
	PC 1	PC 2	PC 1	PC 2	PC 1	PC 2
Mud flat						
Chl <i>a</i>	ns	0.282***	0.331***	0.586***	0.398***	-0.430***
CC	0.601***	-0.715***	0.517***	0.203***	0.425***	-0.345***
EPS	0.686***	-0.192*	0.482***	0.337***	0.474***	-0.447***
Transition						
Chl <i>a</i>	0.213**	0.748**	-0.171*	0.187*	0.463***	0.208**
CC	0.343***	ns	ns	-0.561***	0.551***	ns
EPS	0.326***	-0.558	ns	-0.557***	0.459***	ns
Salt marsh						
Chl <i>a</i>	ns	0.445***	0.418***	0.640***	ns	-0.340***
CC	0.264**	0.319***	0.470***	0.342***	0.163*	ns
EPS	0.534***	ns	0.427***	ns	ns	-0.212*

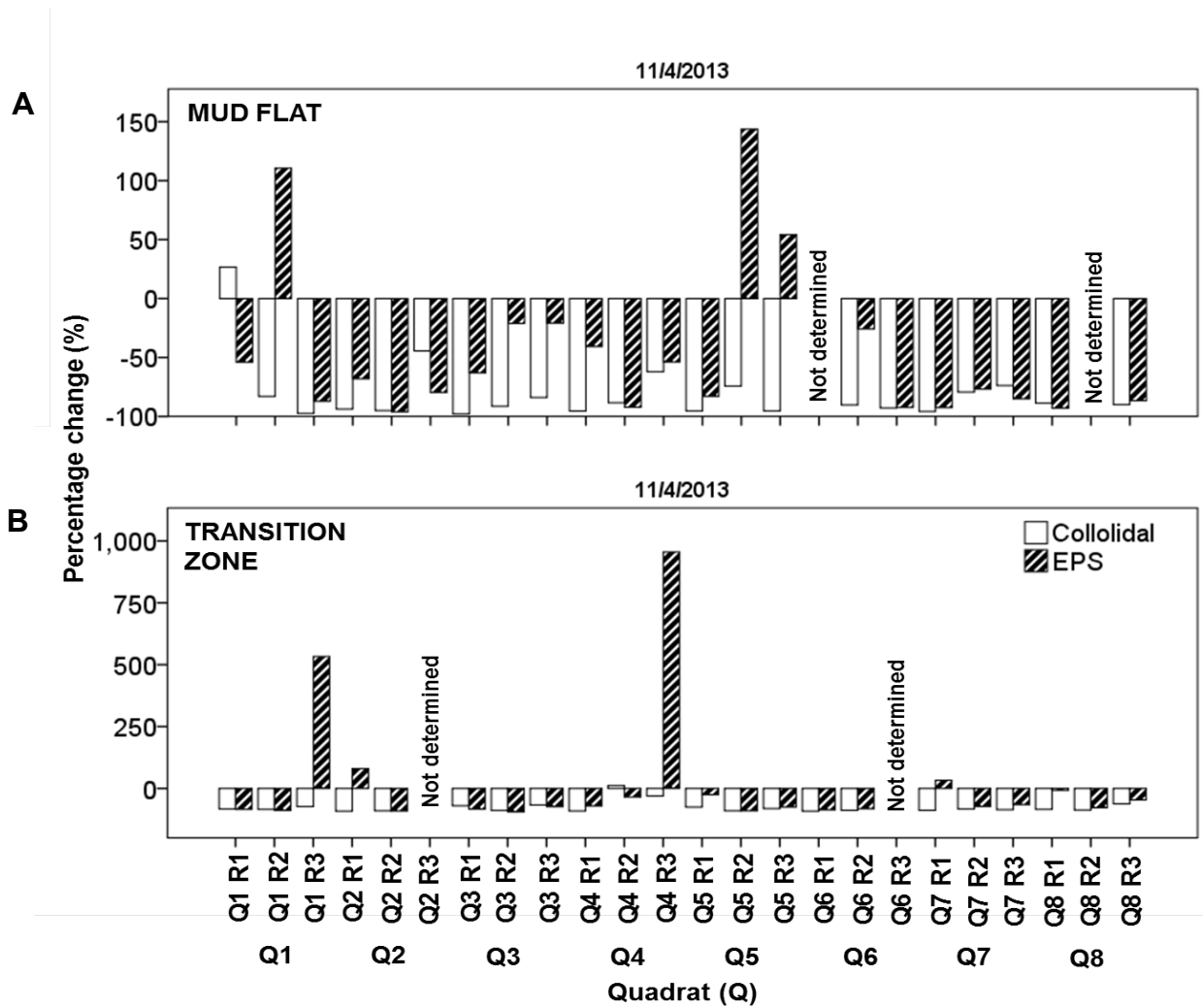


Figure 3.22: Percentage change of CC and EPS concentrations on 11th April on the; A) mud flat and; B) the transition zone. Negative percentage change indicates that most biofilm patches on this day had lower carbohydrates content than previous day (10th April 2013). Q indicates quadrat and R indicates replicate.

3.4 DISCUSSION

3.4.1 Variability of MPB biomass proxies across the intertidal flat

Higher MPB biomass was consistently recorded on the mud flat and the transition zone rather than on the salt marsh. A potentially finer sediment type of the mud flat and the transition zone than on the salt marsh possibly makes these sites more conducive to be inhabited by MPB. This finding agrees with Du et al. (2009) that suggested MPB biomass was positively correlated with mud and fine sand rather than to medium sediment. The mud flat and the transition zone that are exposed to diel tidal cycle must potentially have wetter sediment. Therefore, both zones' sediment surfaces have better nutrient supply than the salt marsh. The MPB on the salt marsh are susceptible to be affected by the desiccation with the zone's increasing height on shore (Underwood, 1997; Jackson et al., 2010; McKew et al., 2011). The salt marsh at our study site is characterized by low exposure to tidal cover which can potentially cause sediment desiccation, which consequently resulted in the zone low Chl *a* concentration. In their stimulated desiccation research, McKew et al. (2011) reported that most tidal flat's diatom cells migrated to wetter sediment downward from the sediment surface. They presumed that the downward migration is an avoidance strategy by the mud flat's diatoms to avoid desiccation. This avoidance strategy potentially can be the main reason for the phenomenon on the salt marsh.

Although there was no significant different in the biomass content between the mud flat and the transition zone, the biomass proxies on the transition zone did show a relatively higher concentration than the mud flat. The transition zone was located adjacent to the salt marsh's bank, and could possibly receive input of MPB from the sediment of eroded bank due to waves and tidal activities. Based on the observation, there was clearly a benthic biofilm covering the top sediment of the bank during emersion. A quite similar finding discussing only sediment by Mitchell et al. (2003), reported that bank erosion positively contributed to greater availability of sediment in water column adjacent to the bank. MPB cells are reported to be significantly

associate with the suspended sediments (De Jonge & Van Beusekom, 1995; Koh et al., 2006; Brito et al., 2012). This further supports the idea that the relatively higher biomass on the transition zone could be attributed to salt marsh's bank's sediment and associated MPB deposition.

The high Chl *a* on both mud flat and transition zone was also reflected by high CC concentration. The mean percentage of EPS in colloidal (CC) extract of respectively 34.14 % and 28.9 % on the mud flat and the transition zone, were in the range of the percentage (11 – 37 %) of EPS in colloidal extract in axenic culture as reported by Underwood and Smith (1997) and below the ~ 40% value as reported by Taylor et al. (2013) from the Colne estuary. The significant correlation between Chl *a* and CC concentrations on the mud flat and the transition zone further supported the idea that the CC and EPS contents on both zones were originated from the MPB. The higher percentage value of 66.33 % of EPS in CC that was recorded on the salt marsh, resulted in a non-significant correlation of Chl *a* and CC on the zone. This confirms that the CC and EPS concentrations on the salt marsh did not purely originate from MPB but also potentially from the vegetation on the salt marsh. The non-significant relationship between Chl *a* and CC in our study was in agreement with study done by Underwood (1997) who also reported a similar non-significant correlation for microbial assemblages consist of less than 30 % diatom cells on a salt marsh restoration site in Blackwater, Essex, UK. His study also proved and stated that only assemblages with more than 50 % diatom cells possess the ability to produce CC in the sediment and gain biostabilization potential. Nonetheless, the non-significant relationship between Chl *a* with CC and EPS on the salt marsh can be due to MPB stress response towards extreme salinity and desiccation (as mentioned in the first paragraph). Downward migration of MPB due to salinity and desiccation (McKew et al., 2011) on the salt marsh may cause the lower benthic Chl *a* and higher CC and EPS on the zone.

Nonetheless, the non-significant Chl *a* and CC on the salt marsh can be attributed to the high occurrence of cyanobacteria in salt marsh sediment (Underwood, 1997; Sullivan &

Moncreiff, 1990), which is characteristically produced more tightly bound polymers than benthic diatoms (Underwood et al., 1995).

3.4.2 Effect of weather-related abiotic factors on biomass proxies variability at multi-scales

It was hypothesized that the temporal variability in the measured weather-related abiotic factors will have different effects on the biofilm patches of different zones, the mud flat, the transition zone and the salt marsh. The chosen weather-related abiotic factors were hypothesized to have different effect on different physical state of biofilm patches of similar zones (within spatial scale < 5 m and < 0.5 m) and across different temporal monthly and daily scales in neap-spring-neap tidal cycle.

3.4.2.1 Chl *a*, CC and EPS variability at monthly or seasonal temporal scale

Investigation on temporal variability of MPB has been commonly carried out to study the correlation between benthic Chl *a* with weather-related abiotic factors (Easley et al., 2005; van der Wal et al., 2010; De Jonge et al., 2012; Benyoucef et al. 2013). This present study however discusses not only relationship between Chl *a* but also the CC and EPS contents in the top 2 mm biofilm patches with weather-related abiotic factors.

Monthly variability in the benthic Chl *a*, CC and EPS of biofilm patches in the Colne estuary at temporal monthly scales was strongly influenced by two chosen abiotic factors, the 'sum of sun' for three days and the sum of rainfall for three days. Biomass proxies on the mud flat and the transition displayed similar response to abiotic factors, the 'sum of sun hours' and the 'sum of rainfall'. Longer period of sun (July 2013) with less rainfall event in Colne estuary resulted in significantly higher Chl *a*, CC and EPS content of the biofilm patches on both zones

than in wet and stormy weather (in October 2013). Therefore this was in agreement with other studies on the positive effect of sunlight either in terms of irradiances (Pan et al., 2013) or attenuation (Ubertini et al., 2015) during emersion period. Also, this confirms that longer 'period of sun hours' in July 2013 (summer) and spring (April 2013) than in October 2013 is certainly as important as the light energy in enhancing the production of MPB as well stimulating the vertical migration (Consalvey et al., 2004; Serôdio et al., 2006) of MPB to top 2 mm of sediment (de Brauwer & Stal, 2001). Seasonally, longer 'period of sun hours' as in July 2013 (summer) which resulted in longer emersion period during periods of daylight, potentially responsible to cause higher biomass on the mud flat and the transition zone than in April 2013 and October 2013.

The response of the biomass proxies on the salt marsh to the sum of sun and sum of rainfall were in contrast to the patterns measured on mud flat and the transition zone. The different weather-biomass relationship that was observed on the salt marsh must be subjected to the zone's obvious different characteristic (as discussed in 3.4.1). On the salt marsh, wetter condition positively increased the Chl *a* of the biofilm patches. Salt marsh sediment that is only covered with water during spring tide is drier than the sediment on the mud flat (Midlen & Ferreira, n.d.; Le Rouzic, 2012). Hence, any input of moisture in the sediment will give a positive effect on the zone's chl *a* concentration (Sullivan & Moncreiff, 1988; Costa et al., 2002).

Tidal range was a significant abiotic factor in determining the monthly variability in the biomass proxies on the salt marsh. However only Chl *a* was significantly and positively affected by the tidal range. The other biomass proxies showed negative correlations. Increased water and nutrient supply due to tidal submersion during spring tide (Le Rouzic, 2012) possibly enhanced the increased in Chl *a* concentration on the salt marsh at our study site. The CCs (CC and EPS) that are not bound to the MPB cells (Underwood et al., 1995) are susceptible to be washed away during the submersion. In addition, wetter conditions due to spring tide cover could also stimulate the upward migration of the MPB that presumably move downward the sediment during neap tide to avoid desiccation (McKew et al., 2011).

3.4.2.2 Daily variability of MPB biomass proxies across the tidal flat

Investigation of the relationships between MPB biomass proxies with weather-related abiotic factors at temporal monthly scale in this study has revealed the strong influence of the sum of rainfall and period of sun. The temporal factor 'month' contributed less than 35 % of the Chl *a*, CC and EPS total variability across Fingringhoe tidal flat. This study also investigated the variability of the MPB biomass proxies across the chosen weather-related abiotic factors at micro-spatial scales < 5 m similar zones within the temporal daily scale. There were complicated weather-biomass relationships which may not be revealed if studies on MPB variability are only done at large temporal and spatial scales.

Daily MPB biomass in the biofilm patches in the mild wet month of April 2013 was showed to mostly affect by the chosen weather-related abiotic factors. High 'sum of rainfall' has been frequently reported as an important driver responsible to wash away the CCs from the sediment surface (Taylor et al., 1965; Orvain et al., 2014) on the mud flat and the transition zone. Therefore rainfall may be responsible for destabilizing the MPB biofilm patches on both zones in April 2013. Consequently, the unstable sediment surfaces of both zones in April 2013 were susceptible to be negatively affected by the resuspension drivers, the mean wind speed (Brito et al., 2012; De Jonge & Van Beusekom, 1995) and the tidal range (Koh et al., 2006; Uncles et al., 1998) during immersion period. Because of the strong significantly positive correlation between the 'mean wind speed' and the wave height ($r = 0.648$, $p < 0.001$) (Figure 3.6), it can also be stated that it was the wind-induced wave and the tidal range that negatively affected the sediment surface (De Jonge & Van Beusekom, 1995; Easley et al., 2005; Ubertini et al., 2015) in April 2013 on both zones during immersion period.

Despite its negative effects on the CC and EPS concentrations on both the mud flat and the transition zones, both mean wind speed and the tidal range were significantly positively correlated with the Chl *a* concentrations of both mentioned zones. As discussed in 3.4.1, the

finding can be due to the adjacent location of the transition to the salt marsh's bank. Therefore, the transition zone could possibly receive input of MPB from the sediment of eroded bank due to waves and tidal activities. Increased energy during the spring tide at my study site was observed to erode the adjacent salt marsh's bank and enhanced the deposition of sediment and its associated MPB on the transition zone. This is further supported by the increasing Chl *a* on the transition zone across the spring tide period in July 2013. A quite similar finding, however discussing only sediment, by Mitchell et al. (2003), suggested that bank erosion contributes to greater availability of sediment in water column which resulted in high suspended sediment that was deposited on the transition zone.

Tidal range was a distinctive factor that differentiates the output of PCA of the mud flat and the transition zone (Figure 3.19 & 3.20). The investigation at monthly temporal scale did not able to highlight the link between the biomass proxies and tidal range on the mud flat and the transition zone. In contrast, at the smaller daily temporal scale, a clearer relationship was observed. The negative relationship as presented in Table 3.3 (April 2013), can be related to the ability of the spring tide's high energy current to wash away and resuspend some biomass-related material of the biofilm patches (Koh et al., 2006; Dupuy et al., 2014) on the mud flat, the transition zone and also the salt marsh. Studies investigating a small temporal scale, the 'between days' MPB variation, successfully demonstrated that the MPB daily variation is strongly affected by the tidal types, the spring tide and the neap tide (Blanchard, et al., 2006; Spilmont, et al., 2007). Therefore, it can be stated that the finding in this present study is comparable to those finding by Blanchard et al., (2006) and Spilmont et al., (2007).

Tidal range was initially hypothesized to have a positive effect on the daily biomass proxies on the salt marsh. However tidal range showed to cause significant decreased in the biomass proxies of the zone. Such condition could be subjected to opposing influences of immersion during spring tide (Le Rouzic, 2012). The so called opposing influences suggests that the effect of periodic sea submersion on the salt marsh not only supplies resources but at the same time destabilizes the salt marsh's sediment surface and allows the resuspension of

microorganisms to happen.

Daily variability in biomass proxies during July 2013 across the intertidal flat showed to significantly positively correlate with the 'sum of rainfall'. This finding was completely different than most studies that have reported the strong negative effect of rainfall on MPB biofilm's biomass concentration (Rasmussen et al., 1983; Costa et al. 2002; Ribeiro et al. 2013). Longer 'sum of sun' for three days in the summer (July 2013), could potentially cause the movement of MPB cells to sediment below towards wetter area to avoid desiccation (McKew et al., 2011). Or perhaps, the longer 'sum of sun' possibly reduced the MPB production (Kwon et al., 2012). Therefore any input of water content in the sediment surface on the tidal flat as from the rainfall event will stimulate the upward vertical migration or stimulates the MPB production, respectively. Hence there was significant increase in the daily mean of the Chl *a* on the mud flat.

Daily mean CC and EPS concentrations on the transition zone were significantly positively correlated with the 'sum of rainfall', whereas, transition zone Chl *a* concentrations showed non-significant correlations with 'sum of rainfall'. The rainfall presumably influences the downward migration (Taylor et al., 1965) of the MPB in the stable biofilm patches. Hence, more CC and EPS are produced and secreted due to cells' movement (Smith & Underwood, 1998). Taylor et al. (1965) suggested that rainfall can be the potential mechanical disturbance that stimulates MPB to migrate downward in advance incoming tide. This might be an explanation for the significant positive correlation between CC and EPS, and the non-significant correlation between the Chl *a* on the transition zone with sum of rainfall in July 2013. There was significantly higher CC:Chl *a* and EPS:Chl *a* ratios on the transition zone on the 3rd July (Appendix 1) than the other sampling days in July 2013. Therefore further supported that the mechanical disturbance by rainfall as reported by (Taylor et al., 1965) potentially caused such condition on the transition zone due to the increased sum of rainfall in July 2013.

3.4.2.3 MPB biomass proxies' variability at spatial scale < 5 m and < 0.5 m across the tidal flat

MPB biomass proxies' daily variability in the top 2 mm of the biofilm patches in October 2013 was the least affected by the weather-related abiotic factors. The low biomass concentration on the sediment surface may be responsible to cause the non-significant effect of the abiotic factors with the daily biomass proxies primarily on the mud flat. The variability in Chl *a*, CC and EPS at spatial scale < 5 however, were shown to be significantly affected by 'sum of sun hours', 'sum of rainfall' and the tidal range.

This present study is the first work that showed the spatial heterogeneity due to the increased 'sum of rainfall' and the tidal range. Often, studies discussed the effect of grazers that causes high micro-spatial heterogeneity by means of fragmented patches (Orvain, et al., 2006; Weerman et al., 2012). Increased 'sum of rainfall' on the other hand caused homogeneity in the daily variability of the biomass proxies of not only the mud flat, but also the transition zone in October 2013. The ability of 'sum of rainfall' to strongly wash away the MPB biomass, primarily CC and EPS as reported by Orvain et al. (2014), may cause homogeneity in the biomass concentration of the biofilm patches. The low MPB biomass potentially caused the biofilm patches losing their ability to self-organize. The effect of rainfall in controlling the self-organized patterns has never been discussed for the MPB, but has been discussed for the vegetation. Barbier et al. (2008) found that decreases in rainfall induce the breakdown of patches into smaller patches, and later prolonged decrease will result in the collapse of the self-organised patches. The different effect of the rainfall on the self-organised patch of vegetation and the MPB biofilm could be subjected to both patches different habitat, body sizes (Azovsky et al., 2004) and potentially different physiology.

Similar to the effect of the abiotic factors on the daily variability, the variability of the MPB biomass proxies at spatial scales < 5 m and < 0.5 m across the tidal flat also showed different

response the abiotic factor according to sampling months and also the zones' height. Study on the effect of weather-related abiotic factors and also other biotic and abiotic factors on the variability of benthic Chl *a*, CC and EPS variability at micro-spatial scales are not only crucial in studying the self-organized pattern of the MPB biofilms but also for better understanding on bio-stabilisation and MPB resuspension. Since it is the changes in the benthic Chl *a* and benthic colloidal carbohydrates of MPB biofilms that control the erosion rates of the sediment and the sediment's associated MPB (Weerman et al., 2012) from the sediment surface of the MPB biofilms.

3.5 Conclusion

My study confirmed that there was a complex interaction between weather-related abiotic factors with Chl *a*, CC and EPS contents of the biofilm patches across the intertidal flat. The effect of weather-related factors is different according to different zones or levels across the Colne estuary. Each of weather-related abiotic factors showed to have a different effect on the benthic Chl *a*, CC and EPS contents across different spatial and temporal scales. For instance, there was weaker effect of rainfall on MPB biofilm patches in summer (July 2013) that has longer period of 'sum sun hours' compared to spring (April 2013) that has shorter 'period of sun hours' and higher 'mean wind speed'. Higher wind speeds intensify the negative effect of increasing tidal range during spring tide on the MPB biomass, especially on the CC and the EPS.

A clearer relationship between weather-related abiotic factors and biomass proxies can be observed at smaller temporal scale rather than at large temporal scale. Study on the correlation between MPB biomass proxies with weather-related factors will be more informative if data on suspended sediment and suspended Chl *a* are included. Weather-related abiotic

factors such as tidal range and mean wind speed not only affected the MPB during emersion but also during immersion period.

Table 3.5 details the addressed hypotheses that have been accepted and rejected in Chapter 3.

Table 3.5: Hypotheses that were addressed in Chapter 3. Also stated whether the hypothesis were accepted or rejected.

Hypotheses (page 15-17)	Accepted	Rejected
A1	/	
A5	/	
B1	Only for mud flat	For transition zone and salt marsh
B2	Chl a on mud flat and transition zone	Chl a on salt marsh
B3	For mud flat and transition zone	Salt marsh
B4	Yes for salt marsh	Yes for mud flat
B5	/	
C1	/	
C2	/	
C3	/	

CHAPTER 4

VARIABILITY IN THE CHL *a* CONCENTRATION OF THE MICROPHYTOBENTHOS (MPB) BIOFILM PATCHES ON AN INTERTIDAL FLAT: INFLUENCE OF SPECIES COMPOSITION ACROSS NEAP-SPRING-NEAP TIDAL CYCLES.

4.1 INTRODUCTION

Intertidal microphytobenthos (MPB), the community of benthic diatoms and associated species that dominate many soft-sediment habitats, often exhibit significant levels of spatial variability in biomass. In chapter 3, it was shown that more than 20 % of Chl *a*, CC (CC) and extracellular polymeric substance (EPS) variability within the Colne Estuary, UK was due to differences between replicates at spatial scale < 0.5 m. As important as these biomass proxies are, an understanding on how diatom species composition changes over varying scales is also vital in studying the ecology of MPB assemblages.

The diatom species assemblage composition is potentially an important factor that influences the temporal and spatial variability of the biomass (Underwood, 1994) on an intertidal flat across tidal variation and across abiotic gradients (Cibic et al., 2007; Thornton et al., 2002). Numerous studies have reported that MPB biomass (in terms of Chl *a*) and MPB assemblage composition displayed similar response to spatial and temporal variability of nutrients (Cibic et al., 2007; Thornton et al., 2002), sediment composition (Du et al., 2010; Woelfel et al., 2007) and also abiotic parameters such as the light intensity (Thornton et al., 2002; Scholz & Liebezeit, 2012) and salinity (Skinner et al., 2006). These cited studies support the idea that there are potentially significant relationships between the MPB biomass, primarily Chl *a*, with the species composition of the same biofilm patch.

Work done by Underwood (1994) in the Severn estuary reported a significant correlation between some of the most abundant species with the community diversity index (H'). He found that the diversity index was negatively correlated with the relative abundance of *Nitzschia pargemina* and *Nitzschia epithemoides* but positively correlated with the abundance of *Coscinodiscus* sp., *Raphoneis minutissima*, *Gyrosigma spencerii* and *Navicula flauaticum*. The study however did not discuss any detailed correlation between MPB assemblages or diversity with MPB biomass proxies. But the work did mention that the seasonal variability observed in the diatom species composition tallied with the seasonal changes of the diatom biomass, and this was positively correlated with the temperature and interrupted by stormy weather (Underwood & Paterson, 1993).

Forster et al. (2006) detailed the relationship between the MPB biomass and diversity in Waterschelde estuary in Netherlands and successfully found a significant relationship between the two proxies. Hence, they concluded that similar to terrestrial plant and soil communities, the MPB on the tidal flat also displayed a significant biodiversity-ecosystem function relationship. One of major findings of their study was that the MPB biomass was inversely correlated with their diversity. Additionally they also reported a significant positive and unimodal relationship between the net primary production and the diversity, which also appeared to be site-specific across a salinity gradient.

The relationship between MPB assemblage with MPB biomass in the Colne estuary was reported in the work done by Thornton et al. (2002). They found that species from the genus *Navicula* was the dominant genus in most MPB assemblages in Colne estuary and caused peaks in Chl *a* concentration when the abundance of single species was more than 65 % of the total abundance. Works by Underwood (1994), Thornton et al. (2002) and Forster et al. (2006) have highlighted the significant relationship between diatom species with MPB community and also biomass concentration on an intertidal flat. Therefore in this chapter, the species composition data were investigated to determine if it is by knowing the species

composition can help in understanding the changes in biomass variability across the neap-spring-neap tidal cycle.

With respect to the questions of whether MPB biomass and MPB species abundance / assemblage display similar responses to a number of abiotic factors, this present work set out to test the following hypothesis; (1) there is a significant relationship between Chl *a* concentration with the diversity of the MPB assemblages; (2) stability in Chl *a* concentration at both temporal and spatial scales must be closely linked to the species richness and the occurrence of dominant species (Thornton et al., 2002) rather than to the species equitability (evenness); (3) the relationship between MPB Chl *a* concentration and MPB assemblage's diversity is controlled by the temporal variability of weather-related abiotic factors, especially the tidal range and wind speed that frequently reported as the drivers in the MPB resuspension on an intertidal flat (De Jonge & Van Beusekom 1995; Ubertini et al. 2012; Ubertini et al. 2015).

4.2 METHODS

4.2.1 Sampling strategy

Sediment samples were collected in three different months; in April, July and October 2013 across Fingringhoe tidal flat in Colne estuary. In each month, seven days of sampling (2 days in early neap tide, 3 days in spring tide and 2 days in later neap tide) were carried out across the neap-spring-neap tidal cycle. Three different zones were chosen at the distance > 5 m apart (mud flat, transition and salt marsh) which lie parallel to River Colne. Both mud flat and transition zones were located on the un-vegetated area of tidal flat. These areas are covered with water in every high tide through the whole tidal cycles. On the other hand, the vegetated salt marsh is only covered with sea water during spring tides. Eight quadrats were built on each zone, in which triplicate samples were obtained using minicore on each sampling day.

4.2.2 Samples preparation for analyses

In the lab, each minicore was extruded so that only the top 2 mm of the sample remained in the syringe. The lower portion of the sediment was discarded while the remaining sample was divided into two. Half of it was placed into 7 ml bijou bottle for Chl *a* analyses. Sediment samples for Chl *a* analyses were freeze dried. The Chl *a* analyses was carried out by following Lorenzen (1967) procedure (detailed in chapter 2). The balance of the sediment was transferred into 15 ml falcon tube and was preserved using 0.5 % glutaraldehyde in 2.3% NaCl for cell identification and cell count.

4.2.3 Cells count

For diatom cell counts, sample in falcon tubes was centrifuged at 1570 g for fifteen minutes. After that, excess glutaraldehyde (supernatant) was discarded using a teat pipette. Five ml distilled water was added into the tube, which then was agitated. Half of the sample was transferred into a sample bottle as a fresh fixed specimen and was preserved in 0.5 % glutaraldehyde. The remaining sample was cleaned following acid washing (32% HCl) procedures for a permanent slide preparation mounted in naphrax solution (Underwood, 1994). Exactly four hundred valves were identified and counted on each slide for the April 2013 and July 2013 samples collected from the mud flat and the transition zones (Table 4.1). While only two hundred and fifty valves were counted for all the salt marsh samples and for October 2013 samples for both mud flat and the transition zone due to their low diatom cells (Table 4.1). A total of 504 samples were counted for each zone to represent the diatom taxonomic data. Diatom species were identified at least to genus level based on the literature by Van der werff & Huls (1976), Snoeijs & Vilbaste (1994), Underwood (1994), Hartley, et al., (1996) and Lange-

Bertalot (2000). The relative abundance of the diatom was calculated as percentage of the total counted cells of each sample.

4.2.4 Statistical analyses

MPB community diversity was calculated from the relative abundance data based on Shannon-Wiener diversity index (H') by using Multi Variate Statistical Package (MVSP) 3.1 software (Kovach, 1999). ANOVA tests were applied to determine the significant differences in temporal and spatial variation of Chl *a* concentration and in MPB assemblage's diversity (H').

Principal component analyses (PCA) were performed on the diatom species relative abundance and the diversity measures (the evenness (E) and / or the species richness) to determine the species that significantly related to the MPB diversity. The test was carried using the FactoMineR package in R. Only species with relative abundance of more than 1 % were included as active variables in this analysis. Only the principal component 1 (PC1) and 2 (PC2) were retained. Pearson correlation coefficients test were carried out on the PC1 with the E values and the species richness of the assemblages, to determine whether there was a significant relationship between the Chl *a* and the species composition of the assemblages with both mentioned diversity functions.

Table 4.1: Counted cells for each sample slide for the samples collected from the mud flat, the transition zone and the salt marsh in three different months. Overall, there were 504 slides counted for the mud flat and the transition zone. Whereas a total of 216 slides were counted for the salt marsh zone.

Zones	Sampling month	Counted cells
MUD FLAT & TRANSITION ZONE	April 2013 and July 2013	400
	October 2013	250
SALT MARSH	April 2013, July 2013 and October 2013	250

4.3 Results

4.3.1 General characteristic of MPB assemblage species composition

Seventy MPB species were identified in the counted samples. *Gyrosigma balticum* was the most common species of the mud flat and the transition zone's assemblages. The species was recorded as the main contributor in most assemblages in both neap and spring tides samples of both zones (Table 4.2 & Table 4.3). The highest mean relative abundance (32.11 ± 1.31 %) of *G. balticum* was in the mud flat neap tide samples in April 2013 (Table 4.2).

The relative abundance data showed that the top ten most common species on the mud flat were often comprised of not only benthic but also centric diatom species such as the *Stephanodiscus* sp1, *Coscinodiscus* spp. and *Actinoptychus splendens* (Table 4.2). The relative abundance of these centric species on the mud flat was relatively increased during spring tides (Table 4.2). There was a higher species richness of centric diatoms in the mud flat's samples during spring tide than in the neap tide. Five out of the top ten species on the mud flat in April 2013 during spring tide were the centric diatoms, the *Odontella aurita*, *Coscinodiscus* sp1, *Coscinodiscus* sp2, *Coscinodiscus* sp3 and *Actinoptychus splendens* (Table 4.2). The occurrence of centric diatoms showed to increase from only two to five recorded species in the top ten most common species in neap and spring tides in April 2013, respectively. There was however no centric diatom recorded in the top ten most occurring species list in spring tide in October 2013 (Table 4.2). On the other hand, spring tide occasion was least likely to cause an increased in centric diatoms occurrence on the transition zone in all months.

MPB assemblages on the salt marsh were comprised of smaller size ($< 50 \mu\text{m}$) diatom species compared to the mud flat and the transition zone. *Opephora* sp1 with the cell length less than $40 \mu\text{m}$ had the highest mean relative abundance during neap tide in both April (11.63 ± 1.21 %) and July 2013 (15.72 ± 1.41 %) samples (Table 4.4). While *Nitzschia vitreae* (cell length less than $< 40 \mu\text{m}$) was the main species of the salt marsh assemblages during neap tide

in October 2013 with mean relative abundance of 15.28 ± 1.68 % (Table 4.3). In the spring tide, the top ten most occurring species on the salt marsh were found to comprise of species that were common on the mud flat and the transition zone, for example, species from the genus *Gyrosigma*, *Navicula*, *Nitzschia* and *Diploneis* (Table 4.3). *Opephora* sp1 that had high relative abundance in neap tide samples in April 2013 (11.63 ± 1.21 %) and July 2013 (15.72 ± 1.41 %) was not recorded as the top ten species in spring tide samples in April and July 2013 (Table 4.3) but was replaced by larger species, *G. balticum* and *P. angulatum* in both April and July 2013 samplings, respectively.

Table 4.2: Relative abundance (%) of the top ten most common diatom taxa identified in the top 2 mm per cm² sediment of the mud flat across the tidal cycle in April 2013, July 2013 and Oct 2013. Values of the RA of neap tide and spring tide are the mean \pm SE of pooled four and three days of neap and spring tides sampling data, respectively. n value for neap tide is 240 and spring tide is 216.

	Neap tide	Relative abundance (%)	Spring tide	Relative abundance (%)
April 2013	<i>Gyrosigma balticum</i>	32.11 \pm 1.31	<i>Gyrosigma balticum</i>	11.53 \pm 0.54
	<i>Nitzschia sigma</i>	4.68 \pm 0.42	<i>Nitzschia sigma</i>	5.13 \pm 0.26
	<i>Stephanodiscus</i> sp1	4.06 \pm 0.22	<i>Odontella aurita</i>	4.75 \pm 0.27
	<i>Gyrosigma fasciola</i>	3.54 \pm 0.22	<i>Nitzschia panduriformis</i>	4.56 \pm 0.13
	<i>Navicula gregaria</i>	3.29 \pm 0.14	<i>Coscinodiscus</i> sp2	4.50 \pm 0.10
	<i>Nitzschia dubia</i>	3.22 \pm 0.18	<i>Stephanodiscus</i> sp1	4.11 \pm 0.19
	<i>Navicula digitoradiata</i>	3.12 \pm 0.20	<i>Coscinodiscus</i> sp3	3.72 \pm 0.22
	<i>Pleurosigma angulatum</i>	3.07 \pm 0.17	<i>Nitzschia formosa</i>	3.42 \pm 0.28
	<i>Gyrosigma scalproides</i>	3.06 \pm 0.22	<i>Actinoptychus splendens</i>	3.26 \pm 0.18
	<i>Coscinodiscus</i> sp2	3.05 \pm 0.21	<i>Caloneis formosa</i>	3.12 \pm 0.24
	other	36.8	other	51.89
July 2013	<i>Gyrosigma balticum</i>	14.44 \pm 0.28	<i>Gyrosigma balticum</i>	19.37 \pm 0.74
	<i>Gyrosigma scalproides</i>	6.07 \pm 0.31	<i>Nitzschia sigma</i>	4.99 \pm 0.30
	<i>Nitzschia sigma</i>	4.30 \pm 0.40	<i>Coscinodiscus</i> sp3	4.41 \pm 0.24
	<i>Pleurosigma angulatum</i>	4.17 \pm 0.33	<i>Nitzschia dubia</i>	4.04 \pm 0.47
	sp1	4.05 \pm 0.42	sp1	3.77 \pm 0.42
	<i>Gyrosigma distortum</i>	3.51 \pm 0.24	<i>Gyrosigma scalproides</i>	3.76 \pm 0.14
	<i>Nitzschia dubia</i> W. Smith	3.38 \pm 0.30	<i>Gyrosigma attenuatum</i>	3.01 \pm 0.35
	<i>Gyrosigma attenuatum</i>	3.37 \pm 0.24	<i>Actinoptychus acuminata</i>	3.01 \pm 0.29
	<i>Actinoptychus splendens</i>	3.19 \pm 0.31	<i>Odontella aurita</i>	2.92 \pm 0.16
	<i>Navicula</i> sp1	2.90 \pm 0.26	<i>Coscinodiscus</i> sp1	2.87 \pm 0.33
	other	50.62	other	47.84
Oct 2013	<i>Gyrosigma scalproides</i>	10.72 \pm 2.93	<i>Gyrosigma balticum</i>	17.24 \pm 0.41
	<i>Gyrosigma balticum</i>	7.95 \pm 0.56	<i>Gyrosigma scalproides</i>	9.20 \pm 0.42
	<i>Pleurosigma angulatum</i>	7.55 \pm 0.24	<i>Pleurosigma angulatum</i>	6.55 \pm 0.40
	<i>Nitzschia minutissima</i>	7.09 \pm 0.46	<i>Tryblionella acuminata</i>	5.06 \pm 0.50
	<i>Nitzschia sigma</i>	6.87 \pm 0.37	<i>Nitzschia sigma</i>	4.32 \pm 0.28
	<i>Diploneis didyma</i>	5.53 \pm 0.48	<i>Scoliolepta tumida</i>	3.96 \pm 0.46
	<i>Navicula cryptocephala</i>	4.60 \pm 0.34	<i>Navicula gregaria</i>	3.82 \pm 0.43
	<i>Tryblionella acuminata</i>	4.35 \pm 0.38	<i>Diploneis didyma</i>	3.79 \pm 0.32
	UI Sp69	4.26 \pm 0.41	<i>Navicula phyllepta</i>	3.48 \pm 0.25
	UI Sp70	3.55 \pm 0.31	<i>Gyrosigma wansbeckii</i>	3.46 \pm 0.35
	other	37.54	other	39.10

Table 4.3: Relative abundance (%) of the top ten most common diatom taxa identified in the top 2 mm per cm² sediment of the transition zone across the tidal cycle in April 2013, July 2013 and Oct 2013. Values are mean \pm SE. Values of the RA of neap tide and spring tide are the mean \pm SE of pooled four and three days of neap and spring tides sampling data, respectively. n value for neap tide is 240 and spring tide is 216

	Neap tide	Relative abundance (%)	Spring tide	Relative abundance (%)
April 2013	<i>Gyrosigma balticum</i>	13.52 \pm 1.00	<i>Gyrosigma balticum</i>	7.33 \pm 0.51
	<i>Diploneis didyma</i>	7.48 \pm 0.50	<i>Diploneis didyma</i>	6.65 \pm 0.63
	<i>Nitzschia sigma</i>	6.47 \pm 0.54	<i>Pleurosigma angulatum</i>	5.88 \pm 0.27
	<i>Gyrosigma wansbeckii</i>	5.97 \pm 0.26	<i>Fallacia forcipata</i>	5.67 \pm 0.33
	<i>Gyrosigma attenuatum</i>	5.93 \pm 0.46	<i>Nitzschia panduriformis</i>	4.6 \pm 0.27
	<i>Nitzschia scalproides</i>	4.25 \pm 0.31	<i>Plagiotropis vitreae</i>	4.51 \pm 0.42
	<i>Gyrosigma scalproides</i>	3.67 \pm 0.34	<i>Stauroneis producta</i>	4.43 \pm 0.30
	<i>Achnanthes longipes</i>	3.51 \pm 0.37	<i>Gyrosigma wansbeckii</i>	4.36 \pm 0.47
	<i>Navicula scopulorum</i>	3.48 \pm 0.45	<i>Gyrosigma scalproides</i>	4.17 \pm 0.51
	<i>Navicula digitoradiata</i>	3.37 \pm 0.43	<i>Navicula scopulorum</i>	3.79 \pm 0.30
	other	42.36	other	48.60
July 2013	<i>Gyrosigma balticum</i>	17.81 \pm 0.33	<i>Gyrosigma balticum</i>	19.36 \pm 0.54
	<i>Gyrosigma attenuatum</i>	9.14 \pm 0.30	<i>Gyrosigma attenuatum</i>	6.79 \pm 0.56
	<i>Gyrosigma scalproides</i>	8.12 \pm 0.17	<i>Diploneis didyma</i>	6.59 \pm 0.51
	<i>Diploneis didyma</i>	7.44 \pm 0.15	<i>Nitzschia sigma</i>	5.66 \pm 0.43
	<i>Nitzschia panduriformis</i>	3.73 \pm 0.24	<i>Gyrosigma scalproides</i>	5.47 \pm 0.47
	<i>Navicula digitoradiata</i>	3.64 \pm 0.30	<i>Hantzschia sp.</i>	4.14 \pm 0.46
	<i>Pleurosigma angulatum</i>	3.23 \pm 0.29	<i>Nitzschia punctate</i>	0.26 \pm 0.30
	<i>Gyrosigma fasciola</i>	3.16 \pm 0.29	UI Sp39	2.53 \pm 0.31
	<i>Nitzschia sigma</i>	3.11 \pm 0.32	<i>Scolioleura tumida</i>	2.42 \pm 0.30
	<i>Hantzschia sp.</i>	2.74 \pm 0.27	<i>Navicula crucigera</i>	2.36 \pm 0.36
	other	37.89	other	42.10
Oct 2013	<i>Gyrosigma balticum</i>	20.72 \pm 0.93	<i>Gyrosigma balticum</i>	24.89 \pm 1.21
	<i>Synedra sp1</i>	7.35 \pm 0.51	<i>Coscinodiscus sp 2</i>	7.46 \pm 0.79
	<i>Gyrosigma wansbeckii</i>	6.71 \pm 0.61	<i>Fallacia forcipata</i>	6.31 \pm 0.58
	<i>Pleurosigma sp1</i>	6.66 \pm 0.58	<i>Navicula crucigera</i>	5.72 \pm 0.66
	<i>Fragilaria sp</i>	6.46 \pm 0.50	<i>Synedra sp1</i>	5.63 \pm 0.52
	<i>Nitzschia panduriformis</i>	4.72 \pm 0.40	<i>Pleurosigma sp1</i>	5.35 \pm 0.67
	UI Sp70	4.40 \pm 0.43	<i>Gyrosigma wansbeckii</i>	4.55 \pm 0.42
	<i>Tryblionella acuminata</i>	4.13 \pm 0.23	<i>Navicula gregaria</i>	4.53 \pm 0.54
	<i>Navicula crucigera</i>	3.63 \pm 0.43	<i>Navicula sp1</i>	4.45 \pm 0.44
	<i>Fallacia forcipata</i>	3.30 \pm 0.23	<i>Nitzschia panduriformis</i>	4.44 \pm 0.43
	other	31.93	other	26.69

Table 4.4: Relative abundance (%) of the top ten most common diatom taxa identified in the top 2 mm per cm² sediment of the salt marsh across the tidal cycle in April 2013, July 2013 and Oct 2013. Values are mean \pm SE. Values of the RA of neap tide and spring tide are the mean \pm SE of pooled four and three days of neap and spring tides sampling data, respectively. n value for neap tide is 240 and spring tide is 216

	Neap tide	Relative abundance (%)	Spring tide	Relative abundance (%)
April 2013	<i>Opephora</i> sp1	11.63 \pm 1.21	<i>Gyrosigma scalproides</i>	8.49 \pm 0.46
	<i>Neidium</i> sp.	11.32 \pm 0.98	<i>Diploneis didyma</i>	7.12 \pm 0.50
	<i>Surirella fastuosa</i>	9.08 \pm 0.82	<i>Diploneis littoralis</i>	5.65 \pm 0.33
	Sp4	6.95 \pm 0.71	<i>Nitzschia sigma</i>	5.50 \pm 0.48
	<i>Nitzschia</i> sp1	6.64 \pm 0.58	<i>Raphoneis ampiceros</i>	5.30 \pm 0.31
	<i>Diploneis stroemii</i>	4.41 \pm 0.64	<i>Nitzschia dubia</i>	5.18 \pm 0.32
	<i>Opephora</i> sp2	4.21 \pm 0.67	<i>Gyrosigma wansbeckii</i>	4.28 \pm 0.35
	<i>Nitzschia panduriformis</i>	4.20 \pm 0.40	<i>Surirella fastuosa</i>	4.15 \pm 0.60
	<i>Diploneis didyma</i>	4.08 \pm 0.48	<i>Navicula gregaria</i>	3.85 \pm 0.26
	<i>Navicula gracilis</i>	4.04 \pm 0.68	<i>Opephora</i> sp2	3.80 \pm 0.48
	other	31.45	other	46.66
July 2013	<i>Opephora</i> sp1	15.72 \pm 1.41	<i>Pleurosigma angulatum</i>	6.24 \pm 0.55
	Sp4	14.13 \pm 1.25	<i>Diploneis didyma</i>	5.92 \pm 0.26
	<i>Nitzschia bilobata</i>	7.87 \pm 0.66	<i>Navicula gregaria</i>	5.78 \pm 0.60
	<i>Nitzschia</i> sp1	6.75 \pm 0.67	<i>Nitzschia bilobata</i>	4.94 \pm 0.53
	<i>Neidium</i> sp	6.18 \pm 0.61	<i>Navicula gracilis</i>	4.76 \pm 0.40
	<i>Nitzschia vitrea</i>	5.23 \pm 0.40	Sp4	4.36 \pm 0.64
	<i>Surirella fastuosa</i>	4.79 \pm 1.22	<i>Diploneis stroemii</i>	4.30 \pm 0.32
	<i>Gyrosigma scalproides</i>	4.23 \pm 0.67	<i>Navicula digitoradiata</i>	4.19 \pm 0.67
	<i>Pleurosigma angulatum</i>	3.50 \pm 0.33	<i>Opephora</i> sp1	4.14 \pm 0.50
	<i>Navicula gregaria</i>	3.46 \pm 0.58	<i>Nitzschia</i> sp1	3.88 \pm 0.37
	other	28.13	other	51.49
Oct 2013	<i>Nitzschia vitrea</i>	15.28 \pm 1.84	<i>Amphora</i> sp1	10.64 \pm 1.11
	<i>Neidium</i> sp.	11.93 \pm 0.60	<i>Gyrosigma wansbeckii</i>	4.87 \pm 0.72
	Sp4	11.85 \pm 0.72	<i>Surirella ovata</i>	4.82 \pm 0.52
	<i>Opephora</i> sp 2	7.54 \pm 1.03	<i>Diploneis stroemii</i>	4.59 \pm 0.90
	<i>Nitzschia</i> sp1	7.48 \pm 0.82	<i>Navicula</i> sp1	4.52 \pm 0.54
	<i>Opephora</i> sp1	7.27 \pm 1.07	<i>Pleurosigma angulatum</i>	4.48 \pm 0.47
	<i>Nitzschia bilobata</i>	7.02 \pm 0.67	<i>Opephora</i> sp2	4.47 \pm 0.49
	<i>Surirella fastuosa</i>	6.27 \pm 0.70	<i>Nitzschia dubia</i>	4.11 \pm 0.52
	<i>Diploneis stroemii</i>	5.06 \pm 0.42	<i>Diploneis didyma</i>	3.99 \pm 0.57
	<i>Achnanthes longipes</i>	3.36 \pm 0.66	<i>Gyrosigma scalproides</i>	3.88 \pm 0.95
	other	16.94	other	49.62

4.3.2 Variability of Chl *a* concentration and MPB assemblage's diversity

There was significant spatial difference in the Chl *a* concentration between sites ($F_{2,1219}=440.85$, $p < 0.001$) at the Fingringhoe tidal flat, Colne estuary. Tukey HSD test revealed that the difference was attributed to significantly lower Chl *a* concentrations on the salt marsh than on the mud flat and the transition zone (all significant at $p < 0.001$) (Figure 4.1). Temporally, both Chl *a* concentration on the mud flat and the transition zone were significantly different between months (mud flat; $F_{2,499}=127.2$, $p < 0.001$ and transition; $F_{2,495}=73.19$, $p < 0.001$) (Figure 4.1). The concentration in October 2013 for both zones (mud flat; $5.31 \pm 0.46 \mu\text{g Chl } a \text{ cm}^{-2}$ and transition; $5.15 \pm 0.53 \mu\text{g Chl } a \text{ cm}^{-2}$) were significantly lower than in April and July 2013 at $p < 0.001$. The significant difference in Chl *a* concentration on the salt marsh between months ($F_{2,500}=87.96$, $p < 0.001$) was attributed to its significantly lower concentration in April 2013 ($1.96 \pm 0.41 \mu\text{g Chl } a \text{ cm}^{-2}$) than in July 2013 ($3.62 \pm 0.44 \mu\text{g Chl } a \text{ cm}^{-2}$) and October 2013 ($4.22 \pm 0.50 \mu\text{g Chl } a \text{ cm}^{-2}$) (both significant at $p < 0.001$) (Figure 4.1).

MPB assemblage diversity values (H') in the Colne estuary ranged between 0.9 and 1.6. Univariate ANOVA tests showed a significant spatial variability in MPB diversity across the three zones ($F_{2,1220}=333.02$, $p < 0.001$). MPB assemblages diversity on the mud flat was significantly higher than the diversity on the transition zone and the salt marsh (both differences significant at $p < 0.001$) (Figure 4.2). The MPB assemblages on the salt marsh had a significantly lower diversity mean value than the other two zones ($p < 0.001$). The diversity of salt marsh MPB assemblages however increased during spring tide in all sampling months. Salt marsh diversity values (H') were significantly higher in spring tide than in neap tide ($F_{1,405}=341.09$, $p < 0.001$) (Figure 4.2).

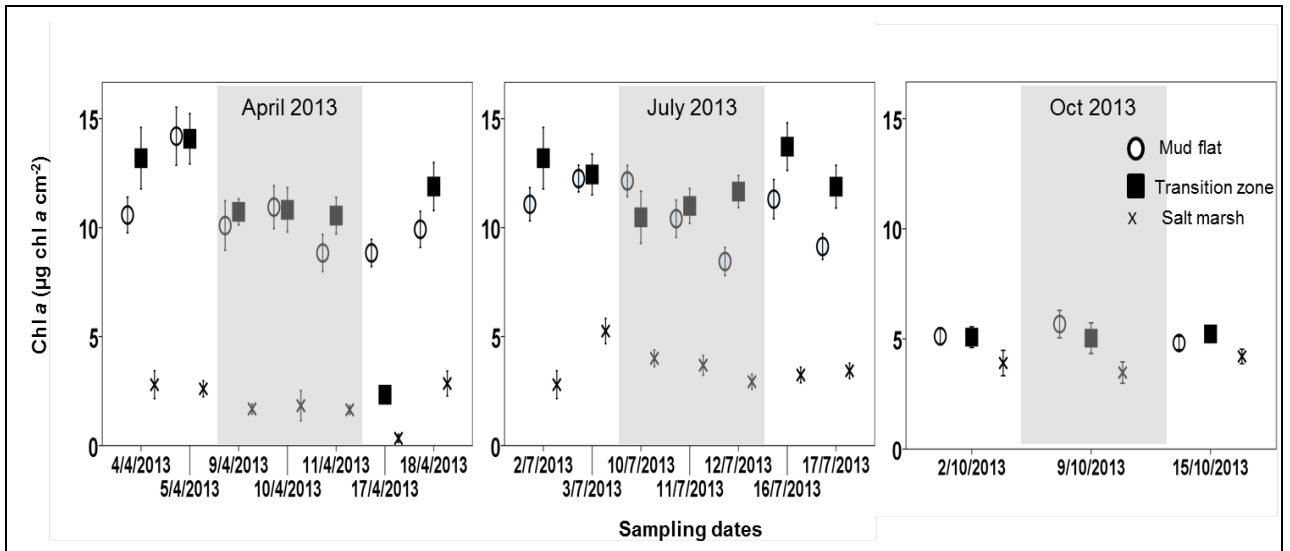


Figure 4.1: Daily Chl a variability in three different sampling months (April 2013, July 2013 and October 2013) on the mud flat, the transition zone and the salt marsh in Fingringhoe tidal flat, Colne estuary across neap (non-shaded area) and spring (shaded area) tidal cycle. Values are mean \pm 1 SE, n = 24.

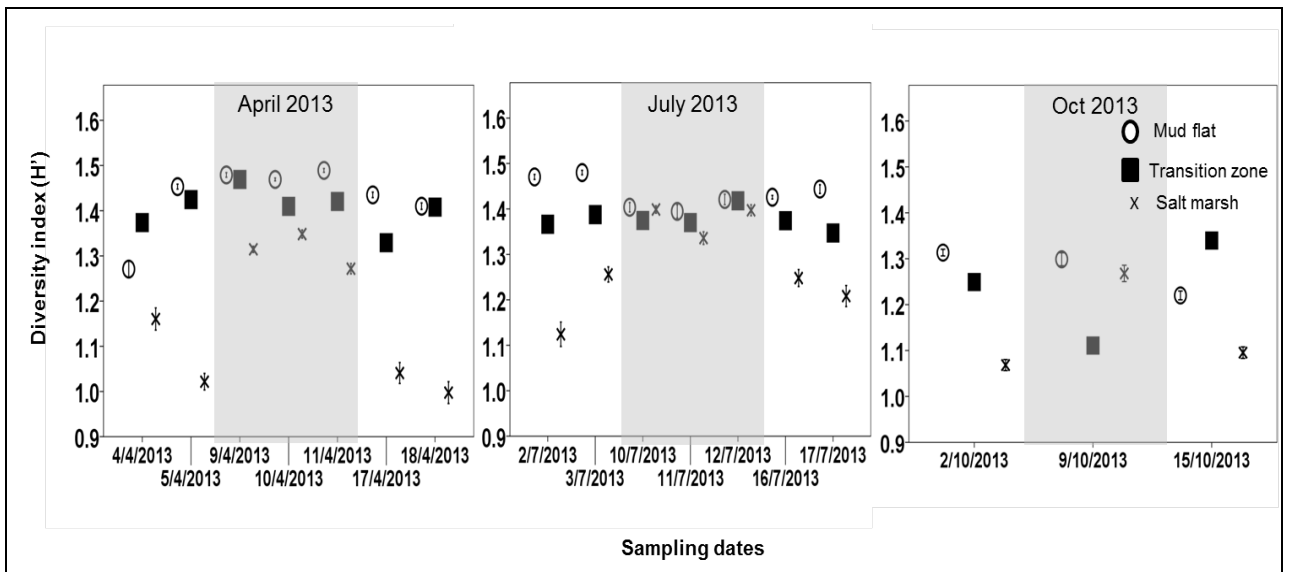


Figure 4.2: Daily Shannon-Wiener diversity index value of MPB assemblages on the mud flat, the transition zone and the salt marsh across the neap and spring tidal cycle in Colne estuary in April 2013, July 2013 and October 2013. Values are mean \pm 1 SE, n = 24.

4.3.3 Relationship between Chl *a* and MPB assemblages diversity

Chl *a* and MPB assemblage diversity (represented by the diversity index (H')) in the Colne estuary at daily temporal scales displayed either significantly positive linear (+ve), significantly positive and curvilinear (+ve curv.), significantly negative (-ve) or unimodal (UM) relationships (Table 4.5). Scatterplots in Figure 4.3, Figure 4.4 and Figure 4.5 shows the relationship patterns recorded for the mud flat, the transition zone and the salt marsh samples, respectively.

Most of the significant correlations on the mud flat and the transition zone during neap tide demonstrated either negative or unimodal patterns (Table 4.5 & Figure 4.3 & 4.4). The significant positive correlation between Chl *a* and the diversity (H') was found in the neap tide samples of the mud flat in April 2013 (17th and 18th April 2013) (Figure 4.3A) and the transition zone on the 2nd Oct 2013 (Figure 4.4C) (Table 4.5). On the salt marsh, most of the significant correlations showed positive pattern (both +ve and +ve curv.) (Table 4.5 & Figure 4.5). The strongest correlation coefficients (r) of the relationship on the salt marsh was recorded in neap tide samples on the 2nd July 2013 with the value of $r = 0.912$, $p < 0.001$ (Table 4.5).

Significant correlations during spring tide periods for all of the zones displayed either linear positive, curvilinear positive and unimodal patterns (Table 4.5 & Figure 4.3 – 4.5). Only the spring tide samples on the salt marsh however displayed the unimodal pattern (Figure 4.5). The strongest correlations between Chl *a* and diversity during spring tide were recorded in the mud flat samples in July 2013 with the Pearson's correlation coefficients (r) values of more than 0.9 for all the samples (Table 4.5 & Figure 4.3). Contrarily, there was no significant correlation recorded for transition zone sample diversity during spring tide in July 2013 (Table 4.5 & Figure 4.4).

The strength of the correlation between the sediment Chl *a* and the H' value of the mud flat and the salt marsh samples in spring tide was significantly positively affected by the tidal

range. The relationship strength (between Chl *a* and H') for both zones in spring tide was found to be significantly positively correlated with increasing tidal range (Figure 4.6A & 4.6B). Both Pearson correlation coefficients for the correlation on the mud flat and the salt marsh were $r = 0.795, p < 0.05$ (Figure 4.6A) and $r = 0.823, p < 0.05$ (Figure 4.6B), respectively. Incorporation of the neap tide data in the correlation strength test of both zones, resulted in a non-significant output. This suggests that the tidal range possibly did not have any significant effect on the relationship between the Chl *a* and the diversity of MPB assemblages during neap tide. The relationship between Chl *a* and the H' for the samples on the transition zone was not significantly affected by the tidal range.

The strength of the correlation between the Chl *a* and the H' for salt marsh's samples was significantly positively controlled by the 'sum of sun' ($r = 0.799, p < 0.01$). However only 'sum of sun hours' below 24 hours showed to responsible in the positive effect. 'Mean wind speed' and 'sum of rainfall' did not have any significant effect on the relationship between the Chl *a* concentration and the diversity index (H') in any of samples.

Table 4.5: Pearson correlation coefficients (r) between Chl *a* concentrations (daily) and MPB assemblages diversity index (H') on three zones in Colne estuary. Also includes the values of measured weather-related abiotic factors. +ve indicates positive correlation. -ve indicates negative correlation. UM indicates unimodal distribution. NP indicates no significant pattern. Significant values of r: $p < 0.05$ *, $p < 0.01$ ** and $p < 0.001$ ***. n = 24.

Dates	Mud flat				Transition zone				Salt marsh				Period of sun (hour)	Tidal range (m)	MWS (ms-1)	Sum of rainfall (m)
	Relationship pattern				Relationship pattern				Relationship pattern							
	+ve	-ve	UM	NP	+ve	-ve	UM	NP	+ve	-ve	UM	NP				
4 th April		-0.591**					+					+	11.8	3.7	14.5	1.4
5 th April				+				+		0.632***			13.8	3.6	8.9	1.4
9 th April	0.508**							+				+	10.9	4.3	6.1	0
10 th April				+				+				+	7.4	4.6	7.7	0.3
11 th April	0.756***				0.366*					0.628***			7.4	4.8	9.3	4.4
17 th April	0.471*							+				+	8.6	3.6	2.4	0
18 th April	0.888***									-0.618***			12.4	3.8	17.4	1
2 nd July				+						-0.518*			21.4	3.9	2.8	0
3 rd July										-0.58**			8.3	4.1	4.0	3.7
10 th July	0.941***							+				+	36.3	5.1	6.1	0
11 th July	0.952***							+		0.726**			30.9	5.4	3.8	0
12 th July	0.911***							+		0.726**			19.1	5.6	6.0	0
16 th July				+						-0.538**			20.5	3.9	3.6	0
17 th July										-0.473*			24.9	4.2	1.9	0
2 nd Oct										0.576**			10.9	3.7	3.2	0.3
9 th Oct	0.539**									0.490*		+	10.3	4.8	4.8	0.6
15 th Oct				+				+				+	2.8	3.9	5.4	18.7

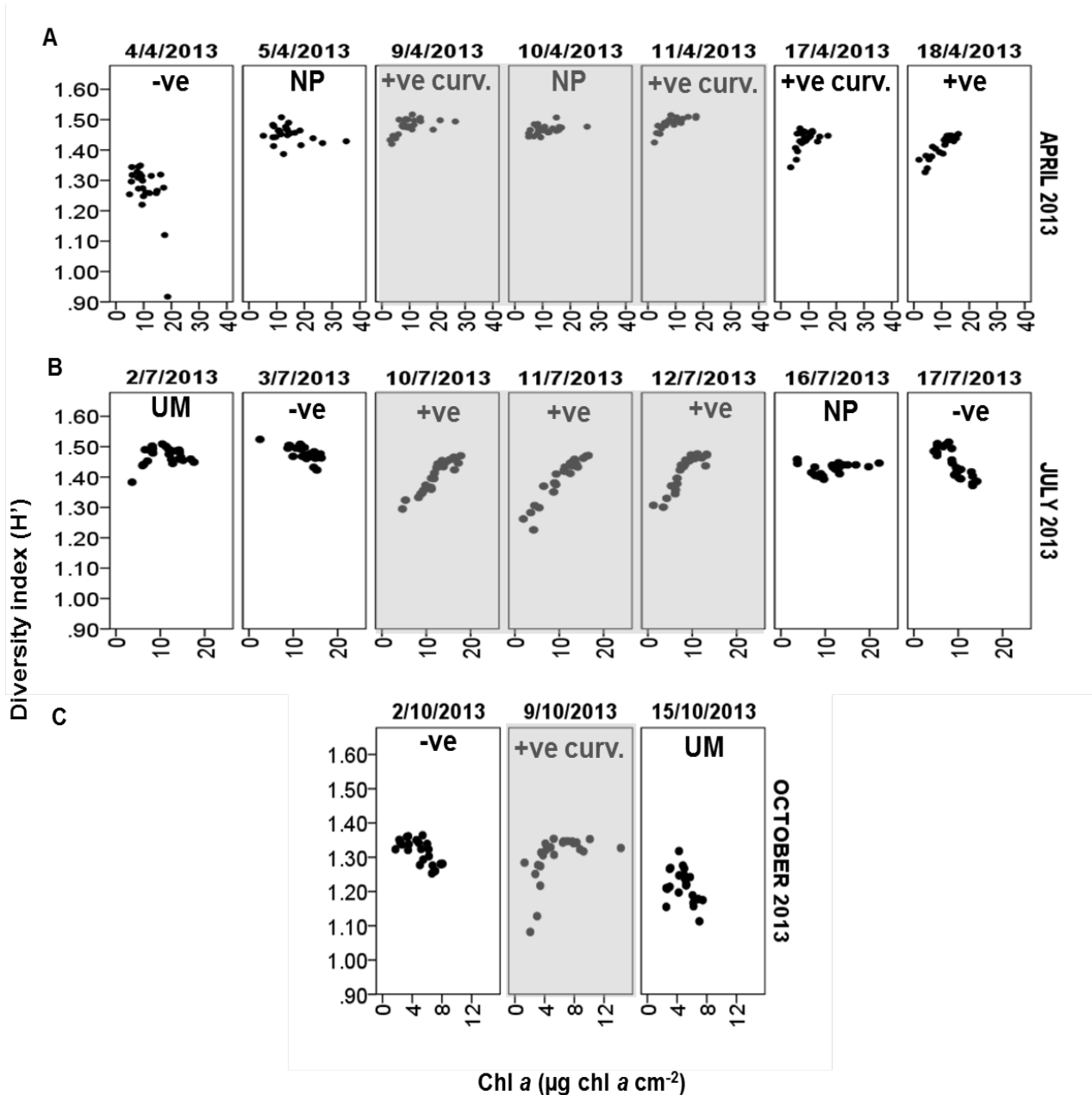


Figure 4.3: Scatterplots showing the relationship between Chl a concentration and the MPB assemblage diversity on the mud flat in A) April 2013, B) July 2013 and C) October 2013. Type of the relationships are indicated by '+ve'=significant positive, '-ve'=significant negative, '+ve curv.'=significant positive (curvilinear), 'UM'=unimodal and 'NP'=no pattern. The Pearson correlation coefficients values (r) are detailed in the Table 4.5. Shaded area represents spring tide while the non-shaded are represents neap tide.

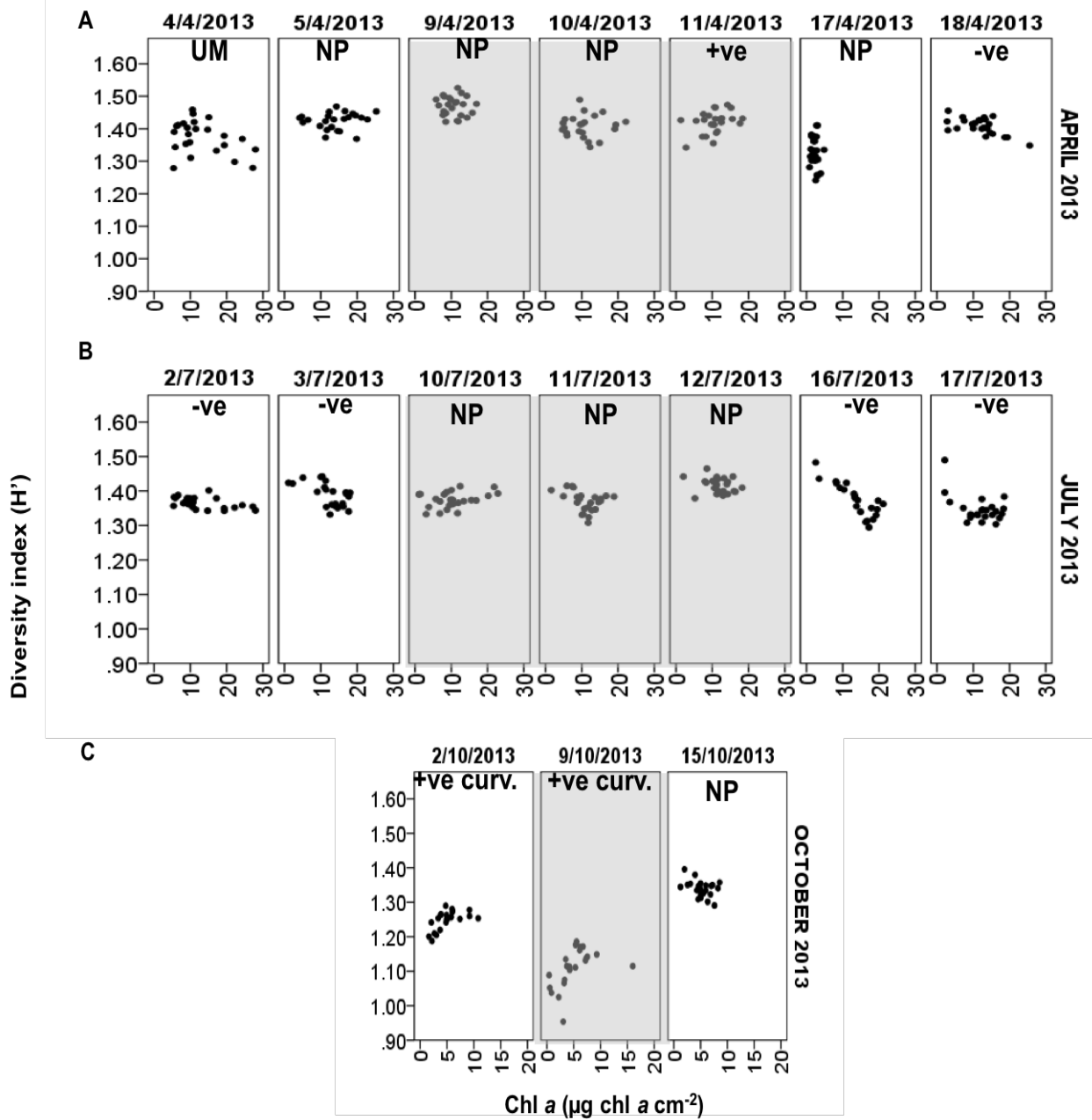


Figure 4.4: Scatterplots showing the relationship between Chl a concentration and the MPB assemblage diversity on the transition zone in A) April 2013, B) July 2013 and C) October 2013. Type of the relationships are indicated by '+ve'=significant positive, '-ve'=significant negative, '+ve curv.'=significant positive (curvilinear), 'UM'=unimodal and 'NP'=no pattern. The Pearson correlation coefficients values (r) are detailed in the Table 4.5. Shaded area represents spring tide while the non-shaded are represents neap tide.

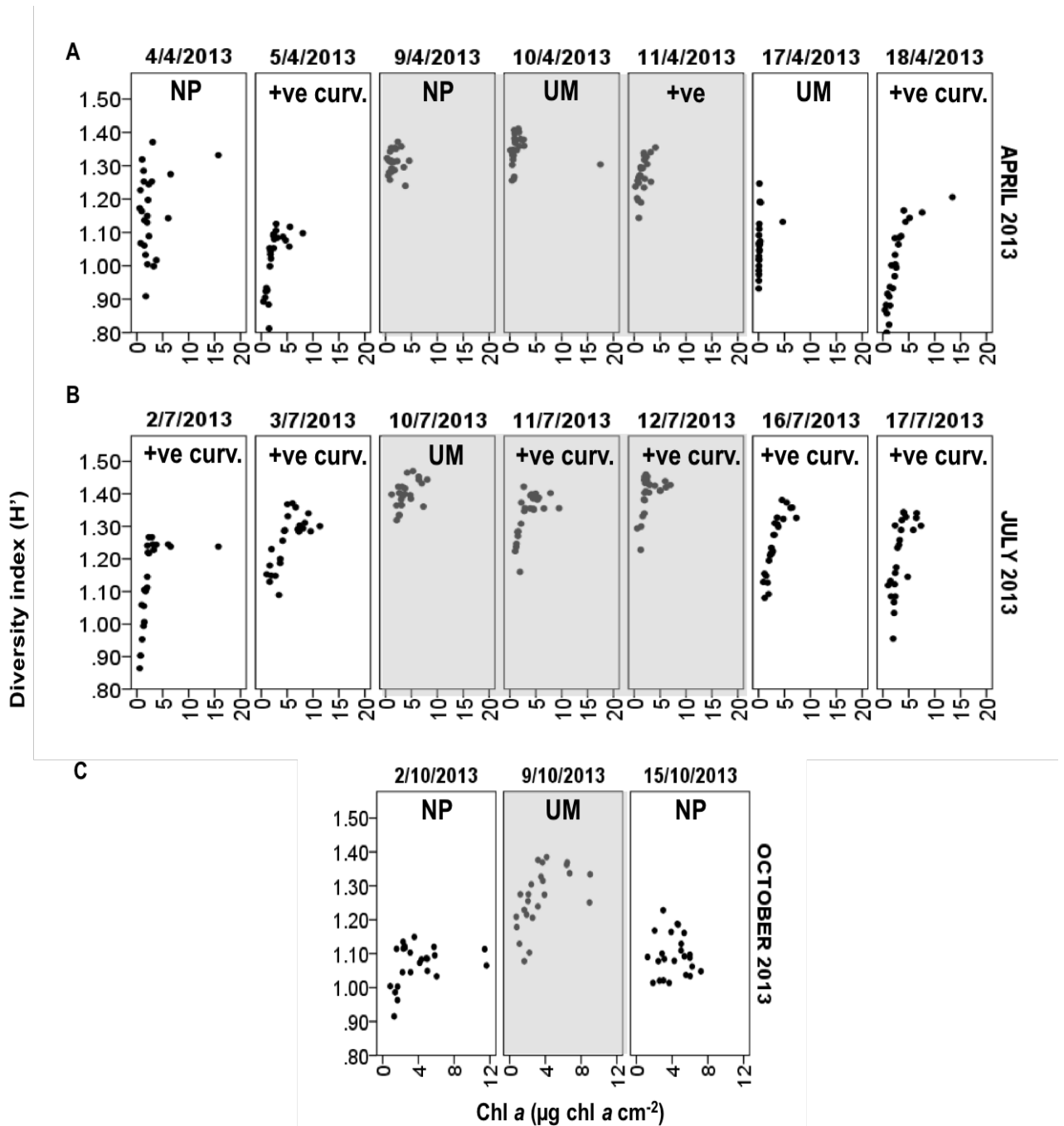


Figure 4.5: Scatterplots showing the relationship between Chl a concentration and the MPB assemblage diversity on the salt marsh in A) April 2013, B) July 2013 and C) October 2013. Type of the relationships are indicated by '+ve'=significant positive, '-ve'=significant negative, '+ve curv.'=significant positive (curvilinear), 'UM'=unimodal and 'NP'=no pattern. The Pearson correlation coefficients values (r) were detailed in the Table 4.5. Shaded area represents spring tide while the non-shaded are represents neap tide.

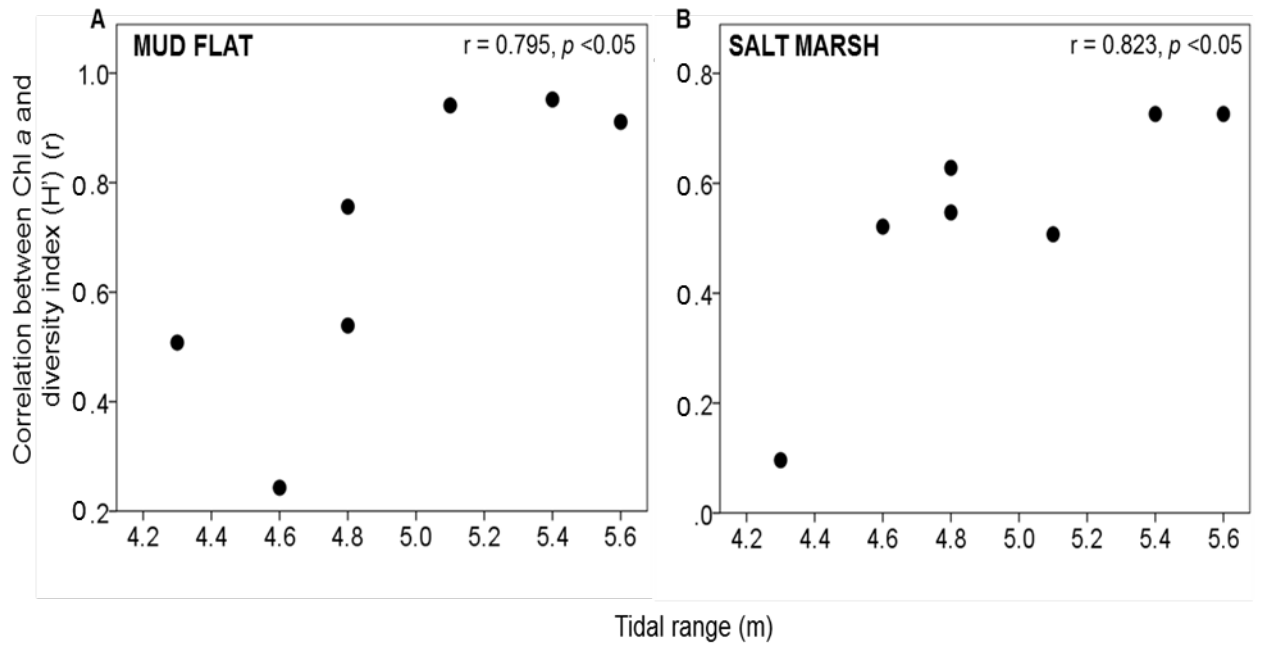


Figure 4.6: Scatterplots showing positive correlations between Pearson correlation coefficients (r) between Chl a and diversity index (H') and tidal range on; A) the mud flat ($r = 0.795, p < 0.05$) and; B) the transition zone ($r = 0.823, p < 0.05$) in spring tide. $n = 7$.

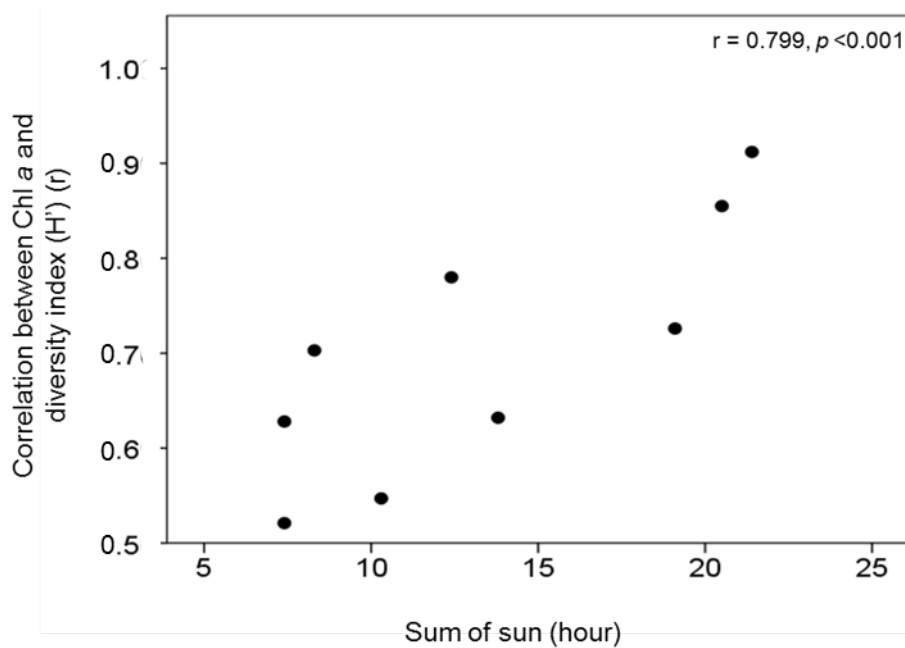


Figure 4.7: Scatterplots showing positive correlations between Pearson correlation coefficients (r) between Chl a and diversity index (H') and sum of sun below 24 hours on the salt marsh ($r = 0.799, p < 0.01$). $n = 9$.

4.3.4 Relationship between Chl *a* concentration, species richness and species equitability (*E*)

The relationship between the Chl *a* concentration and the H' value (as presented in 4.3.3) can be used to determine whether the Chl *a* variability in the samples was closely related to the equitability or the evenness (*E*) or the species richness of the assemblage. This present study found that when Chl *a* concentration was strongly positively correlated with the H' , this was attributed to both *E* and species richness (Figure 4.8A); Chl *a* values that positively and curvilinearly correlated with H' were positively correlated with the species richness (Figure 4.8B); while the samples where Chl *a* concentration that had a negative correlation and unimodal correlation with the H' , were found to be negatively correlated with the *E* value (Figure 4.8C). In discussing this part, the relationship between the Chl *a* concentration and the H' value was termed **Correlation A**.

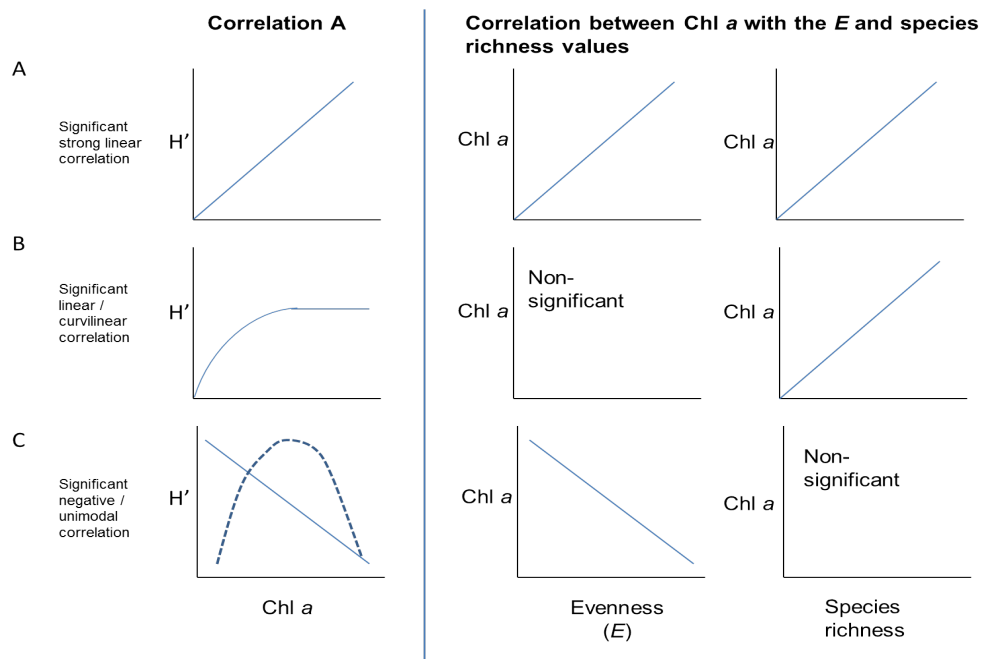


Figure 4.8: Relationship between Chl *a* concentration and MPB assemblage's diversity (H') can be used to predict whether the Chl *a* variability in the samples was attributed to the evenness (*E*) or the species richness of the assemblage. Note that A) Chl *a* concentration that strongly positively correlated with the H' was attributed to both *E* and species richness; B) Chl *a* that positively and curvilinearly correlated with H' was positively correlated with the species richness; while; C) the Chl *a* concentration that have negative correlation and unimodal correlation with the H' showed to negatively correlated with the *E* value.

Chl *a* concentrations of the samples of mud flat that significantly strongly and positively correlated with the *H'* value ($r > 0.90$) were also significantly positively correlated with both the *E* and the species richness. For instance, there were significantly positive correlations between the Chl *a* concentration with both the *E* and the species richness of the MPB assemblages for the spring tide samples of the mud flat on the 10th July (*E*; $r = 0.833$; species richness; $r = 0.870$) (Figure 4.9A) and 11th July (*E*; $r = 0.859$; species richness; $r = 0.894$) (Figure 4.9B) (all significant at $p < 0.001$). Both samples' correlation A value were $r = 0.941$ and $r = 0.952$ (both significant at $p < 0.001$), respectively.

Principal component analyses (PCA) were performed on the log ($n+1$) of the diatom relative abundance and Chl *a* data of the samples for which the Correlation A was $r > 0.90$ (significant, positive, linear relationship) (data on the mud flat on the 10th, 11th and 12th July 2013). PC 1 and PC2 from the PCA explained 56 % of the variation of the data (Figure 4.11A). Chl *a* and diatom species, such as *Navicula phyllepta* (*Navi.phyll*), *P. angulatum* (*Pleur.ang*), *G. fasciola* (*Gyro.fasci*), *Diploneis didyma* (*Diplo.didy*) and also centric diatom species, *Coscinodiscus* sp1 (*Cosci.sp1*), *Stephanodiscus* sp1 (*Stepha.sp1*), *Actinoptychus undulatus* (*Acti.undu*) and *A.splendens* (*Acti.splen*) were significantly positively correlated with the PC 1 (Figure 4.11B). Therefore sample assemblages plotting out on the right side of the scatter plot tended to have high Chl *a* concentration and were associated with the species that explained the right side of the PC 1. There was significant positive correlation between the PC 1 scores with the *E* ($r = 0.702$, $p < 0.001$) and the species richness ($r = 0.792$, $p < 0.001$) of the assemblages (Figure 4.11B). The significant correlation further supported the significant positive correlation between the Chl *a* with both the *E* and the species richness (discussed in previous paragraph). Also, the significant correlation between the PC1 with the diversity functions highlighted the species that significantly and positively correlated with both the *E* and the species richness in the samples with high strength Correlation A value on the mud flat during spring tide in July 2013.

Chl *a* concentration of the samples that were significantly positively correlated in curvilinear relationship with the assemblages' diversity (H') (correlation A) were found to be significantly positively correlated with only the species richness. For instance, the daily data of samples which Correlation A values were $r = 0.912, p < 0.001$ and $r = 0.726, p < 0.001$ showed that the samples' Chl *a* concentration was significantly and positively correlated with the species richness but not the E values (Figure 4.9C & 4.9D). To further investigate the relationship between the species richness with the Chl *a* and the diatom species, PCA was performed on the log transformed ($n+1$) of the diatom relative abundance and the Chl *a* concentration data of the salt marsh and the mud flat's samples that displayed the significant positive curvilinear Correlation A. Eight and four out of the seventeen daily samples of both zones displayed the significant positive curvilinear correlation A, respectively (Figure 4.12 & 4.13, respectively).

The PCA of the salt marsh that mentioned in previous paragraph explained 45.6 % of the total variability (Figure 4.12A). Diatom species such as *Achnanthes longipes* (*Ach.longi*), *Diploneis stroemii* (*Diplo.stroe*), *Gyrosigma scalproides* (*Gyro.scalp*) and *Raphoneis amphiceros* (*Rapho.amphi*) were four out of the twenty-eight diatom species together with the Chl *a*, that significantly positively correlated with the PC1 (Figure 4.12A). The PC1 was significantly explained by larger species such as taxa the genus *Gyrosigma*, genus *Nitzschia*, *Pleurosigma angulatum* (*Pleuro.angu*) and the centric diatom *A.undulatus* (*Acti.undu*) (Figure 4.12A). Salt marsh assemblages during spring tide were located to the right side of the PC1, hence suggested that the assemblages during spring tide had high Chl *a* concentration and had higher relative abundance of the species explained the PC1 (Figure 4.12B). There was significantly positive correlation between the PC1 and the species richness of the assemblages at $r = 0.871, p < 0.001$.

The mud flats PCA for the samples which correlation A showed significant positive curvilinear explained 65.2 % of the total variability (Figure 4.13). Chl *a* together with thirty diatom species, were the variables that significantly correlated with the PC1 (Figure 4.13A) of a PCA that was performed on pooled data of the 9th and the 17th Apr and the 9th Oct 2013. MPB

assemblages in neap and spring tides that were located towards the right side of the PC1 had high Chl *a* and potentially had high abundance of the diatom species that positively explained the PC1. Neap tide assemblages with high Chl *a* also associated with the species that significantly positively correlated with the PC2, such as the *G. balticum* (*Gyro.balti*), *G. distortum* (*Gyro.distor*), *G. scalpoides* (*Gyro.scalp*) and *Petroneis latissima* (*Petro.latis*) (Figure 4.13A & 4.13B). Centric diatom species such as *Coscinodiscus* sp1 (*Cosci.sp1*), *Odontella aurita* (*Odon.auri*), *Odontella alternan* (*Odon.alter*), *Actinoptychus longipes* (*Ach.longi*) and *Stephanodiscus* sp1 (*Stepha.sp1*) were possibly the common species occurring in the assemblages during spring tide with high Chl *a* (9th and 11th Apr) (Figure 4.13B). There was a significantly positive correlation between the PC1 and the species richness at $r = 0.860$, $p < 0.001$. The significant correlation further supported that the high Chl *a* concentration in the samples which correlation A was significant positively curvilinear on the mud flat, was potentially attributed to the increased in species richness. Increased species richness was potentially closely linked to the species that significantly explained the PC1.

There was significant negative correlation between Chl *a* concentration with the *E* value of the assemblages on the mud flat and the transition zone which Correlation A was significantly negative. Figure 4.10A and 4.10B shows that the Chl *a* concentration of two samples which Correlation A were $r = -0.713$, $p < 0.001$ and $r = -0.843$, $p < 0.001$, were significantly negatively correlated with the *E* value ($r = -0.852$ and $r = -0.934$, respectively (both significant at $p < 0.001$)), but not the species richness. PCA were performed on the samples data (log transformed ($n+1$) of diatom relative abundance and the Chl *a* concentration) that displayed significant negative Correlation A on the mud flat and the transition zone during only neap tide (as discussed in 4.3.3) to further investigate the relationship between the Chl *a*, diversity functions, the *E* value and species richness and also the diatom species in such samples.

PC1 and PC2 of the mudflat PCA explained 30.8 % and 19.6 % the variation in the diatom abundance and Chl *a* data. PC1 was significantly positively correlated with the Chl *a* and thirty four diatom species (Figure 4.14A). However, the species that strongly positively

correlated with the PC1 were the *A.splendens* (*Acti.splen*) ($r = 0.884, p < 0.001$), *Coscinodiscus* sp3 (*Cosci.sp3*) ($r = 0.8714, p < 0.001$), Sp3 ($r = 0.858, p < 0.001$), *O.aurita* (*Odon.auri*) ($r = 0.856, p < 0.001$) and *N. navicularis* (*Nitzsc.navi*) ($r = 0.801, p < 0.001$) Therefore some assemblages on the 3rd and 17th July that were plotting out towards the right side of the PC1 tended to have higher Chl *a* and potentially had high abundance of the species explained the PC1 (Figure 4.14B). There was significantly negative correlation between PC1 and the *E* value of the assemblages. This suggests that the species that were significantly correlated with the PC1, were potentially responsible to reduce the equitability in the diversity of the assemblages with high Chl *a* concentration on the mud flat.

PCA of the transition zone was explained by 57.5 % the variability of the data (Figure 4.15A & 4.15B). The PC1 was significantly negatively correlated with the Chl *a* concentration ($r = -0.867, p < 0.001$) and fourteen diatom species (Figure 4.15A), for examples, *G.fasciola* (*Gyro.fasci*), *Diploneis didyma* (*Diplo.didy*) and *G scalproides* (*Gyro.scalp*) (Figure 4.15A). Some assemblages of the samples that showed the significant negative Correlation A plotting towards the left side of the PC1 must had high Chl *a* concentration with high abundance of the fourteen diatom species (Figure 4.15B). The PC1 was significantly positively correlated with the species richness of the assemblages at $r = 0.742, p < 0.001$ (Figure 4.15B). Chl *a* concentration of samples that displayed unimodal trend in the relationship between the Chl *a* concentration and the MPB assemblages' diversity also showed a significantly negative correlation with the *E* value.

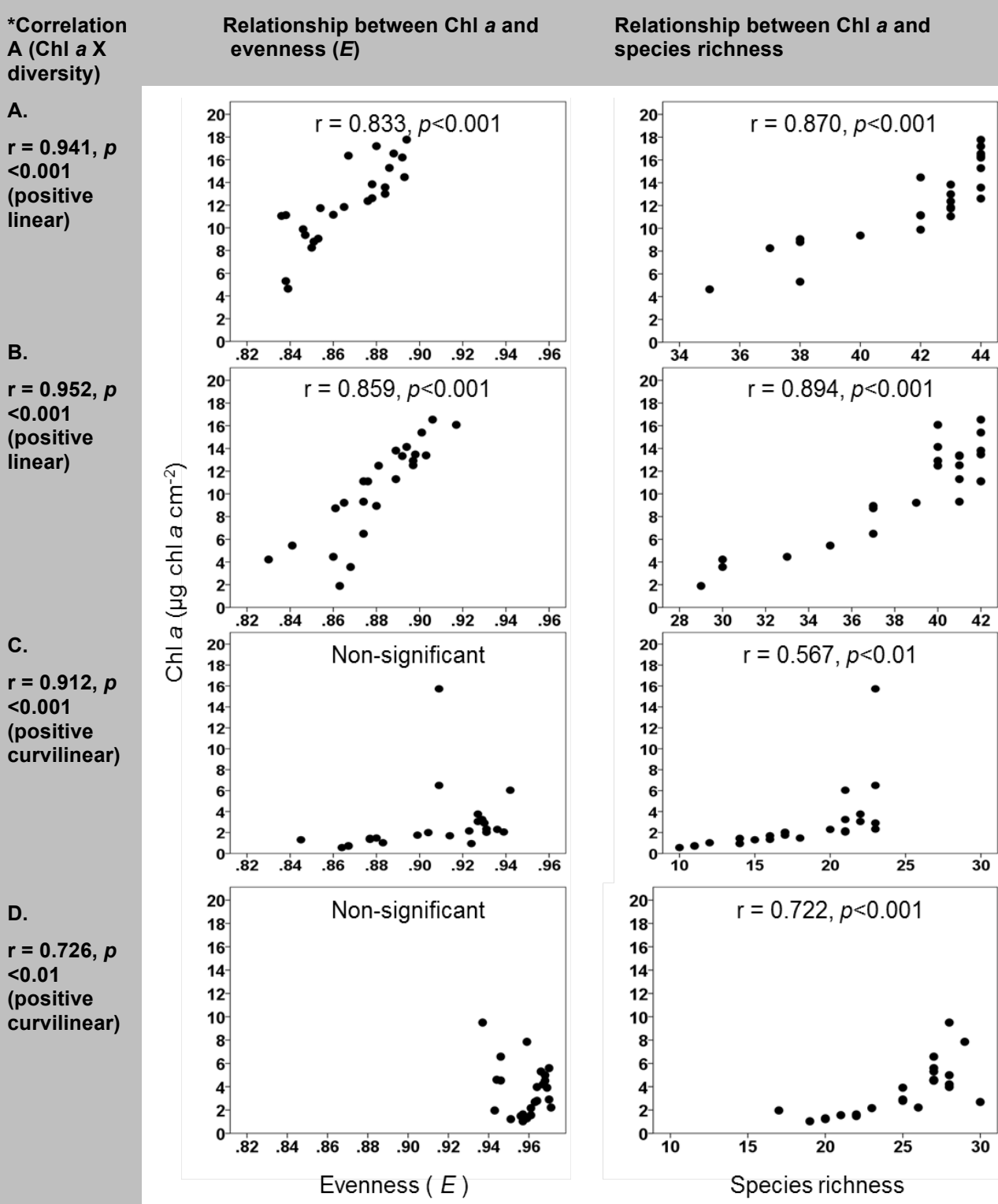


Figure 4.9: Scatterplot showing the relationship between Chl a concentration with the Evenness and the species richness of the samples which MPB assemblages were significantly; A) and B) positively and linearly; C) and D) positively and curvilinear correlated with the Chl a concentration. r is the value of Pearson correlation coefficients, $n = 24$. The term Correlation A was used for relationship between Chl a concentration with MPB assemblage's diversity (H'). Note that the Chl a of samples which Correlation A value was strongly significantly positive, was significantly correlated with both the E value and the species richness. Whereas, the samples which displayed significant curvilinear positive, their Chl a concentration was significantly correlated with on only the species richness and not the E value.

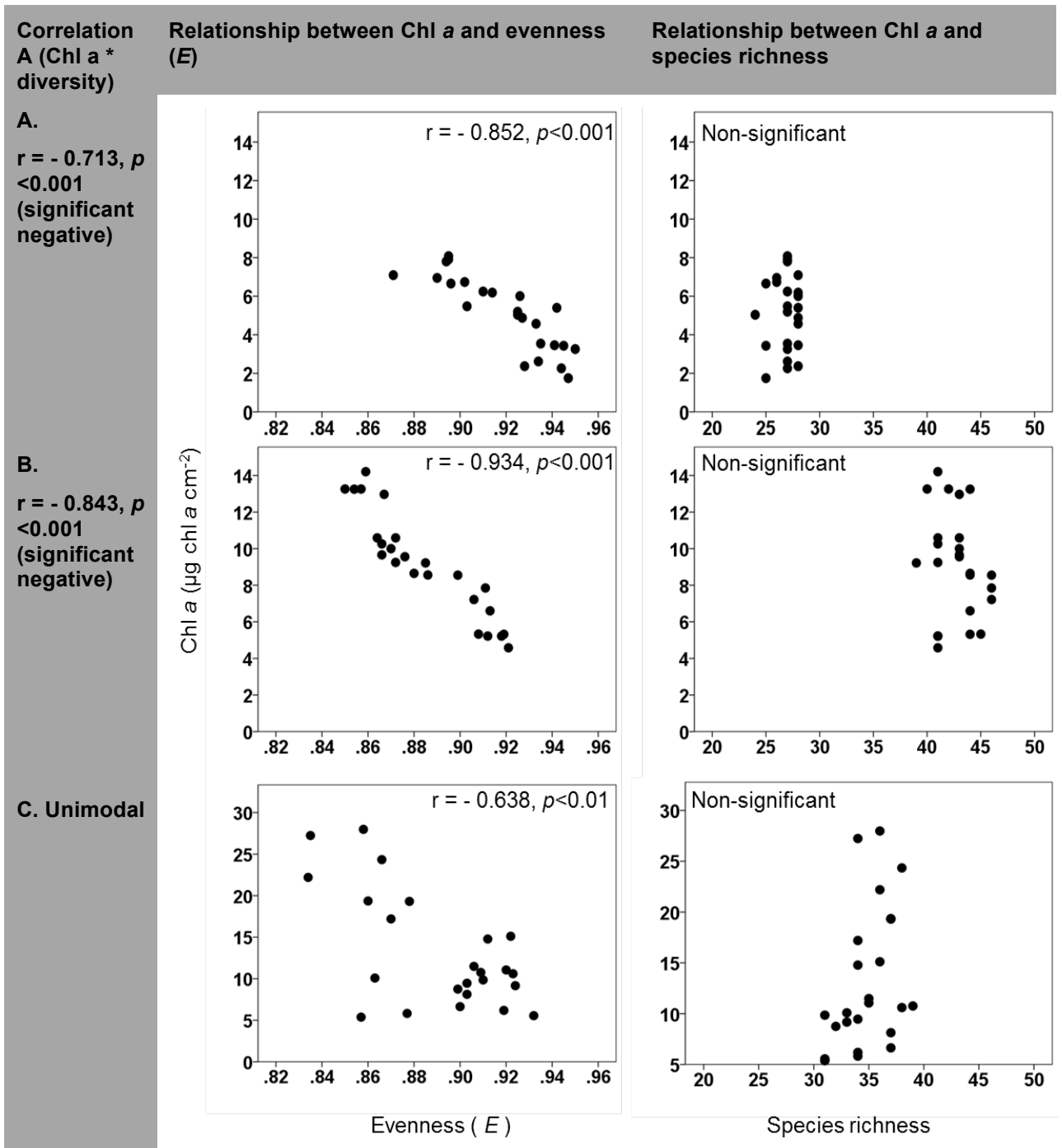


Figure 4.10: Scatterplot showing the relationship between Chl a concentration with the Evenness and the species richness of the samples which MPB assemblages were; A) and B) significantly negatively; and C) unimodal correlated with the Chl a concentration. r is the value of Pearson correlation coefficients, $n = 24$. The term Correlation A was used for relationship between Chl a concentration with MPB assemblage's diversity (H').

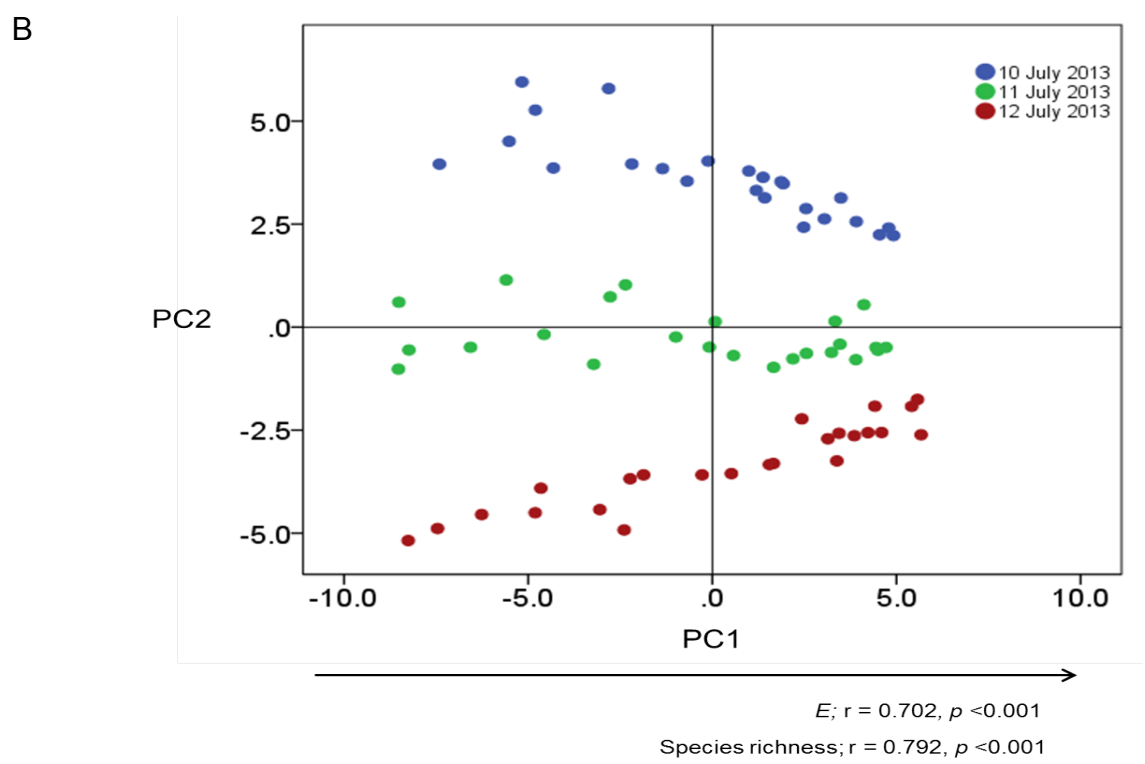
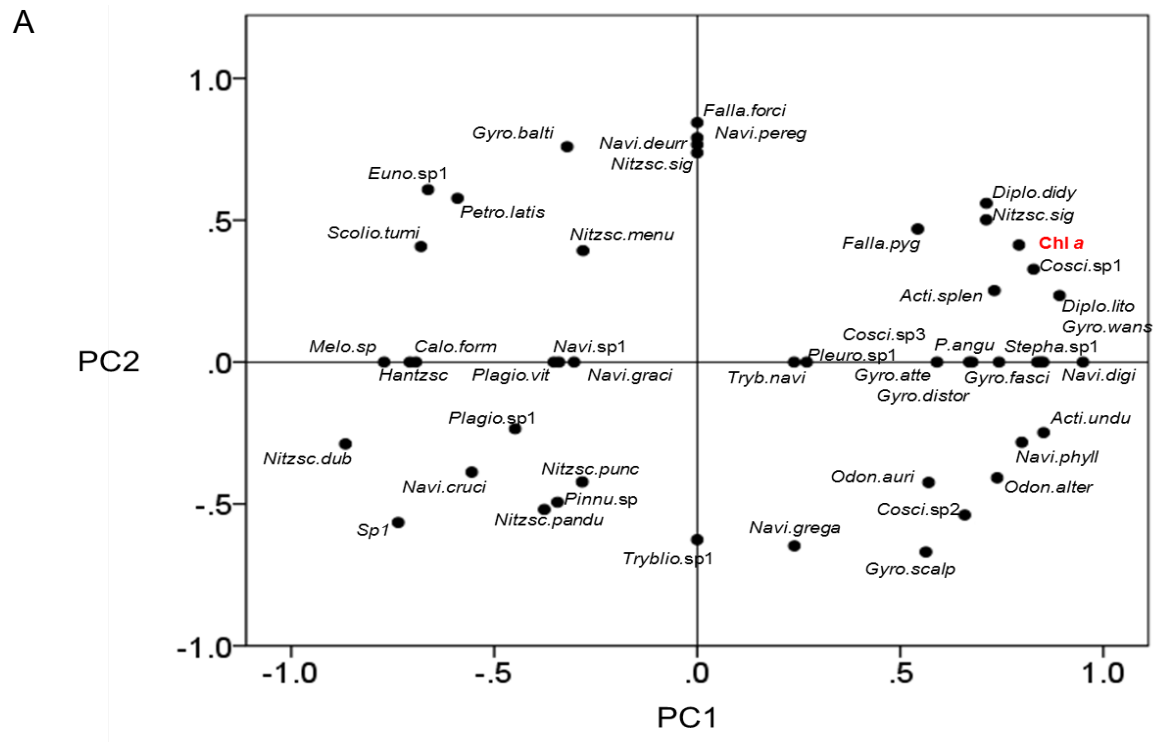


Figure 4.11: A) Variable factor map and the B) individual factor map of the samples which **Correlation A were $r > 0.90$** . The PCA was carried out on the $\log_{10}(n+1)$, n = relative abundance of the species which relative abundance $> 1\%$ and the Chl *a* concentration (supplementary variable) of the samples on the **mud flat** ($n=72$) during spring tide on the 10th, 11th and 12th July 2013. The PC1 was significantly positively correlated with both the E and the species richness values at $r = 0.702$ and $r = 0.792$ (both significant at $p < 0.001$), respectively.

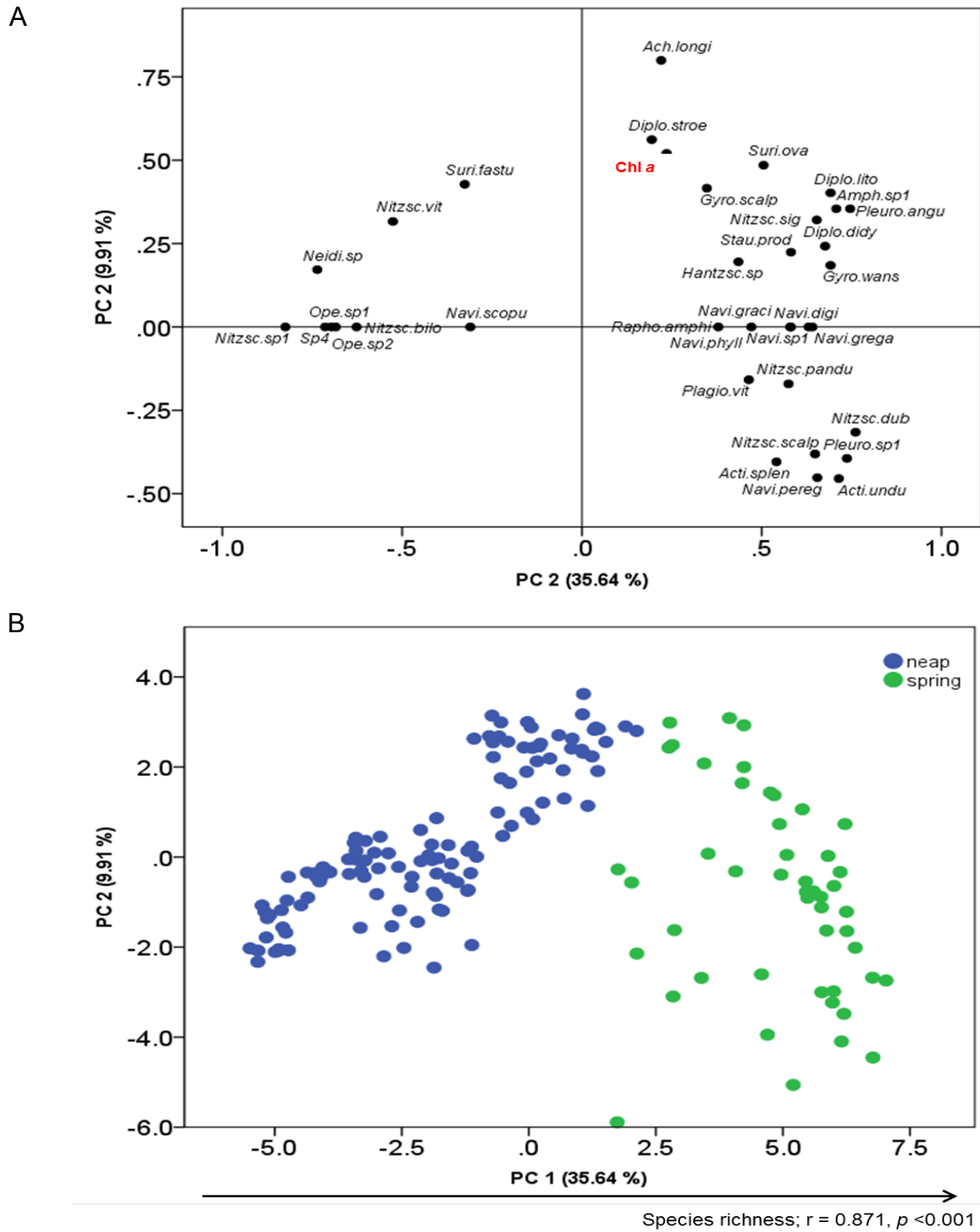


Figure 4.12: A) Variable factor map and the B) individual factor map of the PCA that was performed on the samples which Correlation A showed **significant positive curvilinear relationship** on the **salt marsh** that was only recorded during neap tide on the 5th, 18th April and on the 2nd, 3rd and 17th July 2013 and during spring tide on the 11th, 12th and 16th July 2013. The PCA was performed on the $\log_{10}(n+1)$, n = relative abundance of the species which relative abundance > 1 % and the Chl a concentration (supplementary variable) of the mentioned samples data. Notes that the PC1 was significantly positively correlated with the species richness at $r = 0.871, p < 0.001$.

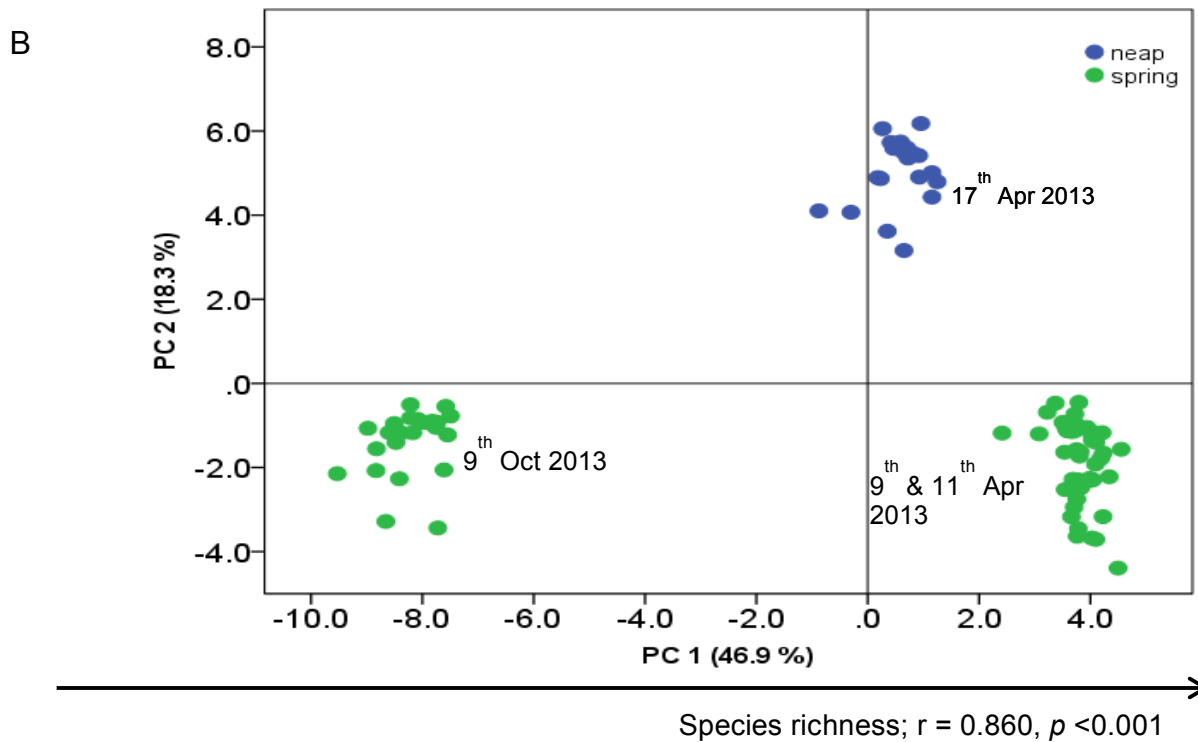
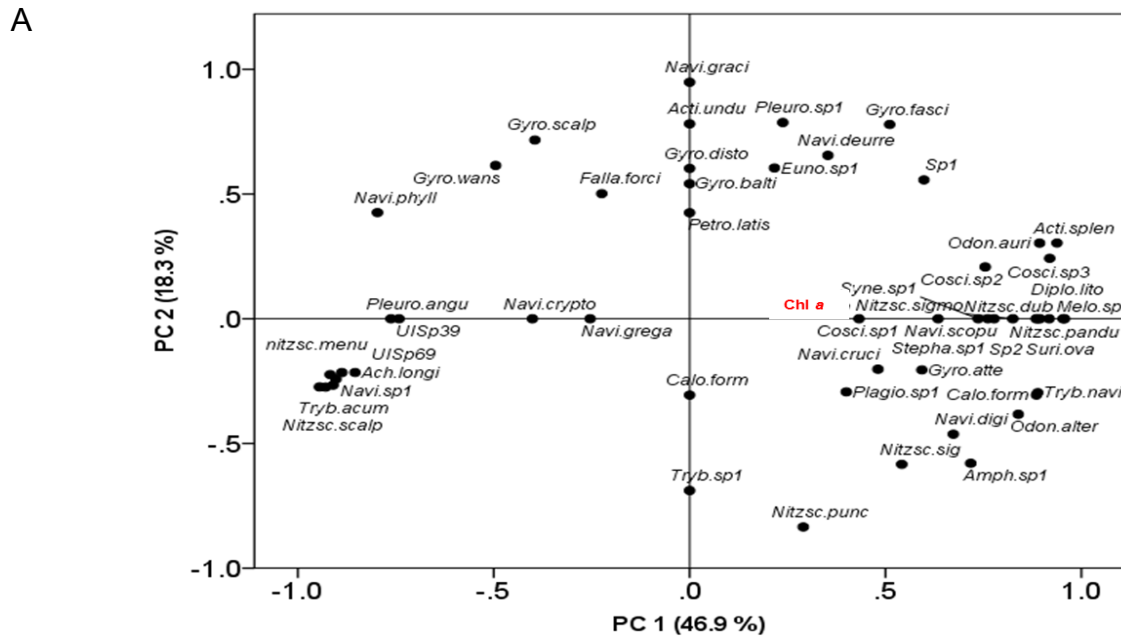


Figure 4.13: A) Variable factor map and the B) individual factor map of the PCA that was performed on the samples which Correlation A showed **significant positive curvilinear relationship** on the **mud flat** during spring (9th and 11th Apr (n = 24) and 9th Oct 2013 (n = 24)) and neap (17th Apr 2013 (n = 24)) tides. The PCA was performed on the $\log_{10}(n+1)$, n = relative abundance of the species which relative abundance > 1 % and the Chl a concentration (supplementary variable) of the mentioned samples data. Notes that the PC1 was significantly correlated with the species richness at $r = 0.860$, $p < 0.001$.

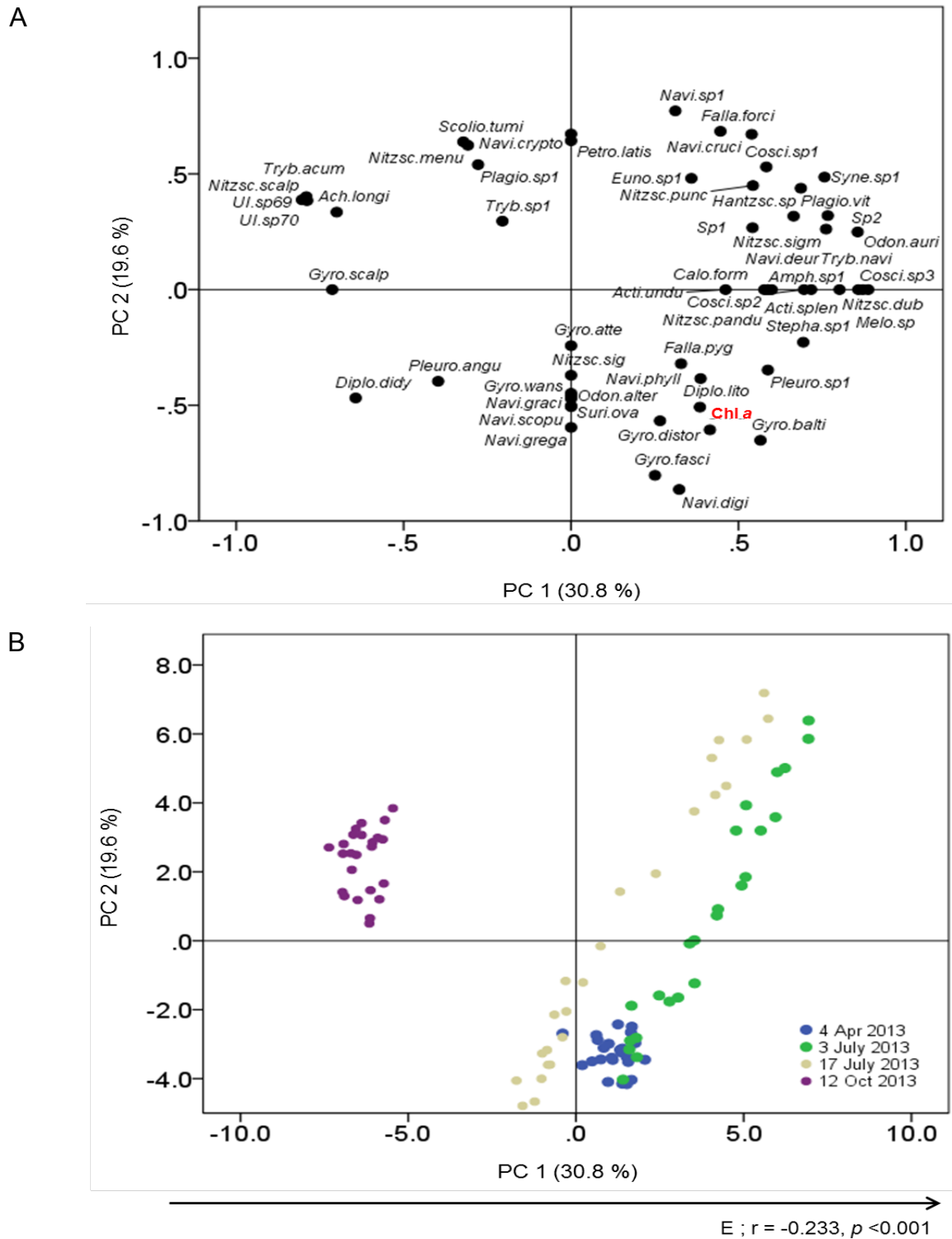


Figure 4.14: A) Variable factor map and the; B) individual factor map of the PCA that was performed on the samples on the **mud flat** which Correlation A showed **significant negative relationship** and was only recorded during neap tide on the 4th April, 3rd and 17th July 2013 and on the 2nd Oct 2013. The PCA was performed on the $\log_{10}(n+1)$, n = relative abundance of the species which relative abundance > 1 % and the Chl a concentration (supplementary variable) of the mentioned samples data. Notes that the PC1 was significantly negatively correlated with the E value at $r = -0.233$, $p < 0.001$.

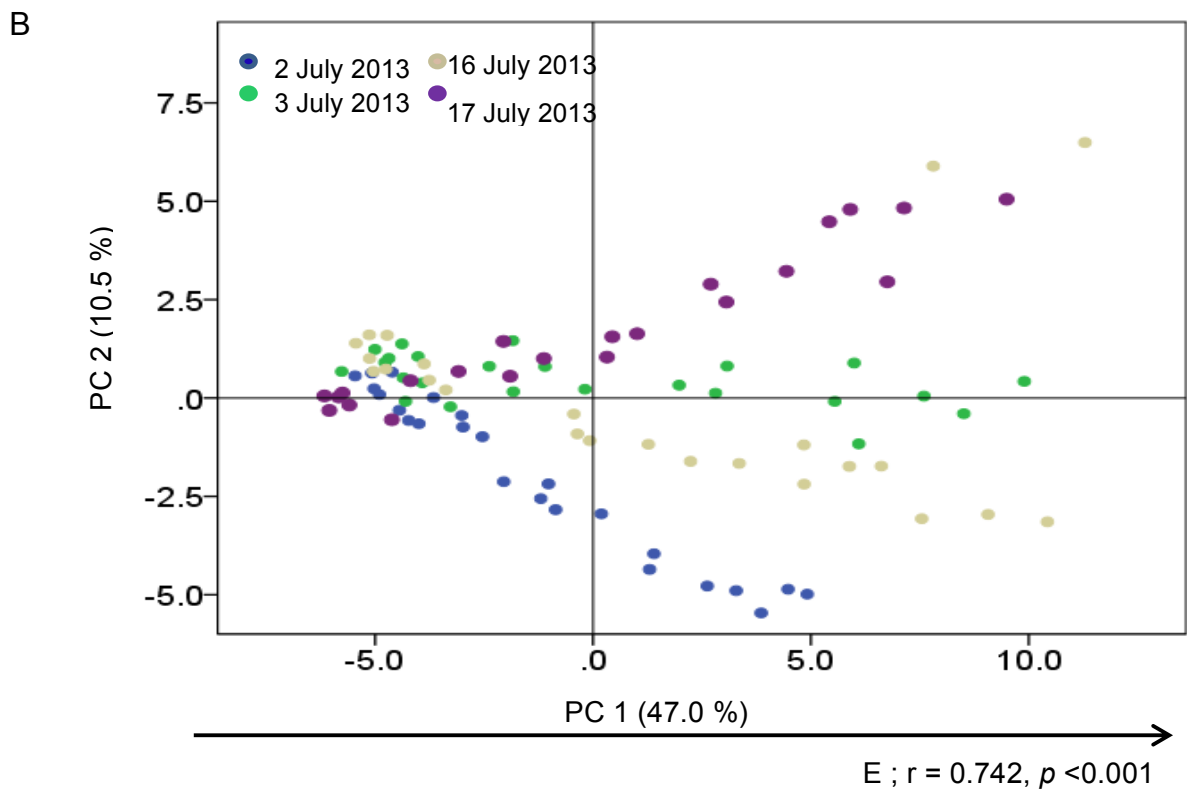
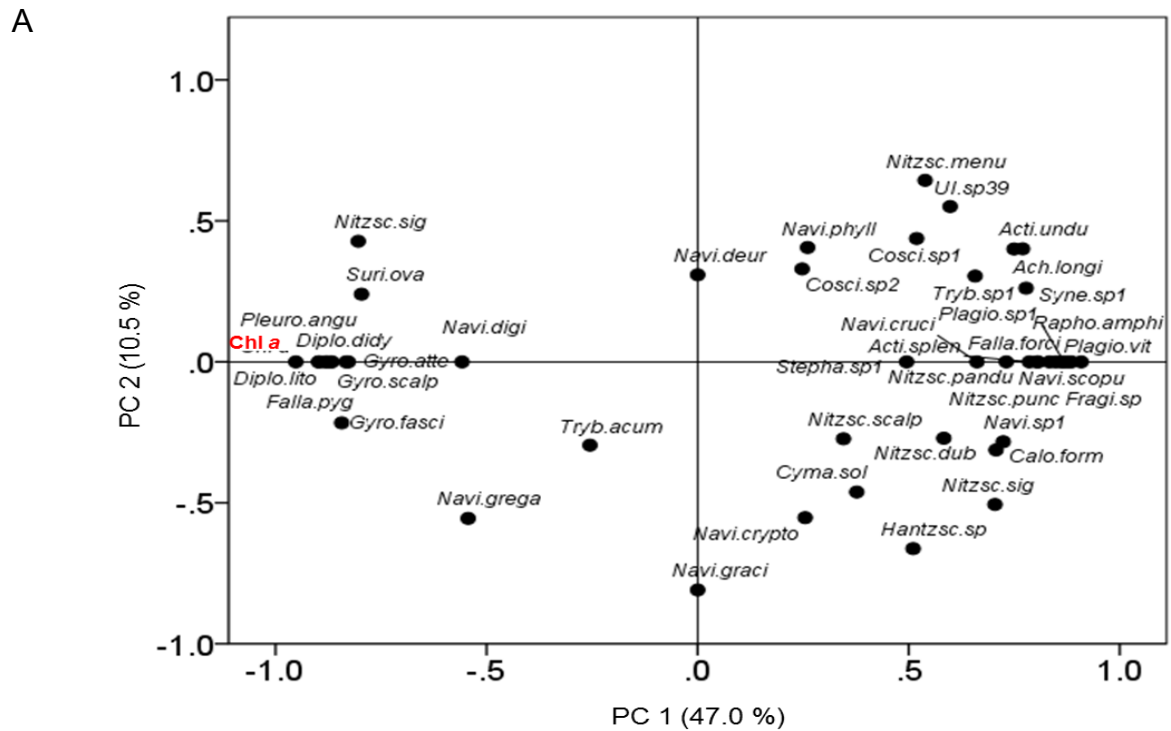


Figure 4.15: A) Variable factor map and the; B) individual factor map of the PCA that was performed on the samples on the **transition zone** which Correlation A showed **significant negative relationship** and was only recorded during neap tide on the 2nd, 3rd, 16th and the 17th July 2013. The PCA was performed on the $\log_{10}(n+1)$, n = relative abundance of the species which relative abundance > 1 % and the Chl *a* concentration (supplementary variable) of the mentioned samples data. Notes that the PC1 was significantly positively correlated with the *E* value at $r = 0.742, p < 0.001$.

4.4 DISCUSSION

4.4.1 Community ecology theory and the relationship between Chl *a* and MPB assemblages diversity on an intertidal flat

This present study is one of very few studies to investigate the relationship between MPB assemblage's diversity and Chl *a* concentration. The relationship pattern was varied across temporal daily and tidal scales. The temporal variability in the species composition of the assemblage must be one of the factors that caused such variability in the daily pattern because some of the diatom species in the assemblage can be either significantly negatively or positively correlated with the diversity of the assemblage which they inhabit (Underwood, 1994).

Strong positive linear relationship between the Chl *a* and the diversity of MPB diatoms in the Colne estuary was common in the mud flat's samples during spring tide. The Chl *a* concentration in these mud flat samples was significantly positively correlated with both the *E* value and the species richness of the assemblages. High occurrences of centric diatom in spring tide samples increased the species richness of the mud flat assemblages, and potentially increased the Chl *a* concentration of the assemblages. This finding is in agreement with the relationship between species diversity and biomass stability model constructed by Hughes & Roughgarden (2000) which hypothesized that in weak species interaction, total biomass would increase linearly with diversity. The potentially weak strength of competition between species in spring tide samples of mud flat in July may result in low number of dominant species (Forster et al., 2006). This finding however is generally opposite of what others have found on mud flats, with high biomass being associated with low diversity such as reported by Thornton et al. (2002). The different pattern potentially attributed to the fact that our present study has investigated the relationship between Chl *a* concentrations and the assemblages diversity at neap-spring tidal cycles, while other studies did not take into account the different in this relationship at the neap-spring tidal cycles.

Strong positive correlations as observed in the mud flat's spring tide samples were also potentially the result of high biomass production due to increased sum of sun hours in summer. The longer sum of sun hours increases the Chl *a* concentration (Austen et al. 1999; Sahan et al. 2007; my study) by providing the diatom communities longer time to photosynthesize (Sahan et al. 2007; Cartaxana et al. 2016). The positive effect of the longer sum of sun hours on MPB biomass was possibly enhanced by the high occurrence of centric species during spring tide on the mud flat. Hence only spring tide samples on the mud flat in summer displayed this significant strong positive correlation. This was supported by the theory of diversity by Putman and Wratten (1984) who proposed that all communities diversify with increased species richness caused by immigration of new species to an area.

Significant positive curvilinear relationship between Chl *a* and MPB diatom diversity was frequently observed in the salt marsh's samples. The Chl *a* concentration in these salt marsh samples displayed significant positive correlations with species richness. This finding can be related to the work done by Walker (1992) on hypothetical associations between biodiversity and biomass stability. Walker (1992) suggested that the positive curvilinear relationship could be the result of species redundancy. This species redundancy phenomenon in Colne estuary must be one of important process to ensure the stability and the reliability of the ecosystem. Redundancy is an insurance against the loss of function of an ecosystem in the event of disturbance (Walker, 2016). The salt marsh that is irregularly covered by the tidal submersions causes extreme condition (Le Rouzic, 2012), therefore potentially only allows certain diatom species as functional species (Forster et al., 2006) on the zone. Although there were species that potentially washed from the mud flat onto the salt marsh during spring tide may increase the biomass concentration on the salt marsh, the species also promotes higher strength of competition that only species that were common or native to the salt marsh could survive. This observation can be related to the study done by Forster et al. (2006), who stated that regular appearance of the same species composition at particular sites indicated that the microphytobenthic system may be resistant to non-native species.

Significant negative relationships between Chl *a* and the assemblages diversity was observed in the neap tide samples of the mud flat and more frequently in the transition zone samples. Chl *a* concentration of the samples that displayed this type of relationship decreased with increased equitability (*E* value) in the diatom species abundance. This finding is comparable to works that reported the high Chl *a* concentration in their samples were attributed to the increase of some dominant diatom species by Underwood (1994) and Thornton et al. (2002) and also simply because of the low evenness of diversity due to increased of unreported species by Sahan et al. (2007). In this type of relationship, it is hypothesized that there must be species that become more productive under certain disturbance (Tilman, 1982). In this present study, i found that the negative relationship were displayed in the samples on the mud flat and the transition zone during period of high mean wind speed, high 'sum of rainfall', and high 'sum of sun hours'. Some possible explanations may be that only certain species can withstand the changes in such weather condition. Species such as *P. angulatum*, *D. didyma*, some genus *Gyrosigma*, *N. digitoradiata* and *N. sigma* which were the large diatom species (> 50 µm) were possibly the least likely species to be washed away due to rainfall and high wind speed. Also, this finding could be link to the species ability to vertically downward moved to wetter sediment to avoid disturbance such as desiccation due to longer period of sun hours (McKew et al., 2011). This could result in these species increase their production and competitively exclude others by being the most productive species (Begon et al., 2005).

4.4.2 Shifts in MPB assemblages species composition across neap-spring tidal cycle and possible resuspension event

Depending on the variability in the weather-related abiotic factors, the Chl *a* concentrations in the Colne estuary increased along with (1) addition of new or rare species whose relative abundance was equitably distributed (2) only addition of rare or non-native species that will cause functional redundancy in other species and (3) high occurrence or high

relative abundance of some species (dominant species). Our finding was not comparable to the work done by Thornton et al. (2002) and Underwood (1997), as both found that the increase in Chl *a* in Colne estuary was correlated with the increases in the relative abundance of a single diatom species. However, their study was only done at large temporal scales, between seasons. Whereas the patterns described in this present study was also done and took into account the variability across higher frequency scales, between days and tidal types.

Tidal range was the important factor in adding the non-native or rare species into the mud flat and the salt marsh MPB diatom assemblages. Higher occurrence of centric diatoms for instance, from the genus *Coscinodiscus* and *Stephanodiscus* and also rare unidentified species such as the Sp2 and Sp3, were recorded in spring tide samples of the mud flat. This observation must be related to resuspension events and the exchange of sediment and associated diatoms between the tidal flat and the adjacent water channel of the Colne estuary. This hypothesis can be further supported by the works of Brito et al. (2012) and Ubertini et al. (2012). Both studies reported the MPB resuspension that occurs in the intertidal area contributes to the MPB species diversity in the water column in tidal flat during immersion and the adjacent water channel. Therefore, if the MPB movement from the tidal flat to the water channel was proven by Brito et al. (2012) & Ubertini et al. (2012), it is expected that the movement of phytoplankton from the water column to the tidal flat is also possible. These phytoplankton species are capable to settle on the sediment together with the benthic species. Migné et al. (2004) reported high amount of phytoplankton cells in the sediment surface during emersion when in the occasion of spring bloom in the water column in the muddy-sand of the Bay of Somme, France. The high phytoplankton cells that was reported in their study, was also coincided with high Chl *a* concentration. The finding by Migné et al. (2004) was also in agreement with the earlier work by Sundbäck et al. (1996), who suggested that the settlement of phytoplankton on sediment significantly contributed to the primary production in the benthic biofilms.

On the salt marsh, species that were commonly recorded on the mud flat and the transition zone were found to contribute to species richness during periods of spring tide. MPB resuspension events that possibly happened on the mud flat and the transition zone may have resulted in some species being washed from the mud flat and the transition zone onto the salt marsh. In addition, the spring tide water may not only provide the salt marsh with nutrients, by increasing species richness but also by increasing the soil moisture and Chl *a* concentration (Sullivan & Moncreiff, 1988 & Le Rouzic, 2012). However, spring tides cover may only benefit the abundance of certain diatom species (the species that were recorded on both the mud flat and the transition zone), but not the species that were only recorded on the salt marsh. The small species that were possibly edaphic and epipellic on the salt marsh had lower relative abundance in the spring tide samples. This finding is supported by Le Rouzic (2012) who found that biofilm destabilization appeared to be the most significant stressor for the dominant taxa (dominant taxa in neap tide) during spring tide submergence in the upper marsh. It can be stated that the tidal cycle able to significantly cause the shift in the species composition of MPB assemblage (Underwood, 1997; Horton et al. 2006). In immersion during spring tide, salt marsh diatom species that are well-adapted in longer emersion period and desiccation (Underwood, 1997) may move to upper sediment, and therefore may be resuspended and washed away from salt marsh (Le Rouzic, 2012) or may vertically migrate downwards the sediment as a response to desiccation (McKew et al., 2011) or to avoid the tidal disturbance.

4.5 CONCLUSIONS

Chl *a* concentration in Colne estuary was closely associated with the species composition of the MPB assemblage. The relationship between Chl *a* and the MPB diversity was controlled by a set of weather-related abiotic factors. Periods of spring tides were the important events that enhanced the occurrence of new or rare species on the mud flat and the salt marsh. However, the diversity of MPB diatoms on the transition zone was disturbed by

spring tide occurrence. Periods of bad weather resulted in the negative correlations between the sediment Chl *a* concentration and the diversity, which indicated the occurrence of dominant species.

MPB biomass (in terms of Chl *a* concentration) in Colne estuary was strongly attributed to addition of new or rare species and the occurrence of dominant diatom species in the assemblage rather to the evenness of the individual abundance of each species. While the increased in Chl *a* concentrations due to both addition of new species and the evenness in the assemblages were uncommon.

The strong positive linear, positive curvilinear, unimodal and negative correlation between Chl *a* and the MPB assemblages diversity in this present study were strongly related to (1) the phase or age of the assemblage, since all communities diversity increases over time (Putman and Wratten, 1984) and (2) the temporal variability of abiotic factors, which controlled the resuspension and the movement of the diatom across the Colne estuary. The relationship also displayed different correlation at different tidal cycles (neap-spring) and at different temporal scales. Our study has highlighted that the investigation of MPB biomass proxies at multi-spatial and temporal scales can reveal more informative findings on the relationship between the MPB biomass proxies with MPB assemblages diversity.

It might be possible that the observed four types of the relationship trends between the Chl *a* and MPB diversity in the Colne estuary are actually the typical relationships that rotate in a cycle as summarized in Figure 4.16.

Table 4.6 details the addressed hypotheses in Chapter 4 that were accepted or rejected.

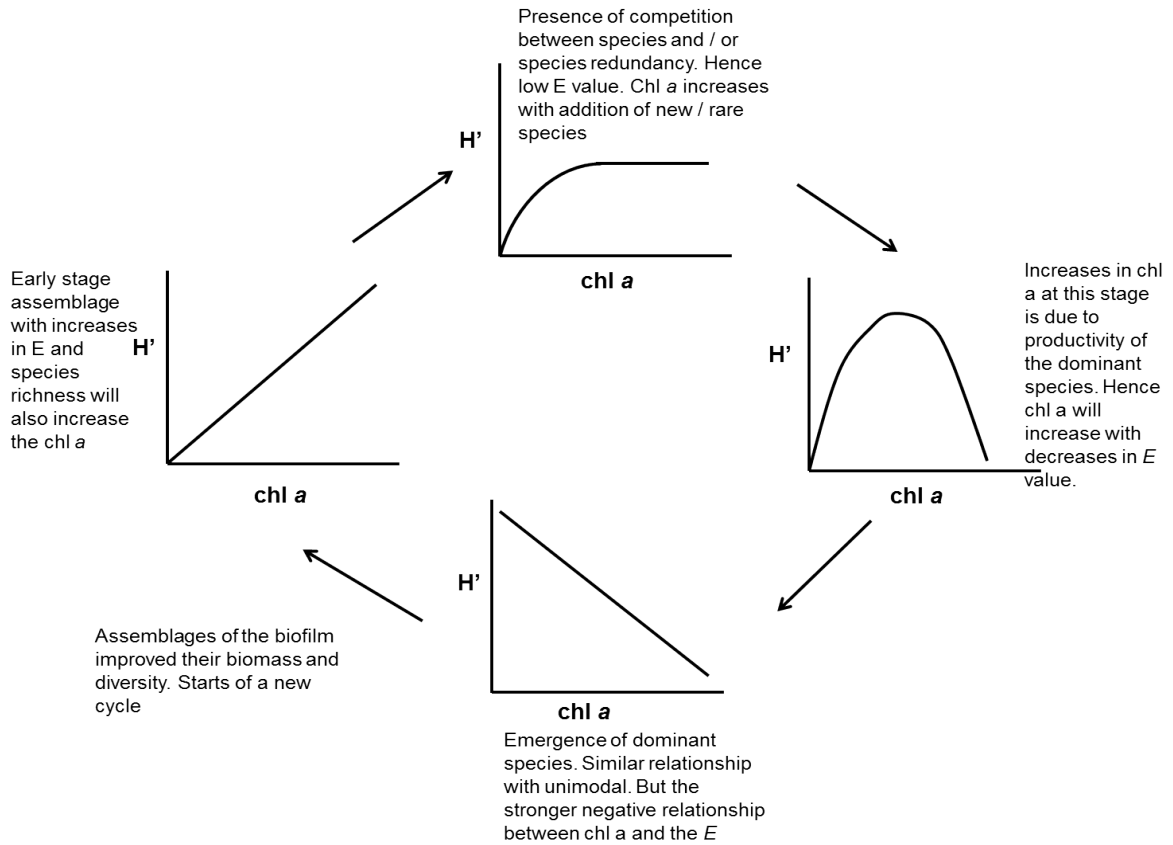


Figure 4.16: Diagram on the possible cycle in the relationship between the Chl a concentration and the MPB assemblage diversity.

Table 4.6: Hypotheses that were addressed in Chapter 4. Also stated whether the hypothesis were accepted or rejected.

Hypotheses (page 15-17)	Accepted	Rejected
A1	/	
A2	/	
A3	/	
A4	/	
B2	Diversity on mud flat and transition zone	Diversity on salt marsh
B3	Diversity on mud flat and transition zone	Diversity on salt marsh
B5 (species richness)	/	
B6	/	
D2	/	

CHAPTER 5

SEDIMENT-WATER COLUMN EXCHANGES OF MICROPHYTOBENTHOS (MPB) ON AN INTERTIDAL FLAT

5.1 Introduction

Sediment-water column exchanges or resuspension of microphytobenthos (MPB) has been reported as one of the main contributors to MPB biomass dynamics and variability across intertidal flats (Koh et al., 2006; Ubertini et al., 2012). The importance of MPB resuspension is reflected by the fact that MPB are the main producers in the intertidal ecosystem (Underwood et al. 2005; Hanlon et al. 2006; Taylor et al. 2013) in the water column during immersion (Brito et al., 2012; Koh et al., 2006) and in the coastal ecosystem (Brito et al., 2012; Ubertini et al., 2012). Therefore, understanding MPB resuspension across an intertidal flat and between the intertidal flat and the water channel are important and should not be ignored when carrying out investigations into MPB distribution. In understanding the multifactorial interactions in MPB distribution, including the study of MPB occurrence and resuspension at different spatial zones, tidal range, wind and wave strengths are critical to picture the sediment-water exchanges of MPB across the intertidal flat.

De Jonge & Van Beusekom (1995) suggested that wind-induced waves were responsible to cause movement of sediment between the tidal flat and water channel, with more than 90 % of phytoplankton inhabiting the water column originating from the mudflat. They also proposed that the effective wind threshold to allow MPB resuspension to happen varies spatially and temporally. This was further supported by Ubertini et al. (2012) who also found significant temporal variability in MPB resuspension in Bays des Veys estuary in France. Higher temporal sampling frequency investigations by Koh et al. (2006) also reported significant variability in

MPB resuspension between neap and spring tidal periods. Because MPB resuspension displays strong temporal and spatial variability, features which are also a typical trait of MPB biomass on sediment surfaces, resuspension can possibly be a key factor that controls the MPB biomass dynamics on an intertidal flat. This suggests that the biomass concentration in terms of Chl *a*, EPS and also species composition may be important factors for each MPB biofilm to avoid resuspension during immersion period.

Chl *a* is the common biomass proxy that has been used in studying the MPB resuspension (De Jonge & Van Beusekom 1995; Koh et al. 2006; Brito et al. 2012). However, it is the extracellular polymeric substances (EPS) that actually is the closely-linked proxy related to MPB resuspension, as EPS controls the biostabilisation of sediment in the biofilm (Ubertini et al., 2012). To date, studies on MPB resuspension has been focusing on the relationship between Chl *a* and suspended sediment (Koh et al. 2006; Brito et al. 2012; Ubertini et al. 2012). There has been no quantitative work on MPB resuspension ever discussing the involvement of MPB species composition. In addition, because MPB abundance is not only significantly correlated to suspended sediment but also settled sediment (Facca et al., 2002), it is worthwhile to investigate the settlement rate of sediment in investigating the MPB resuspension.

Use of sediment traps to study the mineralogy and chemical properties of sediment at mud flats has widely been used by geologists (Green, 2011). Some studies also showed the use of the sediment traps to study the sinking rate of phytoplankton (Trimbee & Harris, 1984) and occasional dinoflagellate bloom (Viner-Mozzin et al., 2003). Green (2011) carried out a study to determine the effect of small waves on resuspension of sediment using sediment traps, however, only the mineralogy aspect was discussed, with information on MPB neglected. There is still no work on the resuspension of MPB by wave or wind activities at tidal flats using sediment traps. Over the past years, in-situ surveys of the resuspended sediment and MPB were simply collected by collecting the water using bottles (De Jonge & Van Beusekom, 1995), by water pumping (Ubertini et al., 2012) and by using Chl *a* and turbidity sensor (Koh et al., 2006).

With aid from sediment traps, the general aim of this present study was to investigate the MPB resuspension in Colne estuary across both spatial and temporal scales. Specifically, this study was carried out 1) to determine the exchanges of sediment and its associated MPB from the sediment surface into the water column on the mud flat and the transition zone over neap-spring-neap tidal cycles. It was hypothesized that there is sediment and MPB being washed away in the Colne estuary during immersion (Figure 5.1). By incorporating the species composition data, we set out to determine if the sediment-associated suspended MPB in the water column really originated from the adjacent sediment surface.

If sediment-water column exchanges of MPB is found, there must be a set of weather related abiotic factors, which control it. Therefore, this work also aimed 2) to investigate the relationship between MPB resuspension with wind speed and also 'sum of rainfall', 'sum of sun hours' and tidal range. It was hypothesized that the MPB resuspension by means of suspended MPB (chl *a* and species composition) is higher in the event of bad weather with increased wind speed (De Jonge & Van Beusekom, 1995) and higher 'sum of rainfall' values, since wet weather or stormy weather will reduce the bio-stabilization ability by the MPB biofilm (Underwood, 1994). The positive effect of bad weather to MPB resuspension will be enhanced by the increased tidal range, because higher water current energies with higher tidal ranges (as in spring tide) will be able to resuspend more sediment and MPB, than the lower energy water currents during neap tides (Koh et al., 2006). Henceforth, finally the aim was 3) to determine the effect of sediment settlement or deposition with the availability of MPB biomass after immersion event across the weather-related abiotic factors variability (Figure 5.1).

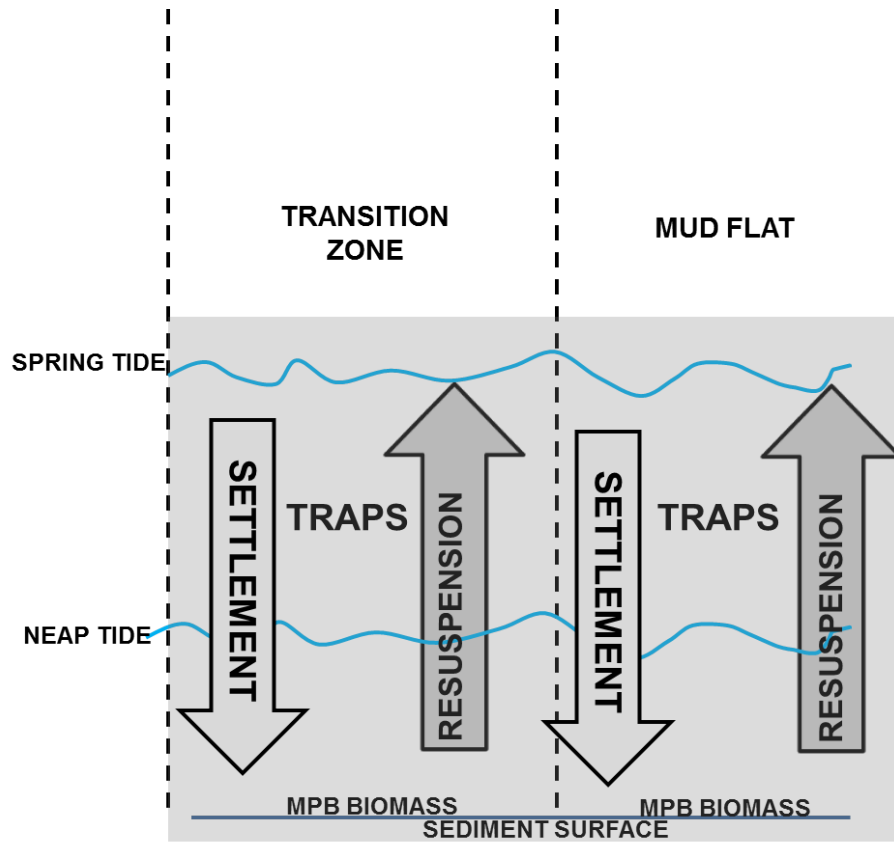


Figure 5.1: Conceptual diagram on sediment-water column exchanges of MPB that allows MPB resuspension to happen on an intertidal flat. In this present study, sediment traps were used to collect suspended sediment and its associated MPB. Traps filled with water were used to determine the net settlement rate of sediment at the study site.

5.2 MATERIALS AND METHODS

5.2.1 Sampling strategy

Sediment samples were collected in three different months; in April, July and October 2013 across Fingringhoe tidal flat in Colne estuary at small spatial scales. In each month, seven days of sampling (2 days in early neap tide, 3 days in spring tide and 2 days in later neap tide) were carried out in neap-spring-neap tidal cycle. Two different zones at spatial scales > 5 m were chosen (the mud flat and the transition) which lie parallel to River Colne. Both mud flat and transition zones were located on the un-vegetated area of tidal flat. These areas are covered with water in every high tide through the whole tidal cycle. Triplicate minicores (top 2 mm of sediment surface) were obtained from eight quadrats on each of the mud flat and the transition zone. Samples were taken within the first two hour's period at the starts of the emersion period.

The top 2 mm sediment samples in the minicores were halved, where the first half was retained and freeze-dried for the Chl *a* and extracellular polymeric substance (EPS) analyses. The Chl *a* and the EPS analyses were carried out following the Lorenzen (1997) and Hanlon et al., (2006)'s procedures, respectively, whereas the other halved sediment samples were retained for cells count which is detailed in 5.2.3.

5.2.2 Sediment Trap Approach (Sample Collection and Processing)

Sediment trap sampling was done once in each of the three different tide cycles in each sampling month (early neap tide, ENT, spring tide, ST, and later neap tide, LNT). Two traps were placed on each of quadrat on the first sampling day of ENT, ST and LNT. Both water and sediment were collected and transferred into 500 ml bottle on the next sampling day. One of the two deployed sediment traps on each quadrat was an empty 850 ml trap which determined the suspended solid load (mg L^{-1}) while the other one, was an identical designed bottle filled with

2.3 % NaCl (the salinity of the site's water) which determined the net vertical sediment settlement ($\text{mg cm}^{-2} \text{ hour}^{-1}$) through the water column during the period of tidal cover (Plate 5.1 & 5.2).

To measure Chl *a* concentration in the trap, 250 ml of the remaining trap sample was filtered using 12 cm GF/F Whatman filter paper that was dried in 80° C oven for 24 hours. Then, sediment on the filter paper was collected and freeze dried. Finally, Chl *a* was extracted from the sediment using the procedure mentioned in chapter 2.

5.2.3 Microphytobenthic cells count for species composition

Diatom cells count was performed using acid washed procedure (Underwood, 1994) (details in chapter 2). A total of 400 valves were counted for the April and July 2013's sediment surface's samples for both the mud flat and the transition zone. Whereas, only 250 valves were counted for October 2013's samples due to their low cells density.

While for each suspended samples, a total of 150 valves were counted for further analyses. A total of 200 ml sample from sediment trap were centrifuged using centrifugation machine (SLC6000) at 1500 rpm for 10 minutes to separate the sediment and associated diatom from water. Supernatant was discarded (100 ml) using soft plastic tubing, while the remaining sample was agitated, collected and transferred into 50 ml tube. After that, the collected sample was centrifuged at 1500 rpm for 10 minutes. For fresh sample, 5 ml of the centrifuged sample was transferred into bijou bottle and was preserved in 0.5 % glutaraldehyde in 2.3 % NaCl. The remaining sample was used in acid washing procedure (Underwood, 1994) for permanent slide preparation.

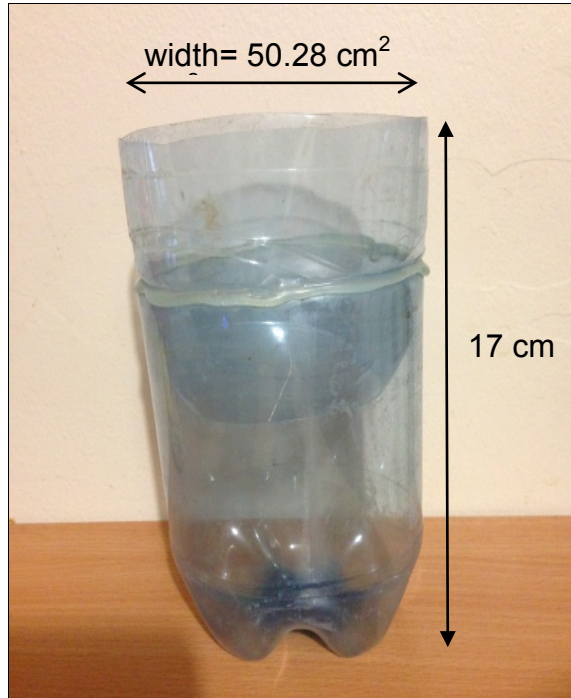


Plate 5.1: Sediment trap that was deployed on the sediment surface.

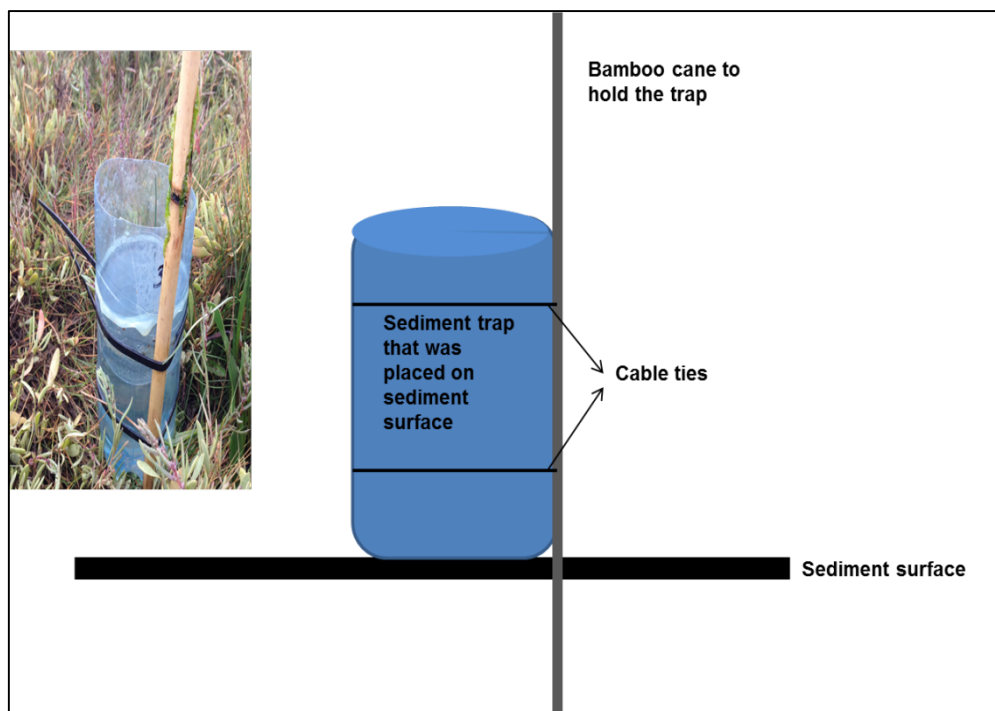


Plate 5.2: Illustration of the sediment traps on the sediment surface of mud flat and transition zone.

5.2.4 Sediment surface and suspended properties data

To investigate the MPB sediment-water column exchanges at our study site, the Chl *a* and EPS data on the sediment surface were compared with the suspended sediment and suspended Chl *a* data. Table 5.1 details the data set 1, 2 and 3 was used in the analyses. The table also details which data that were used in the comparison.

5.2.5 Statistical analyses

Analysis of variance (ANOVA) with Tukey HSD tests were performed on the overall data (log transformed) to determine the spatial trend in the Chl *a* concentration on sediment surface and in the water column, EPS concentration on the sediment surface and the suspended sediment across the study site. Pearson correlation coefficients were used to investigate the relationship and the connection between the suspended sediment and the availability of MPB biomass (Chl *a* and EPS concentration) on the sediment surface.

Principal component analyses were performed using FactoMineR in R stat. The analyses were done on the log transformed of suspended variables (suspended sediment and suspended Chl *a*) and sediment surface variables (Chl *a* and EPS) of pooled mud flat and transition zone data. The individual scores of the PCA were analyzed to identify for temporal trends (monthly scale and neap-spring tidal cycle). Only the first and the second component of the PCA were retained and used in the results and discussion.

Modified Morissita's similarity index was performed to calculate the percentage similarity between the MPB species composition on the sediment surface and in the water column (in the trap), using the Multi Variate Statistical Package (MVSP) 3.1 software (Kovach, 1999). Before the analyses, the overall data for each taxon were averaged and $\log_{(n+1)}$ transformed. The formula for the Modified Morissita's similarity index is;

$$\text{Modified Morissita's coefficient (MMC}_{ij}) = \frac{2 \sum_{k=1}^n X_{ik} X_{jk}}{[\sum_{k=1}^n (X_{ik}^2/N_i^2) + \sum_{k=1}^n (X_{jk}^2/N_j^2)] N_i N_j} \quad (\text{Kovac, 1999})$$

where i and j represents two cases of the data matrix, k represents the column (variable) and therefore X_{ik} is the datum in the k_{th} column of row i . N is the total number of variables.

Table 5.1: Details of the sampling strategies for samples for data set 1, data set 2 and data set 3. The purposes, the location and the dates on which the samples of the data sets were obtained were summarized in the table.

	Data set 1	Data set 2	Data set 3
Samples	Top 2 mm sediment surface	Sediment collected in the trap 1 (without water)	Sediment collected in the trap 2 (filled with NaCl)
Variables measured	Chl a, EPS, cells count (species composition)	Suspended sediment, suspended chl a and suspended cells count (species composition)	Sediment settlement rate
Location	Mud flat & transition zone	Mud flat & transition zone	Mud flat & transition zone
Sampling dates	<p>April 2013 - 4th (NT), 5th (NT), 9th (ST), 10th (ST), 11th (ST), 17th (NT), 18th (NT).</p> <p>July 2013 - 2nd (NT), 3rd (NT), 10th (ST), 11th (ST), 12th (ST), 16th (NT), 17th (NT)</p> <p>Oct 2013 - 2nd (NT), 3rd (NT), 8th (ST), 9th (ST), 10th (ST), 15th (NT), 16th (NT).</p>	<p>Deployed on: April 2013 - 4th, 10th, 17th July 2013 - 2nd, 11th, 16th Oct 2013 - 2nd, 9th, 15th</p> <p>Collected on: April 2013 - 5th, 11th, 18th July 2013 - 3rd, 12th, 17th Oct 2013 - 3rd, 10th, 16th</p> <p>Data of suspended sediment were compared with the sediment surface data of the day the trap were deployed.</p>	<p>Deployed on: April 2013 - 4th, 10th, 17th July 2013 - 2nd, 11th, 16th Oct 2013 - 2nd, 9th, 15th</p> <p>Collected on: April 2013 - 5th, 11th, 18th July 2013 - 3rd, 12th, 17th Oct 2013 - 3rd, 10th, 16th</p> <p>Data of net sediment settlement were compared with the sediment surface data of the day the trap were collected.</p>

5.3 RESULTS

Biomass proxies on the sediment surface and also in the water column were measured to investigate the MPB sediment-water column exchanges at Fingringhoe tidal flat, in the Colne estuary. Three biomass proxies were measured on the sediment surface, which were the Chl *a*, EPS and also the diatom species composition. Chl *a* concentration and also the cells count (species composition) were measured for the suspended sediment (sediment collected in sediment traps). The concentration of suspended sediment was also measured and presented in this work to investigate the effect of MPB availability on the sediment surface and its relation with sediment and MPB resuspension.

5.3.1 Spatial variability in MPB biomass proxies on sediment surface and in suspended sediment across intertidal flat

There was a significant difference in both suspended sediment ($F_{2,399}=9.699$, $p < 0.001$) (Figure 5.2C) and suspended Chl *a* ($F_{2,399}=8.438$, $p < 0.01$) (Figure 5.2D) between the mud flat and the transition zone of Fingringhoe tidal flat in the Colne estuary. Over the whole period of study, both suspended sediment and suspended Chl *a* on the transition zone (suspended sediment; $1187.70 \pm 53.37 \text{ mg L}^{-1}$ and suspended Chl *a*; $112.08 \pm 7.53 \mu\text{g L}^{-1}$) were significantly higher than on the mud flat (suspended sediment; $934.46 \pm 55.83 \text{ mg L}^{-1}$ and suspended Chl *a*; $89.13 \pm 7.57 \mu\text{g L}^{-1}$).

EPS concentration on the sediment surface was significantly different between the two zones ($F_{2,399}=5.528$, $p < 0.05$) (Figure 5.2B) with a higher concentration recorded on the mud flat ($127.14 \pm 6.64 \mu\text{g glucose equiv. cm}^{-2}$) than on the transition zone ($105.03 \pm 6.64 \mu\text{g glucose cm}^{-2}$). There was no significant difference in the Chl *a* concentration on the sediment surface between the two zones (Figure 5.2A).

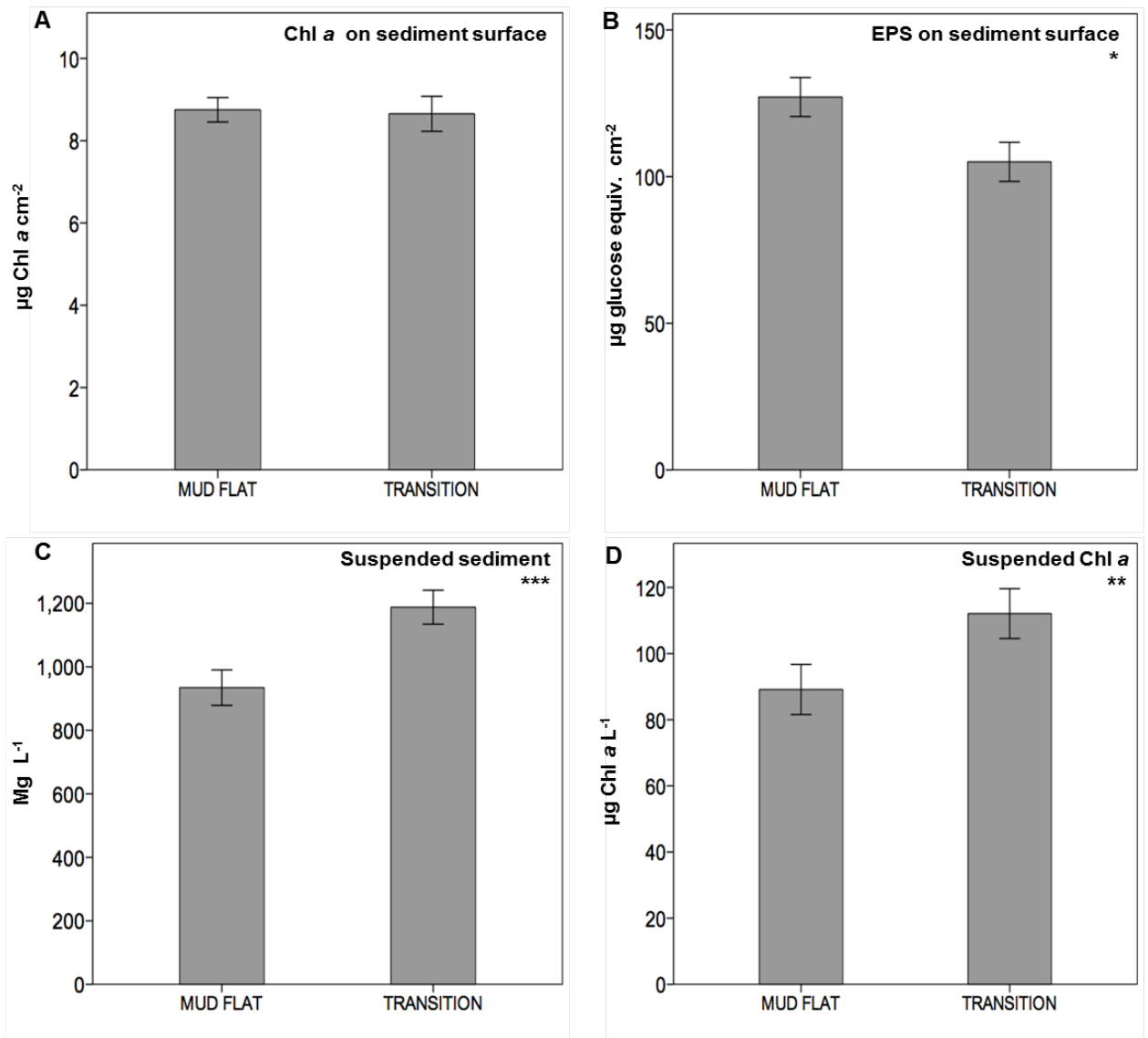


Figure 5.2: Spatial variability of A) Chl *a* and; B) EPS on the sediment surface and; C) suspended sediment and; D) suspended Chl *a* in the water column on two different zones across Fingringhoe tidal flat in Colne estuary. Values are mean \pm SE, $n = 216$. Bar charts were plotted based on the data of two days of neap tide sampling ($n=48$) and one day of spring tide sampling ($n=24$) occasions, across three months sampling in Apr, July and Oct 2013. *** indicates significant difference at $p < 0.001$, ** significant at $p < 0.01$ and * significant at $p < 0.05$.

5.3.2 Characterization of the relationship between suspended sediment and suspended Chl *a*

Suspended sediment in the water column was significantly and positively correlated with the Chl *a* concentration in the water column (Pearson correlation coefficients for overall data, $r = 0.561$, $p < 0.001$) (Figure 5.3A & 5.3B). The relationships between the suspended biomass proxies (suspended sediment and suspended Chl *a*) were explained by more than $R^2 = 0.5$ across all the sampling months on both mud flat and the transition zone. Except in April 2013 on the transition zone where the relationship only explained by 20.9 % of the variability (Figure 5.3B). The relationship between suspended sediment and suspended Chl *a* on the transition zone were explained by relatively lower R^2 than on the mud flat across the sampling months (Figure 5.3). While temporally, the R^2 values were relatively higher in the month of October 2013 than in April and July 2013 on both zones (Figure 5.3).

Values of the slope of the linear regression in Figure 5.3 were presented in Table 5.2 for further investigation on the relationship between suspended sediment and the suspended Chl *a*. There was significant different in the regression slope value for both the mud flat and the transition zone at $F_{2,71}=21.334$, $p < 0.001$ and $F_{2,71}=71.516$, $p < 0.001$, respectively (Table 5.2). The highest slope value on the mud flat was in April 2013 with a mean of $0.11 \pm 0.01 \mu\text{g Chl } a \text{ mg suspended sediment}^{-1}$, whereas the lowest was in October 2013 with the value of $0.02 \pm 0.00 \mu\text{g Chl } a \text{ mg suspended sediment}^{-1}$. The slope of the mud flat regression line was significantly positively correlated with the mean wind speed ($r = 0.644$, $p < 0.001$) and was significantly negatively correlated with the tidal range ($r = -0.396$, $p < 0.001$) and the sum of rainfall ($r = -0.2239$, $p < 0.05$) (Table 5.3). The slope of the transition zone's regression in April 2013 was the highest with the value of $0.08 \pm 0.00 \mu\text{g Chl } a \text{ mg suspended sediment}^{-1}$. While the lowest was in October 2013 ($0.02 \pm 0.00 \mu\text{g Chl } a \text{ mg suspended sediment}^{-1}$) (Table 5.2). There was significant negative correlation between the slope of the transition zone and the sum

of rainfall at $r = -0.339$, $p < 0.01$ (Table 5.3). None of the slope value of both zones had any significant correlation with the sum of sun hours.

The high suspended Chl *a* in April 2013 was reflected by a comparably high suspended sediment of $1550.8 \pm 94.9 \text{ mg L}^{-1}$ and $1506.0 \pm 90.0 \text{ mg L}^{-1}$ on the mud flat (Figure 5.3A) and the transition zone (Figure 5.3B), respectively. The low suspended sediment in July 2013 on the mud flat ($393.0 \pm 36.5 \text{ mg L}^{-1}$) and the transition zone ($796.9 \pm 84.0 \text{ mg L}^{-1}$) coincided with the suspended Chl *a* concentration of $53.5 \pm 3.4 \text{ } \mu\text{g Chl } a \text{ L}^{-1}$ and $84.1 \pm 9.0 \text{ } \mu\text{g Chl } a \text{ L}^{-1}$, respectively (Figure 5.3A and 5.3B). High suspended sediment in October 2013 on both zones was not associated with high suspended Chl *a*. The respective $1013.6 \pm 95.7 \text{ mg L}^{-1}$ and $1187.7 \pm 53.4 \text{ mg L}^{-1}$ of suspended sediment on the mud flat and the transition zone in October 2013 were only reflected by a total of $33.1 \pm 2.0 \text{ } \mu\text{g Chl } a \text{ L}^{-1}$ and $32.8 \pm 1.9 \text{ } \mu\text{g Chl } a \text{ L}^{-1}$ (Figure 5.3). This was relatively lower than the suspended Chl *a* in July 2013 ($53.5 \pm 29.0 \text{ } \mu\text{g Chl } a \text{ L}^{-1}$), the month that recorded to have significantly lower suspended sediment (both zones significant at $p < 0.001$) (Figure 5.3).

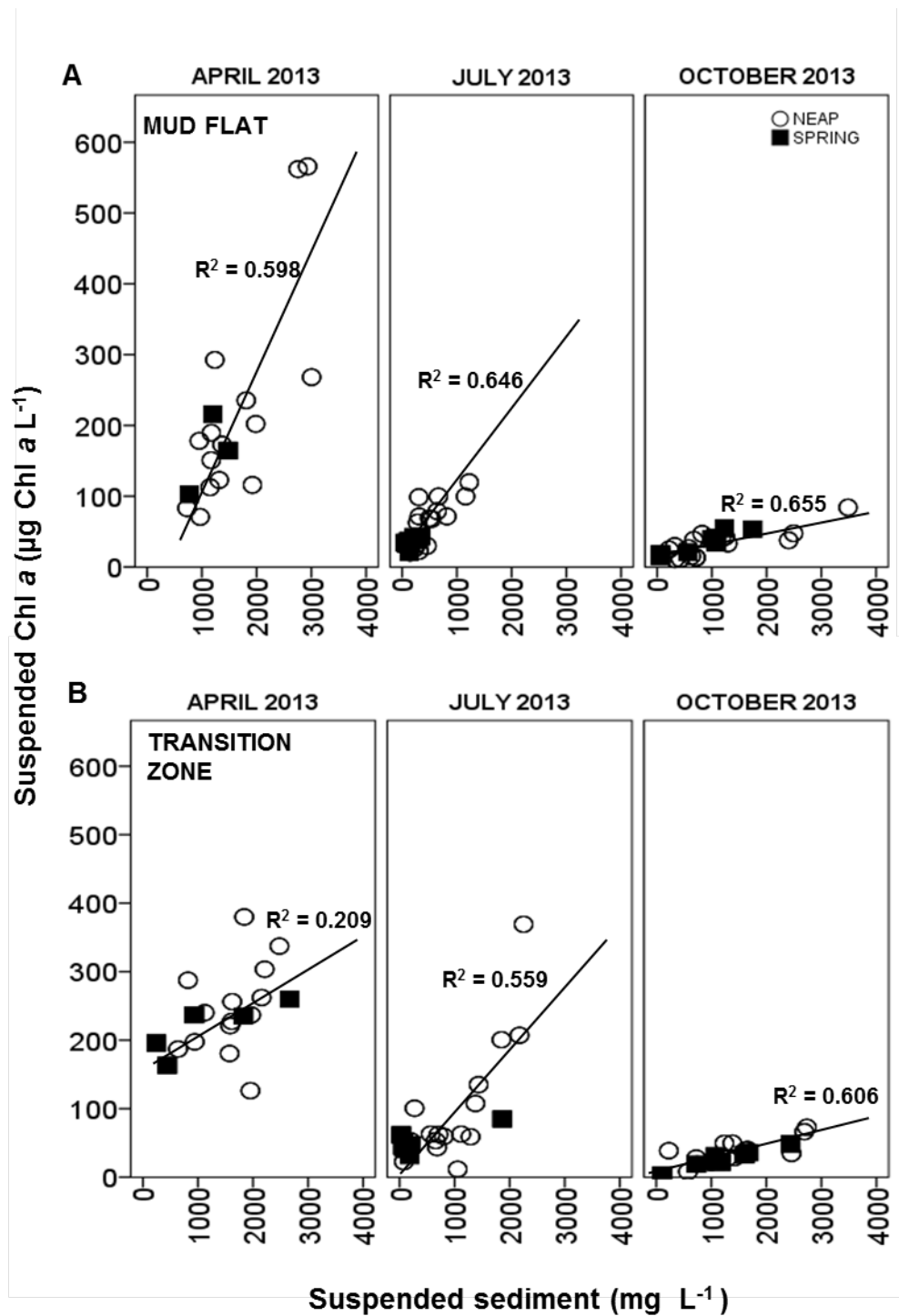


Figure 5.3: Relationship between suspended sediment and suspended Chl a on; A) the mud flat and; B) the transition zone in April 2013, July 2013 and October 2013 across the neap-spring tidal cycle. The scatterplot was plotted using data from the sediment trap which represented the sediment and Chl a in the water column during immersion period. n for each month = 24.

Table 5.2: Slope of the regression line ($\mu\text{g Chl } a \text{ mg suspended sediment}^{-1}$) of the relationship between the suspended sediment and the suspended Chl *a* at daily temporal scales in Apr, July and Oct 2013 on the mud flat and the transition zone. Values are mean \pm SE, n=8.

Month	Date	Mud flat	Transition zone
April 2013	4 th Apr	0.20 \pm 0.61	0.06 \pm 0.04
	10 th Apr	0.10 \pm 0.12	0.03 \pm 0.01
	17 th Apr	0.08 \pm 0.02	0.07 \pm 0.05
July 2013	2 nd July	0.05 \pm 0.02	0.11 \pm 0.04
	11 th July	0.04 \pm 0.02	0.02 \pm 0.00
	16 th July	0.09 \pm 0.03	0.06 \pm 0.01
October 2013	2 nd Oct	0.01 \pm 0.00	0.02 \pm 0.00
	9 th Oct	0.03 \pm 0.00	0.02 \pm 0.00
	15 th Oct	0.02 \pm 0.00	0.02 \pm 0.00

Table 5.3: Correlation coefficients between the slope of regression line and the weather-related abiotic factors, the mean wind speed (ms^{-1}), the sum of sun hours (hour), the tidal range (m) and the sum of rainfall (mm). The correlation strength was based on the output of Pearson's correlation test that were performed on the overall daily data across the three sampling months, n = 9. *** indicates significant difference at $p < 0.001$, ** significant at $p < 0.01$ and * significant at $p < 0.05$.

Weather-related abiotic factor	Zone	
	Mud flat	Transition zone
Mean wind speed (ms^{-1})	$r = 0.644^{***}$	ns
Sum of sun hours (hour)	ns	ns
Tidal range (m)	$r = -0.396^{***}$	ns
Sum of rainfall (mm)	$r = -0.239^*$	$r = -0.339^{**}$

5.3.3 Characterization in the relationship between benthic biomass and suspended biomass

The suspended Chl *a* concentration was hypothesized to closely link to the availability of the Chl *a* present on the sediment surface. This is because, if sediment-water column exchanges or MPB resuspension really happen on the tidal flat, the availability of Chl *a* in the water column must depend on how much available Chl *a* there is on the sediment surface.

A principal component analyses (PCA) was performed on the log-transformed water column variables (suspended sediment and suspended Chl *a*) and sediment surface variables (Chl *a* and EPS concentration) for the pooled mud flat and transition zone data. The PCA explained a total of 67.05 % of the total variation (Figure 5.4). The variable factor map of the PCA showed that the suspended Chl *a* and suspended sediment concentrations were significantly positively correlated with the positive axis of PC 1 which explained 43.81 % of total variation (Figure 5.4). The biomass proxies on the sediment surface, the Chl *a* and the EPS concentrations, were significantly correlated with the negative scores of principal component 1 (PC 1) (Figure 5.4). The output of this PC 1 suggests that there was potentially negative correlation between the Chl *a* and EPS on the sediment surface and the suspended sediment load with its associated Chl *a*. This statement was further supported by the significant negative correlation between PC 1 scores with both sediment surface's Chl *a* and EPS concentration with the values of $r = -0.599$, $p < 0.001$ and $r = -0.604$, $p < 0.001$, respectively (Table 5.4).

The negative relationship between suspended properties (sediment and Chl *a*) and the biomass on sediment surface is exemplified by the data in July 2013. Significantly lower PC 1 score of July 2013 was reflected by its significantly higher Chl *a* ($11.6 \pm 0.4 \mu\text{g Chl } a \text{ cm}^{-2}$) (Figure 5.5A) and EPS ($164.9 \pm 7.6 \mu\text{g glucose equiv. cm}^{-2}$) (Figure 5.5B) concentrations than in April 2013 and October 2013 (all significant at $p < 0.001$). The high biomass (both Chl *a* and EPS concentrations) on July 2013's sediment surface also coincided with significantly lower suspended sediment concentrations in the water column ($594.9 \pm 48.7 \text{ mg L}^{-1}$) than the other

two months (April 2013; $1527 \pm 65.1 \text{ mg L}^{-1}$; October 2013; $1169.9 \pm 64.1 \text{ mg L}^{-1}$) ($p < 0.001$) (Figure 5.5A.i & 5.5B.i). The suspended Chl *a* concentration in July ($68.8 \pm 4.9 \text{ } \mu\text{g Chl } a \text{ L}^{-1}$) however, was significantly higher than in October 2013 ($36.4 \pm 4.1 \text{ } \mu\text{g Chl } a \text{ L}^{-1}$) ($p < 0.001$) and as expected, was significantly lower than in April 2013 ($225.4 \pm 10.1 \text{ } \mu\text{g Chl } a \text{ cm}^{-2}$) ($p < 0.001$) (Figure 5.5A.ii & 5.5B.ii). There was significant negative correlation between the PC 1 and the sum of sun hours (Table 5.4).

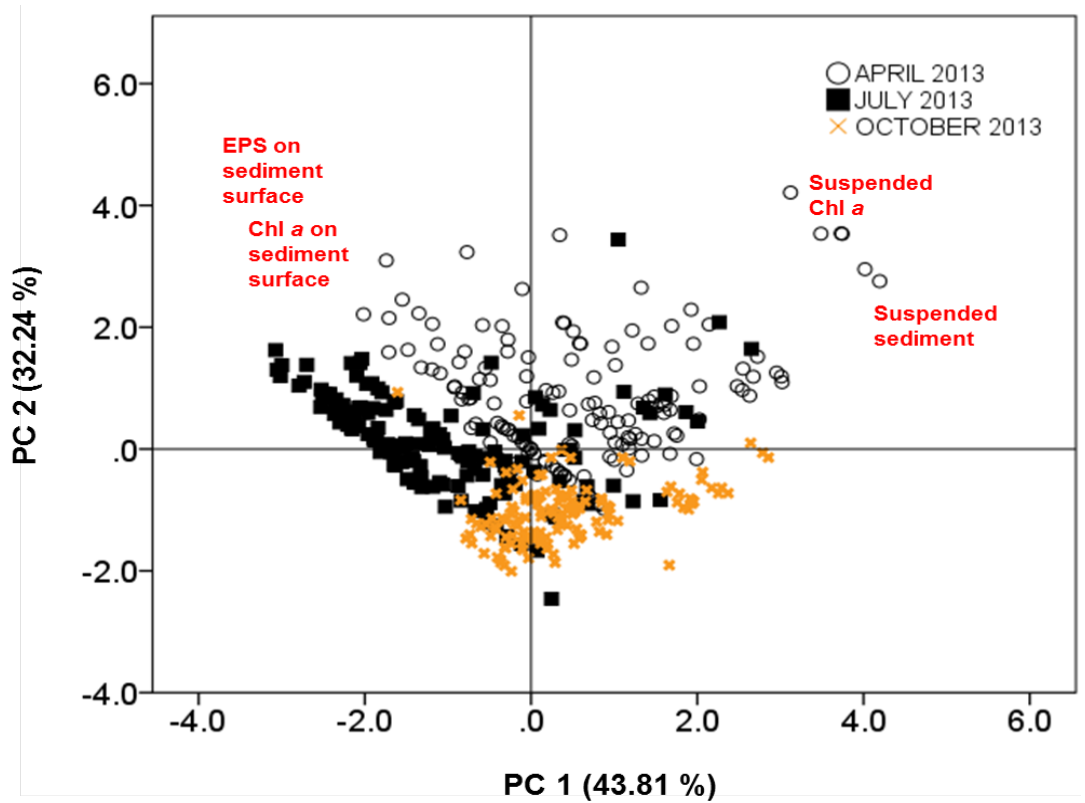
PC 1 was positively correlated with the suspended Chl *a* and suspended sediment and was also significantly positively correlated with mean wind speed ($r = 0.251$, $p < 0.001$) (Table 5.4). Therefore, the PC1 scores for both April 2013 and October 2013 were significantly more positive than July 2013, and were not only characterized by their high suspended sediment and high suspended Chl *a* (only for April 2013), but also by their high mean of 'mean of wind speed of three days' (April 2013; $11.8 \pm 2.7 \text{ ms}^{-1}$; and; October 2013; $5.8 \pm 1.8 \text{ ms}^{-1}$) (Table 5.5). PC 1 was significantly negatively correlated with the tidal range ($r = 0.423$, $p < 0.001$) (Table 5.5). The significantly higher or positive PC 1 scores of neap tide than the spring tide (Figure 5.4B) was reflected by neap tide's significantly higher suspended sediment ($1192.6 \pm 46.2 \text{ mg L}^{-1}$) and suspended Chl *a* ($114.3 \pm 7.0 \text{ } \mu\text{g Chl } a \text{ L}^{-1}$) than in spring tide (Figure 5.5). Sum of rainfall for three days did not show any significant effect on the PC 1.

Similarly to PC 1, principal component 2 (PC 2) was explained by all of the variables (both suspended and sediment surface). All of the variables however were significantly and positively correlated with the PC 2, which explained 32.24 % of total variation (Figure 5.4). Suspended sediment had the lowest correlation value with PC 2. PC 2 suggests that the availability of suspended Chl *a* in the water column was potentially positively related to the availability of the Chl *a* on the sediment surface. October 2013, that had significantly lower PC 2 scores than the other two months ($p < 0.001$), was characterized by significantly lower Chl *a* and EPS than in April 2013 and July 2013 (Figure 5.4) (Figure 5.5A, 5.5B, 5.5C and 5.5D, respectively). Interestingly, regardless the significantly higher suspended sediment in October 2013 than April and July 2013 ($p < 0.001$), the suspended Chl *a* in the water column in this

month was recorded as the lowest (Figure 5.5). Significantly lower Chl *a* concentration on the sediment surface in October 2013 than in April and July 2013 (both significant at $p < 0.001$) must be responsible for the mentioned observation. Therefore, less available Chl *a* was associated with the suspended sediment which reflected the low suspended Chl *a* in October 2013.

The 'sum of rainfall for three days' showed to be significantly negatively correlated with PC 2 ($r = -0.361$, $p < 0.001$) (Table 5.4). Significantly higher sum of rainfall of 6.4 ± 0.8 mm in October 2013 than the other two sampling months (Table 5.5) may be responsible for the low biomass concentration recorded on the sediment surface and also the low suspended Chl *a* recorded in the water column (Figure 5.4).

A



B

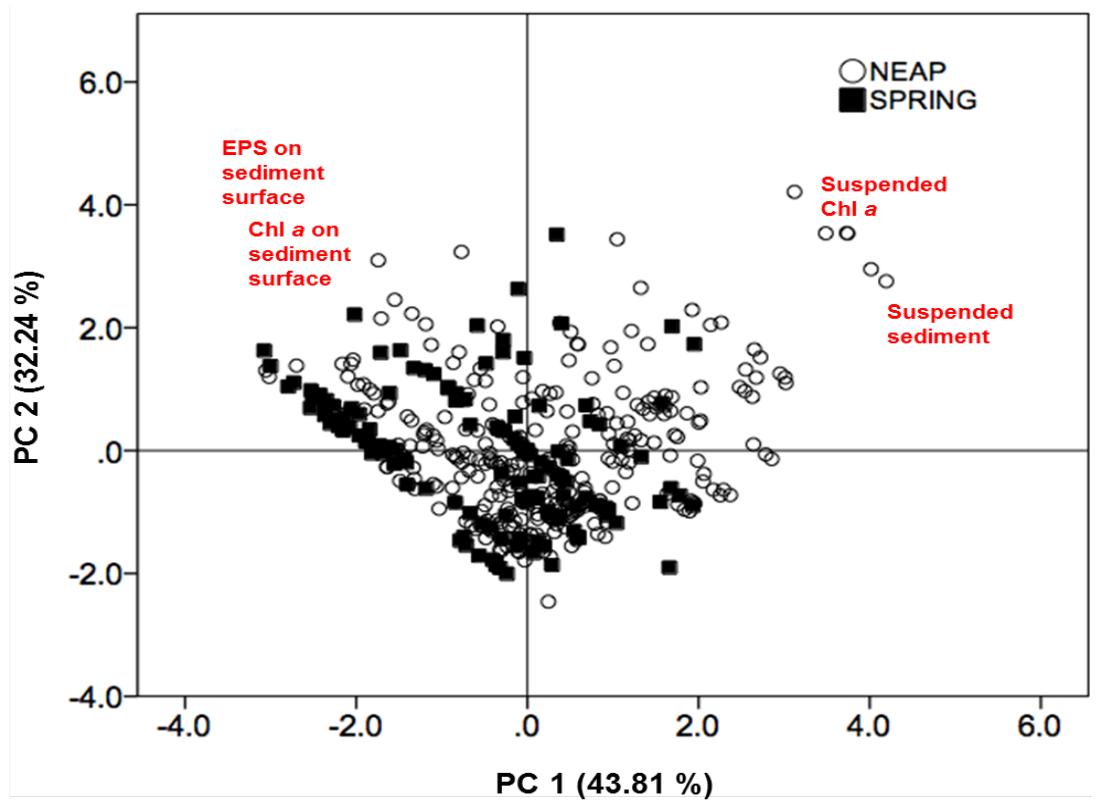


Figure 5.4: Individual variable map of principal component analyses (PCA) done on log-transformed (n) of the pooled data (mud flat and transition zone data) of the biomass on the sediment surface and suspended properties (suspended sediment and suspended Chl a) across three sampling months A) April 2013, July 2013 and October 2013 and in; B) neap-spring tidal cycle.

Table 5.4: Pearson's correlation coefficients (r) between principle component (PC) 1 and 2 with the Chl *a* and EPS concentrations on the sediment surface and also with the measured weather related abiotic factors; the mean wind speed (m s^{-1}), sum of rainfall (mm), sum of sun hours (hour) and tidal range (m). Note that PC 1 was significantly positively correlated with suspended sediment and suspended Chl *a*, and significantly negatively correlated with Chl *a* and EPS concentrations on sediment surface. While PC 2 was significantly and positively correlated with the all four variables. *** indicates significant different at $p < 0.001$, ** indicates significant different at $p < 0.01$ and * indicates significant different at $p < 0.05$.

Principle component (PC)	Biological factors		Weather-related abiotic factors			
	Chl <i>a</i> (on sediment surface)	EPS (on sediment surface)	Mean wind speed	Sum of rainfall	Sum of sun	Tidal range
PC 1	-0.599 ***	-0.604 ***	0.251 ***	ns	-0.505 ***	-0.423 ***
PC 2	0.583 ***	0.565 ***	0.393 ***	-0.361 ***	0.174 ***	ns

Table 5.5: Temporal variability (between daily) of the measured weather-related abiotic factors. MWS is mean wind speed, SOS is sum of sun hours, SOR is sum of rainfall.

MONTH	WEATHER-RELATED FACTORS	SAMPLING DATE							
		4/4/13	5/4/13	9/4/13	10/4/13	11/4/13	17/4/13	18/4/13	
Apr-13	MWS (m s^{-1})	14.5	8.1	6.1	7.7	9.3	2.4	17.4	
	SOS (hours)	11.8	13.8	10.9	7.4	7.4	8.6	12.4	
	SOR (mm)	1.4	1.4	0.0	0.3	4.4	2.4	1.0	
	TIDAL RANGE (m)	3.7	3.6	4.3	4.6	4.8	3.6	3.8	
Jul-13	MWS (m s^{-1})	2/7/13	3/7/13	10/7/13	11/7/13	12/7/13	16/7/13	17/7/13	
	SOS (hours)	2.8	4	6.05	3.75	6.03	3.6	1.9	
	SOR (mm)	21.4	8.3	36.3	30.9	19.1	20.5	24.9	
	TIDAL RANGE (m)	0.0	3.7	0.0	0.0	0.0	0.0	0.0	
Oct-13	MWS (m s^{-1})	2/10/13	3/10/13	8/10/13	9/10/13	10/10/13	15/10/13	16/10/13	
	SOS (hours)	3.2	4.0	3.2	4.8	9.3	5.4	4.0	
	SOR (mm)	10.9	7.0	17.1	10.3	12.3	2.8	1.7	
	TIDAL RANGE (m)	0.3	8.1	0.6	0.6	5.4	18.7	5.8	

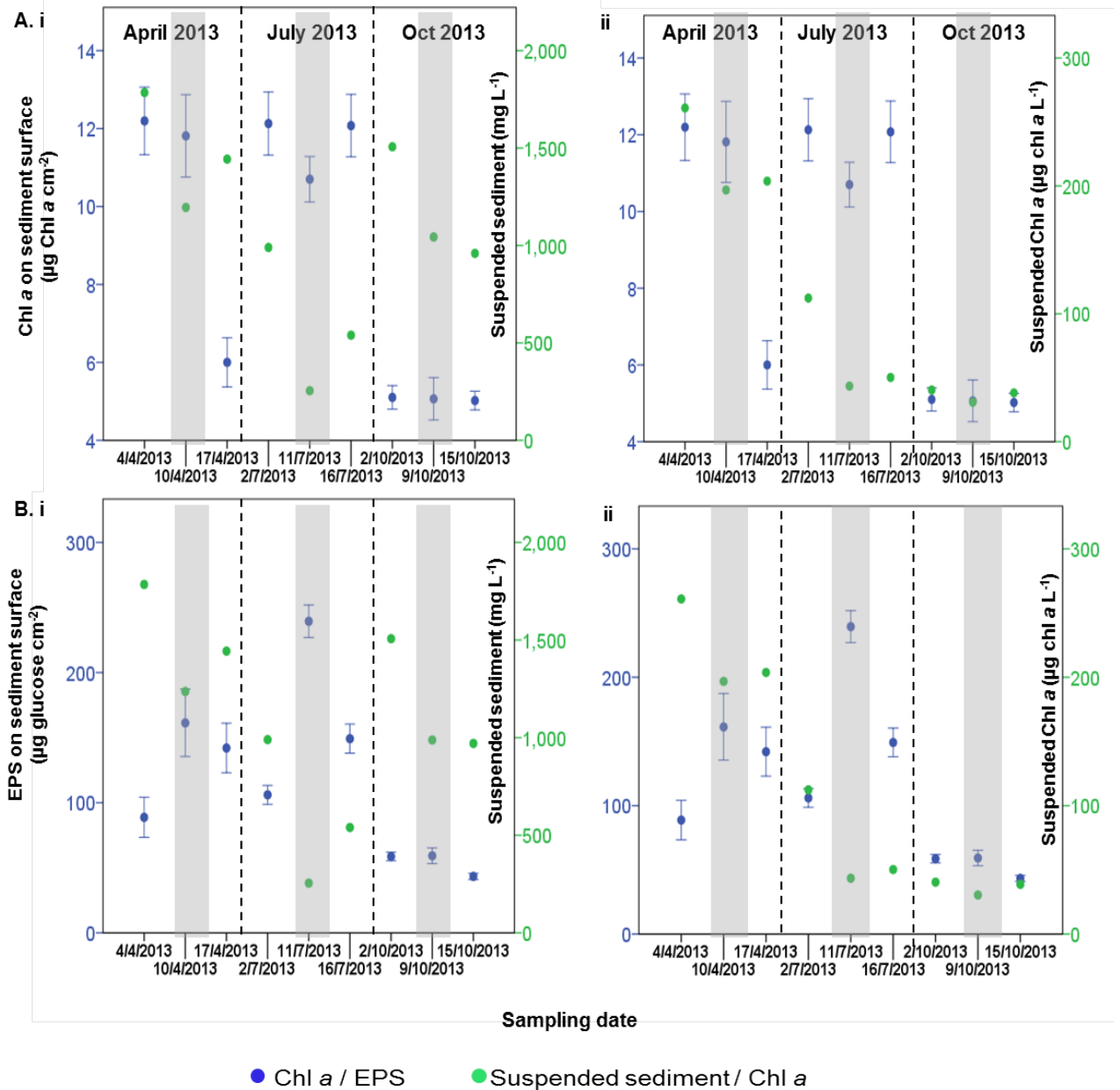


Figure 5.5: Temporal variability of Chl a concentration on the sediment surface with A) suspended sediment in the water column and B) suspended Chl a in the water column during immersion and extracellular polymeric substance (EPS) concentration on sediment surface with C) suspended sediment in the water column and D) suspended Chl a in the water column during immersion across the neap-spring-neap tidal cycle. Values are mean \pm SE, n = 48 (pooled data of both zones). Grey-shaded areas represent spring tide periods.

5.3.4 Exchanges of MPB species composition on the sediment surface and in the water column

This present study also included investigating the MPB species composition data associated with the resuspension information to check whether the sediment-water column exchanges is really happening at the study site.

Table 5.6 listed the relative abundance of the MPB diatom species recorded on both the mud flat and the transition zone across the neap-spring-neap tidal cycle. Overall, there were seventy diatom species identified in the permanent slides of the sediment samples across the study site. Of these seventy identified species, thirty four species (in grey-shaded rows) were also identified in the sediment trap samples of either mud flat or transition zone or both zones. The species collected in the sediment traps potentially originated from the sediment surface and associated with the sediment in the resuspension event during immersion.

Interestingly, all of the listed centric diatom species (in bold), *Actinoptychus splendens*, *A. undulatus*, *Coscinodiscus* sp 1, *Coscinodiscus* sp 2, *Coscinodiscus* sp 3, *Odontella alternan*, *Odontella aurita* and *Stephanodiscus* sp 1 were potentially involved in resuspension events (Table 5.6). Higher tidal range in spring tide than in neap tide occasion may be responsible to increase the occurrence of these centric diatoms on the mud flat and the transition zone. Relatively higher relative abundance of the mentioned species on the sediment surface in the spring tide than in neap tide, were concurrent with their higher relative abundance in the sediment trap during spring tide rather than in neap tide immersion (Table 5.6).

Relative abundance of some common diatom species such as *Gyrosigma balticum*, *G. scalpoides* and *Pleurosigma angulatum* were characteristically found higher on the sediment surface in neap tide sampling than in spring tide (Table 5.6). The low abundances on the sediment surface in the spring tide were characterized by their relatively higher relative

abundance in the water column or in the sediment traps than in the neap tide. However, there was no *G. balticum* ever recorded in the sediment traps on the transition zone (Table 5.6).

Sediment and water column exchanges of MPB diatoms were demonstrated by the positive relationship between the suspended sediment load and the similarity between the species composition on sediment surface and in the water column. Modified Morissita's similarity index was performed on the monthly relative abundance of identified taxa on the sediment surface and in the water column. The species composition percentage similarity was positively correlated with suspended sediment, explaining more than 50 % of the total variability across on both zones in April (R^2 ; 0.545) and July 2013 (R^2 ; 0.604) (Figure 5.6). The relationship in October 2013 only explained 32.3 % of the total variation.

Table 5.6: Relative abundance (%) of the diatom taxa identified on the sediment surface and in the sediment traps (suspended) across the Fingringhoe tidal flat in Colne estuary in neap (NT) -spring (ST) tidal periods. Grey-shaded rows indicate the species that were potentially associated with resuspended sediment during immersion. The table was constructed using the overall data of April, July and October 2013. NT indicates neap tide, ST indicates spring tide and **na** indicates not recorded in the samples. The **species in bold** were the centric species that potentially increased their relative abundance during spring tide.

MPB SPECIES	MUD FLAT				TRANSITION ZONE			
	ON SEDIMENT SURFACE		IN THE TRAP		ON SEDIMENT SURFACE		IN THE TRAP	
	NT	ST	NT	ST	NT	ST	NT	ST
<i>Achnanthes longipes</i>	0.53	0.30	0.99	na	1.38	1.37	3.15	3.42
A. splendens	2.15	3.22	8.44	12.50	1.07	2.00	3.97	5.59
A. undulatus	1.44	2.18	1.54	3.75	0.35	1.10	0.98	3.45
Coscinodiscus sp. 1	1.23	2.79	3.05	6.94	0.36	1.42	3.15	3.85
Coscinodiscus sp. 2	2.42	3.24	0.92	6.08	0.51	2.04	2.20	4.78
Coscinodiscus sp. 3	1.78	3.10	3.45	3.67	0.59	1.18	na	2.19
<i>Diploneis didyma</i>	2.49	2.08	6.62	1.31	5.39	4.91	12.31	8.39
<i>Diploneis littoralis</i>	1.21	1.13	4.50	1.05	1.88	1.70	1.64	2.96
<i>Gyrosigma balticum</i>	16.59	15.87	8.18	10.81	16.93	15.70	na	na
<i>G. fasciola</i>	1.75	0.32	4.57	4.13	1.63	0.55	3.09	2.06
<i>G. wansbeckii</i>	1.72	1.26	4.64	0.79	3.66	2.72	na	5.49
<i>G. scalproides</i>	6.40	4.70	5.77	7.40	5.33	4.19	5.38	8.05
<i>G. attenuatum</i>	2.20	2.65	2.02	1.84	5.17	2.94	5.34	7.54
<i>Navicula crucigera</i>	1.68	2.86	3.13	2.36	1.99	2.40	1.12	3.01
<i>Navicula gracilis</i>	0.78	0.73	1.97	0.79	1.34	1.25	1.57	1.38
<i>Navicula gregaria</i>	2.50	2.25	4.72	4.06	1.52	1.74	3.60	3.45
<i>Navicula scopulorum</i>	0.43	1.13	4.13	1.57	3.10	2.12	5.19	6.61
<i>Navicula sp 1</i>	1.21	1.10	1.06	na	1.52	1.36	1.05	1.33
<i>Nitzschia acuminata</i>	0.86	1.20	3.46	4.32	1.32	1.49	1.84	1.26
<i>Nitzschia dubia</i>	1.87	2.60	2.14	6.23	0.90	1.04	1.88	0.86
<i>Nitzschia scalproides</i>	0.75	0.45	1.65	na	2.42	1.43	5.30	3.41
<i>Nitzschia sigma</i>	4.81	4.89	3.89	0.52	3.70	3.48	6.44	5.82
Odontella alternans	0.25	2.18	2.60	4.31	na	na	2.75	2.77
Odontella aurita	1.68	2.93	1.52	2.36	na	na	0.90	na
<i>Petroneis latissima</i>	1.71	1.47	0.69	na	na	na	na	na
<i>Pleurosigma angulatum</i>	3.92	2.97	4.61	9.42	2.72	3.59	6.78	5.76
<i>Pleurosigma sp 1</i>	0.98	0.84	0.41	na	2.34	1.79	1.01	2.63
<i>Raphoneis ampiceros</i>	na	na	0.53	6.08	0.74	0.94	1.78	1.06
<i>Raphoneis minutissima</i>	2.83	0.89	0.38	na	1.04	0.88	na	na
<i>Stauroneis producta</i>	na	na	0.14	na	0.91	2.01	2.96	3.21
Stephanodiscus sp 1	1.92	2.48	3.41	4.02	0.35	0.53	1.38	1.93
<i>Surirella ovata</i>	0.32	0.53	1.62	1.05	0.45	0.84	3.03	2.68
<i>Fragilaria sp</i>	na	na	1.80	na	2.51	1.31	2.02	2.17
<i>Cymatopleura solea</i>	na	na	na	na	1.16	0.98	0.66	3.25
<i>Amphora sp 1</i>	0.23	0.54	na	na	0.55	0.40	na	na
<i>Caloneis formosa</i>	0.29	1.78	na	na	0.67	1.55	na	na
<i>Diploneis stroemii</i>	na	na	na	na	na	na	na	na
<i>Eunotia sp1</i>	1.66	1.45	na	na	na	na	na	na

Continued

<i>Fallacia forcipata</i>	0.80	0.44	na	na	1.58	3.87	na	na
<i>Fallacia pygmaea</i>	0.91	0.18	na	na	0.58	0.84	na	na
<i>Gyrosigma distortum</i>	1.98	1.85	na	na	1.36	0.86	na	na
<i>Navicula deurrebergiana</i>	0.68	na	na	na	1.07	0.68	na	na
<i>Navicula digitoradiata</i>	1.22	0.88	na	na	2.52	1.86	na	na
<i>Navicula peregrina</i>	1.85	0.64	na	na	1.10	0.39	na	na
<i>Navicula phyllepta</i>	1.63	0.93	na	na	0.56	0.55	na	na
<i>Nitzschia navicularis</i>	0.64	1.33	na	na	na	na	na	na
<i>Nitzschia panduriformis</i>	2.00	2.68	na	na	3.09	3.39	na	na
<i>Nitzschia punctata</i>	0.63	2.70	na	na	1.07	1.52	na	na
<i>Nitzschia sigmoidea</i>	1.38	0.95	na	na	1.07	0.68	na	na
<i>Pinnularia</i> sp	na	0.18	na	na	0.28	na	na	na
<i>Hantzschia</i> sp	0.91	1.05	na	na	1.18	2.70	na	na
<i>Plagiotropis</i> sp 1	1.06	1.63	na	na	0.45	0.12	na	na
<i>Plagiotropis vitreae</i>	0.49	na	na	na	1.34	2.29	na	na
<i>Scolioneis tumida</i>	1.21	1.77	na	na	1.76	1.35	na	na
Sp 1	1.95	1.66	na	na	na	na	na	na
Sp 2	0.41	0.92	na	na	na	na	na	na
Sp 3	1.48	1.78	na	na	0.60	0.83	na	na
Sp 6	na	na	0.46	na	na	na	na	na
Sp 39 (unidentified)	na	na	na	na	0.92	1.41	na	na
Sp 69 (unidentified)	2.68	0.34	na	na	0.43	0.81	na	na
Sp 70 (unidentified)	2.28	0.39	na	na	1.09	na	na	na
<i>Surirella fastuosa</i>	na	na	0.46	na	na	na	na	na
<i>Synedra</i> sp 1	0.35	0.39	na	na	2.28	2.88	na	na
<i>Tryblionella</i> sp 1	0.88	1.20	na	na	0.16	0.11	na	na

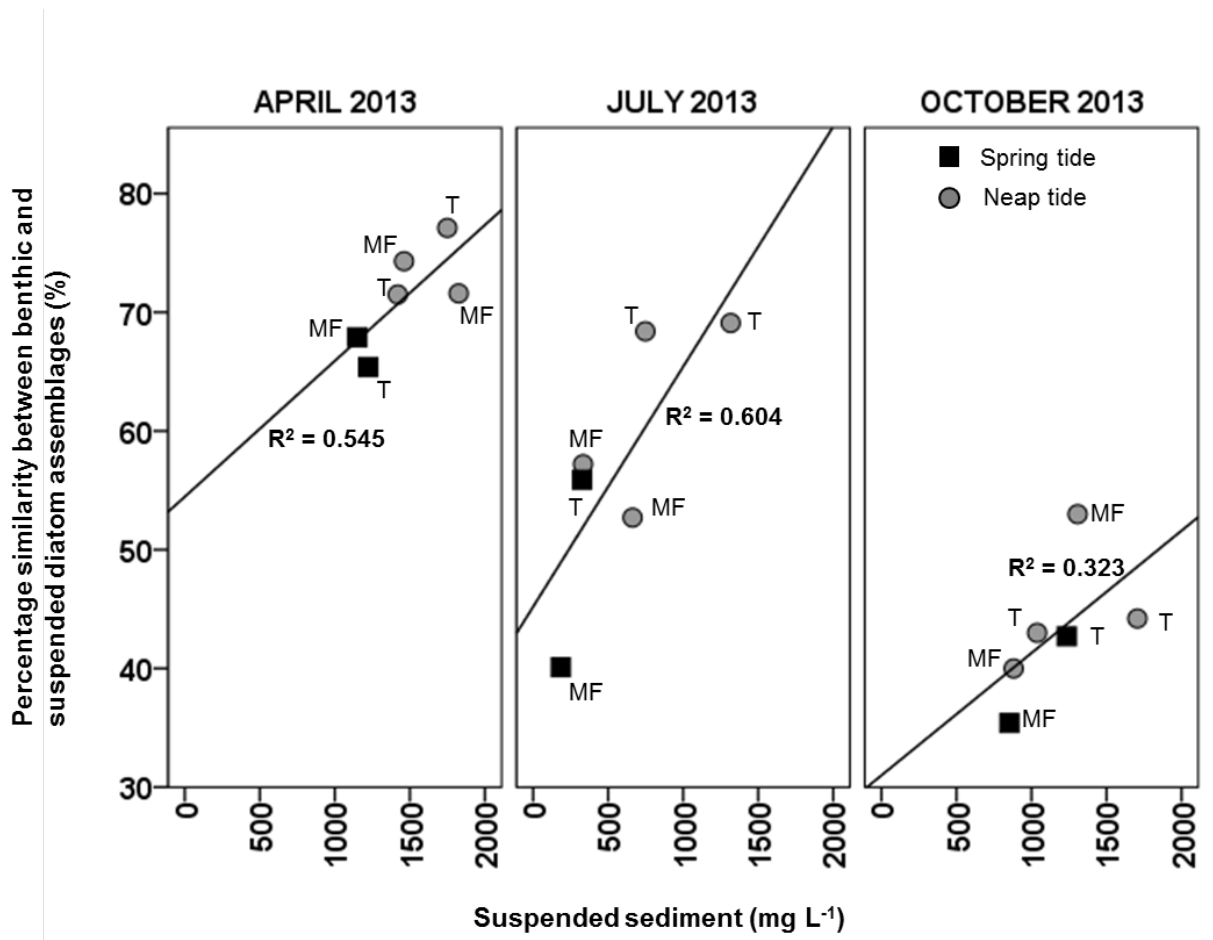


Figure 5.6: Relationship between the suspended sediment load and the percentage similarity between the species composition of diatom on the sediment surface and in the sediment traps (suspended) of the mud flat (MF) and the transition zone (T) in April, July and October 2013. The percentage similarity was determined by using the Modified Morissita's similarity index test.

5.3.5 Sediment settlement and MPB biomass on sediment surface

Sediment settlement or sediment deposition is potentially an important process in controlling the availability of MPB biomass on sediment surface after the MPB resuspension event during immersion period. Both Chl *a* concentration on the sediment surface and the net settlement rate of the sediment displayed similar daily pattern (Figure 5.7A). Figure 5.7A depicts that the high daily net sediment settlement was coincided with relatively high Chl *a* concentration on the sediment surface. This was supported by significant positive correlation between the two variables at $r = 0.211$, $p < 0.01$. There was however no similar daily pattern between the daily changes (percentage changes) of Chl *a* concentration and the sediment settlement after immersion across the tidal flat, with exception in April 2013 (Figure 5.7B).

The significant monthly difference in sediment settlement rate ($F_{2,398}=38.155$, $p < 0.001$) was potentially attributed to temporal variability of the weather-related abiotic factors during immersion period. For instance, higher mean wind speed for three days in April 2013 (Table 5.3) was also characterized by relatively and significantly lower sediment settlement rate ($1.6 \pm 0.1 \text{ mg cm}^{-2} \text{ hour}^{-1}$) than in July 2013 ($1.8 \pm 0.1 \text{ mg cm}^{-2} \text{ hour}^{-1}$) and October 2013 ($2.7 \pm 0.1 \text{ mg cm}^{-2} \text{ hour}^{-1}$) ($p < 0.001$), respectively (Figure 5.7). This was supported by a significantly negatively correlation between the net sediment settlement rate with the mean wind speed (Pearson's correlation coefficients; $r = -0.359$, $p < 0.001$ (pooled data of the mud flat and the transition zone)) (Figure 5.8).

There was significantly higher sediment settlement rate during neap tide ($2.3 \pm 0.7 \text{ mg cm}^{-2} \text{ hour}^{-1}$) than in spring tide ($1.6 \pm 0.9 \text{ mg cm}^{-2} \text{ hour}^{-1}$) ($F_{1,397}=35.824$, $p < 0.001$) (Figure 5.7). The high net sediment settlement during neap tide was also characterized by its significantly higher Chl *a* concentration on sediment surface ($9.95 \pm 0.30 \text{ } \mu\text{g Chl } a \text{ cm}^{-2}$) than in spring tide ($8.29 \pm 0.36 \text{ } \mu\text{g Chl } a \text{ cm}^{-2}$) ($F_{1,427}=11.108$, $p < 0.01$) (Figure 5.7A). This finding was also supported by a significantly negative relationship between the sediment settlement rate and the tidal range ($r = -0.416$, $p < 0.001$) (Figure 5.9). In addition, the higher sediment load during neap

tide compared to during spring tide further supported the net settlement rate was potentially influenced by the sediment availability in the water column.

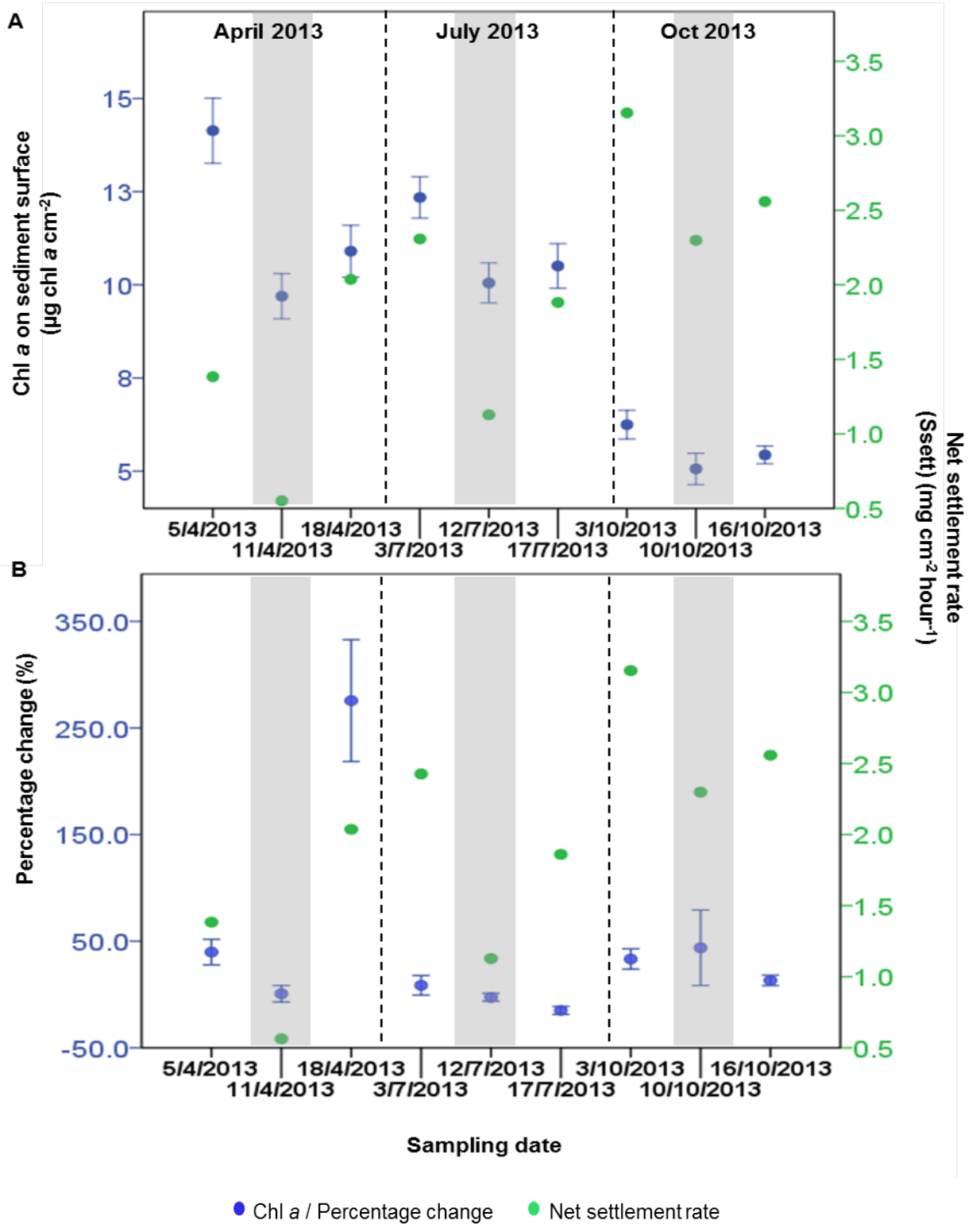


Figure 5.7: Relationship between; A) Chl a on sediment surface; B) daily changes in Chl a on sediment surface with the net settlement rate of sediment across three different sampling months. Values are mean \pm SE. n = pooled mud flat and transition zone data. Shaded areas indicate spring tide sampling.

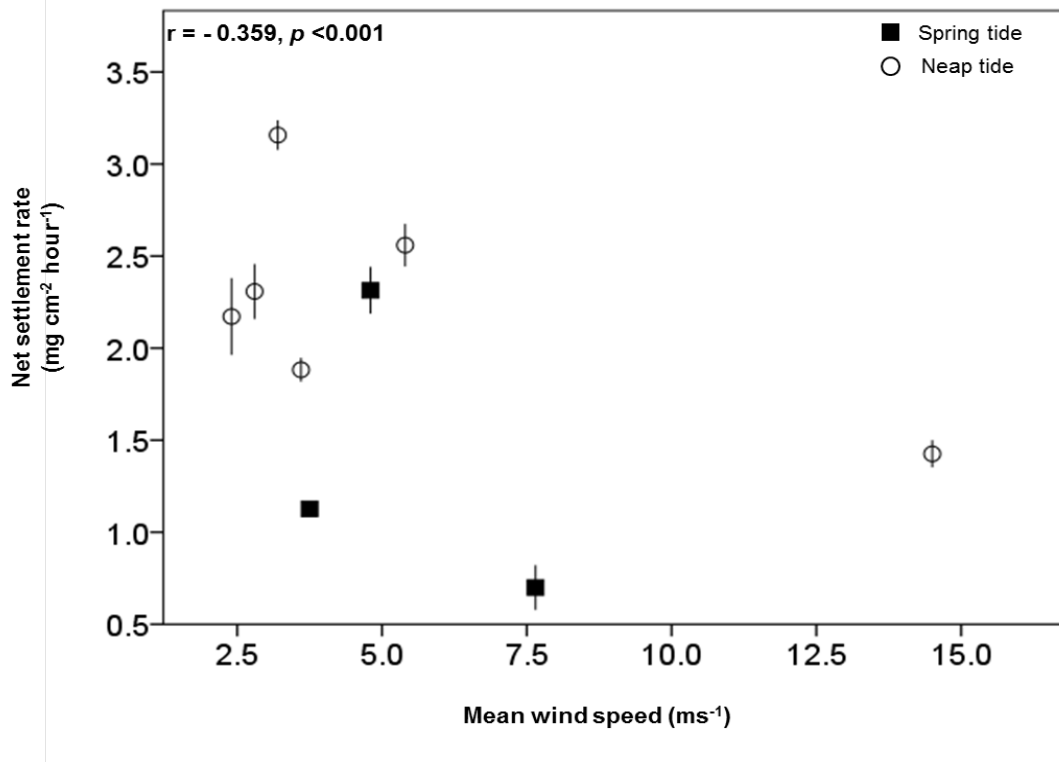


Figure 5.8: Pearson correlation coefficients between the net settlement of sediment and mean wind speed for three days across the neap-spring-neap tidal cycle. Values are mean \pm SE, $n = 48$ (pooled data of the mud flat and the transition zone).

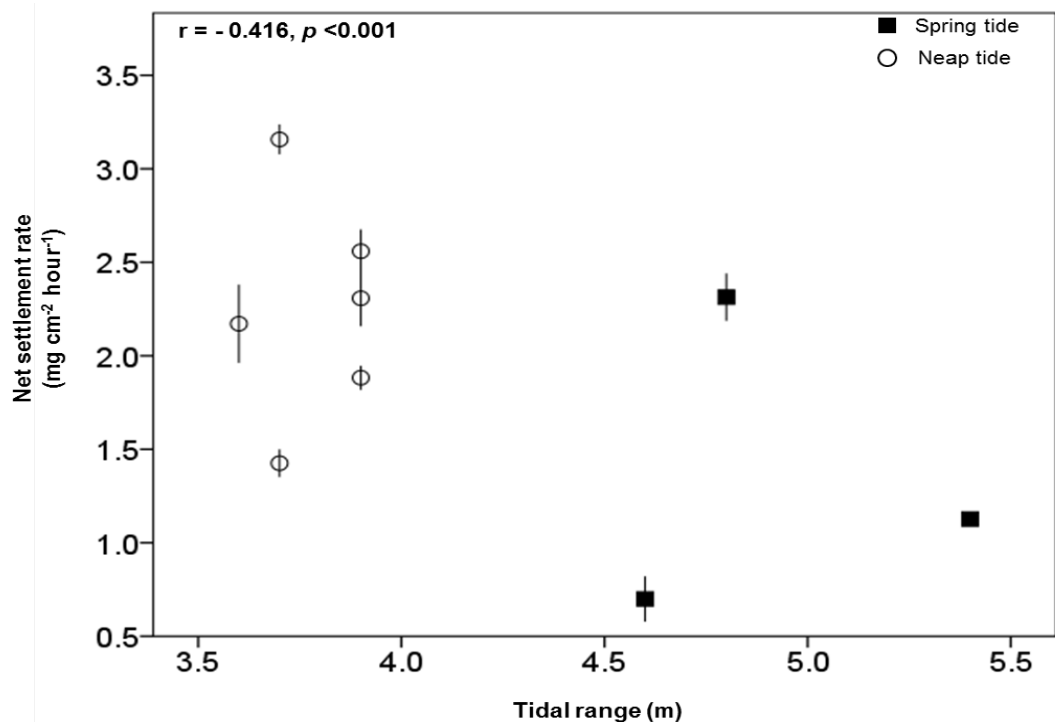


Figure 5.9: Pearson correlation coefficients between the net settlement of sediment and tidal range across the neap-spring-neap tidal cycle. Values are mean \pm SE, $n = 48$ (pooled data of the mud flat and the transition zone).

5.4 DISCUSSION

This present study was developed to investigate the potential for sediment-water column exchanges of MPB on tidal flats by investigating the connection between the MPB biomass properties (Chl *a*, EPS, species composition) on sediment surface (benthic) and in the water column. Data on the suspended sediment was also incorporated in this study to investigate MPB resuspension in Colne estuary.

5.4.1 Spatial variability in MPB biomass on sediment surface and in the water column

Water in the transition zone was typified by higher suspended sediment and Chl *a* concentrations than over the mud flat. The transition zone is located just below the salt marsh bank, and potentially received an input of sediment and associated MPB from the eroded bank during the immersion period. A quite similar finding discussing sediment movements (Mitchell et al., 2003), suggested that the bank erosion contributes to greater availability of sediment in water column which resulted in high suspended sediment at the area adjacent to the bank.

The lower suspended sediment and suspended Chl *a* on the mud flat than the transition zone may be the result of biostabilisation by the MPB (Saint-Béat et al., 2014), which was further explained by the significantly higher sediment EPS concentration on the mud flat than the transition zone.

5.4.2 Does suspended sediment carry along MPB?

This study started out by looking at the relationship between the suspended sediment and the suspended Chl *a*. We found that suspended sediment load was positively associated with suspended MPB biomass (Chl *a*) in both the spring and neap tide on both the mud flat and the transition zone. This finding is comparable to study done by Koh et al. (2007) and Ubertini et al. (2012) who reported significant positive correlations between the suspended particulate matter and suspended Chl *a* concentration during periods of high tide.

Suspended sediment and suspended MPB concentrations were significantly lower in spring tides compared to neap tides. This was different than that reported by Koh et al. (2007), who reported that the high current velocity, (approximately two times higher than in the neap tide at their study site) was responsible to suspend higher sediment loads from the sediment surface. Ubertini et al. (2012) reported that sampling during spring tides provides more understanding on the contribution of resuspended MPB to the total Chl *a* in the water column in their study on spatial variability of benthic-pelagic coupling on tidal ecosystem.

The different finding in our study must be attributed to the dilution effect of the higher water level during spring tide (approximately 1.6 times higher) than in the neap tide, which resulted in low concentrations of sediment being collected in the sediment traps during spring tide than in neap tide. In addition, the higher current velocity in spring tide could potentially cause more sediment being resuspended out of the tidal flat into water channel or to upper marsh. This was further supported by a significantly lower overall mean net sediment settlement rate across the tidal flat by 1.5 fold in the spring tide than in neap tide. The use of sediment traps that were placed exactly on the sediment surface may also be responsible in the different finding in our study. On the other hand, water column sampling to collect suspended sediment in both Koh et al. (2006) and Ubertini et al. (2012) were done by collecting water samples by using hand at water surface and by pumping of water at the level of 1 m from sediment surface, respectively.

5.4.3 Evidence of MPB sediment-water column exchanges

Our data have shown the strong correlation between the suspended sediment and suspended Chl *a*. However, this does not prove that the suspended sediment and the associated Chl *a* originated from the local sediment surface. Therefore, in order to investigate the sediment-water column exchanges of MPB in this study, we compared the data of MPB composition (relative abundance) of the diatom assemblages on the sediment surface and in the water column.

The benthic and suspended data revealed that the occurrence of MPB biomass in the water column during immersion was related to the MPB biomass proxies on the sediment surface (Koh et al., 2007). This strongly proves that the sediment-water column exchanges really happened at the Fingringhoe tidal flat. Interestingly, we found that both sediment surfaces Chl *a* concentration and suspended Chl *a* depicted both negative and positive relationships with each other. The negative relationship explained more variability in the total variation than the positive relationship (PC 1 and PC 2 of PCA, (Figure 5.4)).

The negative relationship between the MPB biomass on the sediment and in the water column indicated the potential biostabilisation effect of MPB biofilms. Increases of MPB biomass linked to EPS concentrations, on the sediment surface decreased the effect of MPB 'wash away' by stabilising the biofilm (Delgado et al., 1991; Austen et al. 1999), and resulted in lower MPB diatom abundance in the traps. Hanlon et al. (2006) further supported this by suggesting that during motility and tidal exposure, MPB produce EPS that combines with other extra cellular carbohydrate, to form mucilage component on the intertidal biofilms (Underwood & Paterson, 2003). These sticky polysaccharide substances are able to decrease the resuspension by holding the MPB in the biofilm together (Blanchard & Forster, 2006). Longer periods of sun, as in July 2013 (summer), not only allowed longer time for MPB production (Woelfel et al., 2007) and stimulates the downwards movement of MPB (Du et al., 2010) but also resulted in less Chl *a* in the water column.

The negative relationship between the suspended and benthic MPB proxies is also comparable to studies on the grazing stress by deposit feeders that cause increases in suspended sediment concentration in water column (Ciutat et al., 2007; Ubertini et al., 2012). Unfortunately, the effect of grazing stress on sediment-water column exchanges of MPB is not the main aim to be discussed in this present study. Based on observation, there was high density of *Hydrobia* sp. on the sediment surface of the mud flat and the transition zone on the Fingringhoe tidal flat (our study site). *Hydrobia* sp. is reported as one of the dominant sediment infauna of the Colne estuary (Chesman et al., 2006; Bellinger et al., 2009), and is also a well-known deposit feeder that significantly affect the erodibility of MPB biofilms on intertidal flats (Hagerthey et al., 2002; Orvain et al., 2004; Orvain et al., 2006). Grazers have been proven to decrease microphytobenthic biomass (Wolfstein et al., 2000) and community (Sahan et al., 2007). This phenomenon directly decreases the production of EPS and was reported to significantly negatively correlate with MPB Chl *a* concentration (Smith & Underwood, 1998) and decrease the ability of MPB biofilms to biostabilize the sediment surfaces of tidal flats.

The positive relationship between the suspended and the benthic MPB biomass proxies is comparable to study by Koh et al. (2006). This relationship was depicted in the PC2 of the water column and the sediment surface data (Figure 5.4) and explained 32.4 % of the total variability, which is proved to be less significant than the negative relationship (explained by PC1 of the PCA). Despite the biostabilisation by MPB biomass on the sediment surface that causes the negative effect on the suspended MPB, the amount of MPB biomass present on the sediment surface is still important in providing a source for the MPB in the water column. This type of positive relationship was observed at large temporal scale, the month but not at daily scale. The low MPB biomass in October 2013 was also reflected by low MPB in the water column but high suspended sediment.

Higher suspended sediment loads that potentially increased the similarity in the MPB species composition on the sediment surface and in the water column, further supported the idea there were MPB sediment-water column exchanges at Fingringhoe tidal flat. This present

study was the first work that discussed this type of relationship. This finding potentially confirms that the suspended diatom species were really originated from the local sediment surface. A similar study by Facca et al. (2002) presented that 71 out of the 166 diatom species recorded in Venice Lagoon were recorded on both sediment surface and in the water column. The study did not report whether the species were originated from the sediment surface or from adjacent water channel. They however stated that there was higher similarity in the MPB species composition on sediment surfaces and the water column species, at station near to the mainland which observed with high sediment resuspension.

5.4.4 Do weather-related abiotic factors drive the sediment-water column exchanges of MPB?

The sediment-water column exchange or coupling at Fingringhoe tidal flat was temporally affected by hydrodynamic and weather conditions as also shown by De Jonge & Van Beusekom (1995), Koh et al. (2006) and Ubertini et al. (2012) and also by the availability of MPB on the sediment surface as previously discussed in 5.3.3.

The MPB sediment-water column exchange varied across sampling months and neap-spring-neap tidal cycles. The temporal variability in sediment-water column exchange was attributed to the wind speed activity. Higher wind speed for three days at our study site significantly increased the suspended sediment and suspended Chl *a* in the water column. This positive effect of wind speed on suspended sediment and suspended Chl *a* in this study was consistent with the studies by Warner et al., (2004), De Jonge & Van Beusekom (1995) and Koh et al. (2006). In addition, the ability of higher mean wind speed to significantly reduce the sediment settlement rate also results in decreased MPB cells being deposited or settled back onto the sediment surface (De Jonge & Van Beusekom, 1995). This, consequently may reduce

the bio-stabilisation of sediment by MPB and promote higher sediment and Chl *a* resuspension to happen (Orvain et al. 2012; Ubertini et al. 2015).

In addition, because of the strong significantly positive correlation between the wind speed and the wave height ($r = 0.648$, $p < 0.001$) (Figure 3.6), it can also be stated that it was the wind-induced wave that positively affected the sediment resuspension (French & Spencer, 1993; Booth et al., 2000) and MPB resuspension (De Jonge & Van Beusekom, 1995; Easley et al., 2005; Ubertini et al., 2015) on the mud flat and the transition zone during immersion periods. Work on the effect between the wave and wind speed on sediment resuspension was discussed by Booth et al. (2000). The study done exclusively on sediments reported that the wave energy, induced bottom sediments resuspension when the wind speeds were higher than 10 m s^{-1} . The finding suggests that the wave could only significantly resuspend the sediment and potentially the MPB when certain wind speed is recorded. Based on our wind data, only the mean wind speed in April 2013 sampling month showed monthly mean speed of 9.4 m s^{-1} , while the monthly mean in July and October were 4.0 and 4.8 m s^{-1} , respectively. Based on the monthly mean of mean wind speed, it could be stated that only MPB resuspension in the month of April 2013 was potentially attributed to wave energy.

The presence of higher MPB biomass (Chl *a* and EPS concentrations) on the Fingringhoe tidal flat were showed to reduce the amount of sediment and MPB resuspensions. This further explained the significant negative correlation between the accumulative sun hours for three days, benthic Chl *a* and benthic EPS with PC 1 (Table 5.2). This is in agreement with a quite similar finding done by Brito et al. (2012), who reported a significant negative relationship between MPB biomass concentration on the sediment surface and phytoplankton biomass in water column in Ria Formosa Lagoon, Portugal. The information on whether the sunlight intensity or hours was responsible to positively enhance the MPB biomass on the sediment surface and potentially resulted in biostabilisation was not reported.

Tidal resuspension potentially had a direct and significant negative effect on both suspended sediment and Chl *a* (also discussed earlier in paragraph 5.4.2). This is similar to a

study done by Koh et al. (2006) who found that MPB resuspension on tidal flat was affected by spring-neap tide variation, and was controlled by tide-induced currents. Our study also found that there was higher occurrence of centric diatoms on the sediment surface in spring tide than in neap tide. High tidal range in the spring tide must have governed the occurrence of the planktonic centric diatom from the adjacent water channel onto the tidal flat (Facca et al., 2002), even though the net sediment settlement rate was low. This finding was in contrast with the study done by Ribeiro et al. (2013) who suggested that higher deposition enhances the presence of both planktonic and tycho planktonic species.

Rainfall for three days (sum of rainfall) was responsible to reduce the MPB biomass on the sediment surface during emersion period (explained in PC 2 of PCA, Figure 5.4). Higher rainfall in October 2013 believed to cause a decrease in sum of sun hours, which an important factor controlling MPB biomass (Costa et al., 2002). Rainfall will result in less MPB productivity (Wolfstein et al., 2000), which causes reductions in MPB biomass from sediment surface (Rasmussen et al., 1983) due to reduce bio-stabilisation effect by MPB biomass. The lower benthic MPB biomass (Chl *a* concentrations) in October 2013 was corresponded with less available suspended Chl *a* in the water column because there was less available MPB biomass on the sediment surface to associate with the sediment in the resuspension event during immersion period. This was further supported by the higher suspended sediment in October 2013 that associated with the low suspended Chl *a*.

Table 5.7 details the accepted and rejected hypotheses in Chapter 5.

Table 5.7: Hypotheses that were addressed in Chapter 5. Also stated whether the hypothesis were accepted or rejected.

Hypotheses (page 15-17)	Accepted	Rejected
A2	/	
C2	/	
C3	/	
D1	/	
D2	/	
E1	/	
E2		/
F1	/	
F2	/	

CHAPTER 6

COUPLING OF MICROPHYTOBENTHOS (MPB) BIOMASS BETWEEN THE TRANSITION ZONE AND THE VEGETATED SALT MARSH DURING SPRING TIDES

6.1 Introduction

In chapter 5, the relationship between MPB distribution and resuspension with weather-related abiotic factors was investigated. It was shown that the weather-related factors control the MPB biomass dynamics on the tidal flat by affecting the stability of the MPB biofilm on the top 2 mm sediment surface.

The relatively shallow water depth over the salt marsh surface even during spring tides on the salt marsh prevented the successful deployment of the sediment traps to collect any suspended sediment samples. Therefore, this limited the ability to study the impact of MPB resuspension on the salt marsh. In this chapter, measurement obtained during the 'super moon' event (the closest approaches the moon makes to the earth in its elliptical orbit) on the 28th September 2015 resulted in increased spring tide range (5.3 m – 6.1 m), with greater flooding of the salt marshes at the Fingringhoe tidal flat. This enabled us to collect suspended sediment samples on the salt marsh during 2015's sampling survey.

The aim of the work presented in this chapter was 1. to investigate the effect of tidal immersion during spring tide on the microphytobenthic biomass (Chl *a*) and species composition on the salt marsh. Higher counts of MPB cells and biomass were expected to be sampled in the water column (suspended) in second high tide of sampling day than in the first high tide of sampling day during spring tides on the salt marsh. This hypothesis is proposed after considering the work by Blanchard et al. (2001), who found that the periodical tidal resuspension was able to replenish the resources (such as nutrients) that otherwise will become limiting on the intertidal flat. However, excessive disturbance in later submersion during spring

tide has also been proven to cause the decrease in microphytobenthic biomass on the salt marshes (Le Rouzic, 2012).

In the early part of our study, we have preliminarily observed the MPB biomass coupling between the transition zone and the salt marsh, based on their relatively high species similarity (Table 6.1). Species similarity was found to be higher during spring tides than in the neap tides (Figure 6.1). This preliminary evidence however is still insufficient to strongly prove movement of the MPB between the two zones. Movement of MPB between the mud flat and the salt marsh has never been discussed in any works on MPB distribution, though it is known that sediments are moved from mudflats to salt marshes during tidal cover (French & Spencer, 1993). Some of the ecologically importance species that are recorded on salt marshes could potentially originate from adjacent mud flat areas. Therefore, the second aim of the work in this chapter was 2. to characterize the movement of MPB between the mud flat (transition zone) and the vegetated salt marsh. Based on the mentioned findings in 2013 research period, it was hypothesized that there is sediment and associated MPB species being carried by the spring tide occasion from the mud flat onto the salt marsh.

In addition, we also aimed 3. to investigate the contribution of flood and ebb tides to the movement of MPB between the two zones by means of species composition. Some common mud flat MPB species such as the *Diploneis didyma*, *Pleurosigma angulatum*, *Surirella ovata*, *Gyrosigma scalproides*, *Gyrosigma wansbeckii* and *Nitzschia sigma*, that showed an increased in their abundance on the salt marsh in spring tide (details in chapter 4), were hypothesized to be associated with the resuspended sediment during flood tide (Koh et al., 2006) from the mud flat to be deposited on the salt marsh. Hence, the flood tide is expected to have higher concentration of suspended sediment and the mentioned associated MPB than the ebb tide.

Table 6.1: Similarity index of MPB species composition between the three zones (the mud flat, the transition zone and the salt marsh) across the Fingringhoe tidal flat, Colne estuary based on data obtained in 2013. The similarity index was determined by using Modified Morissita's similarity index on log-transformed data of overall species composition in Multi Variate Statistical Package (MVSP) 3.1 Software (Kovach, 1999).

Similarity matrix			
	Mud flat	Transition zone	Salt marsh
Mud flat	1		
Transition zone	0.818	1	
Salt marsh	0.462	0.575	1

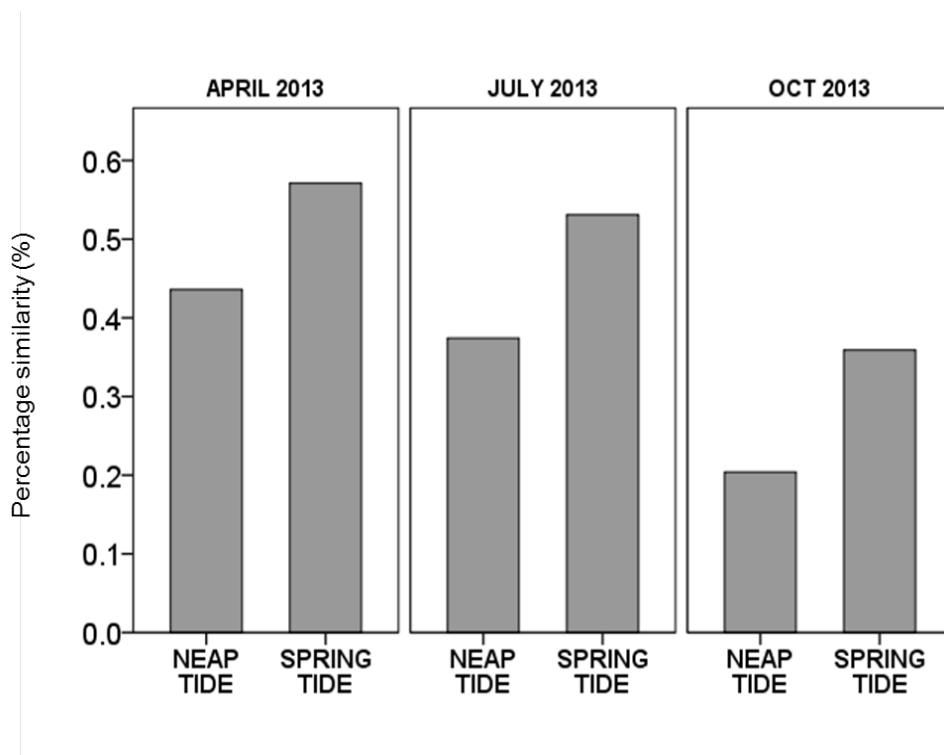


Figure 6.1: Similarity (%) in MPB species composition between the transition zone and the salt marsh during spring and neap tides during the months of April, July and October 2013. The percentage similarity was determined using the Modified Morissita's similarity index that was performed on overall log-transformed (n+1) species composition data of both zones. The values were calculated from averaged community composition.

6.2 Material and methods

6.2.1 Sampling strategy and samples processing

Two sampling surveys were carried out in the month of August 2015 and September 2015. Each sampling survey involved four consecutive sampling days during the spring tide across the transition zone on the mud flat and the salt marsh. A total of five 0.5 m X 0.5 m quadrats were built on both the transition zone and the salt marsh. Fifteen sediment surface samples (top 2 mm) were randomly obtained from each of the quadrats using 2.836 cm² diameter sediment minicores. The sediment surface samples from both zones were collected at low tide, before (LT1) and after (LT2) one high tide occasion of the sampling day (Figure 6.2). Labelled samples were immediately transferred into cold-dark container and were preserved for Chl *a* and CC analyses and also for cells count.

Sediment traps (as described in chapter 2) were used to aid the collection of suspended properties (Chl *a* and species composition) during high tide to investigate the resuspended MPB that were potentially involved in the movement between the two zones. One sediment trap was placed on each of the five quadrats in each zone (Figure 6.2). The suspended sediment samples in the traps were collected, labelled and transferred into 1 litre bottles exactly after the high tide, and were kept in cold and dark container. Triplicates tidal water samples of flood tide (C1) and ebb tide (C3) were collected into 500 ml bottles by hand to investigate the effect of tidal resuspension; the flood tide and ebb tide, on MPB movement between the two zones and MPB resuspension on the salt marsh (Figure 6.2). Both filtered suspended sediment and tidal water samples were analysed for Chl *a*, colloidal carbohydrate (CC) and cells count.

Together, there were three sets of data collected; biomass concentration on the sediment surface (data 1), the suspended biomass collected in the traps (data 2) and the biomass in flood and ebb tides (data 3). All are detailed in Table 6.2.

6.2.2 Samples processing

6.2.2.1 Sediment surface samples

Sediment samples from the fifteen collected minicores within each quadrat were pooled and mixed thoroughly, after which triplicate subsamples (technical replicates) were freeze dried for Chl *a* (Lorenzen, 1967) and CC (Hanlon et al., 2006) analyses. Additionally, another triplicate sediment samples were collected and preserved in 0.5 % w/v glutaraldehyde. These preserved samples were acid washed (Underwood, 1994) for permanent slides preparation for cell count (details in Chapter 2).

6.2.2.2 Sediment traps and tidal levels (flood and ebb tides) water samples

To collect sediments, both suspended (250 ml) and tidal water samples (250 ml) were filtered using 12.5 cm and 4.5 cm GF/F Whatman filter paper. Tidal water samples were filtered through the smaller size filter paper due to low sediment concentration (based on observation). The filtered sediment was freeze dried for Chl *a* (Lorenzen, 1967) and CC (Hanlon et al., 2006) analyses.

For permanent slides preparation and cells count, a volume of 50 ml water samples from both the suspended and tidal water's samples were transferred into plastic 15 ml volume falcon tubes. Before which, both samples were mixed by agitating the sample bottles. Samples in the falcon tube were preserved with 0.5 % w/v glutaraldehyde before going through acid washed for permanent slides preparation following Underwood (1994) procedure (details in Chapter 2).

6.2.3 Microphytobenthic cells count

A total of 300 and 250 valves were counted for the sediment surface's samples for the mud flat and the salt marsh, respectively. Whereas, only 150 and 100 valves were counted for the suspended and tidal water samples, respectively due to their low cells density. Each taxon was expressed in relative abundance (%).

6.2.4 Weather related abiotic factors

There were four abiotic factors chosen in this present study. The factors are the percentage of cloud cover (%), the tidal range (m), the mean wind speed (m s^{-1}) and the sum of rainfall. All of the factors were chosen based on their significant effect on MPB biomass concentration at different spatio-temporal scales as discussed in the Chapter 3. Data for the cloud cover, sum of rainfall and wind speed were obtained online on www.worldweatheronline.com/Colchester-weather-histor/Essex/GB.aspx. While the tidal range data were obtained from Brightlingsea tide tables (<http://www.visitmyharbour.com/tides/90/uk-tables/brightlingsea-tide-tables>).

Cloud cover was chosen to indicate the potential light attenuation and also the weather (cloudy or sunny) at study site. It is presented in percentage of sky covered (%). There was no sun hours data available in 2015 survey due to the shut down of Myland weather centre. Whereas, sum of rainfall in three days which includes sum of rainfall of two days pre sampling and on the sampling day. While the averaged wind speed data for three days which includes two pre sampling days and on sampling day were calculated and named as mean wind speed.

6.2.5 Statistical analyses

T-tests were performed using SPSS 19.0 to evaluate the variability in both Chl *a* (log transformed) and CC (log transformed) concentrations in the top 2 mm sediment surface between before (LT 1) and after (LT 2) tidal immersion on the transition zone and the salt marsh. One-way ANOVA tests were used to investigate the variability of the Chl *a* (log transformed) and CC (log transformed) in both the sediment surface and suspended in the water column among sampling days across the sampling surveys. Weather-related abiotic factors were also analyzed using one-way ANOVA using day and survey as factors to determine their variabilities at both factor level. The significant variability is reported at significant level $p < 0.05$ and lower ($p < 0.01$ and $p < 0.001$).

Daily variability in survey 1 and 2 in Chl *a* in both the flood and ebb tides were investigated by using two way ANOVA. The day and the sampling survey were treated as the factors for the ANOVA analyses. Similar to other variables, the significant variability was also reported at significant level lower than $p < 0.05$.

Pearson correlation coefficients were used to determine the relationship between the measured biomass variables (Chl *a*, CC, suspended Chl *a* and Chl *a* in tidal water samples) with the weather-related abiotic factors.

Modified Morissita's similarity index was performed to calculate the percentage similarity between the MPB species composition on the transition zone and salt marsh sediment surfaces, in sediment traps (on transition zone) and in the flood and ebb tide samples using the Multi Variate Statistical Package (MVSP) 3.1 software (Kovach, 1999). Before the analyses, the overall data for each taxon were averaged and $\log_{10} n+1$ transformed.

6.3 RESULTS

6.3.1 Temporal variability in microphytobenthic and suspended biomass across weather-related abiotic factors gradient

Chl *a* and CC (CC) concentrations in the top 2 mm sediment surface on the tidal flat before (low tide 1) and after (low tide 2) immersion period showed no significant differences. There was a non-significant difference in the Chl *a* concentration between the low tide 1 and 2 on both the transition zone and the salt marsh at daily scale in both surveys (Figure 6.3A & 6.3B, Table 6.3).

CC concentration on the transition zone varied between the two sampling surveys. There was a significant difference in the CC concentration between survey 1 and survey 2 at $F_{1,80} = 235.2$, $p < 0.001$. The CC concentration on the transition zone after immersion was significantly higher on the 30th ($F_{1,10}=7.820$, $p < 0.01$) and 31st August ($F_{1,10}=6.458$, $p < 0.05$) in survey 1 and was significantly lower on the 26th Sept ($F_{1,10}=6.818$, $p < 0.05$) in survey 2 than before immersion period (Figure 6.3C) (Table 6.3). There was significantly higher suspended sediment on the 30th and the 31st August (post hoc Tukey HSD, $p < 0.001$) (Figure 6.4A) and suspended Chl *a* (post hoc Tukey HSD, $p < 0.001$) (Figure 6.4B) in the water column than other days.

Chl *a* and colloidal concentrations in the top 2 mm per cm² sediment displayed a strong temporal variation at daily scale on both zones across both surveys (Figure 6.3A – 6.3C). Both Chl *a* and CC on the transition zones were correlated significantly and positively ($r = 0.812$, $p < 0.001$) across sampling days in both surveys (Figure 6.5). There was significantly higher variability between days in the Chl *a* concentration in survey 1 ($F_{3,40}=80.732$, $p < 0.001$) than in survey 2 ($F_{3,40}=29.341$, $p < 0.001$) on the transition zone (Figure 6.3A). The Chl *a* concentration on the salt marsh relatively depicted stronger daily variability in the drier and sunnier weather

condition (< 50 % cloud cover on all days) in survey 2 ($F_{3,40}=38.173$, $p < 0.001$) than in survey 1 ($F_{3,40}=15.955$, $p < 0.01$) (Figure 6.3B).

Daily mean variability in the Chl *a* concentration on the sediment surface on both zones was closely linked to how much sediment and its associated MPB being suspended in the water column during immersion. There was a significant negative correlation between both suspended sediment load and suspended Chl *a* in the water column during immersion with the concentration of Chl *a* on the sediment surface on the transition zone ($r = -0.605$, $p < 0.001$ (suspended sediment), $r = -0.472$, $p < 0.001$ (suspended Chl *a*)) (Table 6.5). This negative correlation on the transition zone was linked to the significant positive correlation between the Chl *a* concentration with the CC concentration in the top 2 mm sediment surface (Figure 6.5). A lower correlation between benthic Chl *a* with both suspended sediment and suspended Chl *a* was observed on the salt marsh with the values of; $r = -0.398$, $p < 0.001$ (suspended sediment) and $r = -0.260$, $p < 0.001$ (suspended Chl *a*) (Table 6.5).

The mean daily Chl *a* concentration on the transition zone was significantly negatively correlated with all the chosen weather-related abiotic factors (Table 6.5). Cloud cover was the strongest factor significantly negatively correlated with the Chl *a* concentrations (r value > -0.5). The mean (daily) of Chl *a* concentration on the salt marsh, was strongly negatively correlated ($r > -0.5$) with the tidal range (Table 6.5). Salt marsh Chl *a* concentrations were significantly negatively correlated with averaged wind speed for three days ($r = -0.172$, $p < 0.05$) and tidal range ($r = -0.551$, $p < 0.001$) (Table 6.5).

The correlation strength between the suspended Chl *a* with both the mean wind speed and the tidal range was stronger than the factors correlation with the Chl *a* concentration on sediment surface on the transition zone. The Pearson correlation strength between the suspended Chl *a* with the mean wind speed and the tidal range were $r = 0.369$, $p < 0.01$ and $r = 0.649$, $p < 0.001$, respectively (Figure 6.6A and 6.6B, respectively).

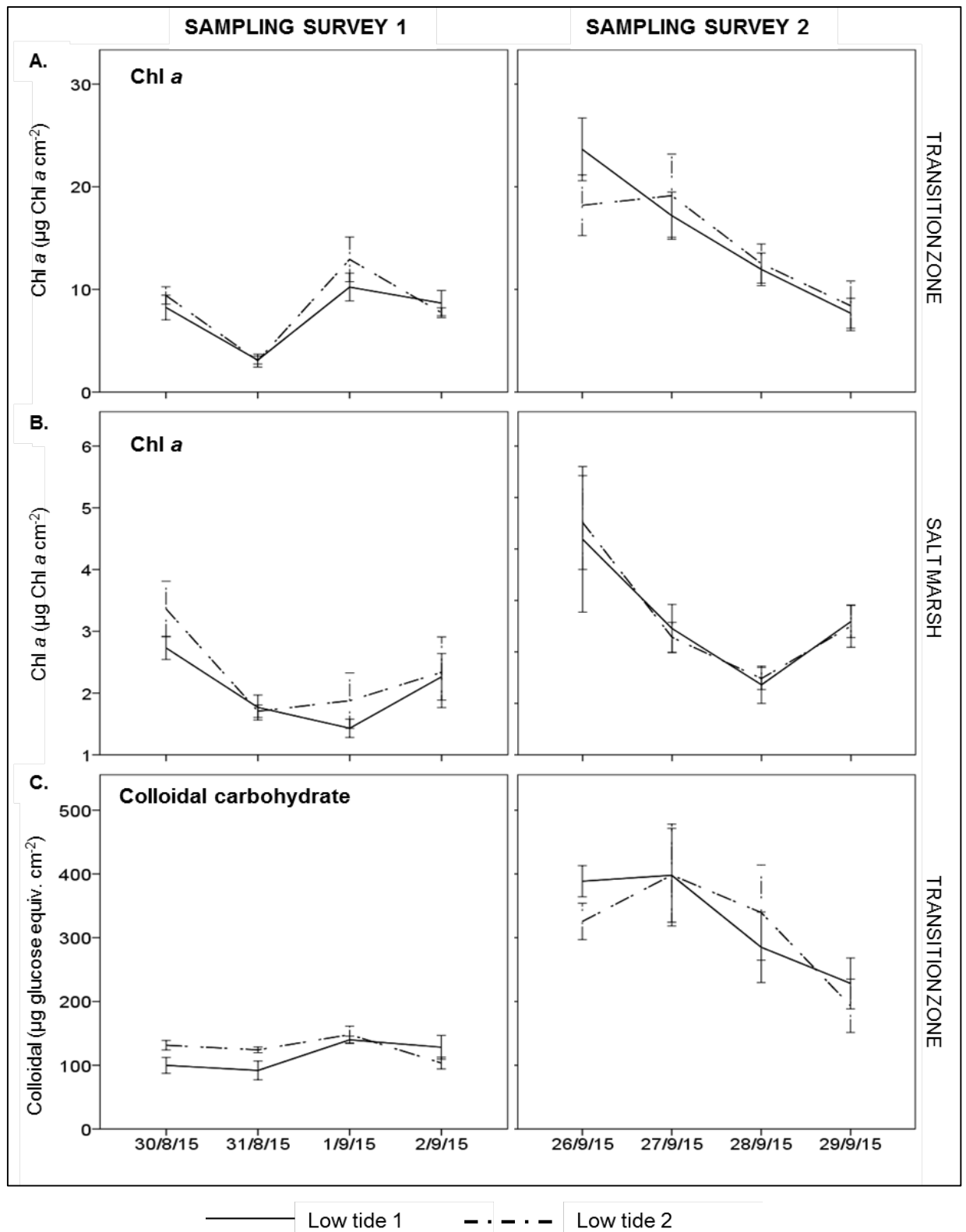


Figure 6.3 : Daily changes in Chl a concentration in the top 2 mm per cm⁻² sediment surface on the; A) transition zone; B) salt marsh and the; C) colloidal carbohydrate on only the transition zone during low tide 1 (LT1) and low tide 2 (LT2) on the transition zone in sampling survey 1 and survey 2. Values are mean \pm SE. n = 5.

Table 6.3: Variability in the Chl *a* and the colloidal carbohydrate concentrations in low tide 1 (LT1) and low tide 2 (LT2) across sampling days in survey 1 and survey 2 on the transition zone and the salt marsh. ns indicate non-significant variability and na indicates no data collected). The F and the p values were obtained from two way ANOVA tests on the log transformed Chl *a* and CC data. n = 10, df = 1 for both variables.

Survey	Date	Variables	ANOVA Between tides (Low tide 1 x Low tide 2)			
			Transition zone		Salt marsh	
			F	p	F	p
1	30 th Aug	Chl <i>a</i>	0.635	ns	1.688	ns
		Colloidal	7.820	< 0.01	na	na
	31 st Aug	Chl <i>a</i>	0.004	ns	0.073	ns
		Colloidal	6.458	< 0.05	na	na
	1 st Sept	Chl <i>a</i>	1.110	ns	0.890	ns
		Colloidal	0.326	ns	na	na
	2 nd Sept	Chl <i>a</i>	0.506	ns	0.011	ns
		Colloidal	1.417	ns	na	na
2	26 th Sept	Chl <i>a</i>	1.642	ns	0.038	ns
		Colloidal	6.818	< 0.05	na	na
	27 th Sept	Chl <i>a</i>	0.174	ns	0.097	ns
		Colloidal	0.010	ns	na	na
	28 th Sept	Chl <i>a</i>	0.052	ns	0.083	ns
		Colloidal	0.344	ns	na	na
	29 th Sept	Chl <i>a</i>	0.066	ns	0.030	ns
		Colloidal	0.370	ns	na	na

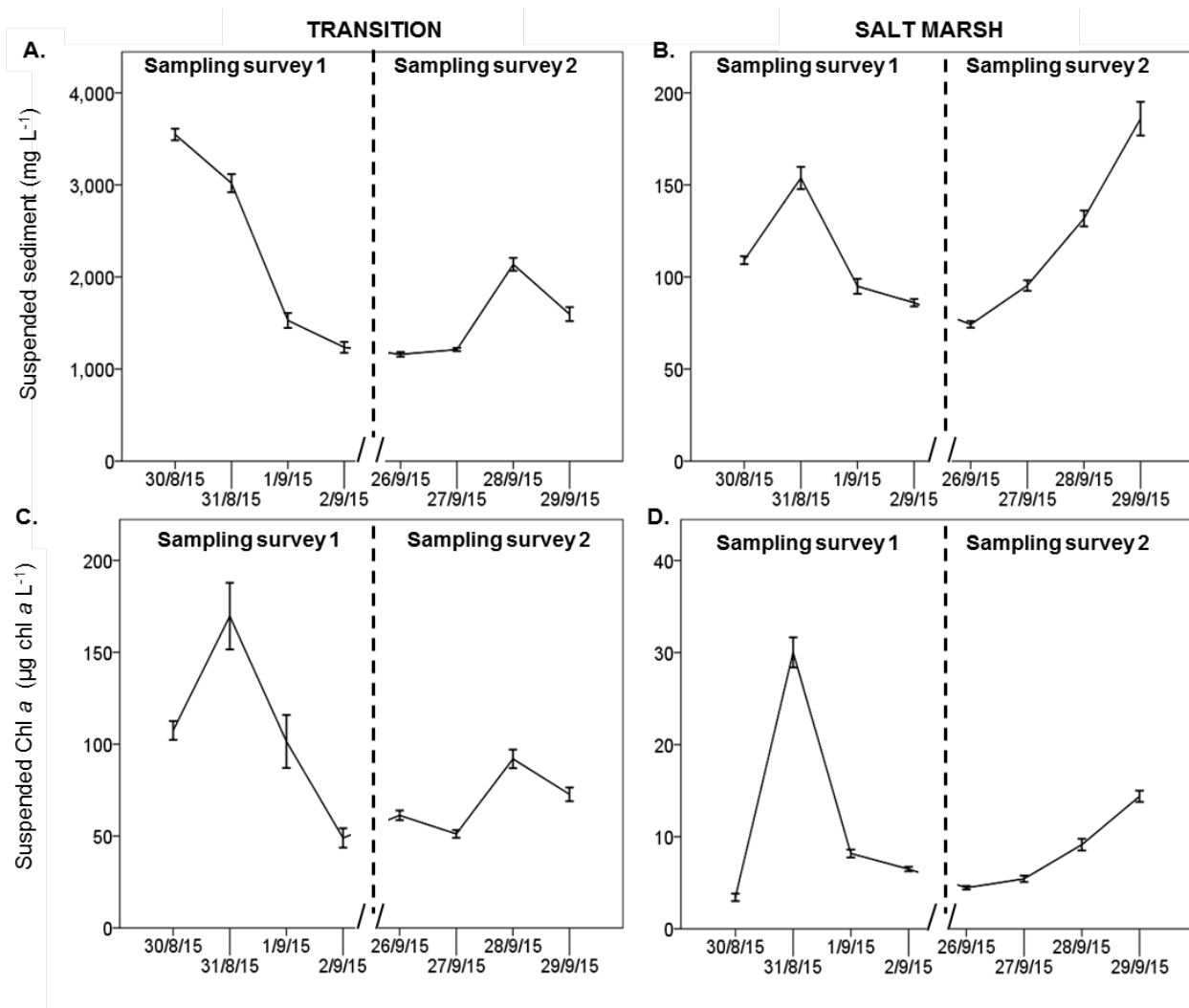


Figure 6.4: Daily changes in suspended sediment per L of water over the; A) transition zone and the; B) salt marsh AND also the daily changes of the suspended Chl a per L of water over the; C) transition zone and the; D) salt marsh during two periods of sampling in August and September 2015. Values are mean \pm SE. n = 5.

Table 6.4: Daily changes in the chosen weather-related abiotic factors during sampling survey 1 and 2.

Sampling survey	Date	Weather-related factors			
		Sum of rainfall (m)	Mean wind speed (ms ⁻¹)	Cloud cover (%)	Tidal range (m)
1	30 th Aug	2.80	2.90	89.00	5.70
	31 st Aug	7.00	3.30	100.00	6.00
	1 st Sept	6.50	3.80	57.00	6.00
	2 nd Sept	6.80	3.80	31.00	5.90
ANOVA (between days)		<i>p</i> < 0.001	<i>p</i> < 0.001	<i>p</i> < 0.001	<i>p</i> < 0.001
2	26 th Sept	6.90	3.10	7.00	5.30
	27 th sept	0.10	2.70	16.00	5.70
	28 th sept	0.10	3.00	47.00	6.10
	29 th Sept	0.10	3.70	30.00	6.10
ANOVA (between days)		<i>p</i> < 0.001	<i>p</i> < 0.001	<i>p</i> < 0.001	<i>p</i> < 0.001
ANOVA (between survey 1 and 2)		<i>p</i> < 0.001	<i>p</i> < 0.001	<i>p</i> < 0.001	ns

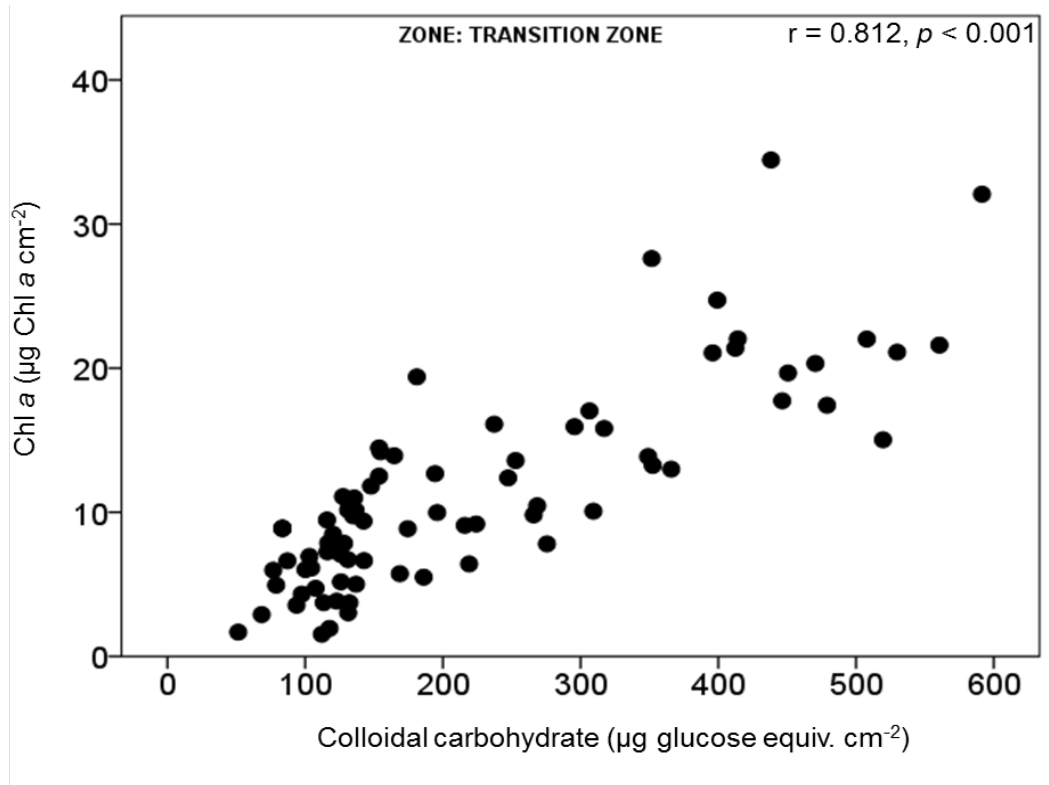


Figure 6.5: Significant positive relationship between the Chl *a* and CC concentration in the top 2 mm sediment surface of the transition zone during August and September 2015. The correlation coefficients were calculated by using the Pearson's correlation coefficients (r) on overall biomass data, $n=80$.

Table 6.5: Correlations between Chl *a* concentration on two different intertidal zones with weather-related abiotic factors and suspended properties during August and September 2015. The Pearson's correlation coefficients were performed on pooled Chl *a* data of survey 1 and 2.

Zones	Pearson correlation coefficients (r)					
	Weather-related abiotic factors				Suspended	
	Sum of rainfall	Mean wind speed	Cloud cover	Tidal range	Suspended sediment	Suspended chl <i>a</i>
Transition zone	-0.207**	-0.299***	-0.652***	-0.462***	-0.605***	-0.472***
Salt marsh	ns	-0.172*	-0.267***	-0.551***	-0.398***	-0.260***

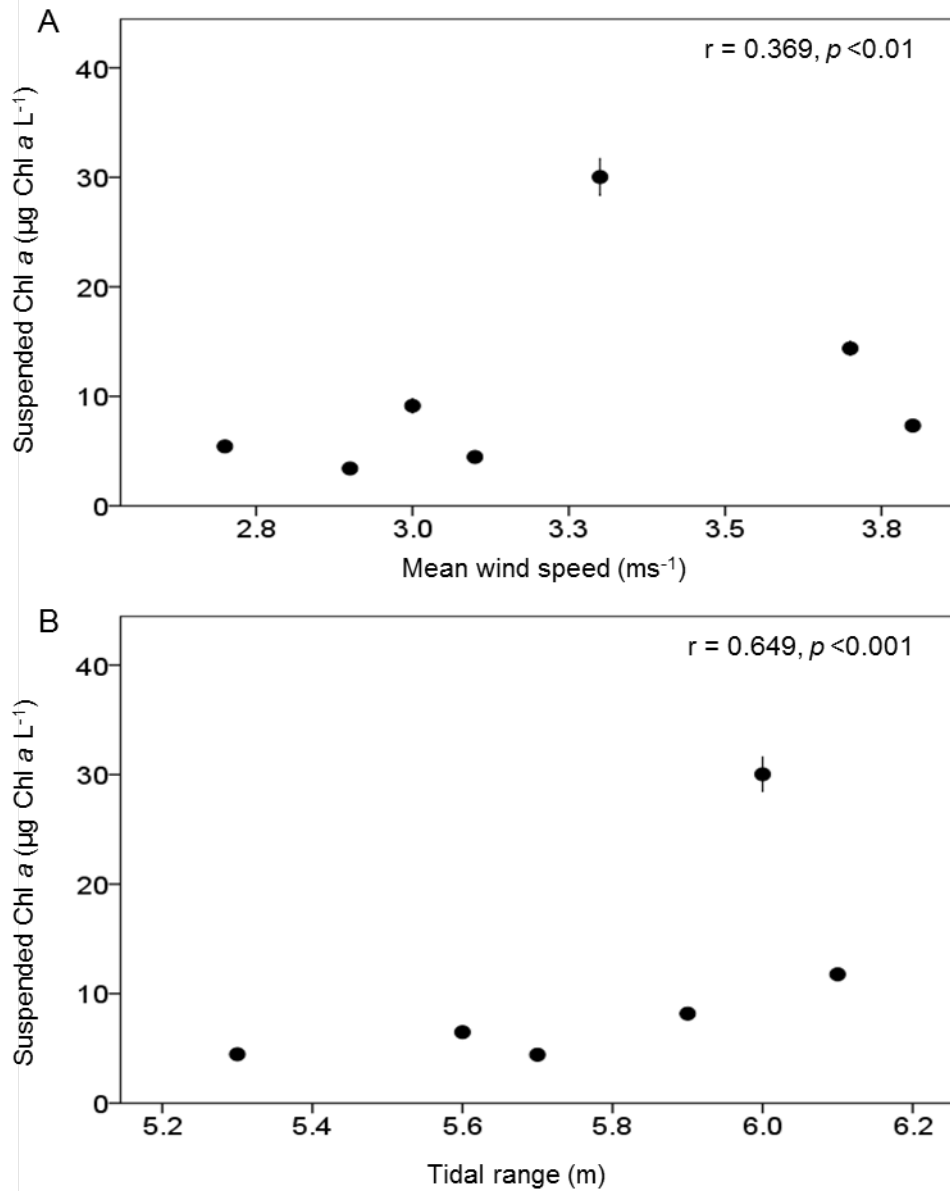


Figure 6.6: Positive relationships between the suspended Chl a concentration over the salt marsh during slack high tide of the spring tide with; A) the mean wind speed and; B) the tidal range. The Pearson's correlation coefficients were performed on the daily mean of Chl a concentration and both weather-related abiotic factors, $n = 5$. Notes that there were similar MWS and tidal range on certain sampling days.

6.3.2 MPB coupling between the transition zone (mud flat) and the salt marsh

Because the coupling of MPB between the mud flat and the salt marsh must take place during flood and ebb tides, it was hypothesized that the flood tidal current is responsible to transfer the resuspended MPB from the mud flat onto the salt marsh, with the ebb tidal current responsible for washing MPB biomass out of the salt marsh (opposing influence).

6.3.2.1 Characterization of MPB across tidal levels, the flood and ebb tides in spring tidal immersion

There was significantly higher Chl *a* in the survey 2 of $14.84 \pm 1.18 \mu\text{g Chl } a \text{ cm}^{-2}$ than in the survey 1 ($7.97 \pm 0.63 \mu\text{g chl } a \text{ cm}^{-2}$) ($F_{1,80} = 26.693$, $p < 0.001$) was concurrent with the survey's relatively lower suspended Chl *a* concentration ($21.59 \pm 1.74 \mu\text{g Chl } a \text{ L}^{-1}$) in the flood tide than in survey 1 ($26.33 \pm 2.12 \mu\text{g Chl } a \text{ L}^{-1}$) (Figure 6.7A). The Chl *a* concentration in flood tide water samples on the salt marsh was significantly negatively correlated with the Chl *a* concentration on transition zone sediment surface at $r = -0.774$, $p < 0.001$ (Figure 6.8A). The correlation strength was stronger than the correlation between the flood tide Chl *a* with the Chl *a* on the salt marsh ($r = -0.410$, $p < 0.001$) (Figure 6.8B).

During ebb tides, there was evidence for the wash away of MPB from the salt marsh. The significantly higher Chl *a* in the top 2 mm salt marsh's sediment surface in survey 2 ($2.71 \pm 0.15 \mu\text{g Chl } a \text{ cm}^{-2}$) than in survey 1 ($2.18 \pm 0.10 \mu\text{g Chl } a \text{ cm}^{-2}$) was potentially connected with relatively lower Chl *a* in the ebb tide water samples in the survey 2 ($17.79 \pm 1.07 \mu\text{g Chl } a \text{ L}^{-1}$) than in survey 1 ($21.13 \pm 1.29 \mu\text{g Chl } a \text{ L}^{-1}$). These data revealed the significant negative relationship between the Chl *a* in the ebb tide's tidal water and in top 2 mm sediment surface of the salt marsh (Figure 6.8B). The correlation strength was higher than the correlation during flood tides (Figure 6.8B).

Chl *a* concentration in the flood tide samples that potentially originated from the mud flat was positively correlated with the cloudy weather (based on the percentage of the cloud cover) ($r = 0.795$, $p < 0.001$) (Figure 6.9C.i). The flood tide Chl *a* concentration was also significantly correlated with the tidal range of the spring tide ($r = 0.629$, $p < 0.01$) (Figure 6.9D.i). Other chosen weather-related abiotic factors, the sum of rainfall and the averaged wind speed for three days did not have any significant effect on the availability of the Chl *a* in the flood tide water samples.

Averaged mean wind speed for three days and the tidal range were significantly and positively correlated with the Chl *a* concentration in the ebb tide's water samples. With the Pearson's correlation coefficients of $r = 0.733$, $p < 0.001$ (Figure 6.9B.ii) and $r = 0.661$, $p < 0.001$ (Figure 6.9D.ii), respectively.

Quantitatively, there was 65.4 % similarity in species composition between the MPB communities on the transition zone before immersion periods and suspended in the water column during high tides (Figure 6.10A). This high similarity, potentially further supported the concept of MPB sediment water column exchanges on the transition zone. Connection between the suspended MPB in the water column of the mud flat with the flood tide samples (sampled on the salt marsh) was supported by a 54.3 % shared species composition (Figure 6.10B). There was high similarity in the species composition between the MPB communities on the salt marsh sediment surfaces and the ebb tide samples at the percentage of 72.6 % (Figure 6.10C). As a whole, the species composition in Group B that was characterized by MPB potentially originated from the mud flat, shared a total of 31.8 % of MPB species composition with MPB originated from the salt marsh sediment surface (Group C) (Figure 6.10).

Species composition data further indicated the ability of flood tide to carry MPB from the transition zone onto the salt marsh. The species involved in the movement between transition zone and salt marsh must be the species present on the sediment surface, the sediment traps and the flood tide water samples. Eighteen out of eighty-four overall identified MPB species were recorded in the suspended sediment of flood tide on the salt marsh during spring tide

immersion period (Table 6.6). MPB species composition data proved that *Pleurosigma angulatum* was recorded as the most abundant species collected in the flood tide samples, with the relative abundance of 3.66 ± 1.99 %.

There were lower relative abundances of MPB species sampled in the tidal water samples during ebb tides than during flood tides. Only fourteen MPB species were recorded in the ebb tide water samples throughout the sampling surveys (Table 6.7). The fourteen species were also recorded on the sediment surface of the salt marsh. Because these fourteen species were recorded in both sediment surface and ebb tidal water samples, the species potentially were resuspended and possibly washed away by ebb tides. Five out of the fourteen recorded species (*Neidium* sp., *Nitzschia bilobata*, sp 1, unidentified Sp4 and *Diploneis stroemii*) were also the species that were dominantly recorded on only the salt marsh during neap tide (detailed in chapter 4). The species are detailed in Table 6.7.

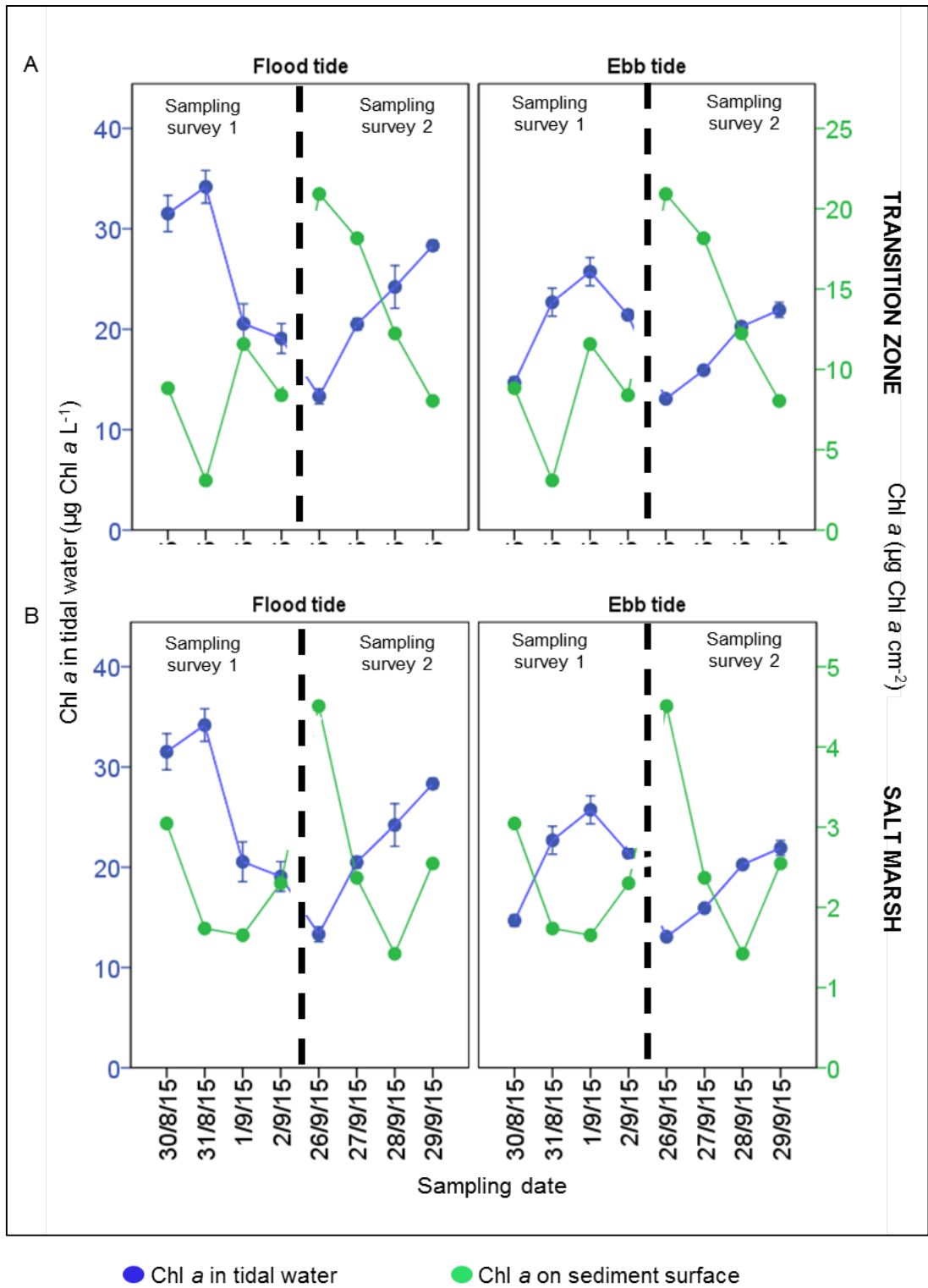


Figure 6.7: Daily variability in Chl a in flood and ebb tidal water and also the concurrent Chl a concentration in the top 2 mm sediment surface on the; A) transition zone and on the; B) salt marsh in both survey 1 and 2. Values are mean \pm SE, n of tidal water= 3. No SE were presented for the Chl a concentration on the sediment surface.

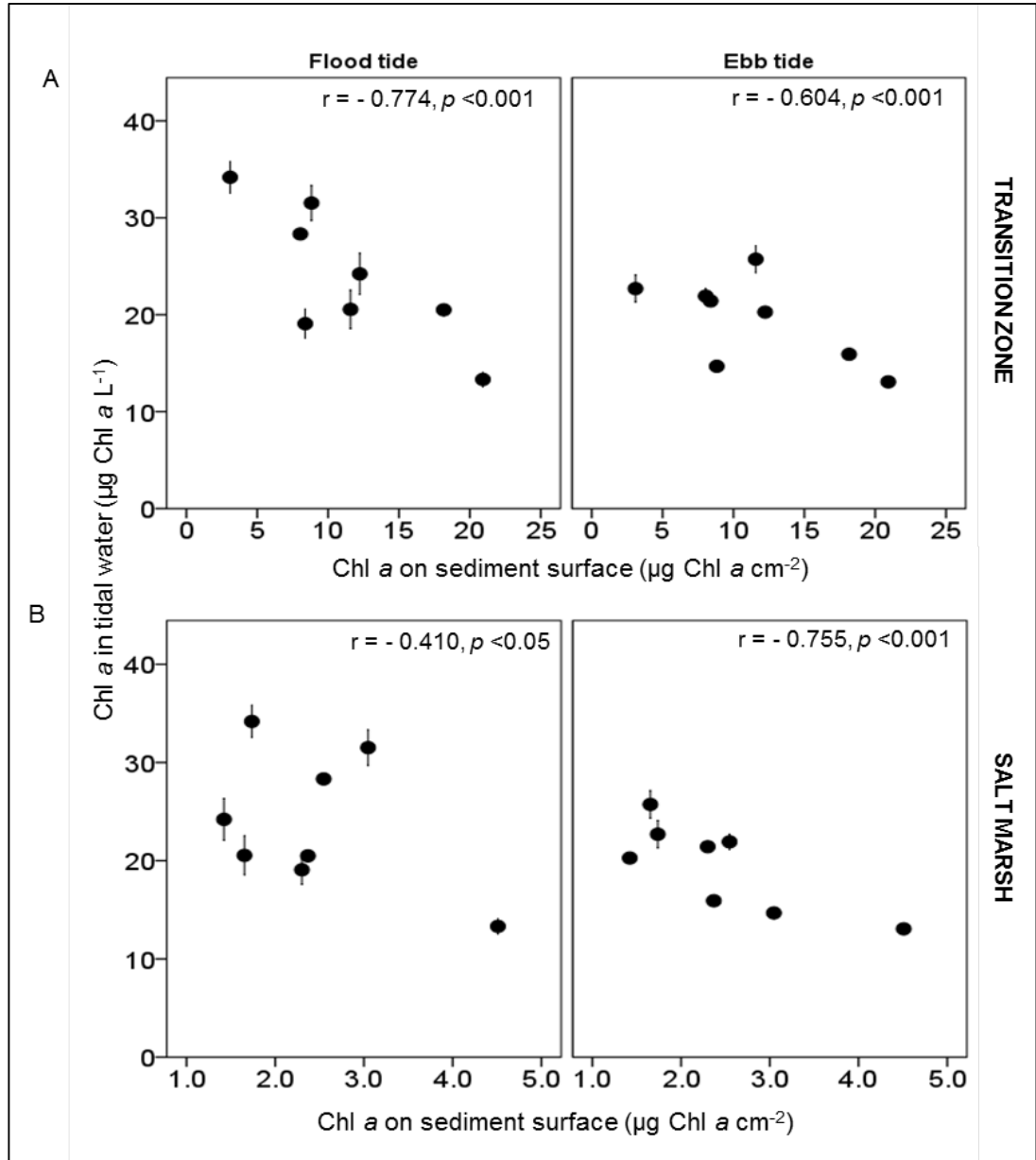


Figure 6.8: Relationship between Chl a concentration per L flood and ebb tidal water with the Chl a concentration in the top 2 mm per cm^2 sediment surface of the; A) transition zone and the; B) salt marsh. r value were calculated based on the Pearson's correlation coefficients on daily mean of flood and ebb data, $n = 3$.

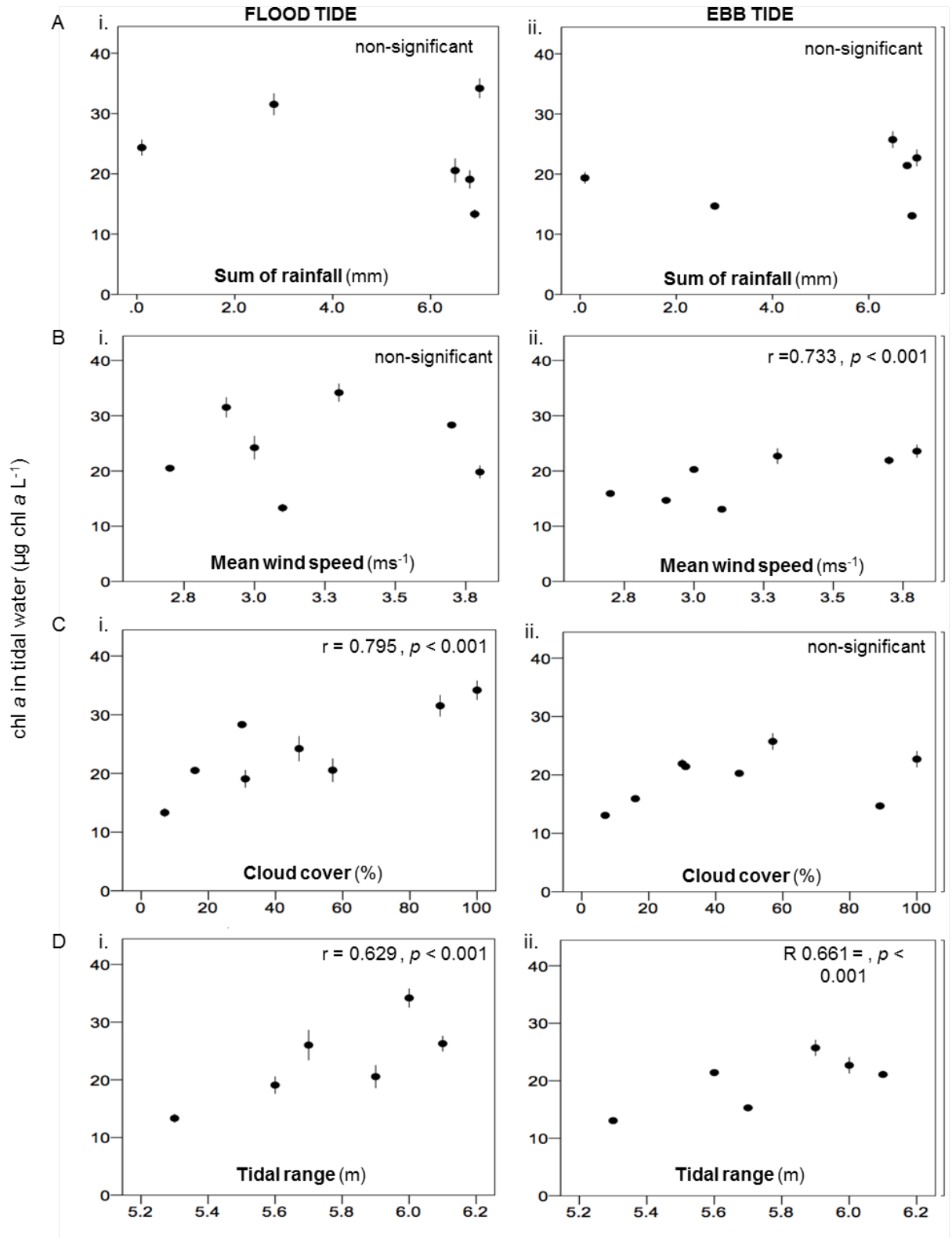
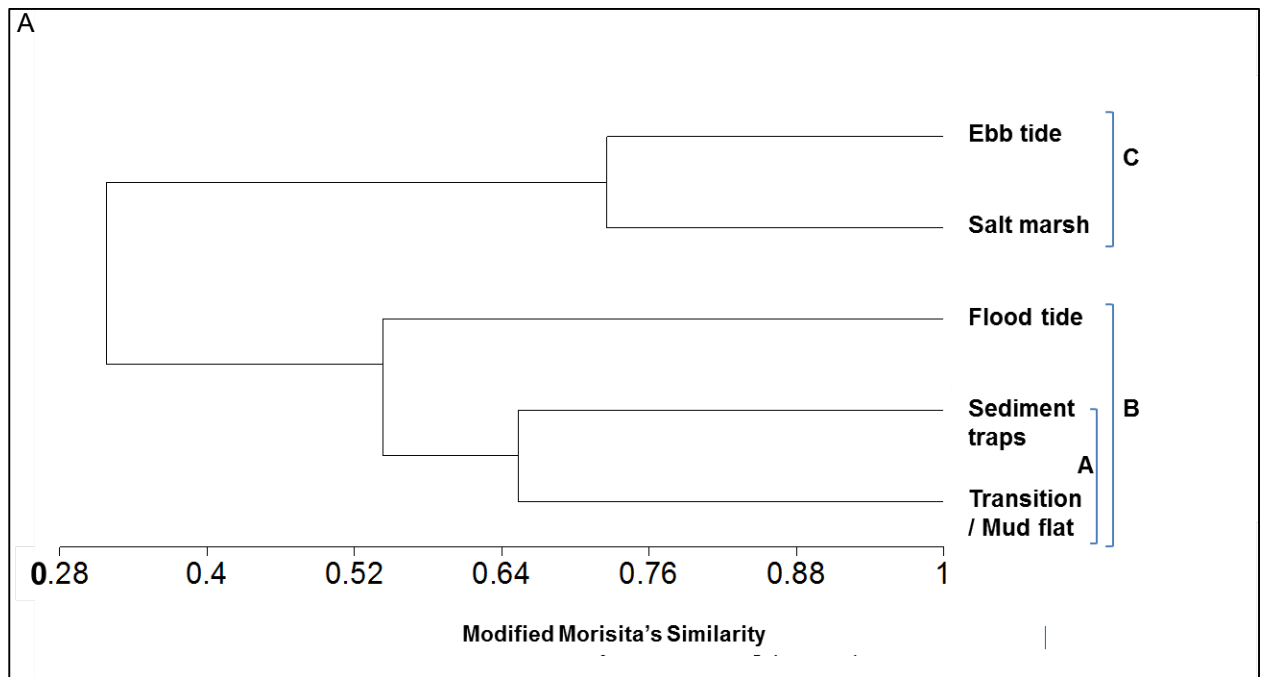


Figure 6.9: Relationship between the Chl a concentration in; i) flood and; ii) ebb tides with the; A) sum of rainfall for three days; B) averaged wind speed for three days; C) percentage of cloud cover and; D) the tidal range across spring tide occasion on the salt marsh. Values are mean \pm SE, $n = 3$.



B

Group	Sample	Sample	Similarity	Number of samples in group
C	Salt marsh	Ebb tide	0.726	2
A	Transition zone	Sediment traps	0.654	2
B	Group A	Flood tide	0.543	3
	Group A	Group C	0.318	5

Figure 6.10: A) Dendrogram on the similarity in the MPB species composition of ebb tide, salt marsh (on sediment surfaces), flood tide, sediment traps (deployed on transition zone) and transition zone (on the sediment surfaces) samples. B) Details on the similarity scores and categorized group.

Table 6.6: Relative abundance \pm SE (%) (n = 24) of MPB species that potentially involved in the movement from the transition zone onto the salt marsh during flood tide periods. The relative abundance was calculated based on the pooled overall (survey 1 and 2) data.

MPB species	On sediment surface		In the trap on the Transition	Collected in flood tide on salt marsh
	Mud flat	Salt marsh		
<i>Achnanthes longipes</i>	1.08 \pm 0.31	0.57 \pm 0.33	2.06 \pm 0.19	0.92 \pm 0.32
<i>Actinoptychus undulatus</i>	0.58 \pm 0.18	0.32 \pm 0.19	0.13 \pm 0.04	1.60 \pm 0.57
<i>Diploneis didyma</i>	5.47 \pm 1.06	3.34 \pm 0.68	5.74 \pm 0.68	1.98 \pm 0.70
<i>Diploneis litoralis</i>	0.78 \pm 0.31	2.20 \pm 0.52	2.21 \pm 0.36	1.30 \pm 0.46
<i>Gyrosigma wansbeckii</i>	4.12 \pm 0.69	0.83 \pm 0.30	3.99 \pm 0.59	1.55 \pm 0.55
<i>Gyrosigma scalproides</i>	5.28 \pm 1.03	3.18 \pm 0.61	4.66 \pm 0.47	1.20 \pm 0.42
<i>Navicula gracilis</i>	0.93 \pm 0.23	1.23 \pm 0.26	0.96 \pm 0.24	1.41 \pm 0.50
<i>Navicula gregaria</i>	1.95 \pm 0.24	3.52 \pm 0.81	1.83 \pm 0.33	1.77 \pm 0.63
<i>Navicula scopulorum</i>	2.40 \pm 0.65	1.02 \pm 0.41	4.76 \pm 0.73	1.36 \pm 0.48
<i>Navicula</i> sp1	2.83 \pm 0.37	0.88 \pm 0.36	0.85 \pm 0.01	1.49 \pm 0.53
<i>Nitzschia dubia</i>	1.05 \pm 0.26	0.70 \pm 0.33	0.78 \pm 0.17	1.92 \pm 0.68
<i>Nitzschia scalproides</i>	2.40 \pm 0.63	0.45 \pm 0.19	2.46 \pm 0.30	1.25 \pm 0.44
<i>Nitzschia sigma</i>	4.02 \pm 0.79	2.18 \pm 0.45	3.85 \pm 0.48	1.83 \pm 0.65
<i>Pleurosigma angulatum</i>	3.32 \pm 0.47	1.89 \pm 0.49	2.95 \pm 0.34	3.66 \pm 1.29
<i>Pleurosigma</i> sp1	3.95 \pm 0.81	0.50 \pm 0.29	1.81 \pm 0.31	1.41 \pm 0.50
<i>Raphoneis amphiceros</i>	1.45 \pm 0.41	1.68 \pm 0.45	0.75 \pm 0.19	0.64 \pm 0.23
<i>Stauroneis producta</i>	0.80 \pm 0.24	0.15 \pm 0.09	2.01 \pm 0.19	1.36 \pm 0.48
<i>Surirella ovata</i>	0.60 \pm 0.24	1.68 \pm 0.33	1.44 \pm 0.25	2.06 \pm 0.19
Species richness	64	34	30	27

Table 6.7: Relative abundance \pm SE (%) (n = 24) of MPB species that potentially involved in the resuspension on the salt marsh during ebb tide. The relative abundance was calculated based on the pooled overall (survey 1 and 2) data.

MPB species	On salt marsh sediment surface	Collected in ebb tide tidal water
<i>Actinoptychus undulatus</i>	0.32 \pm 0.19	8.21 \pm 1.60
<i>Amphora</i> sp 1	1.43 \pm 0.58	8.39 \pm 1.00
<i>Diploneis stroemii</i>	1.99 \pm 0.78	6.96 \pm 1.41
<i>Diploneis didyma</i>	2.75 \pm 0.68	6.12 \pm 0.88
<i>Diploneis litoralis</i>	2.20 \pm 0.52	6.64 \pm 1.28
<i>Neidium</i> sp.	10.68 \pm 1.55	7.42 \pm 1.23
<i>Nitzschia sigma</i>	2.18 \pm 0.44	7.68 \pm 1.19
<i>Nitzschia bilobata</i>	6.27 \pm 0.89	5.56 \pm 1.15
<i>Nitzschia</i> sp 1	7.30 \pm 0.95	7.80 \pm 0.98
<i>Nitzschia vitrea</i>	5.37 \pm 0.59	7.33 \pm 1.09
Sp4	13.95 \pm 1.85	7.68 \pm 1.19
<i>Opephora</i> sp 1	14.3 \pm 1.42	6.71 \pm 1.11
<i>Surirella fastuosa</i>	3.5 \pm 0.82	7.45 \pm 0.72
<i>Surirella ovata</i>	1.68 \pm 0.34	6.04 \pm 0.92
Species richness	34	14

6.4 DISCUSSION

6.4.1 Temporal MPB biomass variability

This present study did not find any significant variability in MPB Chl *a* concentration in the top 2 mm sediment surface between the before and after high tide emersion period during spring tide on both the transition and the salt marsh. The non-significant variability is potentially attributed to the migratory rhythm of the MPB towards the tidal and diel conditions (Smith & Underwood, 1998; Underwood et al., 2005) at our study site. This has been reported to reduce the effect of MPB biofilm 'wash away' by the tidal current (Costa et al., 2002) and its associated wind (De Jonge & Van Beusekom, 1995) and wave (Easley et al., 2005) energies during spring tide immersion. Koh et al. (2007) found a significant positive strong correlation between the daily mean of Chl *a* concentration with both the Chl *a* concentration sampled at two different emersion periods of similar sampling day. This is in agreement with our finding.

6.4.2 Relationship between Chl *a* on sediment surface with suspended Chl *a* on the salt marsh

The ability of MPB biofilms to reduce erosion by increasing the sediment critical erosion threshold has been reported in numerous studies (Underwood & Paterson, 1993; Paterson, 1994; reported in chapter 3 & 4 in this study). Lower Chl *a* concentrations availability on the salt marsh sediment surface causes higher suspended sediment and suspended Chl *a* concentration during immersion in spring tide (Table 6.4). Underwood (1997) reported that MPB assemblages consisting of more than 50 % epipellic diatom on the salt marsh are potentially responsible in producing CC in the sediment surface. Therefore, the biostabilisation on salt marshes in the Colne estuary could be related to MPB biomass.

Wind speed and tidal range in spring tides are the two abiotic factors that are positively important in controlling the MPB resuspension variability on the salt marsh. Loss of Chl *a* from salt marsh biofilms is promoted by increasing tidal range in spring tide (Horton et al., 2006). The negative effect of the tidal range on Chl *a* concentrations on the sediment surface could potentially be associated with the wind speed (Riggs, 2002; van der Wal et al., 2010). This is because of the significant positive correlation between the wind speed and the wave height (presented in chapter 3), it can be stated that the increased in suspended Chl *a* and sediment concentrations on the salt marsh was also a function of wave energy (Leonardi et al., 2015).

As expected, tidal range that positively increased the suspended Chl *a* concentrations and had a significant negative correlation with Chl *a* concentrations on sediment surfaces of the salt marsh (Table 6.4). These two different correlations further supported the occurrence of opposing influences on the salt marsh at our study site, which potentially caused the lower relative abundance of dominant salt marsh MPB species during spring tides as reported in Chapter 4. Tidal current that is reported to replenish the resources (such as nutrients) on the salt marshes sediment (Blanchard et al., 2001), is also reported as one of major disturbance to MPB biofilms of the zone (Horton et al., 2006; Le Rouzic, 2012).

6.4.3 Contribution of tidal levels (flood and ebb tide) in spring tide to MPB variability on the salt marsh

The experiment conducted in 2013 highlighted that the species composition in MPB assemblages on salt marsh, which mostly comprised of small, 'edaphic' and epiphytic species during neap tides, showed to shift their species composition with species common on the transition zone and the mud flat during spring tides.

Suspended Chl *a* concentrations in flood tide samples (sampled on salt marsh) were in strongly association with the transition zone MPB Chl *a* concentrations (Figure 6.8A). This supports the idea that the MPB coupling between the transition zone and the salt marsh occurs during flood tides rather than in ebb tide. Flood tide tidal currents have been reported by Koh et al. (2006) to cause simultaneous MPB resuspension on the mud flat would appear to carry MPB biomass from the transition zone onto the salt marsh during the spring tide.

The percentage of cloud cover was not only closely related to the increased of the suspended Chl *a*, but it also positively enhanced the Chl *a* measured in the flood tide samples sampled on the salt marsh (Figure 6.9C.i). Higher percentage of cloud cover that represents low light attenuation possibly responsible to reduce Chl *a* concentration (Table 6.4) (Serôdio et al., 2006) and biostabilisation effect (Du et al., 2010; Gerbersdorf et al., 2009) by MPB on the transition zone.

Chl *a* concentrations on salt marsh sediment surfaces were negatively correlated with the suspended Chl *a* in ebb and flood tides (Figure 6.8B). The negative relationship showed to be stronger between Chl *a* concentration with the suspended Chl *a* in ebb than in flood tides (Figure 6.8B). MPB species that were only recorded on the salt marshes and are only exposed to tidal range in spring tide are possibly less adapt to tidal disturbance during spring tide (Underwood, 1997). Therefore, 'the ebb tide that was reported by Green (2011) to have larger

wave orbital and larger tidal current with less depth attenuation than in flood tide, was a good factor to cause disturbance on MPB assemblage on the salt marsh.

Species composition data showed that five out of the six dominant MPB species on the salt marsh sediment surface in neap tide were recorded in the ebb tide tidal water samples (Table 6.6). The observation further supported the hypothesis that there was resuspension and possibly wash away of some epipelagic, edaphic and epiphytic salt marsh MPB species during ebb tides.

Table 6.8 details whether the general hypotheses addressed in Chapter 6 were accepted or rejected.

Table 6.8: Hypotheses that were addressed in Chapter 6. Also stated whether the hypothesis were accepted or rejected.

Hypotheses (page 15-17)	Accepted	Rejected
F1	/	
F2	/	

CHAPTER 7

General discussion

7.1 Link between MPB biomass with weather-related abiotic factors, MPB assemblages diversity and sediment resuspension on mud flat and transition zone

The results in Chapter 3 showed that MPB biomass was directly affected by weather-related abiotic factors, as shown in this study with 'Sum of sun hours' and 'sum of rainfall'. The factors directly affected the MPB biomass concentrations in MPB biofilms during emersion periods.

On the mud flat and the transition zone, 'sum of sun hours' stimulated increased in Chl *a*, CC and EPS concentrations. High MPB biomass as recorded in July 2013 reduced the MPB sediment-water column exchanges (MPB resuspension) as reported in Chapter 5. This fits well with studies which have found that MPB biofilms exposed to longer sunlight had high erosion thresholds (Madsen et al., 1993; Austen et al., 1999) due to high MPB biomass (Austen et al., 1999). As discussed in Chapter 3, longer period of sun is as important as the the light energy in enhancing the production of MPB as well stimulating the vertical migration (Consalvey et al., 2004; Serôdio et al., 2006) of MPB to top 2 mm of sediment (de Brauwer & Stal, 2001). In addition, longer period of sun as recorded in July 2013 (summer) caused the emersion periods with longer sum of sun hours, therefore enhanced more MPB biomass production. Stable MPB biofilms in calm weather such as in July 2013 (summer) positively caused the high MPB diversity in the biofilms. In addition, the positive effect was also enhanced with spring tides immersions. This was supported by the strong positive correlation between the Chl *a* concentration and the diversity index (H') on only mud flats during spring tides in July 2013 as reported in Chapter 4. As reported in Chapter 4, high water current and energy in spring tides (Koh et al., 2006; Green, 2011) in calm weather, may carry along a higher density of centric

species onto mud flats from adjacent water channels (River Colne) and consequently increased the diversity of MPB assemblages. The Mud flats that were the nearest zone to water channel, had higher connection to the water channel compared to the transition zone and the salt marsh. The results in Chapter 4 also highlighted that the correlation between the Chl *a* and the diversity (*H'*) was positively stimulated by tidal range. Therefore, it can be stated that although tidal range did not have any significant direct effect on the Chl *a* concentrations (Chapter 3), it had indirect effect on Chl *a* concentration through MPB species compositions and assemblages of MPB biofilms, as discussed in Chapter 4.

High 'sum of rainfall' was showed to have a negative effect on Chl *a* concentrations on both the mud flat and the transition zone. The month of October 2013 was characterized by high sum of rainfall and showed lower Chl *a*, CC and EPS monthly mean concentrations than in April and July 2013 (Chapter 3). The low MPB biomass concentrations potentially resulted in high suspended sediment in the water column. This finding was reported in Chapter 5 and supports the idea that prolonged rainfall enhanced the wash away of MPB from sediment surfaces during emersions periods, therefore reduced the ability of MPB biofilms to biostabilize sediment surfaces. The effectiveness of rainfall to wash away the MPB from sediment surfaces was potentially evident by the low Chl *a* concentration in the water column, despite the high concentration of suspended sediment during prolonged rainfall event. The result from Chapter 4 relatively supported that in the event of bad weather, such as frequent or prolonged rainfall, increased in Chl *a* concentration was attributed to the high density of dominant species. This finding was in agreement with other studies on the relationship between MPB Chl *a* concentration with MPB assemblages diversity (Forster et al., 2006; Thornton et al., 2002).

Wind-induced wave was an important abiotic factor that positively stimulated MPB sediment-water column exchanges on the intertidal flats. The high association between suspended sediment and suspended Chl *a* was shown in the month of April 2013 which was characterized by higher mean wind speed than in July and October 2013 (Chapter 5). Wind-induced waves as an important driver in MPB resuspension has been reported in numerous

studies such as by De Jonge & Van Beusekom (1995), Easley et al., (2005) and Ubertini et al., (2015). The wind can also indirectly affect the Chl *a* concentrations on sediment surfaces by negatively affecting sediment deposition during immersion periods (Austen et al., 1999). Higher net sediment settlement rate in July than in April 2013 could be one of reasons of the month high MPB diversity as presented in Chapter 4. Higher deposition or net settlement rate of sediment reflected the presence of planktonic species after immersion periods (Ribeiro et al., 2013), and in this present study, it was best represented by the centric diatoms species.

Investigation on MPB variability at daily temporal scale in the Chapter 3 highlights that MPB biofilms on the mud flat and the transition zone in April 2013 were the most affected by weather-related abiotic factors. Even when it was windy, the month of April 2013 received quite high sum of sun hours. It was expected that the loss of MPB biomass due to wind induced waves caused higher suspended Chl *a* during immersion (Chapter 5) was balanced by the positive effect of long period of sun in April 2013 (spring) on MPB biomass.

7.2 Role of flood and ebb tides in MPB variability on salt marsh

Differences in the response of MPB between the salt marsh and the mud flat and the transition zone towards weather-related abiotic factors were hypothesized to be caused by the location of salt marsh on the upper tidal flat. At a monthly temporal scale, tidal range was shown to have a direct effect on MPB and positively enhanced the Chl *a* concentration of the salt marsh. Higher similarity in MPB species composition between the salt marsh and the transition zone during the spring tide inspired the work in Chapter 6. The work in Chapter 6 successfully highlights the link between MPB occurrences on the salt marsh with flood and ebb tides during spring tides. Findings in Chapter 6 answered questions that had risen on how spring tides sourced the salt marsh with high MPB biomass and diversity as presented in Chapter 3 and 4.

Results in Chapter 6 showed that there was connection between the MPB species composition in spring tides on the transition zone and salt marsh. MPB sediment-water column exchanges (resuspension) that was reported to be lower in spring tides (Chapter 3) could be attributed to its ability in 'carrying along' MPB properties from transition zone onto salt marsh (Chapter 6). The significant positive correlation between Chl *a* concentrations in flood tides on salt marsh with percentage of cloud cover can be linked to positive effect of 'sum of sun' on Chl *a* on sediment surfaces of transition zone (Chapter 6). Longer sum of sun potentially positively stimulated Chl *a* concentrations on sediment surfaces (Montani et al., 2003) and increased biostabilisation by MPB (Blanchard et al., 2000), therefore possibly decreasing MPB resuspension and decreased Chl *a* concentrations in flood tide on salt marsh. This potential connection between Chl *a* on sediment surfaces of transition zone and Chl *a* in flood tide samples was potentially evidence (in Chapter 4) of MPB movement from transition zone to the salt marsh during flood tide. The results of Chapter 4 also reported the high diversity (*H'*) in salt marsh MPB assemblages during spring tides. This high diversity could be linked to flood tide's potential in carrying the MPB from the lower tidal flat (transition zone). The occurrence of MPB species that were commonly recorded on the transition zone in the top 10 most common diatom taxa on the salt marsh in the event of spring tide events (Chapter 4) further supports the movement of MPB (transition – salt marsh) during flood tides.

In contrast to the role of flood tides, ebb tides are potentially responsible for causing the 'opposing influences' phenomenon on the salt marsh, as discussed in Chapter 3 and 6. MPB species composition in ebb tides samples were comprised of species that were mostly recorded in the top 10 most common species on salt marsh during neap tides. There was also 72.6 % species similarity between the MPB assemblages on salt marsh sediment surfaces and in the ebb tide samples (sampled on the salt marsh). These findings support the theory that MPB being resuspended and possibly washed away from the salt marsh sediment surfaces during spring tides.

7.3 Recommendations for further work

This present study was conducted with several limitations, so there are still questions on MPB spatial and temporal distributions left unanswered. However, fundamental information on how weather-related abiotic factors affected the MPB biomass at multiple spatial scales was answered. The questions of: does the suspended Chl *a* really originated from sediment surfaces? and is the MPB on the salt marsh linked to MPB on the lower part of tidal flat?, were successfully answered. The findings hopefully will help to improve our understanding of MPB variability across tidal flats, in both sediment surfaces and in water column.

Sampling for this work was restricted to the mud flat, the transition zone and the salt marsh area of the Fingringhoe tidal flat. Therefore results were not able to highlight the MPB connection between the tidal flat with the MPB in adjacent water channel. This study would be more informative if the connection between MPB occurrence on the tidal flat sediment surfaces that was ecologically important for Chl *a* concentration in water column during immersion, could also be investigated with the concentration of Chl *a* in the River Colne.

Although this present study has shown that the ebb tides enhanced the MPB sediment – water column exchanges on salt marsh, the fate of MPB after being resuspended are still unknown. It was hypothesized that the resuspended MPB could possibly wash away onto lower area of tidal flat. But none of the recorded MPB that were exclusively recorded on salt marsh and were in the ebb tides samples such as genus *Opephora* and *Neidium* were ever recorded on the mud flat or the transition zone.

Regression analysis looking at the relationship between Chl *a* on sediment surfaces and suspended in the water column during immersions has shown different association strength between these two variables in the three different months across the study site. Other than the effect of weather-related abiotic factors, we hypothesized that the presence of the grazer, the *Hydrobia ulvae* could possibly cause such finding. Therefore, incorporating the biological effect

together with weather-related abiotic factors effect on MPB could potentially important in providing more precise finding.

7.4 Concluding remarks

Overall, the results in this thesis highlights that the Chl *a* concentrations in the top 2 mm of MPB biofilms was closely linked to weather-related abiotic factors, the MPB assemblage diversity of the biofilms and also the resuspension and the net settlement of sediment during immersion period.

Weather conditions which were monitored based on the averaged wind speed for three days, sum of sun hours for three days and sum of rainfall for three days, caused the spatial and temporal variability in Chl *a*, CC and EPS concentrations across the tidal flat. Additionally, the tidal range across the neap-spring-neap tidal cycles had stronger effect on the MPB species composition and diversity rather than on the Chl *a*, CC and EPS concentrations.

The finding in Chapter 3 provides insights on how the weather affected the MPB availability on the sediment surface during emersion and immersion periods. Investigation on multiple scales has highlighted the different effect of the chosen weather-related abiotic factors on the MPB biomass proxies in different months, in different days of month, at different quadrats in each sampling day and at different micro-spatial patches of each quadrat. Chl *a* concentration significantly correlated with MPB assemblages diversity (Chapter 4), could potentially be linked to the variability in MPB biomass proxies at the measured multiple spatio-temporal scales. Additionally, the different in MPB assemblages species composition was potentially one of the main factors to cause high variability even at the smallest micro-spatial scale, < 0.5 m.

The use of sediment traps has provided information on the relationship between the MPB availability on the sediment surfaces with the availability of diatom in the water column during immersion periods. The similarity index analyses on the species composition data,

further supports that suspended diatom during immersions originated from the 'washed away' MPB from the sediment surfaces. This study is the first study ever to report the MPB sediment-water column exchanges with not only Chl *a* data, but also the MPB species relative abundance data. The species composition data has also highlighted the potential water channel (River Colne) – water column – sediment surfaces (on tidal flat) MPB connection, which is driven by the tidal cycles and the tidal range.

Flood tide was an important event to 'wash away' the MPB from sediment surfaces on the mud flat and allowed MPB movement from the lower (mud flat and transition zone) onto the upper area (salt marsh) of the tidal flat. Ebb tide, as expected, was important in 'washing away' or resuspend MPB from the salt marsh sediment surfaces. The movement and resuspension of MPB on both the mud flat and the salt marsh during flood and ebb tides were closely linked to the tidal range and also the sum of sun hours.

REFERENCES

- Aberle-Malzahn, N. (2004). *The microphytobenthos and its role in aquatic food webs* (Doctoral dissertation). Der Christian-Albrechts-Universität zu Kiel.
- Arfi, R., Guiral, D., & Bouvy, M. (1994). Sedimentation modified by wind induced resuspension in a shallow tropical lagoon (Cote d'Ivoire). *Netherlands Journal of Aquatic Ecology*, 28(3–4), 427–431.
- Aspden, R.J., Vardy, S. & Paterson, D. M. (2004). Salt marsh microbial ecology: Microbes, benthic mats and sediment movement. *Coastal and Estuarine Studies*, 59, 115-136.
- Austen, I., Andersen, T. J., & Edolvang, K. (1999). The influence of benthic diatoms and invertebrates on the erodibility of an intertidal mudflat, the Danish Wadden Sea. *Estuarine Coastal and Shelf Science*, 49(1), 99–111.
- Azovsky, A. I., Chertoproud, E. S., Saburova, M. A., & Polikarpov, I. G. (2004). Spatio-temporal variability of micro- and meiobenthic communities in a White Sea intertidal sandflat. *Estuarine, Coastal and Shelf Science*, 60(4), 663–671.
- Barbier, N., Couteron, P., Lefever, R., Deblauwe, V. and Lejeune, O. (2008). Spatial decoupling of facilitation and competition at the origin of gapped vegetation patterns. *Ecology*, 89, 1521–1531.
- Barranguet, C. (1997). The role of microphytobenthos primary production in a Mediterranean mussel culture area. *Estuarine, Coastal and Shelf Science*, 44, 753-765.
- Begon, M., Townsend, C. R. & Harper, J. L. (2006). *Ecology: From individuals to Ecosystems*, 4th edn. Blackwell Publishing, UK.

- Bellinger, B. J., Underwood, G. J. C., Ziegler, S. E., & Gretz, M. R. (2009). *Aquatic Microbial Ecology* 55, 169–187.
- Benyoucef, I., Blandin, E., Lerouxel, A., Jesus, B., Rosa, P., Méléder, V., Barillé, L. (2013). Microphytobenthos interannual variations in a north-European estuary (Loire estuary, France) detected by visible-infrared multispectral remote sensing. *Estuarine, Coastal and Shelf Science*, 136, 43–52.
- Blanchard, F., Guarini, J., Orvain, F., & Sauriau, P. (2001). Dynamic behaviour of benthic microalgal biomass in intertidal mudflats. *Journal of Experimental Marine Biology and Ecology*, 264, 85-100.
- Blanchard, G. F., & Forster, R. M. (2006). Functioning of microphytobenthos in estuaries. Proceedings of the microphytobenthos symposium, Amsterdam, The Netherlands, August 2003. Royal Netherlands Academy of Arts and Sciences.
- Blanchard, G. F., Agion, T., Guarini, J. M., Herlory, O. and Richard, P. (2006). Analysis of the short-term dynamics of microphytobenthic biomass on intertidal mudflats, p. 85–97. In J. Kromkamp [ed.], Functioning of microphytobenthos in estuaries: Proceedings of the microphytobenthos symposium, Amsterdam, The Netherlands, August 2003. Royal Netherlands Academy of Arts and Sciences.
- Blanchard, G. F., Guarini, J. M., Orvain, F. & Sauriau, P. G. (2001). Dynamic behavior of benthic microalgal biomass. *Journal of Marine Biological Association of United Kingdom*, 82, 1027-1028.
- Booth, J. G., Miller, R. L., McKee, B. A., & Leathers, R. A. (2000). Wind-induced bottom sediment resuspension in a microtidal coastal environment. *Continental Shelf Research*, 20(7), 785–806.

- Booth, J., Miller, R., McKee, B. A. & Leathers, R. A. (2000). Wind-induced bottom sediment resuspension in a microtidal coastal environment. *Continental Shelf Research*, 20 (7), 785-806.
- Brito, A. C., Fernandes, T. F., Newton, A., Facca, C., & Tett, P. (2012). Does microphytobenthos resuspension influence phytoplankton in shallow systems? A comparison through a Fourier series analysis. *Estuarine, Coastal and Shelf Science*, 110, 77–84.
- Cartaxana, P., Cruz, S., Gameiro, C., & Kuhl, M. (2016). Regulation of intertidal microphytobenthos photosynthesis over a diel emersion period is strongly affected by diatom migration patterns. *Frontiers in Microbiology*, 7, 1–11.
- Cartaxana, P., Mendes, C. R., van Leeuwe, M. A., & Brotas, V. (2006). Comparative study on microphytobenthos pigments of muddy and sandy intertidal sediments of the Tagus estuary. *Estuarine, Coastal and Shelf Science*, 66(1–2), 225–230.
- Chesman, B. S., Burt, G. R., & Langston, W. J. (2006). Characterisation of European Marine Sites: Essex Estuaries, European Marine Site. *The Marine Biological Association*, (17), 1–208.
- Cibic, T., Blasutto, O., Falconi, C., & Umani, S. F. (2007). Microphytobenthic Biomass, Species Composition and Nutrient Availability in Sublittoral Sediments of the Gulf of Trieste (Northern Adriatic Sea). *Estuarine Coastal and Shelf Science*, 75(1–2), 50–62.
- Ciutat, A., Widdows, J., & Pope, N. D. (2007). Effect of *Cerastoderma edule* density on near-bed hydrodynamics and stability of cohesive muddy sediments. *Journal of Experimental Marine Biology and Ecology*, 346(1–2), 114–126.

- Coastal Geomorphology Partnership (2000). Erosion of the Saltmarshes of Essex Between 1988 and 1998. Department of Marine Sciences and Coastal Management, University of Newcastle, Newcastle, UK.
- Colijn, F., de Jonge, V., & Jonge, V. D. (1984). Primary production of microphytobenthos in the Ems-Dollard Estuary. *Marine Ecology Progress Series*, 14, 185–196.
- Consalvey, M., Paterson, D. M. & Underwood, G. J. C. (2004). The ups and down of life in a benthic biofilm: Migration of benthic diatom. *Diatom Research*, 19(2), 181-202.
- Costa, P. F., Brotas, V. & Fonseca, L. C. (2002). Physical characterisation and microphytobenthos biomass of estuarine and lagoon environments of the Southwest Coast of Portugal. *Limnology*, 21(1-2), 69-79.
- Costa, P., Brotas, V., & Fonseca, L. (2002). Physical characterisation and microphytobenthos biomass of estuarine and lagoon environments of the Southwest coast of Portugal. *Limnetica*, 21(1–2), 69–80.
- Davis, R. A., & Dalrymple, R. W. (2010). Principles of tidal sedimentology. Principles of Tidal Sedimentology. Springer Science & Business Media. New York.
- de Brouwer, J. F. C. & Stal, L. J. (2001). Short-term dynamics in microphytobenthos distribution and associated extracellular carbohydrates in surface sediments of an intertidal mud flat. *Marine Ecology Progress Series*, 2, 33-44.
- de Brouwer, J. F. C., De Deckere, E. M. G. T., & Stal, L. J. (2003). Distribution of extracellular carbohydrates in three intertidal mudflats in Western Europe. *Estuarine, Coastal and Shelf Science*, 56(2), 313–324.
- de Brouwer, J. F. C., Neu, T. R. & Stal, L. J. (2006). Extracellular polymeric substances: function and role in mudflats. pp. 45-64; In C. J. C. Kromkamp, J. F. C. Brouwer, G.F. Blanchard, R. M. Forster & V. Creach [eds.]. Functioning

Microphytobenthos in Estuaries. Royal Netherlands Academy of Arts and Sciences.

- De Jonge, V. N., & Van Beusekom, J. E. E. (1995). Wind- and tide-induced resuspension of sediment and microphytobenthos from tidal flats in the Ems estuary. *Limnology and Oceanography*, 40(4), 776–778.
- De Jonge, V. N., De Boer, W. F., De Jong, D. J., & Brauer, V. S. (2012). Long-term mean annual microphytobenthos chlorophyll a variation correlates with air temperature. *Marine Ecology Progress Series*, 468, 43–56.
- Delgado, M., de Jonge, V. N. & Peletier, H. (1991). Experiments on resuspension of natural microphytobenthos populations. *Marine Biology*, 108, 321–328.
- Delgado, S., Therriault, J. C. & Bourget, E. (1987). Resuspension in the shallow sublittoral zone of macrotidal estuarine environment: Wind influence. *Limnology and Oceanography*, 32, 327-339.
- Du, G. Y., Oak, J.-H., Li, H., & Chung, I.-K. (2010). Effect of light and sediment grain size on the vertical migration of benthic diatoms. *Algae*, 25(3), 133–140.
- Du, G. Y., Son, M., An, S., & Chung, I. K. (2010). Temporal variation in the vertical distribution of microphytobenthos in intertidal flats of the Nakdong River estuary, Korea. *Estuarine, Coastal and Shelf Science*, 86(1), 62–70.
- Du, G., Son, M., Yun, M., An, S., & Chung, I. K. (2009). Microphytobenthic biomass and species composition in intertidal flats of the Nakdong River estuary, Korea. *Estuarine, Coastal and Shelf Science*, 82(4), 663–672.
- Ducker, H. P. (1982). Suspensionsgehalte im Flachwassergebiet-messungen in Watt von scharhorn. *Küste*, 37, 85-184.

- Dupuy, C., Mallet, C., Guizien, K., Montanié, H., Bréret, M., Mornet, F., Orvain, F. (2014). Sequential resuspension of biofilm components (viruses, prokaryotes and protists) as measured by erodimetry experiments in the Brouage mudflat (French Atlantic coast). *Journal of Sea Research*, 92, 56–65.
- Easley, J. T., Hymel, S. N., & Plante, C. J. (2005). Temporal patterns of benthic microalgal migration on a semi-protected beach. *Estuarine, Coastal and Shelf Science*, 64(2–3), 486–496.
- Facca, C., Sfriso, a., & Socal, G. (2002). Changes in Abundance and Composition of Phytoplankton and Microphytobenthos due to Increased Sediment Fluxes in the Venice Lagoon, Italy. *Estuarine, Coastal and Shelf Science*, 54(5), 773–792.
- Fonseca, A. L. P., Machado, E. D., Brandini, F. P., Brandini, N. (2013). Microphytobenthic biomass on a subtropical intertidal flat of Paranagua Bay (Southern Brazil): Spatio-Temporal distribution and the influence of environmental conditions. *Brazilian Journal of Oceanography*, 61(2), 83-92.
- Forster, R. M., Sabbe, K., Vyverman, W., & Stal, L. J. (2006). Biodiversity-ecosystem function relationship in microphytobenthic diatoms of the Waterschelde estuary. *Marine Ecology Progress Series*, 311, 191–201.
- French, A. J. R., Spencer, T., Murray, A. L., Arnold, N. S., Small, T., & Wetlands, T. (2009). Coastal Geostatistical Analysis of Sediment Deposition in two small wetlands, Norfolk, UK. *Journal of Coastal Research*, 11(2), 308–321.
- French, J. R., & Stoddart, D. R. (1992). Hydrodynamics of salt marsh creek systems: Implications for marsh morphological development and material exchange. *Earth Surface Processes and Landforms*, 17(3), 235–252.

- French, R., & Spencer, T. (1993). Dynamics of sedimentation in a tide-dominated backbarrier salt marsh, Norfolk, UK. *Marine Geology*, 110, 315–331.
- Gabrielson, J. O. & Lukatelich, R. J. (1985). Wind related resuspension of sediments in the Peel-Harvey estuarine system. *Estuarine, Coastal and Shelf Science*, 20, 135-145.
- Garstecki, T., Wickham, S. A., & Arndt, H. (2002). Effects of Experimental Sediment Resuspension on a Coastal Planktonic Microbial Food Web. *Estuarine, Coastal and Shelf Science*, 55(5), 751–762.
- Gerbersdorf, S. U., Westrich, B., & Paterson, D. M. (2009). Microbial extracellular polymeric substances (EPS) in fresh water sediments. *Microbial Ecology*, 58(2), 334–349.
- Gottschalk, S., Uthicke, S., & Heimann, K. (2007). Benthic diatom community composition in three regions of the Great Barrier Reef, Australia. *Coral Reefs*, 26(2), 345–357.
- Green, M. O. (2011). Very small waves and associated sediment resuspension on an estuarine intertidal flat. *Estuarine, Coastal and Shelf Science*, 93(4), 449–459.
- Hagerthey, S. E., Defew, E. C., & Paterson, D. M. (2002). Influence of *Corophium volutator* and *Hydrobia ulvae* on intertidal benthic diatom assemblages under different nutrient and temperature regimes. *Marine Ecology Progress Series*, 245, 47–59.
- Hanlon, A. R. M., Bellinger, B., Haynes, K., Xiao, G., Hofmann, T. A., Gretz, M. R., Underwood, G. J. C. (2006). Dynamics of extracellular polymeric substance (EPS) production and loss in an estuarine, diatom-dominated, microalgal biofilm over a tidal emersion-immersion period. *Limnology and Oceanography*, 51(1), 79–93.
- Hartley, B., Barber, H.G., Carter, J.R. (1996). An Atlas of British Diatoms. Biopress Limited, Bristol.

- Herlory, O., Guarini, J. M., Richard, P., & Blanchard, G. F. (2004). Microstructure of microphytobenthic biofilm and its spatio-temporal dynamics in an intertidal mudflat (Aiguillon Bay, France). *Marine Ecology Progress Series*, 282, 33–44.
- Horton, B. P., Corbett, R., Culver, S. J., Edwards, R. J., & Hillier, C. (2006). Modern saltmarsh diatom distributions of the Outer Banks, North Carolina, and the development of a transfer function for high resolution reconstructions of sea level. *Estuarine, Coastal and Shelf Science*, 69(3–4), 381–394.
- Hughes, J. B., & Roughgarden, J. (2000). Species Diversity and Biomass Stability. *The American Naturalist*, 155(5), 618–627.
- Jackson, A. C., Underwood, A. J., Murphy, R. J., & Skilleter, G. A. (2010). Latitudinal and environmental patterns in abundance and composition of epilithic microphytobenthos. *Marine Ecology Progress Series*, 417, 27–38.
- Kocum, E., Nedwell, D. B., & Underwood, G. J. C. (2002). Regulation of phytoplankton primary production along a hypernutrified estuary. *Marine Ecology Progress Series*, 231, 13–22.
- Kocum, E., Underwood, G. J. C., & Nedwell, D. B. (2002). Simultaneous measurement of phytoplanktonic primary production, nutrient and light availability along a turbid, eutrophic UK east coast estuary (the Colne Estuary). *Marine Ecology Progress Series*, 231, 1–12.
- Koh, C. H., Jong, S. K., Araki, H., Yamanishi, H., Mogi, H., & Koga, K. (2006). Tidal resuspension of microphytobenthic chlorophyll a in a Nanaura mudflat, Saga, Ariake Sea, Japan: Flood-ebb and spring-neap variations. *Marine Ecology Progress Series*, 312, 85–100.

- Koh, C. H., Khim, J. S., Araki, H., Yamanishi, H., & Koga, K. (2007). Within-day and seasonal patterns of microphytobenthos biomass determined by co-measurement of sediment and water column chlorophylls in the intertidal mudflat of Nanaura, Saga, Ariake Sea, Japan. *Estuarine, Coastal and Shelf Science*, 72(1–2), 42–52.
- Kovach, W. L. (1999). A multivariate statistical package. Kovach Computing Service. Anglesey, Wales.
- Kwon, B. O., Khim, J. S., Park, J., Ryu, J., Kang, S. G., & Koh, C. H. (2012). Short-term variability of microphytobenthic primary production associated with in situ diel and tidal conditions. *Estuarine, Coastal and Shelf Science*, 112, 236–242.
- Lake, S. J., & Brush, M. J. (2011). The contribution of microphytobenthos to total productivity in upper Narragansett Bay, Rhode Island. *Estuarine, Coastal and Shelf Science*, 95(2–3), 289–297.
- Le Hir, P., Roberts, W., Cazaillet, O., Christie, M., Bassoullet, P., & Bacher, C. (2000). Characterization of intertidal flat hydrodynamics. *Continental Shelf Research*, 20(12–13), 1433–1459.
- Le Rouzic, B. (2012). Changes in photosynthetic yield (Fv/Fm) responses of salt-marsh microalgal communities along an osmotic gradient (Mont-Saint-Michel Bay, France). *Estuarine, Coastal and Shelf Science*, 115, 326–333.
- Leonardi, N., Ganju, N. K., & Fagherazzi, S. (2015). A linear relationship between wave power and erosion determines salt-marsh resilience to violent storms and hurricanes. *Proceedings of the National Academy of Sciences*, 113(1), 64–68.
- Lorenzen, C. J. (1967). Determination of chlorophyll and phaeo-pigments: Spectrophotometric equations. *Limnological Oceanography*, 12, 343–346.
- Mann, D. G. 1999. The species concept in diatoms. *Phycologia*, 38(6):437-495.

- McKew, B. A., Taylor, J. D., McGenity, T. J., & Underwood, G. J. C. (2011). Resistance and resilience of benthic biofilm communities from a temperate saltmarsh to desiccation and rewetting. *The ISME Journal*, 5(1), 30–41.
- McLachlan, D. H., Brownlee, C., Taylor, A. R., Geider, R. J., & Underwood, G. J. C. (2009). Light-induced motile responses of the estuarine benthic diatoms *Navicula perminuta* and *Cylindrotheca closterium* (bacillariophyceae). *Journal of Phycology*, 45(3), 592–599.
- Midlen, A. & Ferreira, M. (n.d.). Essex estuaries (united kingdom). Erosion Case Study.
- Migné, A., Spilmont, N., & Davoult, D. (2004). In situ measurements of benthic primary production during emersion: Seasonal variations and annual production in the Bay of Somme (eastern English Channel, France). *Continental Shelf Research*, 24(13–14), 1437–1449.
- Miklasz, K. (2012). *Physical constraints on the size and shape of microalgae* (PhD dissertation). Stanford University. USA.
- Mitbavkar, S. & Anil, A. C. (2006). Diatoms of the microphytobenthic community in a tropical intertidal sand flat influenced by monsoons: spatial and temporal variations. *Marine Biology*, 148, 693-709.
- Mitchell, S. B., Couperthwaite, J. S., West, J. R. & Lawler, D. M. (2003). Measuring sediment exchange rates on Intertidal bank at Blacktoft, Humber estuary, UK. *Science Total Environment*, 535-549.
- Montani, S., Magni, P., & Abe, N. (2003). Seasonal and interannual patterns of intertidal microphytobenthos in combination with laboratory and areal production estimates. *Marine Ecology Progress Series*, 249, 79–91.

- Murphy, R. J., Tolhurst, T. J., Chapman, M. G., & Underwood, A. J. (2009). Seasonal distribution of chlorophyll on mudflats in New South Wales, Australia measured by field spectrometry and PAM fluorometry. *Estuarine, Coastal and Shelf Science*, *84*(1), 108–118.
- Nedwell, D. B., Underwood, G. J. C., McGenity, T. J., Whitby, C., & Dumbrell, A. J. (2016). The Colne Estuary: A long-term microbial ecology observation. *Advances in Ecological Research*, *55*, 227-281.
- Ogilvie, B., Nedwell, D. B., Harrison, R. M., Robinson, A., & Sage, A. (1997). High nitrate, muddy estuaries as nitrogen sinks: The nitrogen budget of the River Colne estuary (United Kingdom). *Marine Ecology Progress Series*, *150*(1–3), 217–228.
- Orvain, F., De Crignis, M., Guizien, K., Lefebvre, S., Mallet, C., Takahashi, E., & Dupuy, C. (2014). Tidal and seasonal effects on the short-term temporal patterns of bacteria, microphytobenthos and exopolymers in natural intertidal biofilms (Brouage, France). *Journal of Sea Research*, *92*, 6–18.
- Orvain, F., Lefebvre, S., Montepini, J., Sébire, M., Gangnery, A., & Sylvand, B. (2012). Spatial and temporal interaction between sediment and microphytobenthos in a temperate estuarine macro-intertidal bay. *Marine Ecology Progress Series*, *458*, 53–68.
- Orvain, F., Sauriau, P.G., Bacher, C., & Prineau, M. (2006). The influence of sediment cohesiveness on bioturbation effects due to *Hydrobia ulvae* on the initial erosion of intertidal sediments: A study combining flume and model approaches. *Journal of Sea Research*, *55*(1), 54–73.
- Orvain, F., Sauriau, P.G., Sygut, A., & Joassard, L. (2004). Interacting effects of *Hydrobia ulvae* bioturbation and microphytobenthos on the erodibility of mudflat sediments. *Marine Ecology Progress Series*, *278*, 205–223.

- Pan, J., Bournod, C. N., Cuadrado, D. G., Vitale, A., & Piccolo, M. C. (2013). Interaction between Estuarine Microphytobenthos and Physical Forcings: The Role of Atmospheric and Sedimentary Factors. *International Journal of Geosciences*, 4, 352–361.
- Paterson, D. M. (1986). The migratory behaviour of diatom assemblages in a laboratory tidal micro-ecosystem examined by low temperature scanning electron microscopy. *Diatom Research*, 1, 227-239.
- Perkins, R. G., Honeywill, C., Consalvey, M., Austin, H. A., Tolhurst, T. J., Paterson, D. M. (2003). Changes in microphytobenthic chlorophyll a and EPS resulting from sediment compaction due to de-watering: opposing patterns in concentration and content. *Continental Shelf Research*, 23, 575-586.
- Perkins, R. G., Underwood, G. J. C., Brotas, V., Snow, G. C., Jesus, B. & Ribeiro, L. (2001). Responses of microphytobenthos to light: primary production and carbohydrate allocation over an emersion period. *Marine Ecology Progress Series*, 223, 101-112.
- Peterson, C. H., & Peterson, N. M. (1979). The Ecology of Intertidal Flats of North Carolina: A Community Profile. University of North Carolina. Morehead City.
- Piccard, V. A., Larga, C., & Marta, S. (2010). *Microphytobenthos*. *Biological Marine Mediterranean*, 17(1), 754–800.
- Potapova, M. (2011). *Navicula cryptocephala*. In *Diatoms of the United States*. http://westerndiatoms.colorado.edu/taxa/species/navicula_cryptocephala.
- Putman, R. J. & Wratten, S. D. (1984). Principles of Ecology. University of California Press. USA.

- Rasmussen M.B, Henriksen, K., Jensen, A. (1983). Possible causes of temporal fluctuations in primary production of the microphytobenthos in the Danish Wadden Sea. *Marine Biology*, 73, 109–114.
- Reiss, H., Wieking, G., & Kröncke, I. (2007). Microphytobenthos of the Dogger Bank: A comparison between shallow and deep areas using phytopigment composition of the sediment. *Marine Biology*, 150(6), 1061–1071.
- Ribeiro, L., Brotas, V., Rincé, Y., & Jesus, B. (2013). Structure and Diversity of Intertidal Benthic Diatom Assemblages in Contrasting Shores: A Case Study from the Tagus Estuary. *Journal of Phycology*, 49(2), 258–270.
- Riggs, S.R. (2002). Life at the edge of North Carolina's coastal system: the geo-logic controls. In: Beal, C., Prioli, C. (Eds.), *Life at the Edge of the Sea: Essays on North Carolina's Coast and Coastal Culture*, Vol I. Coastal Carolina Press, Wilmington, NC, pp. 63-95.
- Risgaard-Peterson, N. (2003). Coupled nitrification denitrification in autotrophic and heterotrophic estuarine sediments on the influence of the benthic microalgae. *Limnology and Oceanography*, 48, 93-105.
- Sahan, E., Sabbe, K., Creach, V., Hernandez-Raquet, G., Vyverman, W., Stal, L. J., & Muyzer, G. (2007). Community structure and seasonal dynamics of diatom biofilms and associated grazers in intertidal mudflats. *Aquatic Microbial Ecology*, 47(3), 253–266.
- Saint-Béat, B., Dupuy, C., Agogué, H., Carpentier, A., Chalumeau, J., Como, S., Niquil, N. (2014). How does the resuspension of the biofilm alter the functioning of the benthos-pelagos coupled food web of a bare mudflat in Marennes-Oléron Bay (NE Atlantic). *Journal of Sea Research*, 92, 144–157.

- Scholz, B., & Liebezeit, G. (2012). Microphytobenthic dynamics in a Wadden Sea intertidal flat – Part II: Seasonal and spatial variability of non-diatom community components in relation to abiotic parameters. *European Journal of Phycology*, 47(2), 120–137.
- Seitzinger, S. P. (1973). Denitrification in freshwater and coastal marine ecosystems: Ecological and geochemical significance. *Limnological Oceanography*, 33(2), 702–724.
- Serôdio, J., Coelho, H., Vieira, S., & Cruz, S. (2006). Microphytobenthos vertical migratory photoresponse as characterised by light-response curves of surface biomass. *Estuarine, Coastal and Shelf Science*, 68(3–4), 547–556.
- Seuront, L. and Leterme, C. (2006). Microscale patchiness in microphytobenthos distributions: evidence for a critical state. In Blanchard, G and R. Forster (eds), *Functioning of microphytobenthos in estuaries*. Royal Netherlands Academy of Arts and Sciences, Netherlands, 167-185.
- Skinner, T., Adams, J. B., & Gama, P. T. (2006). The effect of mouth opening on the biomass and community structure of microphytobenthos in a small oligotrophic estuary. *Estuarine, Coastal and Shelf Science*, 70(1–2), 161–168.
- Smith, D. J., & Underwood, G. J. C. (1998). Exopolymer production by intertidal epipellic diatoms. *Limnology and Oceanography*, 43(7), 1578–1591.
- Snøeijs, P. and Vilbaste, S. (1994). Intercalibration and distribution of diatom species in the Baltic Sea. Vol. 2, The Baltic Marine Biologists Publication, Opulus Press, Uppsala.
- Spilmont, N., Migné, A., Seuront, L., Davoult, D. (2007). Short-term variability of intertidal benthic community production during emersion and the implication in annual budget calculation. *Marine Ecology Progress Series*, 333, 95-101.

- Spilmont, N., Seuront, L., Meziane, T., & Welsh, D. T. (2011). There's more to the picture than meets the eye: Sampling microphytobenthos in a heterogeneous environment. *Estuarine, Coastal and Shelf Science*, 95(4), 470–476.
- Sullivan, M. J., Montcreiff, C. A. (1988). Primary production of edaphic algal communities in a Mississippi salt marsh. *Journal of Phycology*, 24, 49-58.
- Sundbäck, K., & Miles, A. (2002). Role of microphytobenthos and denitrification for nutrient turnover in embayments with floating macroalgal mats: A spring situation. *Aquatic Microbial Ecology*, 30(1), 91–101.
- Sundbäck, K., Carlson, L., Nilsson, C., Jönsson, B., Wulff, A., & Odmark, S. (1996). Response of benthic microbial mats to drifting green algal mats. *Aquatic Microbial Ecology*, 10(2), 195–208.
- Taylor, J. D., McKew, B. A., Kuhl, A., McGenity, T. J., & Underwood, G. J. C. (2013). Microphytobenthic extracellular polymeric substances (EPS) in intertidal sediments fuel both generalist specialist EPS-degrading bacteria. *Limnology and Oceanography*, 58(4), 1463–1480.
- Taylor, P., Round, F. E., & Haphey, C. M. (1965). Persistent vertical-migration rhythms in benthic microflora. *British Phycological Bulletin*, 2, 37–41.
- Thornton, D. C. O., Dong, L. F., Underwood, G. J. C., & Nedwell, D. B. (2002). Factors affecting microphytobenthic biomass, species composition and production in the Colne Estuary (UK). *Aquatic Microbial Ecology*, 27(3), 285–300.
- Tilman, D. (1982). Resource competition and community structure. Princeton University Press, Princeton.
- Trimbee, A. M., & Harris, G. P. (1984). Phytoplankton population dynamics of a small reservoir: Use of sedimentation traps to quantify the loss of diatoms and recruitment of

summer bloom-forming blue-green algae. *Journal of Plankton Research*, 6(5), 897–918.

Tyler, A. C., McGlathery, K. J. & Anderson, I. C. (2003). Benthic algae control sediment-water column fluxes of organic and inorganic nitrogen compounds in a temperate lagoon. *Limnology and Oceanography*, 48, 2125-2137.

Ubertini, M., Lefebvre, S., Gangnery, A., Grangeré, K., Le Gendre, R., & Orvain, F. (2012). Spatial Variability of Benthic-Pelagic Coupling in an Estuary Ecosystem: Consequences for Microphytobenthos Resuspension Phenomenon. *PLoS ONE*, 7(8), 1-17.

Ubertini, M., Lefebvre, S., Rakotomalala, C., & Orvain, F. (2015). Impact of sediment grain-size and biofilm age on microphytobenthos resuspension. *Journal of Experimental Marine Biology and Ecology*, 467, 52–64.

Uncles, R. J., Easton, A. E., Griffiths, M. L., Harris, C., Howland, R. J. M., Joint, I., Plummer, D. H. (1998). Concentrations of suspended chlorophyll in the tidal Yorkshire Ouse and Humber Estuary. *Science of the Total Environment*, 210–211, 367–375.

Underwood, G.J.C. & Smith, D. J. (1998). Predicting epipellic diatom exopolymer concentrations in intertidal sediments from sediment chlorophyll *a*. *Microbial Ecology*, 35,116–125.

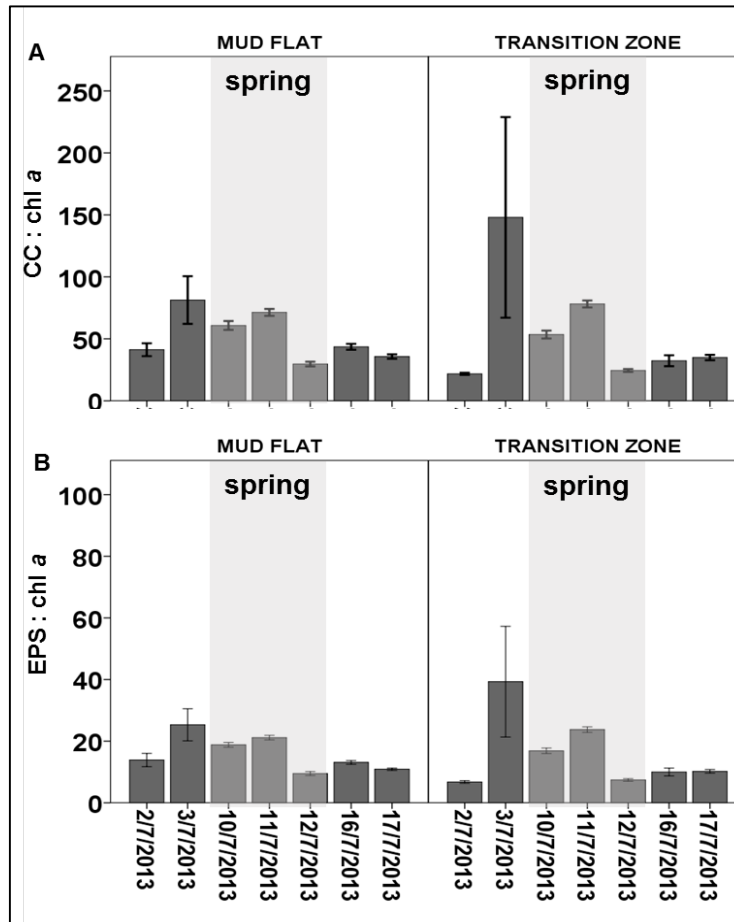
Underwood, G. J. C. & Paterson, D. M. (1993). Recovery of intertidal benthic diatoms after biocide treatment and associated sediment dynamics. *Journal of the Marine Biological Association of the UK*, 73, 25-45.

Underwood, G. J. C. (1994). Seasonal and spatial variation in epipellic diatom assemblages in the Severn estuary. *Diatom Research*, 9, 451-472.

- Underwood, G. J. C. (1997). Microalgal colonization in a saltmarsh restoration scheme. *Estuarine Coastal and Shelf Science*, 44, 471–481.
- Underwood, G. J. C. and Kromkamp, J. (1999). Primary production by phytoplankton and microphytobenthos in estuaries. *Advanced Ecological Research*, 29, 93-153.
- Underwood, G. J. C., Hanlon, A. R. M., Oxborough, K., & Baker, N. R. (2005). Patterns in microphytobenthic primary productivity: Species-specific variation in migratory rhythms and photosynthetic efficiency in mixed-species biofilms. *Limnological Oceanography*, 50(3), 755–767.
- Underwood, G. J. C., Paterson, D. M., & Parkes, R. J. (1995). The measurement of microbial carbohydrate exopolymers from intertidal sediments. *Limnological Oceanography*, 7, 1243–1253.
- Underwood, G., Phillips, J., & Saunders, K. (1998). Distribution of estuarine benthic diatom species along salinity and nutrient gradients. *European Journal of Phycology*, 33(2), 173–183.
- van der Wal, D., Wielemaker-van den Dool, A., & Herman, P. M. J. (2010). Spatial synchrony in intertidal benthic algal biomass in temperate coastal and estuarine ecosystems. *Ecosystems*, 13(2), 338–351.
- Van Der Werff, A. & Huls, H. (1976). *Diatomeenflora van Naderland (Diatom Flora of the Netherland)*. Otto Koeltz Science Publishers, West Germany.
- Viner-Mozzin, Y., Zohary, T., & Gasith, A. (2003). Dinoflagellate bloom development and collapse in Lake Kinneret: A sediment trap study. *Journal of Plankton Research*, 25(6), 591–602.
- Walker, B. H. (1992). Biodiversity and Ecological Redundancy. *Society for Conservation Biology*, 6, 18–23.

- Warner, J.C., Schoellhamer, D.H., Ruhl, C.A., Burau, J.R. (2004). Floodtide pulses after low tides in shallow subembayments adjacent to deep channels. *Estuarine Coastal Shelf Science*, 60 (2), 213–228.
- Webster, I., Ford, P., Hodgson, B. (2002). Microphytobenthos contribution to nutrient-phytoplankton dynamics in a shallow coastal lagoon. *Estuaries*, 25, 540-551.
- Weerman, E. J., Van Belzen, J., Rietkerk, M., Temmerman, S., Kéfi, S., Herman, P. M. J., & Van De Koppel, J. (2012). Changes in diatom patch-size distribution and degradation in a spatially self-organized intertidal mudflat ecosystem. *Ecology*, 93(3), 608–618.
- Woelfel, J., Schumann, R., Adler, S., Hübener, T., & Karsten, U. (2007). Diatoms inhabiting a wind flat of the Baltic Sea: Species diversity and seasonal succession. *Estuarine, Coastal and Shelf Science*, 75(3), 296–307.
- Wolfstein, K., Colijn, F., & Doerffer, R. (2000). Seasonal Dynamics of Microphytobenthos Biomass and Photosynthetic Characteristics in the Northern German Wadden Sea, Obtained by the Photosynthetic Light Dispensation System. *Estuarine, Coastal and Shelf Science*, 51(5), 651–662.
- Xin, P., Li, L., & Barry, D. A. (2013). Tidal influence on soil conditions in an intertidal creek-marsh system. *Water Resources Research*, 49(1), 137–150.

APPENDICES



Appendix 1: Daily ratio of A) CC (CC) and B) extracellular polymeric substance (EPS) to Chl a content in top 2 mm per cm² sediment across July 2013 sampling month on the mud flat and the transition zone. Values are mean ± 1SE, n= 24. Notes the high CC : Chl a and EPS : Chl a values on both zones on the 3rd July 2013 (one day rainfall event in July 2013) and on the 10th and 11th July 2013 (longer period of sun).

Appendix 2: Plate of some recorded MPB species in Fingringhoe tidal flat, Colne estuary.

— represents 10 μm .

Plate	Species	Literature
	<p>Plate 1</p> <p><i>Gyrosigma balticum</i> (Ehrenberg)</p> <p>Length = 225 μm, valve is linear and sigmoidal towards ends, sigmoidal raphae towards the centre.</p> <p>Habitat : Mud flat and transition zone</p>	<p>Van der werff, A & Huls, H. (1976).</p>
	<p>Plate 2</p> <p><i>Gyrosigma scalproides</i> (Rabenhorst)</p> <p>Length= 52.85 μm, valve is sigmoid, central fissure is straight.</p>	<p>Van der werff, A & Huls, H. (1976).</p>
	<p>Plate 3</p> <p><i>Nitzschia sigma</i></p> <p>Length= 178.2 μm</p>	<p>Van der werff, A & Huls, H. (1976).</p>

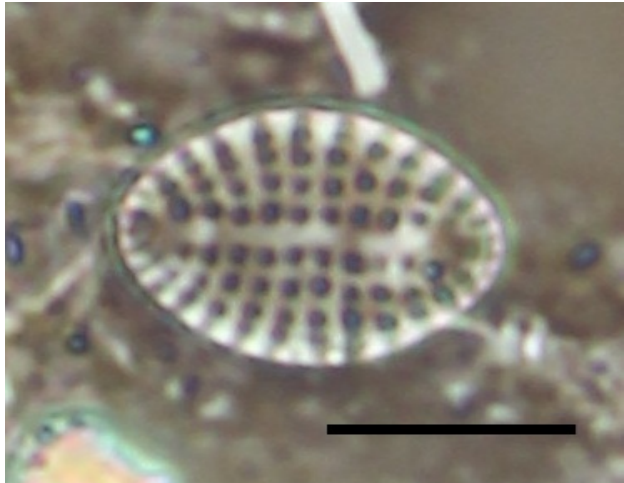
Plate	Species	Literature
	<p>Plate 4 <i>Nitzschia minutissima</i> Length = 13.5 μm</p>	<p>Underwood, G. J. C. (1994).</p>
	<p>Plate 5 <i>Gyrosigma attenuatum</i> (Kutzing) Rabenhorst Length= 162 μm</p>	<p>Van der werff, A & Huls, H. (1976).</p>
	<p>Plate 6 <i>Scoliopleura tumida</i>. Length= 125.4 μm, striation= curve radiate (pointing downwards), raphae= straight</p>	<p>Van der werff, A & Huls, H. (1976).</p>

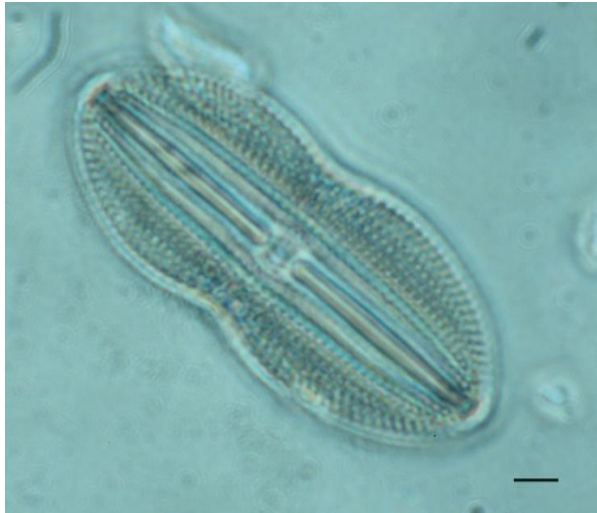
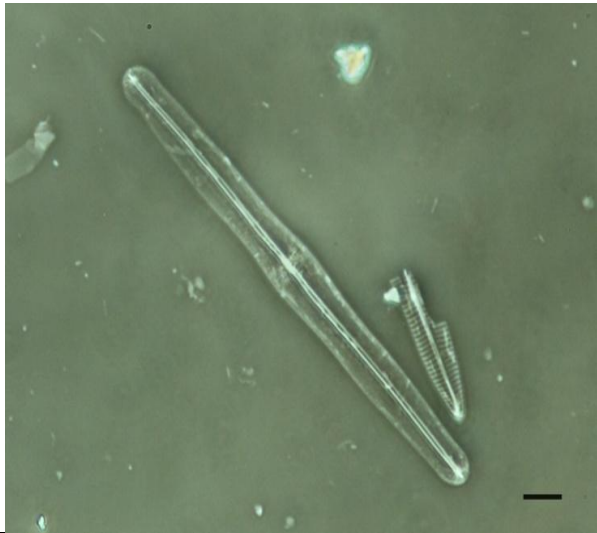
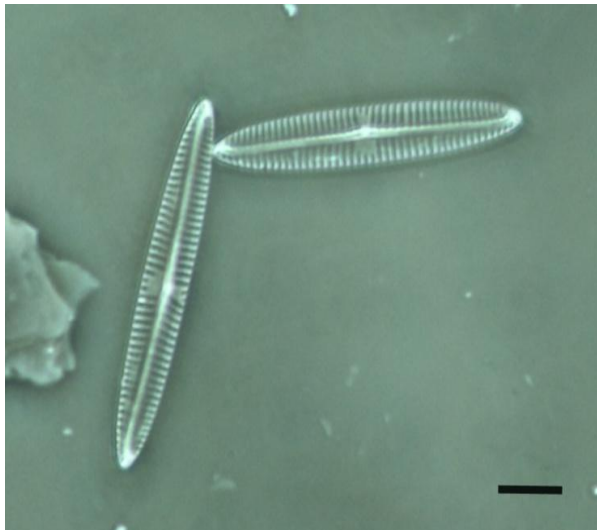
Plate	Species	Literature
	<p>Plate 7 <i>Diploneis didyma</i> Length= 64.8 μm</p>	<p>Van der werff, A & Huls, H. (1976).</p>
	<p>Plate 8 <i>Navicula scopulorum</i> Length= 110.8 μm</p>	<p>Van der werff, A & Huls, H. (1976).</p>
	<p>Plate 9 <i>Navicula gracilis</i> Length= 51.3 μm</p>	<p>Van der werff, A & Huls, H. (1976).</p>

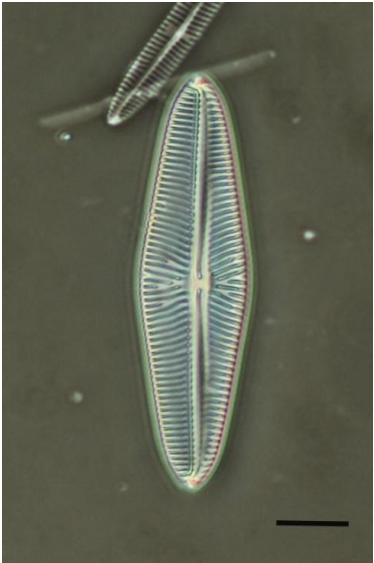
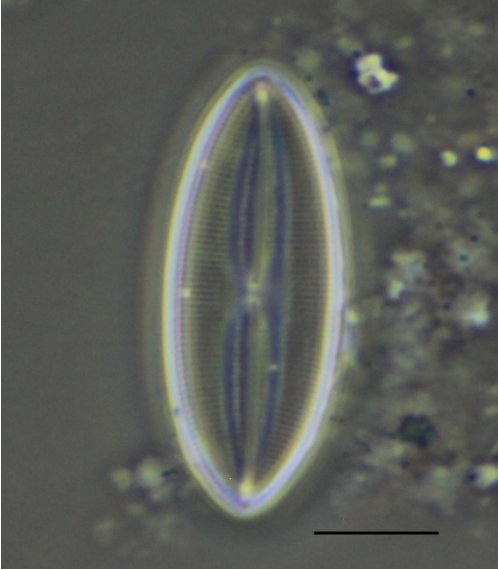
Plate	Species	Literature
	<p>Plate 10 <i>Navicula digitoradiata</i> Length= 67.5 μm</p>	<p>Van der werff, A & Huls, H. (1976).</p>
	<p>Plate 11 <i>Raphoneis amphiceros</i> Length= 32.4 μm</p>	<p>Lange-Bertalot, H. (2000).</p>
	<p>Plate 12 <i>Fallacea pygmaea</i> (Kutzing) A. J. Stickle & D. G. Mann</p>	<p>Snoeijs, P. & Vilbaste, S. (1994).</p>

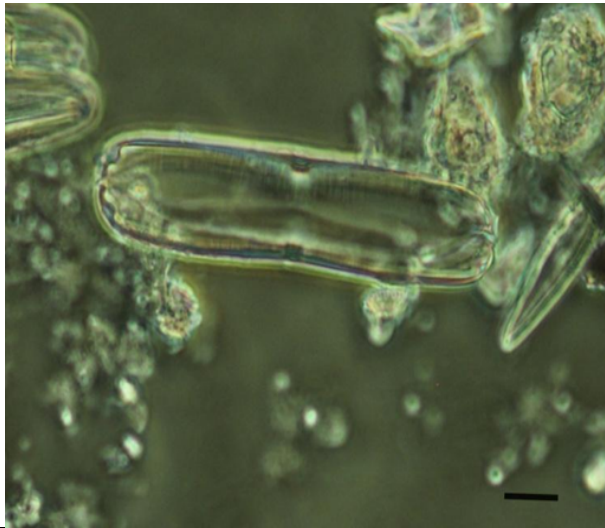
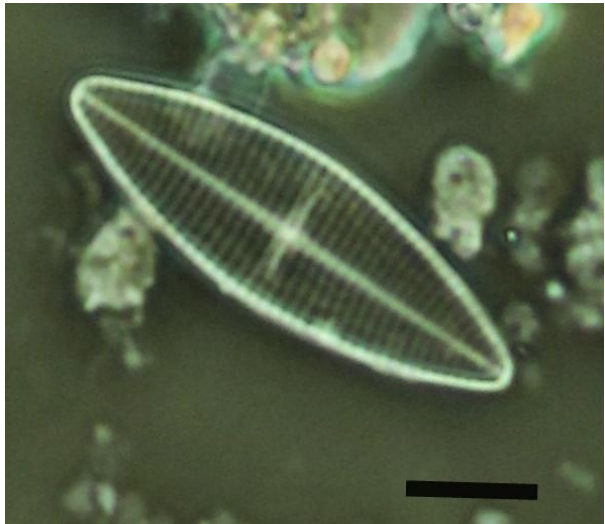
Plate	Species	Literature
	<p>Plate 13 <i>Fragilaria</i> sp. Length= 116.1 μm</p>	<p>Van der werff, A & Huls, H. (1976).</p>
	<p>Plate 14 <i>Plagiotropis vitreae</i> Length= 71 μm</p>	<p>Hartley, et al., (1996).</p>
	<p>Plate 15 <i>Navicula gregaria</i> Length= 40.5 μm</p>	<p>Underwood, G. J. C. (1994).</p>

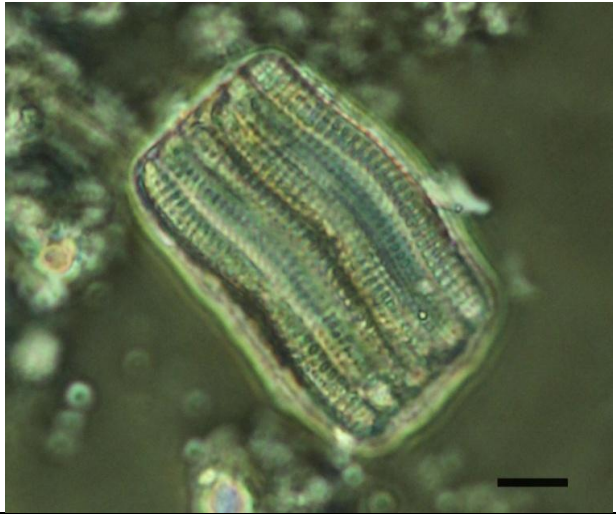
Plate	Species	Literature
	<p>Plate 16 <i>Nitzschia scalproides</i> Length= 124.2 μm</p>	<p>Van der werff, A & Huls, H. (1976).</p>
	<p>Plate 17 <i>Achnanthes longipes</i> Length= 52.65 μm</p>	<p>Van der werff, A & Huls, H. (1976).</p>
	<p>Plate 18 <i>Hantzschia</i> sp.</p>	<p>Lange-Bertalot, H. (2000).</p>

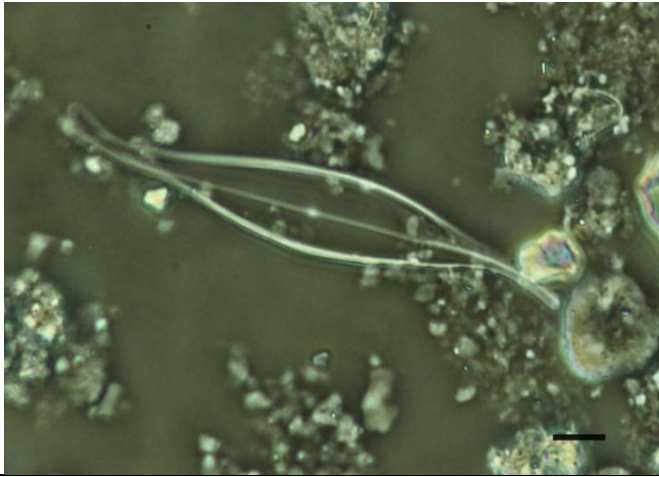
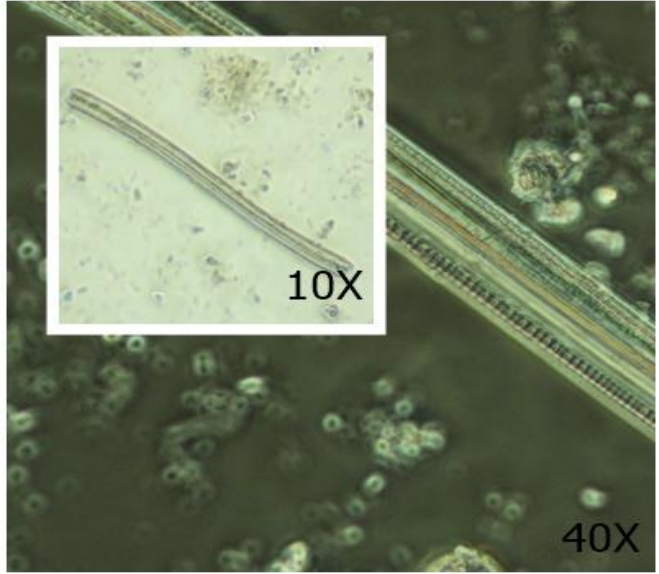
Plate	Species	Literature
	<p>Plate 19 Sp1 Length= 108 μm</p>	
	<p>Plate 20 <i>Gyrosigma fasciola</i> Length= 105.3 μm</p>	<p>Van der werff, A & Huls, H. (1976).</p>
	<p>Plate 21 <i>Nitzschia sigmoidea</i></p>	<p>Van der werff, A & Huls, H. (1976).</p>

Plate	Species	Literature
	<p>Plate 22 <i>Actinoptychus undulatus</i> (Bailey) Ralfs</p>	<p>Van der werff, A & Huls, H. (1976).</p>
	<p>Plate 23 <i>Pleurosigma angulatum</i> Length= 140.4 μm</p>	<p>Van der werff, A & Huls, H. (1976).</p>
	<p>Plate 24 <i>Fallacia forcipata</i> Length= 40.5 μm</p>	<p>Van der werff, A & Huls, H. (1976).</p>

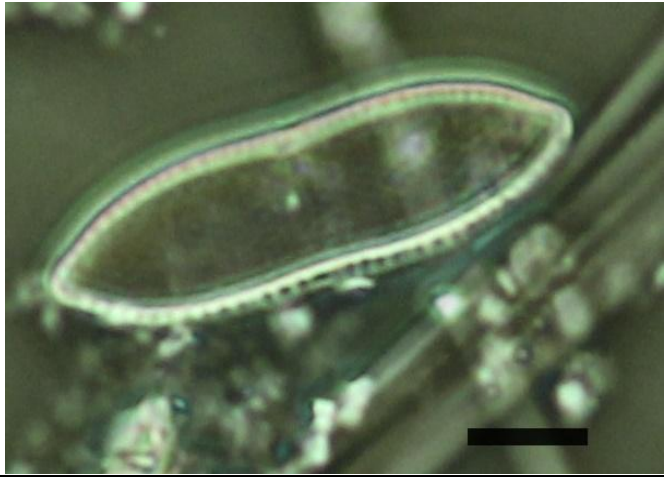
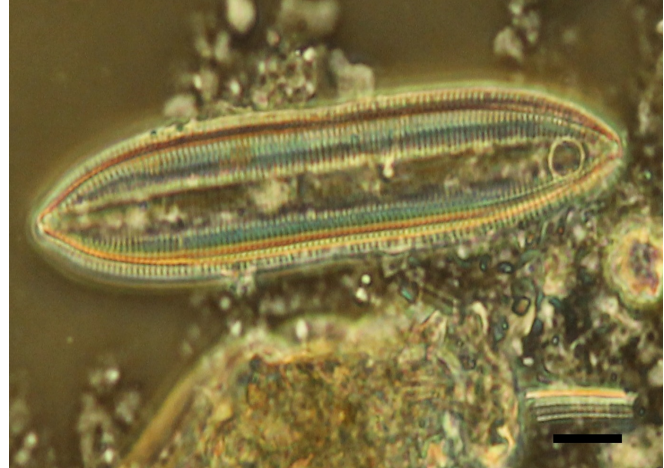
Plate	Species	Literature
	<p>Plate 25 <i>Nitzschia panduriformis</i> Gregory Length= 45.5 μm</p>	<p>Hartley, et al., (1996).</p>
	<p>Plate 26 <i>Caloneis formosa</i> Length=118.8 μm</p>	<p>Van der werff, A & Huls, H. (1976).</p>
	<p>Plate 27 <i>Tryblionella acuminata</i> W. Smith Length=89.1 μm</p>	<p>Hartley, et al., (1996).</p>

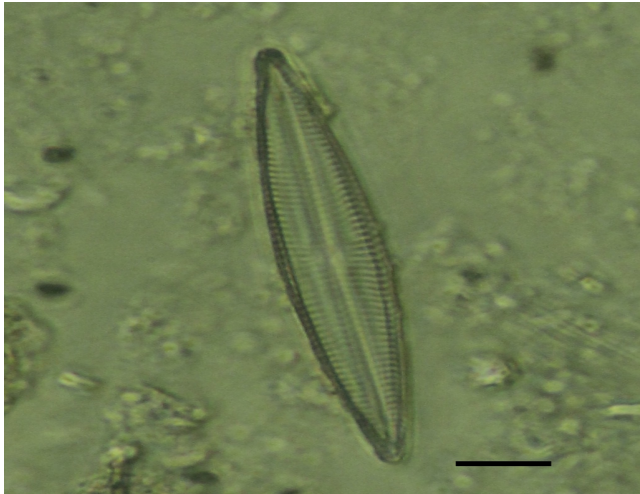
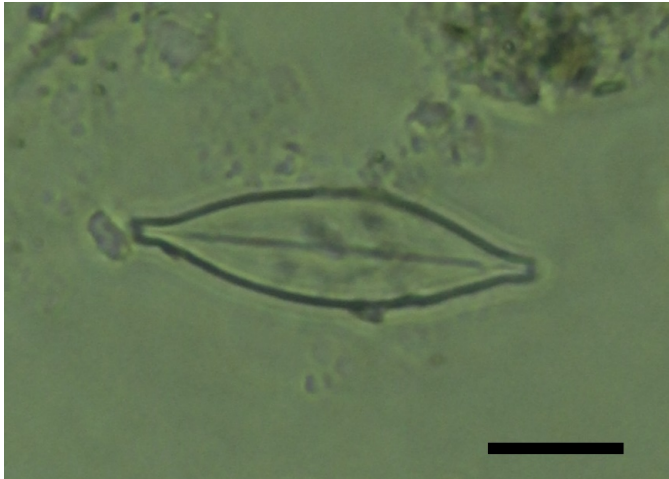
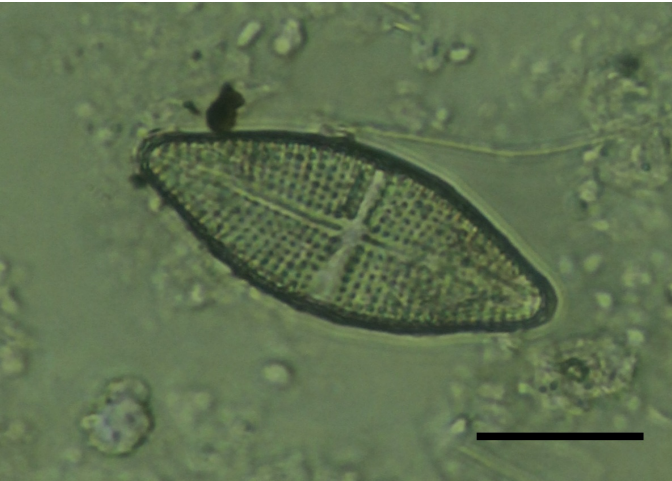
Plate	Species	Literature
	<p>Plate 28 <i>Navicula phyllepta</i> Length= 72.9 μm</p>	<p>Underwood (1994)</p>
	<p>Plate 29 <i>Navicula</i> sp1</p>	
	<p>Plate 30 <i>Stauroneis producta</i> Grunow Length= 24.3 μm</p>	<p>Van der werff, A & Huls, H. (1976).</p>

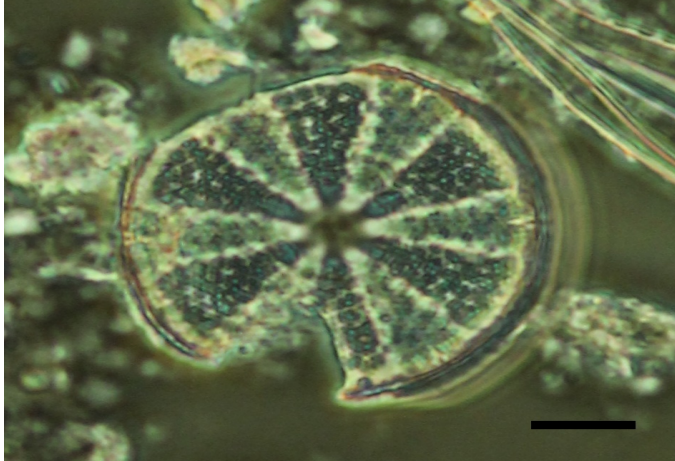
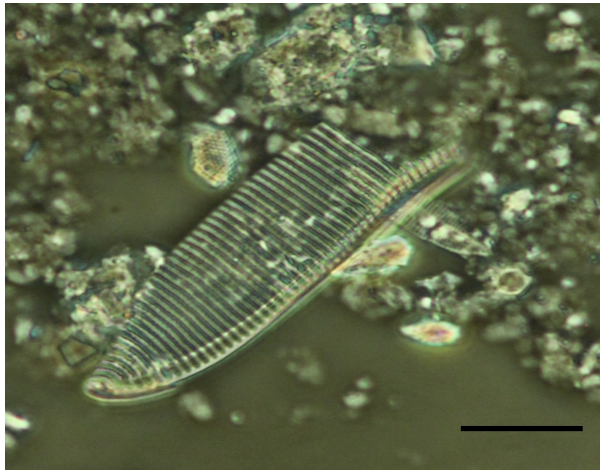
Plate	Species	Literature
	<p>Plate 31 <i>Gyrosigma wansbeckii</i> Length= 135 μm</p>	<p>Van der werff, A & Huls, H. (1976).</p>
	<p>Plate 32 <i>Actinoptychus splendens</i> (Shadbolt) Ralfs Length= 43.2 μm</p>	<p>Van der werff, A & Huls, H. (1976).</p>
	<p>Plate 33 <i>Nitzschia dubia</i> W. Smith (Half frustule) Length = 71 μm</p>	<p>Van der werff, A & Huls, H. (1976).</p>

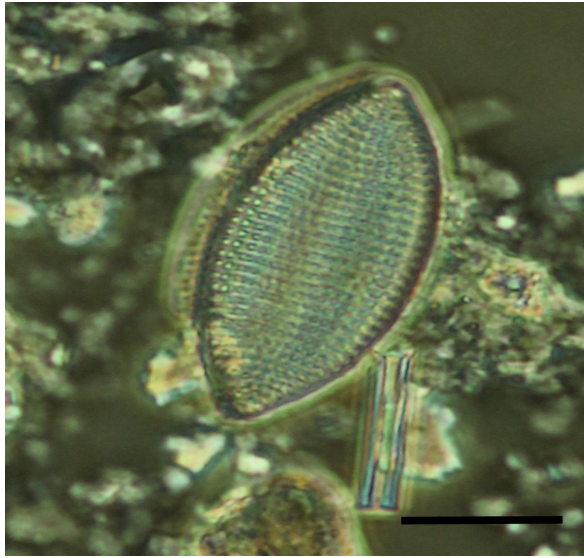
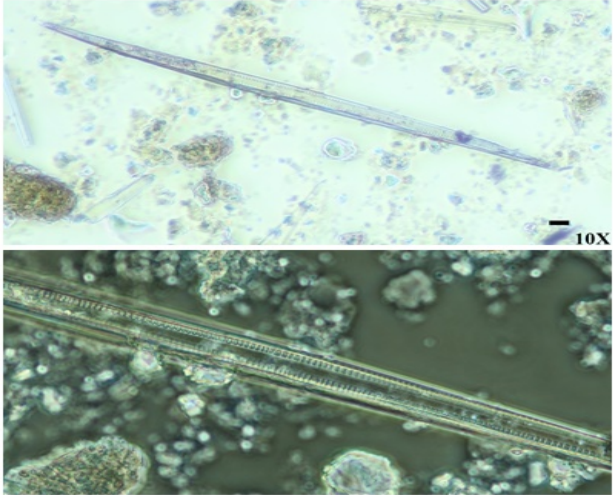
Plate	Species	Literature
	<p>Plate 34 <i>Nitzschia punctata</i> W. Smith</p> <p>Length= 29.7 μm</p>	<p>Hartley, et al., (1996).</p>
	<p>Plate 35 <i>Synedra</i> sp.</p> <p>Length=324 μm</p>	<p>Van der werff, A & Huls, H. (1976).</p>
	<p>Plate 36 <i>Diploneis litoralis</i> (Donkin) Cleve</p> <p>Length=51.3 μm</p>	<p>Van der werff, A & Huls, H. (1976).</p>

Plate	Species	Literature
	<p>Plate 37 <i>Gyrosigma distortum</i> (W. Smith) Cleve</p> <p>Length= 116.1 μm</p>	<p>Van der werff, A & Huls, H. (1976).</p>
	<p>Plate 38 <i>Navicula cryptocephala</i> (Ehrenberg) Kutzing</p>	<p>Potapova, M. (2011)</p>
	<p>Plate 39 UI Sp39</p>	

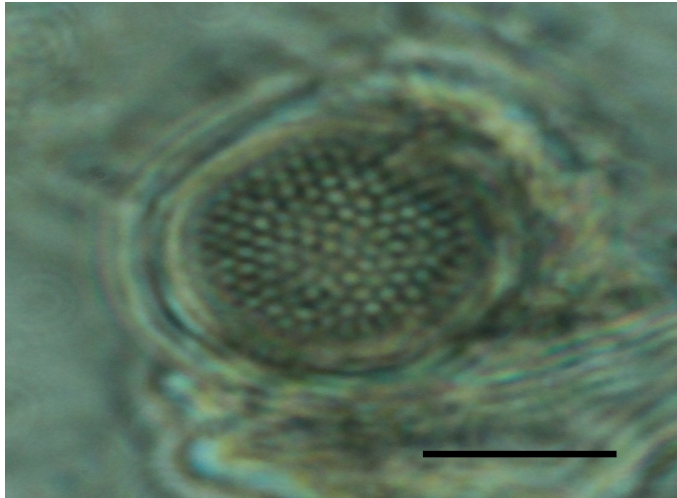
Plate	Species	Literature
	<p>Plate 40 <i>Coscinodiscus</i> sp. 1 Length= 16.5 μm</p>	<p>Van der werff, A & Huls, H. (1976).</p>
	<p>Plate 41 <i>Stephanodiscus</i> sp. 1 Length= 24.3</p>	<p>Van der werff, A & Huls, H. (1976).</p>
	<p>Plate 42 <i>Pleurosigma</i> sp. 1</p>	<p>Van der werff, A & Huls, H. (1976).</p>

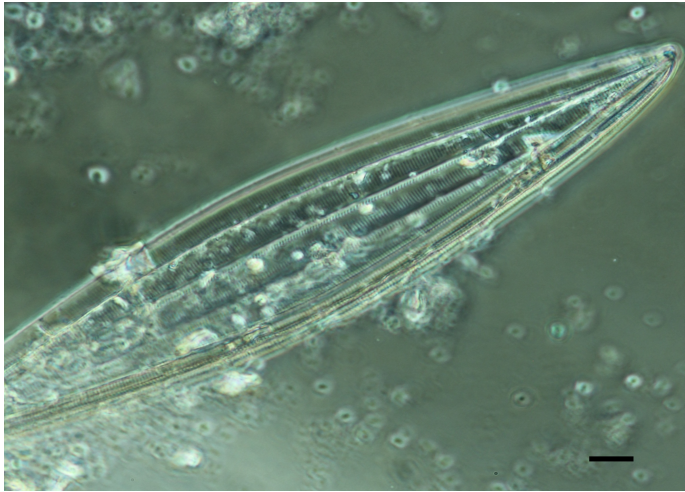
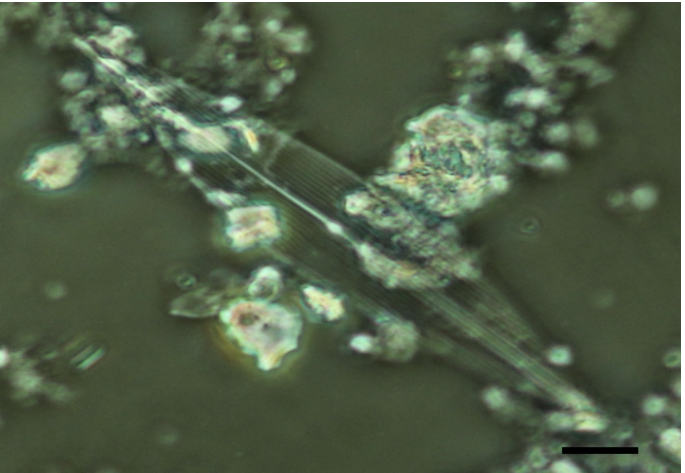
Plate	Species	Literature
	<p>Plate 43 <i>Surirella ovata</i> Kutzing Length= 54 µm</p>	<p>Hartley, et al., (1996).</p>
	<p>Plate 44 <i>Plagiotropis</i> sp. 1</p>	<p>Van der werff, A & Huls, H. (1976).</p>
	<p>Plate 45 <i>Navicula deurrebergiana</i> Length= 94.5 µm</p>	<p>Van der werff, A & Huls, H. (1976).</p>

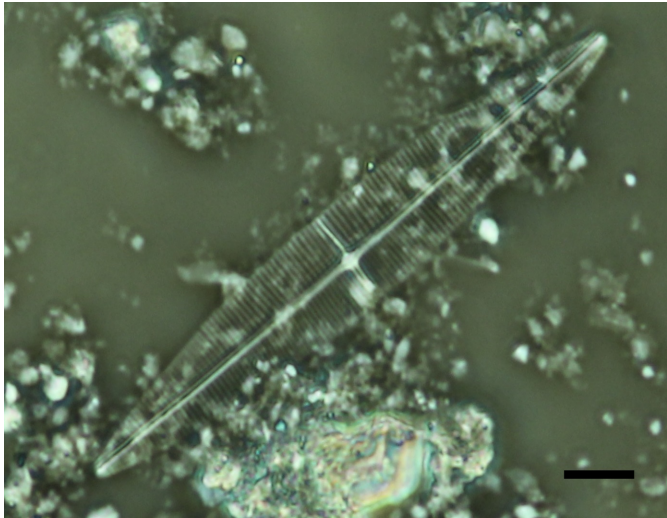
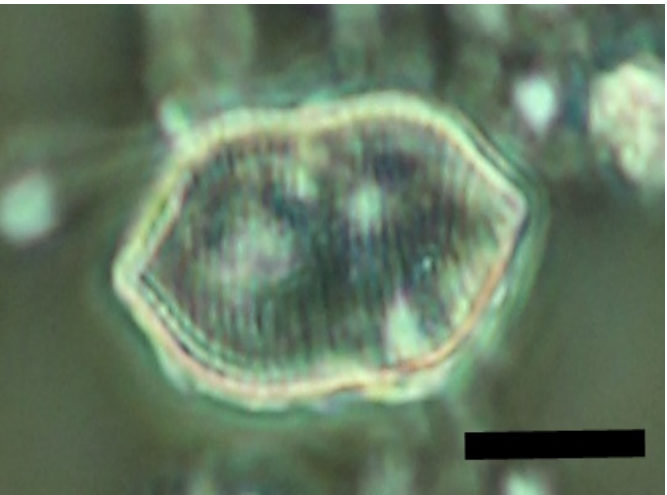
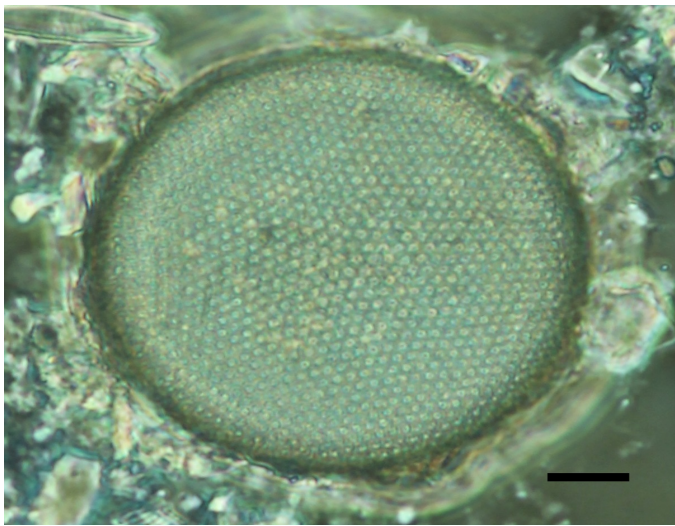
Plate	Species	Literature
	<p>Plate 46 <i>Navicula crucigera</i> Length= 105.3 μm</p>	
	<p>Plate 47 <i>Tryblionella</i> sp. 1 Length= 24.3 μm</p>	<p>Hartley, et al., (1996).</p>
	<p>Plate 48 <i>Coscinodiscus</i> sp. 2 Length= 59.4 μm</p>	<p>Van der werff, A & Huls, H. (1976).</p>

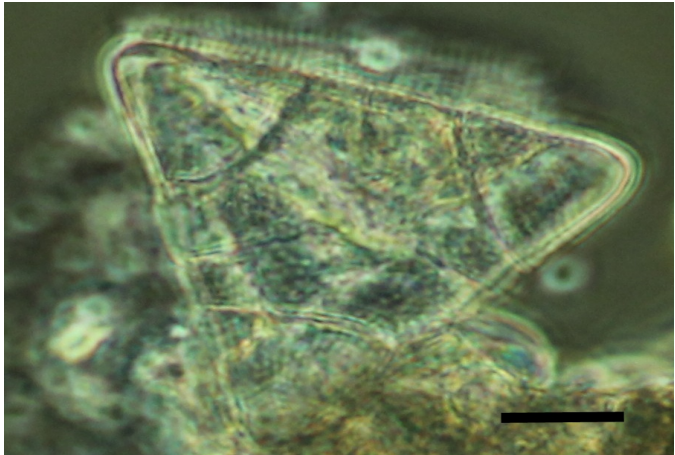
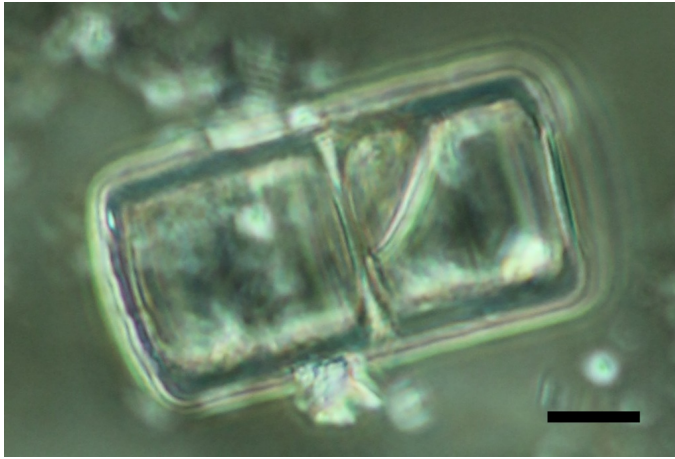
Plate	Species	Literature
	<p>Plate 49 <i>Odontella alternan</i> Bailey Length= 51.3 μm</p>	<p>Van der werff, A & Huls, H. (1976).</p>
	<p>Plate 50 Sp1 Length of one cell= 24.3 μm</p>	
	<p>Plate 51 <i>Tryblionella navicularis</i> Length= 56.7 μm</p>	<p>Van der werff, A & Huls, H. (1976).</p>

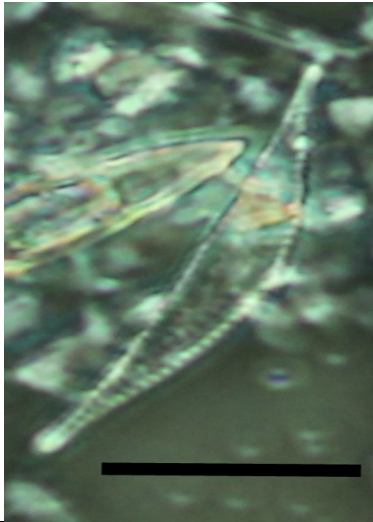
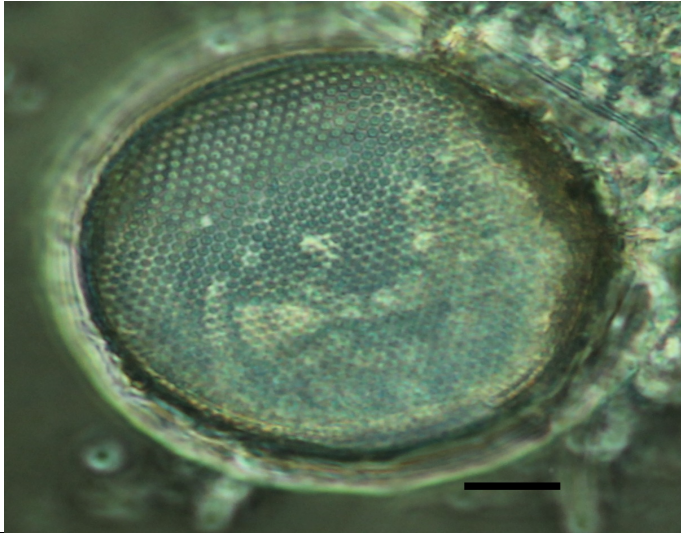
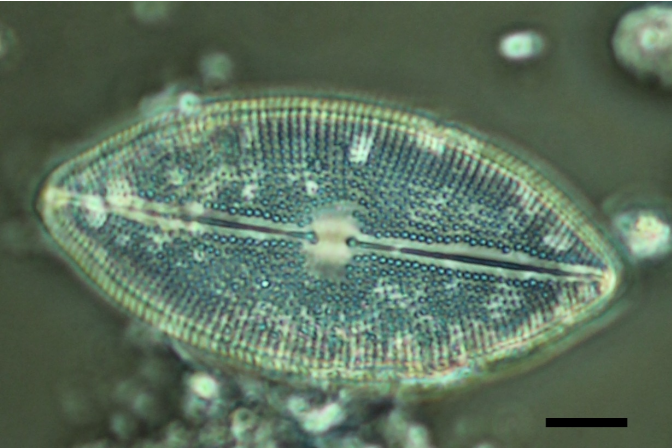
Plate	Species	Literature
	<p>Plate 52 <i>Amphora</i> sp. 1 Length= 27 μm</p>	<p>Van der werff, A & Huls, H. (1976).</p>
	<p>Plate 53 <i>Coscinodiscus</i> sp. 3 Diameter= 62.1 μm</p>	<p>Van der werff, A & Huls, H. (1976).</p>
	<p>Plate 54 <i>Petroneis latissima</i> (W. Gregory) A. J. Stickle & D. G. Mann Length= 72.9 μm</p>	<p>Van der werff, A & Huls, H. (1976).</p>

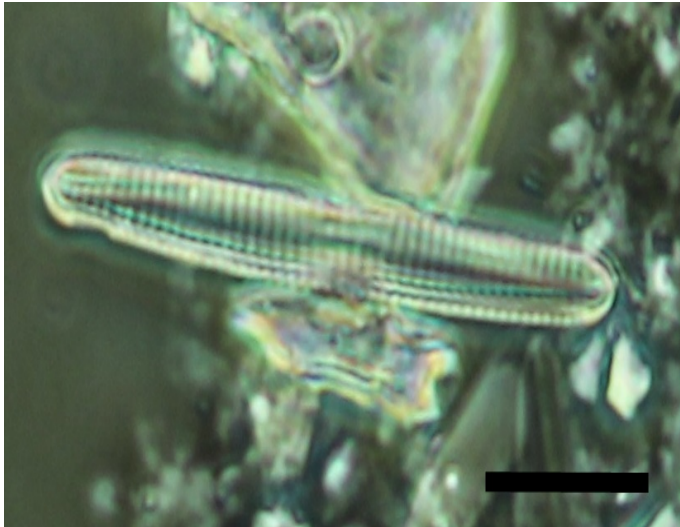
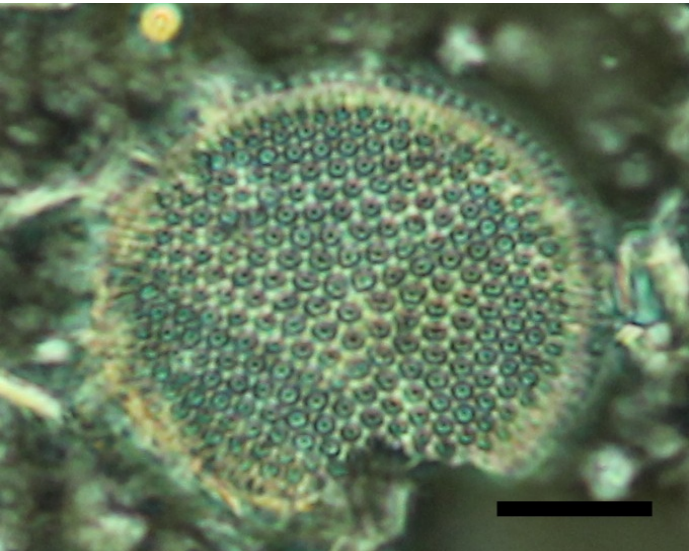
Plate	Species	Literature
	<p>Plate 55 <i>Eunotia</i> sp. 1 Length= 35.1 μm</p>	<p>Van der werff, A & Huls, H. (1976).</p>
	<p>Plate 56 <i>Cymatopleura solea</i> Length= 102.6 μm</p>	<p>Van der werff, A & Huls, H. (1976).</p>
	<p>Plate 57 Sp 2 Diameter= 32.4 μm</p>	

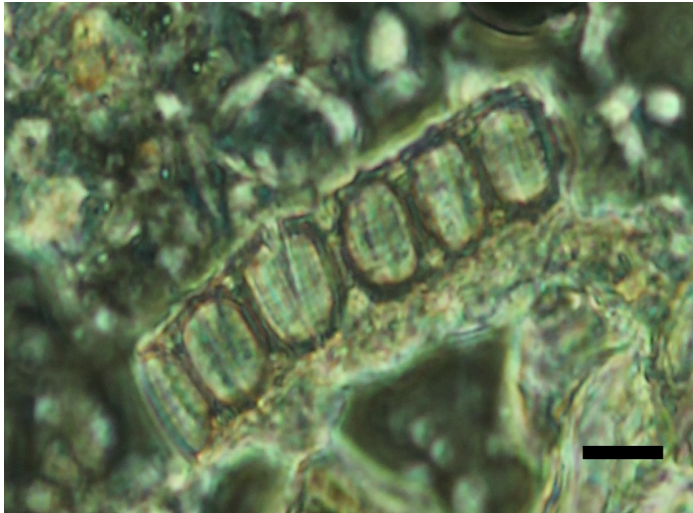
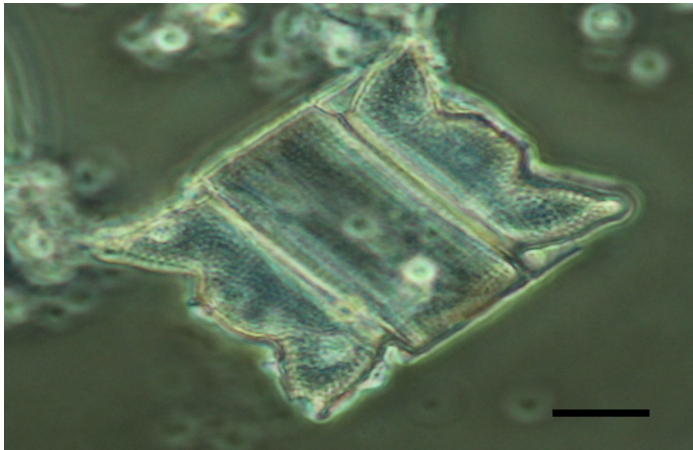
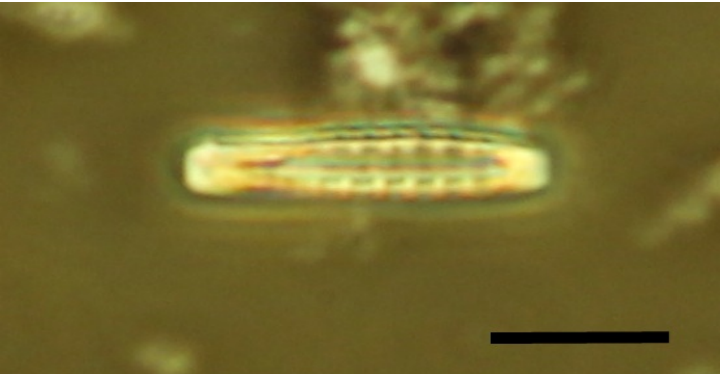
Plate	Species	Literature
 <p>A high-magnification micrograph showing a portion of a diatom frustule. The structure is composed of several rectangular cells arranged in a row, with distinct transverse and longitudinal striations. A black scale bar is visible in the lower right corner.</p>	<p>Plate 58 <i>Melosira</i> sp. Length= 8.1 μm</p>	
 <p>A micrograph of a diatom frustule, likely <i>Odontella aurita</i>. The frustule is elongated and tapers at both ends, showing a complex arrangement of cells with prominent longitudinal striations. A black scale bar is located in the lower right corner.</p>	<p>Plate 59 <i>Odontella aurita</i> (Lyngbye) De Brebisson et Godey</p>	<p>Van der werff, A & Huls, H. (1976).</p>
 <p>A micrograph of a diatom frustule, identified as <i>Opephora</i> sp. 1. The frustule is elongated and spindle-shaped, with a distinct central region and a black scale bar in the lower right corner.</p>	<p>Plate 60 <i>Opephora</i> sp 1 Length= 100x 19eg</p>	<p>Hartley, et al., (1996).</p>

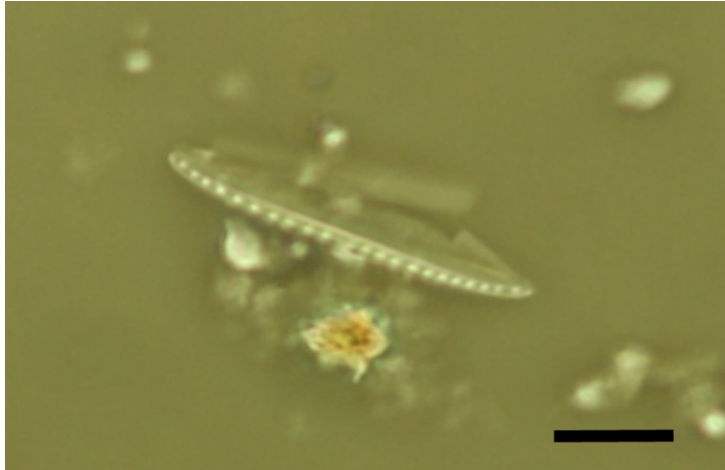
Plate	Species	Literature
	<p>Plate 61 <i>Neidium</i> sp. Length= 30 μm</p>	<p>Hartley, et al., (1996).</p>
	<p>Plate 62 <i>Nitzschia bilobata</i> Length= 52.3 μm</p>	<p>Hartley, et al., (1996).</p>
	<p>Plate 63 <i>Nitzschia</i> sp1 Length= 32.5 μm</p>	<p>Hartley, et al., (1996).</p>

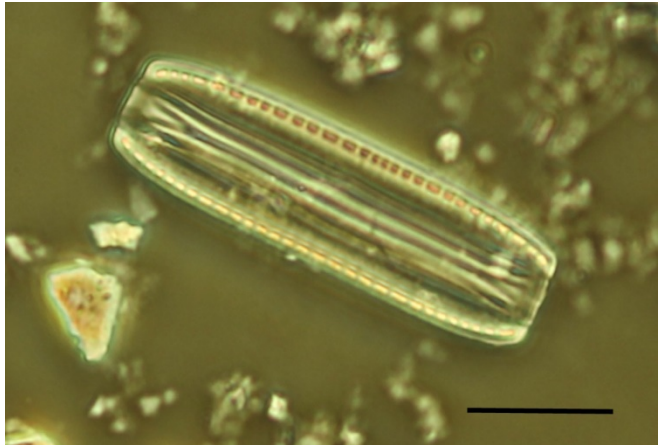
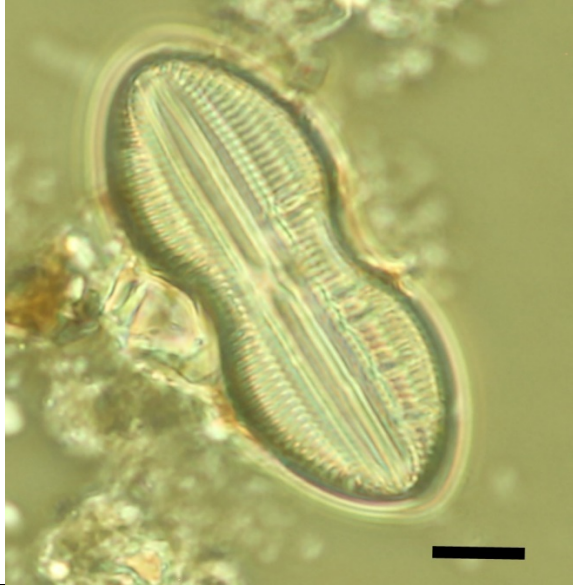
Plate	Species	Literature
	<p>Plate 64 <i>Nitzschia vitreae</i> Length= 32.5 μm</p>	<p>Hartley, et al., (1996).</p>
	<p>Plate 65 <i>Diploneis stroemii</i> Length= 55 μm</p>	<p>Van der werff, A & Huls, H. (1976).</p>
	<p>Plate 66 <i>Surirella fastuosa</i> Length= 47.5 μm</p>	<p>Van der werff, A & Huls, H. (1976).</p>

Plate	Species	Literature
 A light micrograph showing a single, elongated, spindle-shaped organism with a distinct internal structure, likely a flagellum or similar appendage. The organism is stained and appears as a bright, elongated shape against a darker background. A black scale bar is located in the lower right corner of the image.	Plate 67 <i>Opephora</i> sp2 Length= 12.5 μ m	Hartley, et al., (1996).